Identification of SPRED2 as a Novel Regulator of Hypothalamic-Pituitary-Adrenal Axis Activity and of Body Homeostasis

Dissertation zur Erlangung des

naturwissenschaftlichen Doktorgrades

der Julius-Maximilians-Universität Würzburg

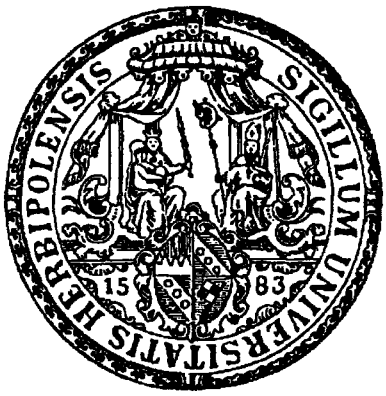

vorgelegt von

Melanie Ullrich

aus Karlstadt

Würzburg 2014

Eingereicht bei der Fakultät für Biologie am:

_____

Mitglieder der Promotionskommission:

Vorsitzender: _____

1. Gutachter: _____

2. Gutachter: _____

Tag des Promotionskolloquiums:

_____

Doktorurkunde ausgehändigt am:

_____

Eidesstattliche Erklärung

Hiermit erkläre ich an Eides statt, dass ich meine Dissertation mit dem Titel „Identification of SPRED2 as a Novel Regulator of Hypothalamic-Pituitary-Adrenal Axis Activity and of Body Homeostasis“ eigenständig, d.h. insbesondere selbstständig und ohne Hilfe einer kommerziellen Promotionsberatung angefertigt habe und keine anderen als die von mir angegebenen Quellen oder Hilfsmittel benutzt habe.

Des Weiteren versichere ich, dass ich die Gelegenheit zum Promotionsvorhaben nicht kommerziell vermittelt bekommen habe und dass ich insbesondere nicht eine Person oder Organisation eingeschaltet habe, die gegen Entgelt Betreuer bzw. Betreuerinnen für die Anfertigung von Dissertationen sucht.

Ich erkläre außerdem, dass die Regeln der Universität Würzburg über gute wissenschaftliche Praxis eingehalten wurden, dass die Dissertation weder in gleicher noch in ähnlicher Form bereits in einem anderen Prüfungsverfahren vorgelegen hat und dass ich akademische Grade weder bereits früher erworben noch zu erwerben versucht habe.

Würzburg, 2014

_____

Melanie Ullrich

Die vorliegende Arbeit wurde unter Betreuung von

Herrn Prof. Dr. Kai Schuh

am Physiologischen Institut

der Julius-Maximilians-Universität Würzburg angefertigt.

Teile dieser Dissertation wurden bereits in

wissenschaftlichen Publikationen

oder in Form von

Abstracts zur Präsentation auf wissenschaftlichen Kongressen

veröffentlicht.

Publikationen

Wissenschaftliche Publikationen

Benz, P.M., Merkel, C.J., Offner, K., Abeßer, M., **Ullrich, M.**, Fischer, T., Bayer, B., Wagner, H., Gambaryan, S., Ursitti, J.A., Adham, I.M., Linke, W., Feller, S.M., Fleming, I., Renné, T., Frantz, S., Unger, A., Schuh, K. (2013): Mena/VASP and αII-Spectrin complexes regulate cytoplasmic actin networks in cardiomyocytes and protect from conduction abnormalities and dilated cardiomyopathy. Cell Commun Signal. 11:56.

Ullrich, M., Bundschu, K., Benz, P.M., Abesser, M., Freudinger, R., Fischer, T., Ullrich, J., Renné, T., Walter, U., and Schuh, K. (2011): Identification of SPRED2 (Sprouty-related protein with EVH1 domain 2) as a negative regulator of the hypothalamic-pituitary-adrenal axis. J Biol Chem. 286 (11): 9477-88.

Ullrich, M. and Schuh, K. (2009): Gene trap - knockout on the fast lane. Methods Mol Biol. 561, 145-159.

Johne, J., Blume, C., Benz, P.M., Pozgajová, M., **Ullrich, M.**, Schuh, K., Nieswandt, B., Walter, U., and Renné, T. (2006): Platelets promote coagulation factor XII-mediated proteolytic cascade systems in plasma. Biol Chem. 387, 173-78.

Bundschu, K., Knobeloch, K.-P., **Ullrich, M.**, Schinke, T., Amling, M., Engelhardt, C.M., Renné T., Walter, U., and Schuh, K. (2005): Gene disruption of Spred-2 causes dwarfism. J Biol Chem. 280 (31), 28572-80.

Wissenschaftliche Publikationen in Revision

Fischer, T., Rokita, A.G., Benz, P.M., Fissler, B., **Ullrich, M.**, Abeßer, M., Seibold, S., Reichle, J., Lars, S., Maier, L.S., Ritter, O., Seidlmayer, L.K., Zuern, C., Wohlschlaeger, J., Baba, H.A., Schuh, K.: ATIP1 is a suppressor of cardiac hypertrophy and modulates AT2-dependent signaling in cardiac myocytes.

Andere wissenschaftliche Artikel in den Medien

http://www.nationalgeographic.de/aktuelles/koerpereigene-stressbremse-entdeckt
http://www.innovationsreport.de/html/berichte/biowissenschaften_chemie/stressbremse_versagt_172042.html
http://derstandard.at/1297820667155/Forscher-identifizieren-Stressbremse

Abstracts zur Präsentation auf wissenschaftlichen Kongressen

Ullrich, M., Weber, M., Post, A., Popp, S., Guerrero, H., and Schuh. K. (2014): SPRED2 – a Critical Regulator of Synaptic Protein Expression and of Behavior?
Posterpräsentation, Jahrestagung der Deutschen Physiologischen Gesellschaft, Mainz

Augustin, A.M., **Ullrich M.,** Abesser, M., and Schuh K. (2014): Antagonizing aldosterone reduces cardiac effects of SPRED2-deficiency only partially.
Posterpräsentation, Jahrestagung der Deutschen Physiologischen Gesellschaft, Mainz

Ullrich, M., Abesser, M., Augustin, A.M., and Schuh, K. (2013): SPRED2 - A Novel Modulator of Cardiac Hypertrophy and Electrical Conduction in the Heart?
Posterpräsentation, Jahrestagung der Deutschen Physiologischen Gesellschaft, Heidelberg

Ullrich, M., Abesser, M., Augustin, A.M., and Schuh, K. (2012): SPRED2 - A Novel Modulator of Cardiac Hypertrophy and Electrical Conduction in the Heart?
Posterpräsentation, Jahrestagung des Deutschen Zentrums für Herzinsuffizienz, Kloster Banz

Ullrich, M. and Schuh, K. (2012): Physiological Role of SPRED2 in the Mammalian Heart.
Vortrag, Begutachtung des DZHI-Projekts B10, ESAB-Meeting des DZHI, Würzburg

Ullrich, M. and Schuh, K. (2011): Identification of SPRED2 as a negative regulator of the HPA axis.
Posterpräsentation, Jahrestagung der Deutschen Physiologischen Gesellschaft, Regensburg

Bundschu, K., Schuh, K., Walter, U., and **Ullrich, M.** (2010): SPRED2 (Sprouty-related protein with EVH1 domain 2) regulates bone growth and hypothalamic-pituitary-adrenal hormone secretion.
Posterpräsentation, EMBO Meeting, Barcelona

Ullrich, M., Bundschu, K., Walter, U., and Schuh, K. (2010): Dysregulated hypothalamic-pituitary-adrenal (HPA) hormone secretion in SPRED2-deficient mice.
Posterpräsentation, Jahrestagung der Deutschen Physiologischen Gesellschaft, Kopenhagen.

Ullrich, M., Walter, U., and Schuh, K. (2009): Dysregulated hypothalamic-pituitary-adrenal (HPA) hormone secretion in SPRED2-deficient mice.

Posterpräsentation, Jahrestagung der Deutschen Vereinten Gesellschaft für Klinische Chemie und Laboratoriumsmedizin, Leipzig

Ullrich, M., Bundschu, K., Freudinger, R., Gattenloehner, S., Walter, U., and Schuh, K. (2009): Dysregulation of hypothalamic-pituitary-adrenal hormone secretion in SPRED2-deficient mice.
Posterpräsentation, Jahrestagung der Deutschen Physiologischen Gesellschaft, Giessen.

Ullrich, M., Freudinger, R. Bundschu, K., Walter, U., and Schuh, K. (2008): Phenotype puzzle in Spred-2-deficient mice.
Posterpräsentation, Jahrestagung der Deutschen Vereinten Gesellschaft für Klinische Chemie und Laboratoriumsmedizin, Mannheim

Ullrich, M., Bundschu, K., Freudinger, R., Gattenloehner, S., Walter, U., and Schuh, K. (2008): Hormone, ion, and fluid imbalance in Spred-2$^{-/-}$ mice.
Posterpräsentation, Graduate School of Life Sciences, Würzburg

Ullrich, M., Bundschu, K., Walter, U., and Schuh, K. (2008): Phenotype puzzle in Spred-2-deficient mice.
Posterpräsentation, Jahrestagung der Deutschen Physiologischen Gesellschaft, Köln.

Ullrich, M., Bundschu, K., Gattenloehner, S., Walter, U., and Schuh, K. (2007): Dwarfism and kidney failure in Spred-2-deficient mice.
Posterpräsentation, Jahrestagung der Deutschen Physiologischen Gesellschaft, Hannover.

Ullrich, M., Bundschu, K., Walter, U., and Schuh, K. (2006): Spred-2 deficiency results in dwarfism and kidney failure.
Vortrag und **Posterpräsentation**, Experimental Biology Meeting, San Francisco

Ullrich, M., Schmitteckert, E., Renné, T., Walter, U., and Schuh, K. (2006): Generation of a system for thrombocyte-specific gene deletion.
Posterpräsentation, Jahrestagung der Gesellschaft für Thrombose und Hämostase, Basel

Preise und Auszeichnungen

„1. Posterpreis“ auf der Jahrestagung des Deutschen Zentrums für Herzinsuffizienz (DZHI) in Kloster Banz

„FEPS Best Poster Award” auf dem European Young Physiologists Symposium im Rahmen der Physiologentagung in Kopenhagen

„Travel Award” im Rahmen des Experimental Biology Meetings in San Francisco

Das Genie beginnt die schönen Werke, aber nur die Arbeit vollendet sie.

Joseph Joubert

Meiner Familie

Danksagung

An dieser Stelle möchte ich mich bei all den Personen bedanken, ohne die die Durchführung und Vollendung meiner Dissertation nicht möglich gewesen wäre:

Mein größter Dank gilt Herrn Prof. Dr. Kai Schuh, der mir die Bearbeitung dieses Dissertationsthemas in seiner Arbeitsgruppe ermöglicht hat. Lieber Kai, du warst mir in all den Jahren ein ganz hervorragender Betreuer. Ich konnte sowohl in wissenschaftlicher als auch in menschlicher Hinsicht wirklich sehr viel von dir lernen. Ganz herzlichen Dank für die Freiheit sowohl bei der experimentellen als auch bei der schriftlichen Gestaltung dieser Arbeit, für deine stets offene Tür, für deine unerschöpfliche Diskussionsbereitschaft, für deine Geduld, deine Motivation und deinen Glauben an mich. Durch deine immerwährende Unterstützung konnte ich die Ergebnisse dieses schönen Projekts publizieren und als meine Doktorarbeit zu Papier bringen.

Ein herzliches Dankeschön gilt auch Herrn Prof. Dr. Georg Krohne für die Bereitschaft, nach meiner Diplomarbeit auch meine Dissertation als Vertreter der biologischen Fakultät zu begutachten. Vielen Dank für die stets unkomplizierte Zusammenarbeit.

Ganz besonders bedanken möchte ich mich bei allen aktuellen und ehemaligen Kolleginnen und Kollegen der AG Schuh. Lieben Dank an euch, Doreen, Krissi, Anne, Ruth, Priscilla, Carla, Feli, Chris, Constanze, Marco, Peter, Tobi, Hans und Robert für das stets konstruktive und freundschaftliche Miteinander im Labor. Auch die vielen schönen Unternehmungen zusammen mit euch außerhalb des Labors, wie die Cocktailabende im Joes, die diversen (Geburtstags-) Partys, der Besuch der Wilhelma in Stuttgart mit gemütlichem Ausklang im Bierzelt auf dem Cannstatter Wasen und die Bootstour auf dem Main werden mir immer in Erinnerung bleiben.
Vielen Dank an die AG von Prof. Dr. Michaela Kuhn mit Birgit, Katharina, Sabrina, Heike, Franziska, Annett, Thomas, Hitoshi und Wen. Danke euch allen für das fröhliche Arbeitsklima und für die unterhaltsamen Mittagspausen.
Ganz lieben Dank auch an die AG von Prof. Dr. Andreas Friebe mit Barbara, Dieter, Ronald und Noomen. Speziell dir, liebe Barbara, möchte ich ganz herzlich für die seelische Unterstützung und die vielen lieben und aufmunternden Worte besonders gegen Ende meiner Promotionsphase danken. Unvergesslich werden für mich die abenteuerlichen Bierwanderungen, die legendären Weihnachtsfeiern mit Schrottwichteln, die lustigen Skiausflüge nach Fügen und nach Au und natürlich auch die geselligen Sommerabende auf den Weinfesten Würzburgs mit euch bleiben.

Weiterhin danken möchte ich den Tierpflegerinnen Iris, Kerstin und Evi für die unkomplizierte und freundschaftliche Zusammenarbeit und für die gute und umfassende Betreuung meiner nicht ganz so pflegeleichten SPRED2 KO-Mauslinie.

Ganz kuscheligen Dank an Katze Floh und Kater Kalle, für die seelische Unterstützung beim Zusammenschreiben dieser Arbeit in Form von beruhigendem Schnurren auf meinem Schoß oder auf dem Schreibtisch. Ich danke euch auch für das ausgiebige Schlafen auf der Computertastatur, die so immer warm gehalten wurde, auch wenn es mit dem Schreiben mal nicht so lief.

Zu guter Letzt möchte ich von ganzem Herzen meiner Familie danken.
Liebe Julia, danke für die Überraschungspäckchen per Hauspost und für die vielen Telefonate in guten und in schlechten Zeiten. Ich denke, das hat bei uns beiden einiges bewegt…und ich zieh es jetzt durch!
Liebe Mama, lieber Papa, herzlichen Dank, dass ihr immer bei mir im Labor vorbeigeschaut habt, wenn ihr in Würzburg wart, für den alljährlichen Besuch auf dem Würzburger Weihnachtsmarkt mit Oma und für das viele gute Essen, das ihr jedesmal für mich mitgebracht habt.
Danke für eure immer dagewesene Unterstützung, für das Vertrauen und den Rückhalt, den ihr mir gebt und gegeben habt, diese akademische Karriere zu beginnen und bis zum Doktortitel fortzuführen.

Table of Contents

Summary

1

SPRED proteins are inhibitors of the Ras/ERK/MAPK signaling pathway, an evolutionary highly conserved and very widespread signaling cascade regulating cell proliferation, differentiation, and growth. To elucidate physiological consequences of SPRED2 deficiency, SPRED2 KO mice were generated by a gene trap approach. An initial phenotypical characterization of KO mice aged up to five months identified SPRED2 as a regulator of chondrocyte differentiation and bone growth. Here, the loss of SPRED2 leads to an augmented FGFR-dependent ERK activity, which in turn causes hypochondroplasia-like dwarfism. However, long term observations of older KO mice revealed a generally bad state of health and manifold further symptoms, including excessive grooming associated with severe self-inflicted wounds, an abnormally high water uptake, clear morphological signs of kidney deterioration, and a reduced survival due to sudden death. Based on these observations, the aim of this study was to discover an elicitor of this complex and versatile phenotype.

The observed kidney degeneration in our SPRED2 KO mice was ascribed to hydronephrosis characterized by severe kidney atrophy and apoptosis of renal tubular cells. Kidney damage prompted us to analyze drinking behavior and routine serum parameters. Despite polydipsia, which was characterized by a nearly doubled daily water uptake, the significantly elevated Na^+ and Cl^- levels and the resulting serum hyperosmolality could not be compensated in SPRED2 KOs. Since salt and water balance is primarily under hormonal control of aldosterone and AVP, we analyzed both hormone levels. While serum AVP was similar in WTs and KOs, even after experimental water deprivation and an extreme loss of body fluid, serum aldosterone was doubled in SPRED2 KO mice. Systematic investigation of contributing upstream hormone axes demonstrated that hyperaldosteronism developed independently of an overactivated Renin-Angiotensin system as indicated by halved serum Ang II levels in KO mice. However, aldosterone synthase expression in the adrenal gland was substantially augmented. Serum corticosterone, which is like aldosterone released from the adrenal cortex, was more than doubled in SPRED2 KOs, too. Similar to corticosterone, the production of aldosterone is at least in part under control of pituitary ACTH, which is further regulated by upstream hypothalamic

CRH release. In fact, stress hormone secretion from this complete hypothalamic-pituitary-adrenal axis was upregulated because serum ACTH, the mid acting pituitary hormone, and hypothalamic CRH, the upstream hormonal inductor of HPA axis activity, were also elevated by 30% in SPRED2 KO mice. This was accompanied by an upregulated ERK activity in paraventricular nucleus-containing hypothalamic brain regions and by augmented hypothalamic CRH mRNA levels in our SPRED2 KO mice. *In vitro* studies using the hypothalamic cell line mHypoE-44 further demonstrated that both SPRED1 and SPRED2 were able to downregulate CRH promoter activity, CRH secretion, and Ets factor-dependent CRH transcription. This was in line with the presence of various Ets factor binding sites in the CRH promoter region, especially for Ets1.

Thus, this study shows for the first time that SPRED2-dependent inhibition of Ras/ERK/MAPK signaling by suppression of ERK activity leads to a downregulation of Ets1 factor-dependent transcription, which further results in inhibition of CRH promoter activity, CRH transcription, and CRH release from the hypothalamus. The consecutive hyperactivity of the complete HPA axis in our SPRED2 KO mice reflects an elevated endogenous stress response becoming manifest by excessive grooming behavior and self-inflicted skin lesions on the one hand; on the other hand, in combination with elevated aldosterone synthase expression, this upregulated HPA hormone release explains hyperaldosteronism and the associated salt and water imbalances. Both hyperaldosteronism and polydipsia very likely contribute further to the observed kidney damage. Taken together, this study initially demonstrates that SPRED2 is essential for the appropriate regulation of HPA axis activity and of body homeostasis.

To further enlighten and compare consequences of SPRED2 deficiency in mice and particularly in humans, two follow-up studies investigating SPRED2 function especially in heart and brain, and a genetic screen to identify human SPRED2 loss-of-function mutations are already in progress.

Zusammenfassung 2

SPRED-Proteine sind Inhibitoren des hochkonservierten und in allen Geweben verbreiteten Ras/ERK/MAPK-Signalwegs, welcher Proliferation, Differenzierung und das Wachstum von Zellen reguliert. Um physiologische Konsequenzen der SPRED2-Defizienz im lebenden Modellorganismus aufzuklären, haben wir SPRED2-KO-Mäuse mithilfe der „gene trap“-Methode generiert. Eine erste Studie zur phänotypischen Charakterisierung mit KO-Mäusen bis zu einem Alter von fünf Monaten identifizierte SPRED2 als Regulator der Chondrozytendifferenzierung und des Knochenwachstums. So bewirkt der Verlust der SPRED2-Proteinfunktion eine erhöhte FGFR-vermittelte ERK-Aktivität, was wiederum einen Hypochondroplasie-ähnlichen Minderwuchs verursacht. Allerdings offenbarten Langzeitbeobachtungen älterer KO-Mäuse einen im Allgemeinen sehr schlechten Gesundheitszustand und weitere facettenreiche Symptome, darunter exzessives Putzverhalten mit schweren, selbst zugefügten Wunden, einen abnorm hohen täglichen Wasserkonsum, klare morphologische Anzeichen einer Nierenschädigung und eine reduzierte Überlebenswahrscheinlichkeit durch plötzlichen Tod. Ziel dieser Studie war es, basierend auf unseren Beobachtungen, einen Auslöser für diesen komplexen und vielseitigen Phänotyp zu finden.

Die beobachtete Nierendegeneration in unseren SPRED2-KO-Mäusen war auf eine Hydronephrose zurückzuführen, welche durch schwere Atrophie des Nierengewebes und Apoptose von Nierentubuluszellen gekennzeichnet war. Aufgrund des Nierenschadens haben wir Trinkverhalten und gängige Serumparameter analysiert. Trotz der Polydipsie, die sich durch eine nahezu verdoppelte tägliche Wasseraufnahme manifestierte, konnten signifikant erhöhte Na^+- und Cl^--Werte und die daraus resultierende Hyperosmolalität im Serum der SPRED2-KOs nicht kompensiert werden. Weil Salz- und Wasserhaushalt zum größten Teil unter der hormonellen Kontrolle von Aldosteron und ADH stehen, haben wir beide Hormonspiegel untersucht. Während die ADH-Werte im Serum von WT- und KO-Mäusen vergleichbar waren, insbesondere nach experimentellem Wasserentzug und einem extremen Verlust von Körperflüssigkeit, waren die Serumspiegel von Aldosteron in den SPRED2-KO-Mäusen verdoppelt. Die systematische Untersuchung übergeordneter regulatorischer Hormonachsen

ergab, dass sich der Hyperaldosteronismus unabhängig von einer erhöhten Aktivität des Renin-Angiotensin-Systems entwickelte, da die Serum-Ang II-Spiegel in den SPRED2-KOs etwa um die Hälfte reduziert waren. Die Expression der Aldosteronsynthase in der Nebenniere war jedoch wesentlich erhöht. Für Kortikosteron, das wie Aldosteron von der Nebennierenrinde freigesetzt wird, konnten wir ebenfalls mehr als doppelt so hohe Werte im Serum der KO-Tiere detektieren. Die Aldosteron-Produktion steht, ähnlich wie bei Kortikosteron, zumindest teilweise unter der Kontrolle des hypophysären Hormons ACTH, dessen Sekretion wiederum übergeordnet durch die Freisetzung von CRH aus dem Hypothalamus geregelt wird. Tatsächlich war die Stresshormon-Sekretion entlang dieser gesamten Hypothalamus-Hypophysen-Nebennierenrinden-Achse erhöht, da Serum-ACTH, das mittlere, hypophysäre Hormon, und hypothalamisches CRH, der übergeordnete hormonelle Induktor der HPA-Achse, in den SPRED2-KOs auch um 30% erhöht waren. Zusätzlich waren die ERK-Aktivität ebenso wie die CRH-mRNA-Spiegel im paraventrikulären Nukleus des Hypothalamus in unseren SPRED2-KO-Mäusen deutlich höher. *In vitro* Studien mit der Hypothalamus-Zelllinie mHypoE-44 zeigten weiterhin, dass sowohl SPRED1 als auch SPRED2 die Aktivität des CRH-Promotors, die CRH-Sekretion und die Ets-Faktor-abhängige CRH-Transkription reduzieren können. Passend dazu enthält die CRH-Promotorregion zahlreiche verschiedene Bindungsstellen für Transkriptionsfaktoren der Ets-Familie, speziell für Ets1.

Somit zeigt diese Studie zum ersten Mal, dass die durch SPRED2-vermittelte Hemmung der Ras/ERK/MAPK-Signalkaskade mittels Unterdrückung der ERK-Aktivität zu einer Herunterregulation der Ets1-Faktor-abhängigen Transkription führt, was eine Hemmung der CRH-Promotoraktivität, der CRH-Transkription und der CRH-Freisetzung aus dem Hypothalamus zur Folge hat. Die daraus resultierende Hyperaktivität der gesamten HPA-Achse in unseren SPRED2-KO-Mäusen spiegelt eine erhöhte endogene Stress-Reaktion wider und äußert sich durch übermäßiges Putzverhalten und durch selbst zugefügte Hautläsionen auf der einen Seite; auf der anderen Seite erklärt dies, in Kombination mit der erhöhten Aldosteronsynthase-Expression, den Hyperaldosteronismus und das damit verbundene Ungleichgewicht in Salz- und Wasserhaushalt. Weiterhin tragen sowohl Hyperaldosteronismus als auch Polydipsie sehr wahrscheinlich zu den beobachteten Nierenschädigungen bei.

Zusammengefasst ist diese Studie ein erster Hinweis, dass SPRED2 wesentlich an der adäquaten Regulation der HPA-Achsen-Aktivität beteiligt ist und essentiell ist für die Aufrechterhaltung der Homöostase im Körper.

Um die Folgen von SPRED2-Defizienz in Mäusen und vor allem im Menschen weiter aufzuklären und zu vergleichen, erforschen wir in zwei Folgeprojekten die Funktion von SPRED2 speziell im Gehirn und im Herzen und führen parallel ein genetisches Screening zur Identifikation von funktionellen SPRED2-Mutationen im Menschen durch.

Introduction 3

3.1. MAPK Signaling – Control of Proliferation and Growth

The mitogen-activated protein kinase (MAPK) cascades are evolutionary conserved pathways that respond to various extracellular signals in transmitting them to their intracellular targets. Within these cascades, the signal is propagated by phosphorylation and activation of sequential kinases, resulting in phosphorylation and activation of regulatory target proteins in cytoplasm and nucleus. Thereby, they control a large number of fundamental cellular processes including proliferation, differentiation, growth, motility, stress response, survival, and apoptosis (for review see (Plotnikov et al., 2011; Raman et al., 2007)). To date, four different mammalian MAPK cascades have been identified and named according to their corresponding MAPKs: extracellular signal-regulated kinase 1 and 2 (ERK1/2), c-Jun N-terminal kinase (JNK), p38, and ERK5. Other kinases like ERK3/4 and ERK7/8 indeed share sequence similarities with the typical MAPKs but show a different mode of activation, suggesting that they are not components of genuine MAPK cascades (Coulombe and Meloche, 2007).

3.1.1. The Ras/ERK/MAPK Pathway

The MAPK pathway first elucidated and until today considered as the “classical” MAPK cascade is the ERK1/2 pathway (Figure 1). In contrast to other MAPK pathways, its function mainly concentrates on the regulation of cell proliferation and differentiation (Seger and Krebs, 1995). It is preferentially activated in response to mitogens and growth factors (GFs), e.g. epidermal growth factor (EGF), fibroblast growth factor (FGF), vascular endothelial growth factor (VEGF), platelet-derived growth factor (PDGF), nerve growth factor (NGF), but also by cytokines like stem cell factor (SCF), interleukins (IL-3, IL5), and tumor necrosis factor α (TNF α). These various ligands bind to receptor tyrosine kinase (RTK) monomers, induce receptor dimerization

through monomer crosslinking and thereby the activation of the RTK. RTK monomers consist of an extracellular N-terminal region, a single hydrophobic transmembrane-spanning domain, and an intracellular C-terminal region (Ullrich and Schlessinger, 1990). The extracellular N-terminal region exhibits a variety of conserved elements, which are characteristic for each subfamily and of which the most occurring are immunoglobulin (Ig)-like domains and cysteine-rich regions (Ullrich and Schlessinger, 1990; van der Geer et al., 1994). It primarily contains the ligand binding site, and after extracellular ligand binding RTK activation is translated across the membrane into activation of intracellular domains. The intracellular C-terminal region comprises catalytic domains responsible for the kinase activity and thus catalyzes reciprocal autophosphorylation of RTK monomers on key tyrosine residues (Ullrich and Schlessinger, 1990). Via its Src (Sarcoma) homology 2 (SH2) domain, the adapter protein growth factor receptor-bound protein 2 (GRB2) binds to phosphotyrosine interaction modules of activated receptors (Lowenstein et al., 1992). Beyond direct interaction with tyrosine phosphorylated RTKs, GRB2 can also bind to intermediary adapter proteins, such as SHC (Src homology and collagen protein) (Skolnik et al., 1993), FRS2 (fibroblast growth factor receptor substrate 2) (Kouhara et al., 1997), IRS-1/2 (insulin receptor substrate 1/2) (Skolnik et al., 1993), GAB1 (GRB2-associated binding protein 1) (Holgado-Madruga et al., 1996), and SHP2 (Src homology 2 domain containing protein-tyrosine phosphatase 2, also PTPN11=Tyrosine-protein phosphatase non-receptor type 11) (Hadari et al., 1998). These adapters are associated with the receptor via SH2 or phosphotyrosine-binding (PTB) domains and are tyrosine phosphorylated upon binding.

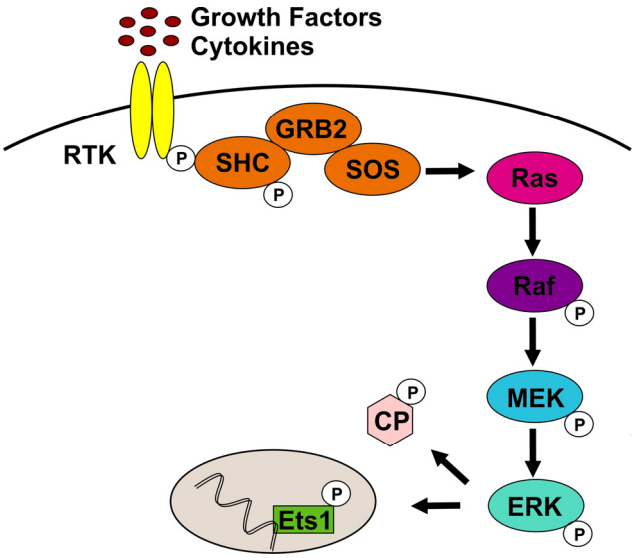

Figure 1: The Ras/ERK/MAPK Pathway - A Critical Regulator of Cell Proliferation, Differentiation and Growth
Stimulation of RTKs by GFs or cytokines results in the activation of the "classical" MAPKs ERK1 and ERK2. ERK further phosphorylates cytoplasmic and nuclear targets, which are able to regulate the transcription of target genes (CP = cytoplasmic proteins). *Figure based on (Bundschu, 2005).*

Via its Src homology 3 (SH3) domain, GRB2 also interacts with the proline-rich motif of SOS (son of sevenless) (Chardin et al., 1993). When the GRB2-SOS complex docks to tyrosine phosphorylated RTKs or adapter proteins at the cell membrane, SOS becomes activated. There, GRB2-SOS interacts with and activates Ras (rat sarcoma) (Egan et al., 1993). Ras comprises a family of small GTPases, which were identified as proto-oncogenes and of which H-Ras, N-Ras, and K-Ras are the most common family members (Malumbres and Barbacid, 2003). Ras contains an N-terminal G domain, which binds guanosine nucleotides, and a C-terminal CAAX box, which is lipid-modified and required for its plasma membrane targeting (Hancock et al., 1989; Temeles et al., 1985; Willumsen et al., 1984). SOS is a RasGEF (guanine nucleotide exchange factor) that activates Ras by catalyzing the exchange of bound GDP to GTP (Chardin et al., 1993). The activated GRB2-SOS complex binds exclusively to the inactive Ras-GDP-bound form, destabilizes the Ras-GDP binding, and promotes the dissociation of GDP from Ras. Because the cytosolic ratio of GTP is much higher than GDP (10:1), GTP associates with the GTPase, which results in the release of the GRB2-SOS complex and to the activation of Ras at the plasma membrane (Bos et al., 2007). Ras activates Raf (rapidly accelerated fibrosarcoma), the MAPKKK of the ERK pathway, which phosphorylates target kinases on serine and threonine kinase. The Raf family comprises three members, namely A-Raf, B-Raf, and C-Raf/Raf-1. Like Ras, Raf was identified as proto-oncogenic, whereas only B-Raf shows a high mutation rate in human cancers (Davies et al., 2002; Wellbrock et al., 2004). Raf kinases share a conserved domain structure containing an N-terminal regulatory domain and a C-terminal kinase domain (Wellbrock et al., 2004). Active Ras binds directly to the regulatory domain of Raf (Zhang et al., 1993) and thereby recruits the kinase to the plasma membrane, which is indispensable for its activation (Leevers et al., 1994; Stokoe et al., 1994). The phosphorylation and activation of Raf is Ras-independent and mediated by Src family protein-tyrosine kinases and other protein-serine/threonine kinases (King et al., 2001; Marais et al., 1995). Activated Raf catalyzes the activation of the MAPKKs MEK1 and MEK2 by phosphorylation on 2 serine residues (Kyriakis et al., 1992; Macdonald et al., 1993). MEK1/2 are dual specificity kinases that can act as both tyrosine and serine/threonine kinases. They are highly specific for their downstream components, the MAPKs ERK1 (also known as MAPK3 or p44 MAPK) and ERK2 (also known as MAPK1 or p42 MAPK) (Crews et al., 1992). ERK1/2 are activated by sequential phosphorylation of their regulatory tyrosine and threonine residues in the Thr-Glu-Tyr domain (Haystead et al., 1992). ERK, like Raf a serine/threonine kinase, further phosphorylates and activates more than 200 different substrates localized mainly in the nucleus but also in the cytoplasm or in other cellular organelles (Yao and Seger, 2009; Yoon and Seger, 2006). Among the cytosolic targets are kinases, phosphatases, cytoskeletal and signaling proteins, involved in processes like

translation, mitosis, and apoptosis. However, the main ERK1/2 targets are transcription factors and other transcriptional regulators (see list in (Yoon and Seger, 2006)). Target cytoplasmic proteins or transcription factors can be regulated directly by ERK but also by ERK-regulated MAPKAPKs (=Mitogen-activated protein kinase-activated protein kinases), such as ribosomal S6 kinases (RSKs), MAPK interacting kinases (MNKs), and mitogen and stress-activated kinases (MSKs). ERK, in order to phosphorylate and activate nuclear transcription factors, or transcription factors that have already been phosphorylated by ERK or ERK target kinases in the cytoplasm are translocated into the nucleus. Thus, nuclear ERK regulates a great variety of transcription factors, including c-Jun and c-Fos, which are part of the heterodimeric transcription factor AP-1 (activator protein 1), NF-κB (nuclear factor kappa-light-chain-enhancer of activated B cells), c-Myc (avian myelocytomatosis virus oncogene cellular homolog), and several family members of the Ets (E-twenty six) transcription factor family, especially Ets1 and Elk-1 (Chang et al., 2003). In this manner, ERK is involved in chromatin remodeling, in nuclear disintegration in mitosis, and in induction or suppression of transcription (Yao and Seger, 2009; Yoon and Seger, 2006).

3.1.2. Ras/ERK/MAPK Pathway Dysregulation – Causes of Cancer and Rasopathies

Ras/ERK/MAPK signaling has to be strictly regulated because upregulation of this pathway has been linked to malignant phenotypes including increased cell proliferation, migration, metastasis and invasiveness, defects in apoptosis, and the ability to induce neovascularization in tumors. Constitutive active mutants of Ras or B-Raf occur at a high frequency in almost all human cancers including pancreas, thyroid, lung, liver, kidney, bladder, breast, colorectal, gastric, and ovarian carcinoma, melanoma, seminoma, and leukaemia (Davies et al., 2002; Dhillon et al., 2007; Hilger et al., 2002; Malumbres and Barbacid, 2003; Montagut and Settleman, 2009). Thus, the activation of the Ras/ERK/MAPK pathway has to be strictly regulated because uncontrolled proliferation is a necessary step for the development of all cancers.

Overactivation of the Ras/ERK/MAPK pathway is also causative for a growing group of diseases bundled as “rasopathies”. They are mainly caused by constitutive active mutants of Ras or Raf, but also by mutations of other pathway components or regulators that lead to upregulation of Ras-dependent signaling. All rasopathy-syndromes profoundly impact the development of various tissues and exhibit overlapping phenotypical features including facial dysmorphologies, cardiac defects, cutaneous abnormalities, neurocognitive delay, and a predisposition to malignancies (Tidyman and Rauen, 2009).

A variety of drugs are able to target and inhibit selectively Ras/Raf/ERK pathway components, e.g. Ras farnesyl transferase, Raf, MEK, and tyrosine kinase inhibitors (Dhillon et al., 2007; Hilger et al., 2002; Montagut and Settleman, 2009). In healthy species, of course, the Ras/Raf/ERK pathway also exhibits intrinsic regulation mechanisms. As shown above, the pathway comprises a set of protein kinases that are activated one by one and thereby transmit signals from receptor to nucleus. The activity of these kinases is regulated by sequential phosphorylation, autoregulation, protein phosphatases, and negative feedback regulation by pathway components or by independent regulators induced by cascade activation.
Examples for such independent regulators are the SPRED proteins, which have been shown to potently inhibit the Ras/ERK/MAPK cascade in response to a wide range of mitogenic stimuli.

3.2. SPREDs – Inhibitors of the Ras/ERK/MAPK Pathway

The SPRED (**Spr**outy-related protein with **E**VH1 **d**omain) protein family was detected twelve years ago in a yeast two-hybrid screen by their interaction with the tyrosine kinase domain of c-Kit. Together with the structural related Sprouty proteins, SPREDs represent a family of MAPK signaling inhibitors (Wakioka et al., 2001).

3.2.1. SPRED Isoforms

SPRED has first been identified in *Drosophila melanogaster,* where it is expressed in photoreceptor cells. The *Drosophila* orthologue AE33 therefore seems to play a role in the differentiation of photoreceptor cells during the development of the *Drosophila* eye (DeMille et al., 1996; Freeman et al., 1992; Treisman and Rubin, 1996). SPREDs seem to be ubiquitously expressed in most animal species, and besides the *Drosophila* AE33, two *Xenopus tropicalis*, three murine, and three human SPREDs have been described (Kato et al., 2003; Sivak et al., 2005; Wakioka et al., 2001). In mammalians, all three *Spred* genes are located on different chromosomes: In mice, *Spred1* is located on 2E5 and in humans on 15q14, *Spred2* on 11A3 and on 2p14, and *Spred3* on 7B1 and 19q13, respectively ((Kato et al., 2003) and ENSEMBL database). Thus, in mice and men, the SPRED family consists of three members, namely SPRED1, SPRED2, and SPRED3. There is also first evidence for existing splice variants, e.g. Eve-3 (EVH1 enhanced), a splice variant of human SPRED3 (King et al., 2006).

3.2.2. SPRED Domain Structure and Functions

SPRED family members show a characteristic domain structure consisting of an N-terminal **E**nabled (Ena)/**V**asodilator-stimulated phosphoprotein (VASP) **h**omology **1** (EVH1) domain, a central c-**K**it **b**inding **d**omain (KBD), and a C-terminal **Spr**outy-related (SPR) domain (Figure 2) (Kato et al., 2003; Wakioka et al., 2001). SPRED3 lacks a functional KBD (Kato et al., 2003), and its splice variant Eve-3 consists of merely a single EVH1 domain (King et al., 2006).

The *Spred2* mouse gene contains 1233 protein-coding nucleotides and the corresponding protein has a calculated molecular mass of 46 kDa. It comprises six exons, of which exons 1-3 encode the EVH1 domain, exons 4 and 5 encode the region between EVH1 domian and KBD, and exon 6 encodes the KBD and the SPR domain (Figure 2) (ENSEMBL Transcript ID: ENSMUST00000093298). The genomic structure of murine *Spred1* (1335 bp coding sequence/49 kDa) is very similar, but it contains one more exon than *Spred2,* which encodes a part of the EVH1/KBD interregion (ENSEMBL Transcript ID: ENSMUST00000028829) (Bundschu, 2005; Bundschu et al., 2005). With six exons, *Spred3* (1227 bp coding sequence/45 kDa) has a similar genomic arrangement like *Spred2* but lacks a functional KBD domain due to the replacement of a critical arginine by a glycin (ENSEMBL Transcript ID: ENSMUST000000489239) (Kato et al., 2003).

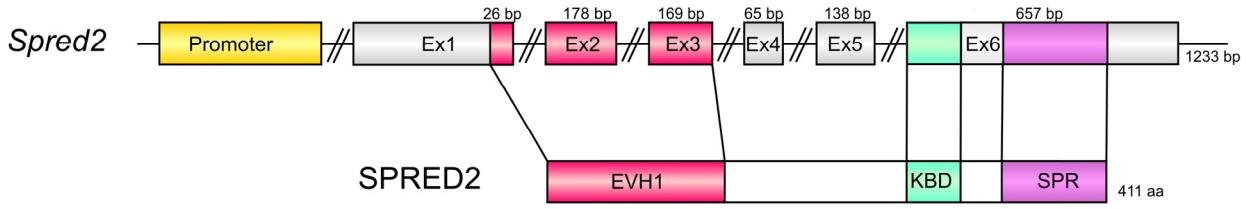

Figure 2: SPRED2 Protein Structure and its Corresponding Genomic Exon/Intron Organization
Exons (Ex) 1, 2, and 3 of *Spred2* are coding for the EVH1 domain, exons 4 and 5 for the middle part, and exon 6 for both the KBD and the SPR domain. Numbers above the exons represent the 1233 protein-coding nucleotides of the *Spred2* cDNA, which are translated into the 411 amino acid-containing SPRED2 protein. *Figure based on (Bundschu, 2005).*

3.2.2.1 The EVH1 Domain

The EVH1 domain is an evolutionary conserved protein domain containing about 115 amino acids. It represents a protein interaction module, which recognizes and binds specifically to proline-rich sequences (Ball et al., 2002; Niebuhr et al., 1997). To date, four classes of proteins that contain EVH1 domains have been identified, namely the Ena/VASP proteins, the Homer/Vesl proteins, the Wiskott-Aldrich syndrome proteins (WASP), and the SPRED proteins.

Their common EVH1 domain is implicated e.g. in the regulation and remodeling of the actin cytoskeleton and cell motility (Gertler et al., 1996; Reinhard et al., 2001; Reinhard et al., 1995; Reinhard et al., 1996; Renfranz and Beckerle, 2002; Samarin et al., 2003), in axonal guidance (Menzies et al., 2004), in synaptic signal transduction (Sala et al., 2001; Xiao et al., 2000), and in cell proliferation and differentiation (Bundschu et al., 2006b, 2007). High-resolution structures of the EVH1 domains of all four protein classes were solved (Ball et al., 2002; Callebaut et al., 1998). However, the EVH1 domain of SPREDs shows a narrower peptide-binding groove indicating that it binds to less proline-rich sequences as compared to its related domains (Harmer et al., 2005; Zimmermann et al., 2004). Indeed, NBR1 (neighbor of BRCA1=breast cancer1) and NF1 (neurofibromin1), the only two identified proteins that interact with SPRED by binding to the EVH1 domain; show no canonical proline-rich binding sequences in their critical SPRED-interacting regions (Mardakheh et al., 2009; Stowe et al., 2012).

The EVH1 domain has shown to be essential for SPRED protein function because N-terminal deletion mutants of SPRED1 and SPRED2 lost their ability to suppress ERK phosphorylation in response to different stimuli (King et al., 2005; Stowe et al., 2012; Wakioka et al., 2001). *Vice versa*, Eve-3 harboring exclusively the EVH1 domain is fully potent in inhibiting GF-induced MAPK signaling and cell cycle progression (King et al., 2006). Exceptionally, ΔN-SPRED2 is still functional in the suppression of hematopoietic cell differentiation in aorta-gonad-mesonephro-cultures (Nobuhisa et al., 2004) indicating a differential regulation of EVH1 function in the different SPRED isoforms, which is dependent on the cellular and mechanistic background.

3.2.2.2 The c-Kit Binding Domain

The KBD represents a binding sequence for the oncogenic receptor tyrosine kinase c-Kit located in the central region of SPRED1 and SPRED2, and comprises approximately 50 amino acids. It is not related to any previously identified tyrosine kinase interaction domain such as SH2, PTB, or c-Met binding domain (Wakioka et al., 2001). The KBD seems to be involved but not essential for SPRED protein function. Thus, SPRED3 lacking the KBD as well as ΔKBD-SPRED1 mutants are still able to suppress GF-induced ERK phosphorylation, although inhibitory potential is reduced (Kato et al., 2003; Nonami et al., 2004; Wakioka et al., 2001).

3.2.2.3. The Sprouty Domain

SPREDs contain a highly-conserved cysteine-rich Sprouty-related domain at their C-terminus consisting of about 110 amino acids. As the name implies, this SPR domain is homologous to the C-terminus of Sprouty proteins comprising a family of four homologous mammalian

members (de Maximy et al., 1999). Both in *Drosophila* and in vertebrates, Sproutys, similar to SPREDs, have been described as negative regulators of MAPK signaling downstream of a variety of RTKs (Casci et al., 1999; Hacohen et al., 1998; Kim and Bar-Sagi, 2004; Kramer et al., 1999; Reich et al., 1999).

In SPRED2, the SPR domain is essential and sufficient for MAPK pathway inhibition (King et al., 2005; Nobuhisa et al., 2004; Sasaki et al., 2003), whereas in SPRED1 it is not required to inhibit ERK phosphorylation in response to various stimuli (King et al., 2005). ΔC-SPRED2 has been shown to fail to inhibit Ras/ERK/MAPK signaling and to even enhance it by exerting a dominant negative effect on SPRED function (King et al., 2005). Although ΔC-SPRED1 seems to retain the inhibitory potential (King et al., 2005), contrarily a dominant negative effect on MAPK activation has also been published (Nonami et al., 2004; Wakioka et al., 2001).

Endogenous and functional SPRED is localized in vesicle-like structures (Engelhardt et al., 2004; Mardakheh et al., 2009; Phoenix and Temple, 2010) at the plasma membrane, where it exerts its inhibitory effect on possible MAPK pathway targets, like Ras or Raf, which are also recruited to the membrane upon activation (King et al., 2005; Wakioka et al., 2001). However, ΔC-SPREDs localize either in the cytoplasm (Kato et al., 2003; Stowe et al., 2012; Wakioka et al., 2001) or in the nucleus (Mardakheh et al., 2009). Therefore, according to Sproutys, the SPR domain is essential for the membrane anchoring of SPREDs and targets them to phosphatidylinositol 4,5-bisphosphate in plasma membranes upon MAPK pathway stimulation (Kato et al., 2003; Lim et al., 2002; Wakioka et al., 2001). Additionally, SPRED1 and SPRED2 are able to form stable heterodimers mediated exclusively by their SPR domains (King et al., 2005).

Taken together, the biochemical inhibitory function of SPREDs on the Ras/ERK/MAPK pathway is thought to reside mainly in the EVH1 domain, whereas the SPR domain mostly mediates the protein localization to cell membranes and the association with interaction partners, all required for appropriate protein function.

3.2.3. SPRED Expression Patterns and Localizations

To date, SPRED expression has been investigated well in humans, rats, and mice by monitoring endogenous *Spred* promoter activity and by visualizing expression on RNA and protein levels (Figure 3). Investigation of especially *Spred2* promoter activity was enabled using SPRED2 knockout (KO) mice generated by an insertion of a gene trap vector-encoded reporter gene into the *Spred2 gene* (Figure 12) (Bundschu et al., 2006a; Ullrich and Schuh, 2009). During mouse embryongenesis from day E7.5 to E13.5 the endogenous *Spred2* promoter was highly active in ectodermal and mesodermal tissues in early stages and later in developing

neural tissues, heart, lung, intestine, urogenital tract, and limbs (Figure 3 A) (Tuduce et al., 2010). In newborn and adult SPRED2 KO mice, *Spred2* promoter activity was nearly congruent and similarly ubiquitous compared to the embryos. The highest activity was detected in various parts of the brain, in the telencephalon especially in frontoparietal cortex and hippocampus, and in the cerebellum mostly in cortex and Purkinje cells. A comparable highly activated promoter was also seen in other neural tissues like spinal cord and spinal nerves. A strong activity was observed in glands like salivary gland, prostate and mucus epithelial glands in stomach and colon, in the kidney, especially in the cortex, and in vascular, intestinal, and uterine smooth muscle cells. Weaker activity was detected in heart, lung, liver, bones, and testis and almost no activity was seen in skeletal muscle and spleen (Bundschu et al., 2006a).

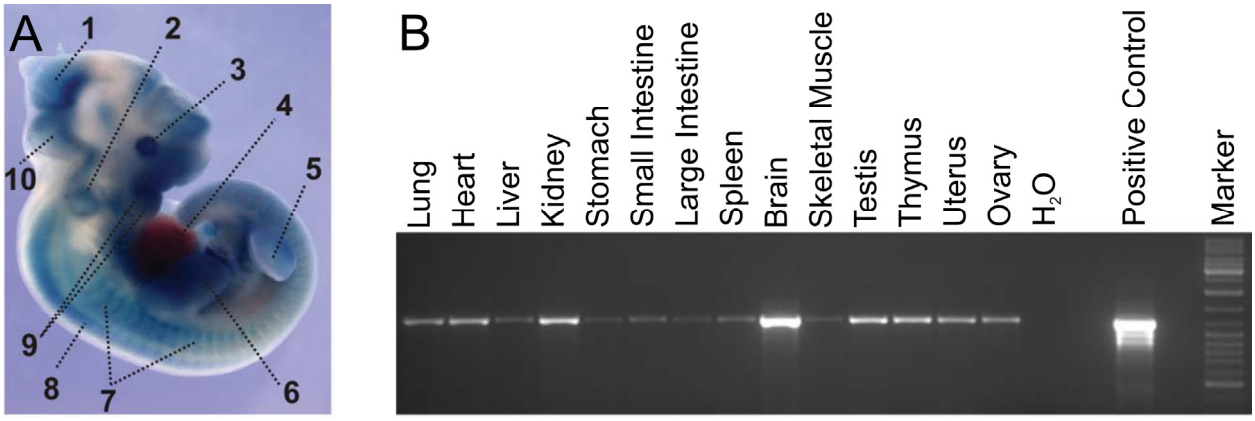

Figure 3: Ubiquitous *Spred2* Promoter Activity and SPRED2 Expression in Embryonic and Adult Mice
A) Lateral right view of an X-Gal-stained whole mount SPRED2 HET embryo at day E11.5 demonstrating *Spred2* promoter activity by blue staining. 1: Mesencephalon, 2: otic vesicle, 3: optic vesicle, 4: liver, 5: hindlimb bud, 6: forelimb bud, 7: somites, 8: neuroepithelium of neural tube, 9: maxillar and mandibular component of first branchial arch, 10: rhombencephalon. *Figure in part reproduced from (Tuduce et al., 2010) with permission from Wiley*. **B)** RT-PCR of different tissues of adult mice showing widespread SPRED2 expression on mRNA level. *Figure in part reprinted from (Engelhardt et al., 2004) with permission from Spriger.*

Determination of *Spred2* RNA levels by RT-PCR (Figure 3 B) and Northern blot, and of SPRED2 protein levels by Western blot again confirmed the ubiquitous expression pattern of SPRED2 in mainly brain, glands, and kidney (Engelhardt et al., 2004; Kato et al., 2003). In contrast to the ubiquitous SPRED2 expression, murine SPRED1 expression has predominantly been detected in brain tissues, and SPRED3 expression exclusively in brain, as shown by RT-PCR, Northern blot, and Western blot (Engelhardt et al., 2004; Kato et al., 2003).
In situ hybridisation of fetal rat tissue demonstrated a similar SPRED1 and SPRED2 expression in rat with high levels of RNA transcripts in brain, spinal cord, lung, heart, intestine, and skin (Hashimoto et al., 2002).

Immunohistochemistry with human tissue revealed high SPRED2 protein levels in glandular tissues like salivary glands, prostate, and sweat glands, which is consistent with high glandular expression also seen in mice. There, SPRED2 especially localized in vesicle-like granules indicated by colocalization with specific endosome markers (Engelhardt et al., 2004).
Taken together, SPRED2 shows a widespread expression pattern in men and mice, with varying intensity depending on the regarded tissue but present from early embryonic stages up to adulthood.

3.2.4. SPREDs and Suppression of Ras/ERK/MAPK Signaling

SPREDs suppress Ras/ERK/MAPK pathway activity downstream of multiple RTKs (e.g. FGFR, EGFR, VEGFR, PDGFR, NGFR) in response to a wide range of mitogenic stimuli like different growth factors (e.g. FGF, EGF, VEGF, PDGF, NGF, HGF, SCF), serum, cytokines (e.g. ILs), and chemokines (Bundschu et al., 2005; Inoue et al., 2005; Kato et al., 2003; King et al., 2005; Miyoshi et al., 2004; Nobuhisa et al., 2004; Nonami et al., 2004; Nonami et al., 2005; Sasaki et al., 2003; Sasaki et al., 2001; Sivak et al., 2005; Wakioka et al., 2001), for review see (Bundschu et al., 2007). The inhibitory effect is mediated by interaction with defined pathway components at different positions of the Ras/ERK/MAPK pathway.
Caveolin1, not a direct participating component in the Ras/ERK/MAPK pathway but a designated regulator of signal transduction, is localized in caveolae. In these lipid-rich invaginations of the plasma membrane it associates with SPRED1 and other pathway components like EGFR (Couet et al., 1997) or Ras (Song et al., 1996). The interaction of Caveolin1 with the SPR domain of SPRED1 increases the inhibitory effect of SPRED1 on ERK phosphorylation; however, the underlying mechanism remains to be shown (Nonami et al., 2005).
Under unstimulated conditions, SPREDs seem to be constitutively associated with RTKs. Thus, via the SPR domain, SPRED1 is bound to FGFR-like 1 (FGFRL1) (Zhuang et al., 2011), and SPRED2 to EGFR from where it dissociates upon EGF stimulation in order to exert its suppressive effect (Meng et al., 2012). The RTKs itself can be a target of SPREDs inhibitory function because EVH1 domain–mediated interaction of SPRED2 with NBR1 induces lysosomal degradation of the FGFR, thus silencing FGF-dependent ERK activation (Mardakheh et al., 2009).
Via the conserved Raf-binding motif (RBM) within the SPR domain, SPREDs as well as Sproutys are able to interact with the C-terminal catalytical domain of Raf1 (Sasaki et al., 2003). The small GTPase Ras (Wakioka et al., 2001) acting upstream of Raf kinase in the MAPK pathway also binds to SPREDs, but the binding sites have yet to be identified. Accordingly, one

possible SPRED target has been shown to be located between Ras and Raf (Figure 4). SPRED is able to interact with Ras in the Ras-Raf complex, but does not prevent the activation of Ras. However, although Ras is still capable of recruiting Raf to the membrane, Raf is thought to be not accessible to its kinase when SPRED is bound to the Ras-Raf complex (Wakioka et al., 2001). SPRED has further been shown to decrease Ras-GTP levels, possibly by inhibiting RasGEF or enhancing RasGAP activity, and thus the second identified SPRED target lies upstream of Ras (King et al., 2005) (Figure 4). Indeed, SPREDs have been shown to interact with the RasGAP NF1 via their EVH1 domain. SPRED1 enables and enhances the RasGAP activity of NF1 by recruiting it to the plasma membrane, where it accelerates the hydrolysis of active Ras-GTP to the inactive Ras-GDP form (Stowe et al., 2012).

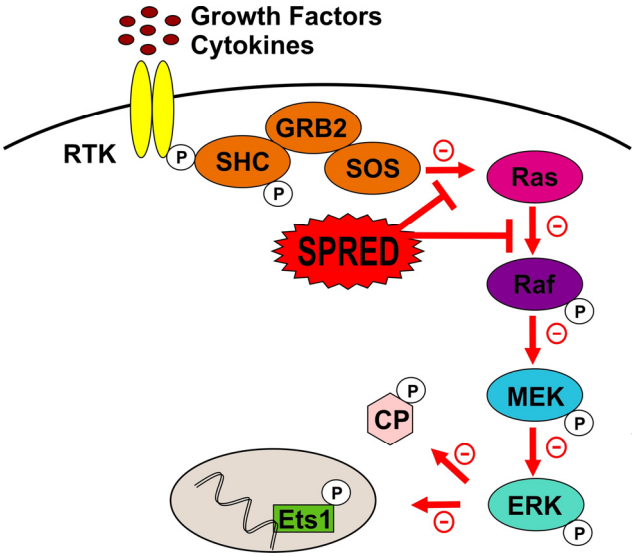

Figure 4: SPREDs – Inhibitors of the Ras/ERK/MAPK Cascade
SPREDs suppress Ras/ERK/MAPK signaling at different sites of action. Possible SPRED targets have been described to be located upstream of Raf or between Ras and Raf (CP = cytoplasmic proteins). *Figure based on (Bundschu, 2005).*

In sum, point and mechanism of Ras/ERK/MAPK pathway regulation by SPREDs seems to be variable dependent on cell type, tissue or developmental process to be regulated. According to current knowledge, SPREDs do not affect other cellular pathways like e.g. JAK–STAT, PLC, JNK, and p38MAPK pathways. Thus, the suppressive effect of SPREDs seems to be exclusively restricted to Ras/Raf/ERK signaling (King et al., 2006; King et al., 2005; Miyoshi et al., 2004; Nobuhisa et al., 2004; Nonami et al., 2004; Sivak et al., 2005; Wakioka et al., 2001).

3.2.5. Regulation of SPRED-mediated Ras/ERK/MAPK Pathway Inhibition

Protein expression, activity, and function can be regulated by pretranslational or posttranslational processes. Pretranslational alternative splicing takes place within the SPRED

family and has been demonstrated by Eve-3, a liver specific splice variant of SPRED3. The functional EVH1 domain conserves its inhibitory effect on MAPK signaling, whilst the loss of the SPR domain causes an altered localization pattern in cytoplasmic punctae rather than at the cell membrane (King et al., 2006). Besides Eve-3, a variety of further splice mutants may exist (see ENSEMBL database and (Ullrich et al., 2011)).

SPRED expression can also be regulated pretranslationally by microRNAs (miRs), short non-coding RNAs that function as negative regulators of gene expression. Thus, SPREDs and their inhibitory function on Ras/ERK/MAPK signaling is downregulated by miRs like miR-126 (Fish et al., 2008; Wang et al., 2008), miR-221, and miR-485-3p (Liu et al., 2012).

Among the posttranslational modifications, phosphorylation and ubiquitination have been shown to be critical for SPRED regulation. Murine SPRED1 and 2 are tyrosine phosphorylated in response to stimulation by various growth factors (Wakioka et al., 2001). c-Kit may be critical for SCF-induced tyrosine phosphorylation because the KBD is required and because SPRED3 without a functional KBD can not be tyrosine phosphorylated (Kato et al., 2003; Nonami et al., 2004; Wakioka et al., 2001). Two recent studies identified defined tyrosine phosphorylation sites in murine SPREDs, which are critical for their inhibitory effect. Thus, Y377 and Y420 in the SPR domain of mouse SPRED1 and 2 have to be phosphorylated for mediating Ras/ERK/MAPK pathway suppression. *Vice versa*, interaction of the protein tyrosine phosphatase SHP2 with the EVH1/KBD interregion of SPRED1 and 2 causes dephosphorylation of Y420, hence attenuating SPRED-mediated pathway inhibition (Quintanar-Audelo et al., 2011). Similarly, phosphorylation of Y303, Y343, and Y353 within SPR of SPRED2 seems to trigger its dissociation from the EGFR upon EGF stimulation and is essential for the interaction of SPRED2 with the p85 subunit of phosphatidylinositol 3 kinase. This interaction in turn is thought to enhance the SPRED2-mediated inhibitory effect via increased Ras binding to SPRED2 and to decrease SPRED2 ubiquitination (Meng et al., 2012). In humans, comparable tyrosine phosphorylation required for the inhibitory effect of SPREDs could not yet be detected; however, phosphorylation of serine and threonine residues has been demonstrated in human SPREDs (King et al., 2005).

Ubiquitination is a posttranslational enzymatic process, by which ubiquitin is ligated to a target protein and thus labels it for degradation. It can also be regulated by phosphorylation, whereas phosphorylation of the above mentioned Y303, Y343, and Y353 in SPR domain of SPRED2 seems to prevent SPRED degradation (Meng et al., 2012). However, phosphorylation of Y228 and/or Y231 in the c-Kit binding domain of SPRED2 is required for the interaction with Cbl (Casitas B-lineage lymphoma) E3 ubiquitin ligase and thus enhances SPRED ubiquitination (Lock et al., 2006).

In sum, a combination of differential splicing, miRs, phosphorylation, and ubiquitination enables a fine tuning of SPRED functions and expression levels.

3.2.6. SPRED Functions in Mice and Men

SPRED proteins are inhibitors of Ras/ERK/MAPK signaling, a pathway that regulates cell proliferation and differentiation in a tremendous variety of cell types, from unicellular eukaryotes over fungi and plants up to all animals, from early development up to old age. ERK is activated by multiple RTKs in response to an even greater diversity of ligands and itself activates an immense amount of nuclear and cytoplasmic target proteins. Due to their involvement in this highly conserved and ubiquitous pathway, SPREDs play a role in a great variety of developmental processes.

3.2.6.1. *In vitro* Studies and Mouse Models

To date, five different mouse models are available to study *Spred1* and *Spred2* gene function: First, one SPRED1 (Denayer et al., 2008; Inoue et al., 2005; Nonami et al., 2004) and one SPRED2 KO mouse model (Nobuhisa et al., 2004; Wakabayashi et al., 2012) both backcrossed to C57BL/6 background and generated by a Japanese group. Second, one knockdown mouse line for SPRED1 (Phoenix and Temple, 2010). Third, the SPRED2 KO mouse model generated by us and kept on a mixed C57BL/6 x 129P2/OlaHsd background (Bundschu et al., 2005; Ullrich et al., 2011).

Hematopoiesis

The first function that has been described for SPREDs is its role as a regulator of hematopoiesis. In mouse embryos, SPRED2 is expressed in the AGM (aorta-gonad-mesonephros) region, a primary site of embryonic hematopoiesis. In SPRED2 KO mice the production of $CD45^+$ hematopoietic stem cells and colony formation is upregulated compared to WT controls. Accordingly, overexpression of SPRED2 significantly reduces ERK phosphorylation and the number of $CD45^+$ cells in an AGM culture (Nobuhisa et al., 2004).

SPRED1 is highly expressed in mature hematopoietic cells. Thus, in different IL-3-dependent hematopoietic cell lines, overexpression of SPRED1 reduces ERK activation, cell proliferation and colony formation. *Vice versa*, in bone marrow-derived mast cells of adult SPRED1-deficient mice, Ras/ERK/MAPK signaling and proliferation was augmented (Nonami et al., 2004). In an allergic asthma model, adult SPRED KO mice develop airway eosinophilia and hyperresponsiveness, indicating that SPRED1 also downregulates IL-5-induced Ras/ERK/MAPK pathway activation required for eosinophil production (Inoue et al., 2005). Taken together, due to their suppressive effect on ERK-dependent cell proliferation and

differentiation, SPRED2 negatively regulates embryonic hematopoiesis, while SPRED1 rather regulates late-phase hematopoiesis by inhibiting hematopoietic cytokine signaling.

Angiogenesis and Lymphangiogenesis

Angiogenesis is mainly regulated by GFs like FGF and VEGF, which stimulate MAPK pathways that mediate the generation of new vessels by inducing escape of endothelial cells from their original blood vessel, proliferation, and sprouting. Recently, miRNAs have been identified as novel pretranslational regulators of angiogenesis (Suarez and Sessa, 2009). SPRED1 was shown to be a target of the miR-126, expressed specifically in endothelial cells and regulating VEGF-mediated angiogenesis by repression of target genes. miR-126 deficiency in mice (Wang et al., 2008) and knockdown in zebrafish (Fish et al., 2008) resulted in loss of vascular integrity, hemorrhage, and partial embryonic lethality. Both studies demonstrate that ablation of miR-126 normally repressing SPRED1 expression leads to a decrease in ERK signaling in response to VEGF. Thus, the resulting impaired endothelial cell proliferation, migration, and angiogenesis is a consequence of forced SPRED1-mediated inhibition of angiogenic signaling (Fish et al., 2008; Wang et al., 2008).

Lymphangiogenesis is mediated in part also by VEGF/ERK-dependent signaling and regulates the growth of lymphatic vessels form pre-existing vessels. SPRED1 and SPRED2 seem to play an important role in lymphangiogenesis because their deficiency in mice results in embryonic lethality due to severe subcutaneous hemorrhage, edema, and dilated lymphatic vessels filled with erythrocytes. These SPRED1/2-double KO mice show increased numbers of lymphatic vessels and resemble mouse models defective in the separation of lymphatic vessels from blood vessels. Because VEGF-C-mediated ERK activation was enhanced in SPRED1/2-double KO embryos, SPREDs seem to be inhibitors of VEGF-induced lymphatic endothelial cell proliferation (Taniguchi et al., 2007).

Brain Development and Learning

All SPRED proteins show a high expression pattern in brain and spinal cord, which is indicative for their functional requirement there. Indeed, in fetal mouse brain, SPRED1 was shown to be highly enriched in central nervous system (CNS) germinal zones during neurogenesis, especially in the ventricular and subventricular zone of the cortex, where neural progenitor cells (NPC) reside. Knockdown of SPRED1 *in vitro* in embryonic cortical cells revealed increased ERK phosphorylation, elevated self-renewal, and proliferation in NPCs. *In vivo* knockdown of SPRED1 in mouse embryos also leads to an increase in NPC proliferation and periventricular heterotopia, a developmental abnormality characterized by a mislocalization of cell masses in or next to the subventricular zone due to abnormal neuronal migration. Thus, SPRED is critical for

normal cortical development and, by controlling MAPK/ERK-dependent NPC proliferation, helps to maintain the integrity of germinal zones (Phoenix and Temple, 2010).

Besides their role in brain development, SPREDs are also critical for proper brain function. Behavioral characterization of a SPRED1 KO mouse line revealed unaltered neuromotor performance and normal sensory perception to visual, auditory, or pain stimuli but an impaired spatial and visual learning and memory. In this manner, the ability to find and remember the position of a dry platform in a swimming pool (Morris water maze) or to discriminate between black and white colored doors and remember the color of the door with a reward behind in a T-shaped land maze (T-maze) was impaired in SPRED1 KO mice. Moreover, electrophysiological recordings on hippocampal slices revealed reduced excitatory postsynaptic potentials (EPSPs) and defects in short and long term synaptic plasticity, both underlining the observed deficits in hippocampus-dependent learning and memory formation. These deficits seem to be related to hyperactivation of the Ras/ERK/MAPK pathway because after induction of long term potentiation, ERK phosphorylation was increased in brain slices of SPRED1 KO mice (Denayer et al., 2008).

DYRK1A (dual specificity tyrosine-phosphorylation-regulated kinase 1A), a kinase thought to play a role in Down syndrome, shows overlapping expression patterns with SPREDs in the brain and has been identified as a new SPRED1/2 binding partner. The interaction of SPREDs via their SPR domain with the kinase domain of DYRK1A prevents it from phosphorylating its targets like STAT3 and Tau. By competing with DYRK1A substrates for binding and without affecting its kinase activity, SPREDs are able to inhibit DYRK1A-mediated cell proliferation and, as DYRK1A regulators, may impact Down syndrome development (Li et al., 2010).

Embryonic Development and Growth

FGF/FGFR signaling plays a critical role in embryonic development including mesoderm induction, anterior-posterior patterning, neural induction, and limb development. SPREDs are highly expressed already during embryonic development especially in ectodermal and mesodermal tissues (Tuduce et al., 2010) and are critical regulators of FGF-dependent cell proliferation. During gastrulation of *Xenopus tropicalis*, *Xt*SPREDs inhibit mesoderm specification by inhibiting FGF-dependent MAPK activation (Sivak et al., 2005). In the pancreas mesenchyme of the embryonic mouse, SPRED1 expression is stimulated by FGF-9 signaling (Sylvestersen et al., 2011). In the lung mesenchyme of embryonic rats, SPREDs are also coexpressed with FGF-9 and-10 and seem to be essential for normal lung branching (Hashimoto et al., 2002). Hepatospecific Eve-3 regulates the regenerative capacity, growth, and mass of the mature liver by suppressing ERK/MAPK singnaling (King et al., 2006).

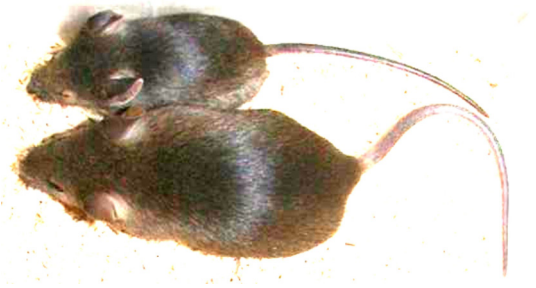

Figure 5: SPRED2 Deficiency in Mice Causes Dwarfism
SPRED2 KO mice have a short stature and decreased long bone growth already from birth on, which is similar to hypochondroplasia in humans.

FGFR pathways are also critical regulators of bone development, especially FGFR3-mediated signaling, which suppresses long bone growth. Thus, FGFR3 gain-of-function mutations leading to increased ERK/MAPK signaling result in dwarfism. Accordingly, SPRED2 deficiency in mice provoked hypochondroplasia-like dwarfism (Figure 5) associated with reduced growth and body weight, shortened bones, and narrowed growth plates. Because FGF-stimulated chondrocytes of SPRED2 KO mice showed earlier and augmented ERK phosphorylation, SPRED2 regulates long bone growth by suppression of FGF-dependent ERK activation (Bundschu et al., 2005).

Cytoskeleton and Vesicular Trafficking

MAPK signaling is not only a critical regulator of cell proliferation and differentiation but also impacts cell motility. Similar to the related VASP, SPREDs have been shown to play a role in the reorganization of the actin cytoskeleton. SPREDs are able to directly interact with RhoA (Ras homolog gene family, member A) and to inhibit Rho-mediated ROCK (Rho-associated protein kinase) activation, actin stress fiber formation, and cell migration (Miyoshi et al., 2004). A second SPRED target in the RhoA/ROCK pathway is TESK1 (testis-specific protein kinase 1), a downstream target of ROCK that modulates actin reorganization via phosphorylation of cofilin. While unphosphorylated and active cofilin induces disassembly of actin filaments, phosphorylated and inactive cofilin induces stress fiber formation. SPRED1 inhibits TESK1 by SPR domain-dependent interaction and prevents TESK1 to phosphorylate cofilin. The resulting stress fiber breakdown renders the actin network dynamic (Johne et al., 2008).

Via its SPR domain, SPRED1 has further been shown to interact with MARKK (microtubule affinity-regulating kinase-activating kinase), which causes the breakdown of microtubules by phosphorylation and activation of downstream targets. However, the functional impact of this interaction has yet to be identified (Johne et al., 2008).

Associated with a putative role of SPREDs in microtubule dynamics, there are some first hints that SPREDs might play a role in microtubule-guided vesicular trafficking. SPRED2 colocalizes with NBR1 in cytoplasmic punctae representing late endosomes as identified by costaining with Ras-related protein (Rab) 7. Via interaction with SPRED2, NBR1 indirectly enhances SPREDs

inhibitory effect on ERK phosphorylation. SPRED2-NBR1 induces the targeting activated FGFRs to late endosomes for lysosomal degradation (Mardakheh et al., 2009). Similarly, the periventricular heterotopia characterized by CNS germinal zone disruption occurring in SPRED1 knockdown mice is reminiscent of mouse models harboring mutations of genes associated with vesicular trafficking (Phoenix and Temple, 2010).

Rab-GTPases regulate many steps of membrane traffic, including vesicle formation, vesicle movement, and membrane fusion. Colocalization of SPREDs has been demonstrated not only with the late endosome markers Rab7 (Mardakheh et al., 2009), but also with Rab5 and Rab11 in transfected HEK 293 T cells (Engelhardt et al., 2004) and in NPCs of mouse embryos (Phoenix and Temple, 2010). Whereas SPRED1 seems to extensively colocalize with early endosome marker Rab5, but to a lesser extent with the recycling endosome marker Rab11 (Phoenix and Temple, 2010), SPRED2 rather colocalizes with Rab11 than with Rab5 (Engelhardt et al., 2004).

Tumorigenesis and Metastasis

SPREDs, arising from their function as negative regulators of Ras/ERK/MAPK signaling, a main regulator of cell proliferation and differentiation, have a putative role in preventing the development of tumors and metastasis. In this manner, an *in vitro* study with Hela cells, in which large tumor suppressors (LATS) 1 and 2 were knocked down, show increased proliferation and migration associated with dysregulated expression of various oncogenes, hereunder SPRED1, which was downregulated (Visser and Yang, 2010). Similarly, in a tumorigenic murine keratinocyte cell line (PDV), endogenous SPRED2 expression was decreased compared with a non-tumorigenic control. However, stable expression of SPRED2 in these PDV cells suppresses transforming growth factor-β1 (TGF-β1)-induced ERK activation, urokinase type plasminogen activator (uPA) expression, epithelial mesenchymal transition, and cell migration, all contributing to tumor invasion and metastasis (Villar et al., 2010).

The anti-tumorigenic and anti-metastatic effect of SPREDs could also be confirmed by *in vivo* studies in different mouse models. In the highly metastatic mouse osteosarcoma cell line LM8*,* SPRED1 expression inhibits ERK activation, proliferation, and migration *in vitro*. Accordingly, in nude mice injected with LM8 cells overexpressing SPRED1, LM8 cell-mediated tumor growth and metastasis was suppressed (Miyoshi et al., 2004). SPRED1 overexpression also reduces tumorigenesis in a hepatocellular carcinoma (HCC) model in nude mice. Accordingly, in cultured HCC cells, overexpression of SPRED1 suppresses cell proliferation, ERK activation, cell motility, and the expression of matrix metalloproteinase (MMP) 2 and 9, which are required for extracellular matrix degradation and metastasis (Yoshida et al., 2006). The same effect on HCC was shown for SPRED2, both in HCC cultures and in a nude mouse model, with the additional

outcome that SPRED2 overexpression induces the activation of caspase-3 and apoptosis (Ma et al., 2011). Similarly, SPRED2 seems to have a tumor-suppressive effect on prostate cancer both *in vivo* and *in vitro* (Kachroo et al., 2013). Somewhat different, an immunological study with C57BL/6 mice injected with the murine colon adenocarcinoma cell line MC38 reveals TGF-β-induced impaired functionality of $CD8^+$ cytotoxic T cells in the tumor microenvironment. This is characterized by hyporesponsiveness to cytokines, downregulation of TCR pathway components, reduced T cell proliferation, and decreased ERK activation, which is in this case contributed by upregulation of SPRED1 expression in the cytotoxic T cells (di Bari et al., 2009).
SPRED expression levels seem to be further responsive to and coefficient with cancer pharmaceuticals. The anti-tumorgenic silibinin increases the expression of SPRED1/2 in a human hepatocellular carcinoma cell model (Hep G2) (Momeny et al., 2008). Furthermore, Imatinib, a common drug used for chronic myeloid leukemia (CML) treatment, promotes endogenous SPRED2 levels in the human CML cell line K562 (Liu et al., 2010).

3.2.6.2. First Lessons from Humans

Since the discovery of SPREDs and their identification as negative Ras/ERK/MAPK cascade regulators in 2001, there are now some clear indications of what a missing or altered SPRED expression causes in humans. While dysregulated human SPRED expression has been linked to the development of cancers, mutations in human SPRED1 leading to complete or partial deficiency are causative for rasopathies, a genetically related group of neuro-, cardio-, facio-, and cutaneous-developmental disorders.

Cancer

To date, only two studies investigating the impact of SPREDs in human cancer have been published. In tumors of human HCC patients, ERK phosphorylation was increased, while expression of SPRED1/2 was downregulated. Interestingly, in HCC patients with low SPRED expression levels, the incidence of tumor invasion and metastasis was higher than in patients with higher SPRED levels, indicating an inverse correlation between SPRED expression and tumorigenesis (Yoshida et al., 2006). In prostate cancer tumors, SPRED2 was also downregulated, while SPRED1 expression remained unchanged, indicating a unique role for SPRED2 in prostate cancer (Kachroo et al., 2013). Although SPRED mutations have not yet been shown to be causative for any kind of cancer, they are, due to the observed downregulation in cancers and due to their anti-proliferative effect, prognostic factors and potential targets for anti-cancer and anti-metastatic therapies.

Legius Syndrome

Just recently, Legius syndrome has been described as an autosomal dominant human disorder, which was detected due to its symptomatic similarity to neurofibromatosis type 1 (Brems et al., 2007). In a neurofibromatosis clinic, five families were identified at first, showing clinical features of neurofibromatosis type 1 but lacking any mutation in the neurofibromin gene NF1. A genome-wide linkeage scan revealed germline loss-of-function mutations in the *Spred1* gene in these patients (Brems et al., 2007). Legius syndrome and neurofibromatosis type 1 belong to the family of rasopathies, of which the most prominent are Costello syndrome, Noonan syndrome, LEOPARD syndrome, and cardio-facio-cutaneous syndrome. All these diseases show overlapping phenotypes, originating from germline mutations in genes encoding a component or a regulator of the Ras/ERK/MAPK pathway and leading to pathway upregulation (Tidyman and Rauen, 2009). While neurofibromatosis type 1 and Legius syndrome are caused by loss-of-function mutations of the pathway inhibitors NF1, a RasGAP (Cawthon et al., 1990; Viskochil et al., 1990; Wallace et al., 1990), and SPRED1 (Brems et al., 2007), respectively, the other rasopathies are caused by gain-of-function mutations of direct Ras/ERK pathway components like PTPN11/SHP2 (Digilio et al., 2002; Legius et al., 2002; Tartaglia et al., 2001), Sos (Roberts et al., 2007; Tartaglia et al., 2007), H-Ras (Aoki et al., 2005), K-Ras (Niihori et al., 2006; Schubbert et al., 2006), C-Raf (Pandit et al., 2007; Razzaque et al., 2007), B-Raf (Niihori et al., 2006; Rodriguez-Viciana et al., 2006), and MEK1/2 (Rodriguez-Viciana et al., 2006).

Until today, about 100 different *Spred1* mutations have been described in about 150 unrelated individuals (Brems et al., 2007; Brems et al., 2012; Denayer et al., 2011; Laycock-van Spyk et al., 2011; Messiaen et al., 2009; Muram-Zborovski et al., 2010; Pasmant et al., 2009b; Spencer et al., 2011; Spurlock et al., 2009; Stevenson et al., 1993). Most of the described mutations are point mutations, including nonsense, missense, and frameshift mutations, but also in-frame and whole gene deletions as well as intronic mutations have been reported. The mutations affect both the EVH1 and the SPR domain, and *in vitro* experiments with subcloned *in vivo* detected *Spred1* mutations revealed a reduced inhibitory effect on ERK activation regardless of the mutations domain localization (Brems et al., 2007). All known *Spred1* gene variants are collected in the public and regularly updated SPRED1 database of ARUP Laboratories and the University of Utah: http://www.arup.utah.edu/database/SPRED1/SPRED1_welcome.php (Sumner et al., 2011).

Legius syndrome in humans is characterized by cutaneous café au lait macules with or without axillary freckling, lipomas, learning disabilities, developmental delays, and macrocephaly (Brems et al., 2007; Brems et al., 2012). Very strikingly, SPRED1 KO mice also show learning disabilities (Denayer et al., 2008) and facial abnormalities (Inoue et al., 2005), and therefore reflect a demonstrable congruent phenotype with that of Legius syndrome patients. These

phenotypical features of Legius syndrome are also characteristic for neurofibromatosis type 1. The additional predisposition to malignancies like tumors of the peripheral and central nervous system (neurofibromas, astromas, optic pathway gliomas), Lisch nodules, and osseus lesions in neurofibromatosis type 1 is completely absent in Legius syndrome (Brems et al., 2007; Messiaen et al., 2009; Pasmant et al., 2009a). Hence, genetic testing to clearly distinguish between neurofibromatosis type 1 and the milder Legius syndrome is indispensable for proper disease diagnosis and prognosis. Mutational analysis of *Spred2* in Legius syndrome patients did not detect any mutations (Spurlock et al., 2009) and thus, a human correlate of SPRED2 deficiency remains to be identified.

3.3. The Mouse - A Research Model for Human Gene Function and Disease

The human and mouse genomes were fully sequenced at the beginning of the new millennium (Lander et al., 2001; Venter et al., 2001; Waterston et al., 2002). Now, one major challenge facing the scientific community is to elucidate the *in vivo* function of the 20,000-25,000 identified protein-coding genes. Large-scale generation of genetically modified *Drosophila*, *C. elegans*, *Xenopus*, and zebrafish organisms has been carried out for many years. Although these non-mammalian animals have provided indispensable insights into gene function, the mouse is considered to be the most valuable model to study mammalian gene function. A great advantage of the mouse is its genetic similarity with humans because human and murine genes are homologous to 99% (Lander et al., 2001; Venter et al., 2001; Waterston et al., 2002). But also mouse development, physiology, anatomy, behavior, and diseases have much in common with those of humans due to their common ancestry. Although the same is true for rats, most techniques for genetic manipulation that result in gene knockouts, knockins, or in conditional mutations depend on the ability to culture and manipulate embryonic stem (ES) cells. Whereas the mouse genome supports modifications in ES cells, it was not possible for a long time to generate ES cells from rats with the same potential to provide pluripotency, genetic manipulation, and germ line transmission like in mice. ES cells have been available from inbred mice since 1981 (Evans and Kaufman, 1981; Martin, 1981); however, the first equivalent rat ES cells have been generated much later (Buehr et al., 2008; Li et al., 2008). Therefore, manipulating techniques not requiring ES cells, e.g. the generation of transgenic models by microinjection of DNA into fertilized oocytes, are feasible in both rats and mice according to the

experimental intent. However, for global or conditional knockout or knockin approaches involving ES cell manipulation and culture, the mouse is still the model of choice.

3.3.1. Mutagenesis Strategies in Mice

The use of mice as a model organism to study human diseases and to identify therapeutic targets by mutating or knocking out genes has a more than 100 year old history. It started with the collection of naturally occurring and visible mouse mutants. The development of mouse genetics to a formalized science enabled a more systematic collection and analysis of spontaneous mutants like agouti (Bultman et al., 1992), reeler (D'Arcangelo et al., 1995), and obese (Zhang et al., 1994) and facilitated their mapping to the mutated genes. Because the frequency at which spontaneous mutations occur is very low (~5 x 10^{-6} per locus), the first X-ray mutagenesis experiments were carried out in the 1930s (Russell et al., 1958), followed by studies with chemical mutagens like chlorambucil (Russell et al., 1989) and N-Ethyl-N-nitrosourea (ENU) (Russell et al., 1979). Whereas the mutagenesis frequency induced by radiation or chemical mutagens is 20-300 times greater than that of spontaneous occurring mutants, both X-ray and chlorambucil mutagenesis can cause chromosomal rearrangements. Therefore, on the one hand, they provide a landmark for identifying and cloning the affected gene(s), but on the other hand, these methods mostly affect multiple genes and thus impede the dissection of individual gene function. In contrast, ENU is easily administrable, amenable to high throughput, and the generated mutations are primarily single gene mutations (point mutations or small deletions not exceeding 50 bp). Hovewer, it does not provide obvious molecular landmarks for cloning.

Since the late 1970s, insertional mutagenesis began to be hotly pursued in the mouse, and the possibility to directly introduce exogenous genetic material into the mouse embryo predates the widespread use of recombinant DNA techniques these days. In two independent studies, Rudolf Jaenisch et al. showed that viral DNA sequences can be integrated into the mouse genome both after microinjection into the blastocoel of mouse blastocysts and after viral infection of preimplantation mouse embryos, and that germline transmission is possible (Jaenisch, 1976; Jaenisch and Mintz, 1974). Shortly after, the first successful introduction of a cloned gene into the mouse genome was reported. Therefore, DNA was microinjected into the male pronucleus of a one-cell stage fertilized embryo, which was reimplantated into foster mothers (Gordon et al., 1980). In 1981, several groups were not only successful in introducing cloned genes by this technique, but also in germline transmission of these genes. Thus, the first transgenic mice were generated (Brinster et al., 1981; Costantini and Lacy, 1981; Gordon and Ruddle, 1981; Harbers et al., 1981; Wagner et al., 1981a; Wagner et al., 1981b). Transgenic mice mainly

represent gain-of-function mutations. Their most common use is on the one hand the study of tissue- and developmental-specific gene regulation, on the other hand the research of the phenotypic effects resulting from transgene expression. The random insertional mutagenesis is a valuable by-product of the generation of transgenic mice causing a wide variety of phenotypic effects. In approximately 5-10% of transgenic animals, the coding sequence of endogenous genes is disrupted and their expression is suppressed. Furthermore, the inserted DNA tags the mutated genes and enables their cloning and identification. However, tandem arrays of transgenes can also generate chromosomal rearrangements and deletions and thereby hinder the isolation of the affected genes, precluding insertional mutagenesis by transgenes from being developed for the effective knockout of genes with high throughput (Gridley, 1991; Jaenisch, 1988; Meisler, 1992).

In strong contrast to the hit-and-miss nature of these highly random mutagenesis strategies is gene targeting, the deletion of single genes with a molecularly well-defined nature in the germ line of mice. Gene targeting was enabled by two principal developments in the 1980s. First, methods were developed to culture ES cells derived from mouse blastocysts *in vitro* (Evans and Kaufman, 1981; Martin, 1981). Furthermore, after injection into host blastocysts and reimplantation of the embryos into foster mothers, these ES cells were shown to be capable of contributing to all tissues in chimeras, including the germ line (Bradley et al., 1984). Second, it was shown that ES cells can be genetically manipulated and that mutated ES cells are still germ line competent. The method was further perfected by the possibility to introduce directed, precise, and preplanned mutations into any gene in ES cells by the homologous recombination method. Therefore, a cloned targeting vector containing a combination of sequences homologous to the wild-type (WT) gene and the desired mutation is microinjected into ES cells. After homologous recombination, the desired mutation gets part of the mouse genome and replaces the endogenous sequence (Doetschman et al., 1987; Thomas and Capecchi, 1987). For the development of these groundbreaking techniques, Mario R. Capecchi, Martin Evans, and Oliver Smithies were awarded the Nobel Prize for Medicine in 2007 because the combination of gene targeting (Doetschman et al., 1987; Thomas and Capecchi, 1987) with ES cell culture (Evans and Kaufman, 1981; Martin, 1981) led to the generation of the first KO mouse in 1989.

An emerging technology for post-genomic mutation of gene expression is RNA interference (RNAi), which is mediated by small interfering RNA (siRNA). siRNA like miRNA is a class of double-stranded RNA molecules comprising 20-25 bp. siRNA binds to complementary sequences on target mRNA transcripts, usually resulting in translational repression or target degradation and gene silencing. To induce long-term knockdown phenotypes in mice, stable siRNA expression constructs have been developed. They integrate into the mouse genome

after microinjection of DNA into one cell mouse embryos or after transfecting ES cells. These vectors contain RNA polymerase III promoter-driven expression elements of short hairpin RNA (shRNA), which is further processed to the silencing siRNA (Hasuwa et al., 2002; Kunath et al., 2003). However, RNAi-mediated knockdowns often show some persisting residual expression of the silenced gene and the knockdown efficiency is variable in different cell types. Furthermore, siRNA gene knockdown may also exert non-specific effects, e.g. initiate an immune response because it may be recognized as a viral by-product within the cell, or inadvertently downregulate genes with incomplete complementarity.

3.3.2. Gene Trapping - Knockout on the Fast Lane

In comparison to completely random mutations induced by radiation, chemical mutagens, or retroviral/transgene insertion, and in contrast to molecularly defined mutations generated by gene targeting, gene trapping takes a middle path by combining random insertional mutagenesis with the ability to easily identify and clone the mutated gene. For this mutagenesis strategy, a gene trap vector is introduced into the mouse genome by electroporation or retroviral infection of ES cells, ES cells with the integrated gene trap vector are injected into blastocysts, and the latter are reimplanted into foster mothers (Figure 6).

A standard gene trap vector consists of a promoterless reporter gene, e.g. *lacZ,* which allows expression profiling of endogenous promoter activity. It further comprises a selectable genetic marker, mostly an antibiotic resistance gene like *neoR*, which enables the positive selection of ES cells with gene trap vector integration in antibiotic-containing culture medium. These genes are flanked upstream by a splice acceptor site and intronic sequences, and downstream by a polyadenylation sequence and plasmid vector backbone, ensuring a proper vector integration, splicing, transcription, and translation (Figure 12). Thus, a gene trap vector also provides a DNA tag for the rapid identification of the disrupted gene (Ullrich and Schuh, 2009).

Gene trap vectors are designed to function when inserted in an intron of an expressed gene. After intronic insertion, the gene trap cassette is transcribed from the promoter of the trapped gene, resulting in the expression of a fusion transcript, in which the exon(s) upstream of the insertion site is spliced in frame to the reporter/selectable marker gene. Since transcription is terminated prematurely at the inserted polyadenylation site, the processed fusion transcript encodes a truncated or disrupted non-functional version of the affected endogenous gene and the reporter/selectable marker gene. Thus, gene trapping is a powerful tool to simultaneously ablate gene function and to report expression and promoter activity of the trapped gene (Ullrich and Schuh, 2009).

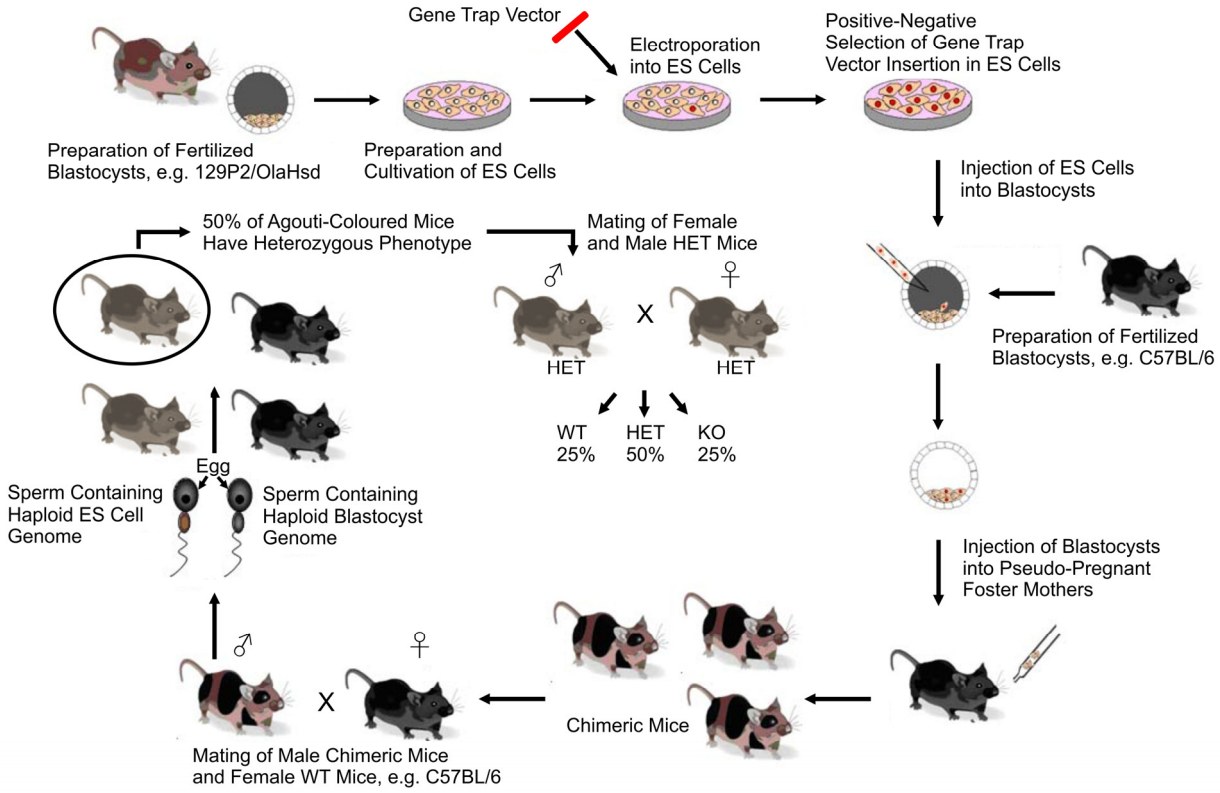

Figure 6: General Gene Trapping Strategy
By electroporation of a gene trap vector into murine ES cells, a gene is disrupted randomly by integration of the gene trap vector into the ES cell genome. ES cells containing a random modification in the desired gene are selected, microinjected into fertilized and isolated mouse blastocysts, and re-implanted into the uterus of pseudo-pregnant foster mothers. Chimeric male offspring born from these embryos are mated with female WTs in order to transmit the modified gene to their progeny. Selected heterozygous (HET) female and male mice are mated with each other to generate complete KO mice.
Figure in part reproduced from: http://proj.ncku.edu.tw/research/commentary/e/20071116/images/c2_1.jpg.

Despite of less flexibility in the design of the mutated alleles, despite the preference of gene trap vectors to integrate to large transcription units and genes highly expressed in ES cells, and despite the uncertainty to generate complete null alleles, gene trapping has striking advantages compared to gene targeting. Besides the possibility to mutate and report the expression of the trapped gene in parallel, gene trapping is rapid, cost-effective, and does not require the knowledge of structure and sequence of the mutated gene. Accordingly, the long-lasting time- and work-consuming cloning of homologous recombination vectors essential for gene targeting is not necessary. Due to the requirement of only one common and standardized gene trap vector for all knockout approaches performed by gene trapping, this method enables the fast and easy generation of a large variety of insertional mutations throughout the whole mouse genome and therefore is amenable to high throughput and large-scale mutagenesis.

The International Gene Trap Consortium (IGTC) consists of laboratories all around the world working together to generate a public library of all mutated murine ES cell lines. The IGTC ensures a broad availability of a wide collection of ES cell clones with a huge variety of identified trapped genes that can be obtained on a non-collaborative basis for nominal handling fees by every scientist. In addition to ES cell clones producing standard loss-of-function alleles, the IGTC also offers ES cell lines with newer gene trap vectors that enable post-insertional modification for the generation of other experimental alleles. In these new vectors, Cre/loxP (cyclisation recombination/locus of X-over of P1) and/or FLP/FRT (flippase/flippase recognition target) recombinase systems are combined with conventional gene trapping strategies. This allows, for example, the rescue and conversion of complete KOs that result in embryonic lethality to temporally and spatially-controllable conditional KOs in a single mouse line.
The IGTC, together with the members of the International Mouse Phenotyping Consortium (IMPC), aim to mutate all protein-coding genes in the mouse, using a combination of conventional/conditional gene trapping and gene targeting in C57BL/6 mouse ES cells. Owing to the continuous progress of these large-scale mouse mutagenesis programs, targeted and/or trapped ES cells are available for about 18,000 of the approximately 25,000 identified protein-coding mouse genes to date.

3.4. Hormonal Regulation of Body Homeostasis

3.4.1. The Hypothalamic-Pituitary-Adrenal Axis

The hypothalamic-pituitary-adrenal (HPA) axis is essential for the maintenance of homeostasis and enables the organism to prepare for and manage either physical or emotional stress. It comprises a complex set of direct influences and feedback interactions among the hypothalamus, the pituitary gland, and the adrenal glands and constitutes a major part of the neuroendocrine system. Triggered by the limbic system, activation of the HPA axis begins with the release of corticotropin-releasing hormone (CRH) from the hypothalamus, which in turn stimulates the secretion of adrenocorticotropic hormone (ACTH) from the anterior pituitary and further results in the release of mineralocorticoids like aldosterone and glucocorticoids like cortisol or corticosterone from the adrenal gland (Figure 7).

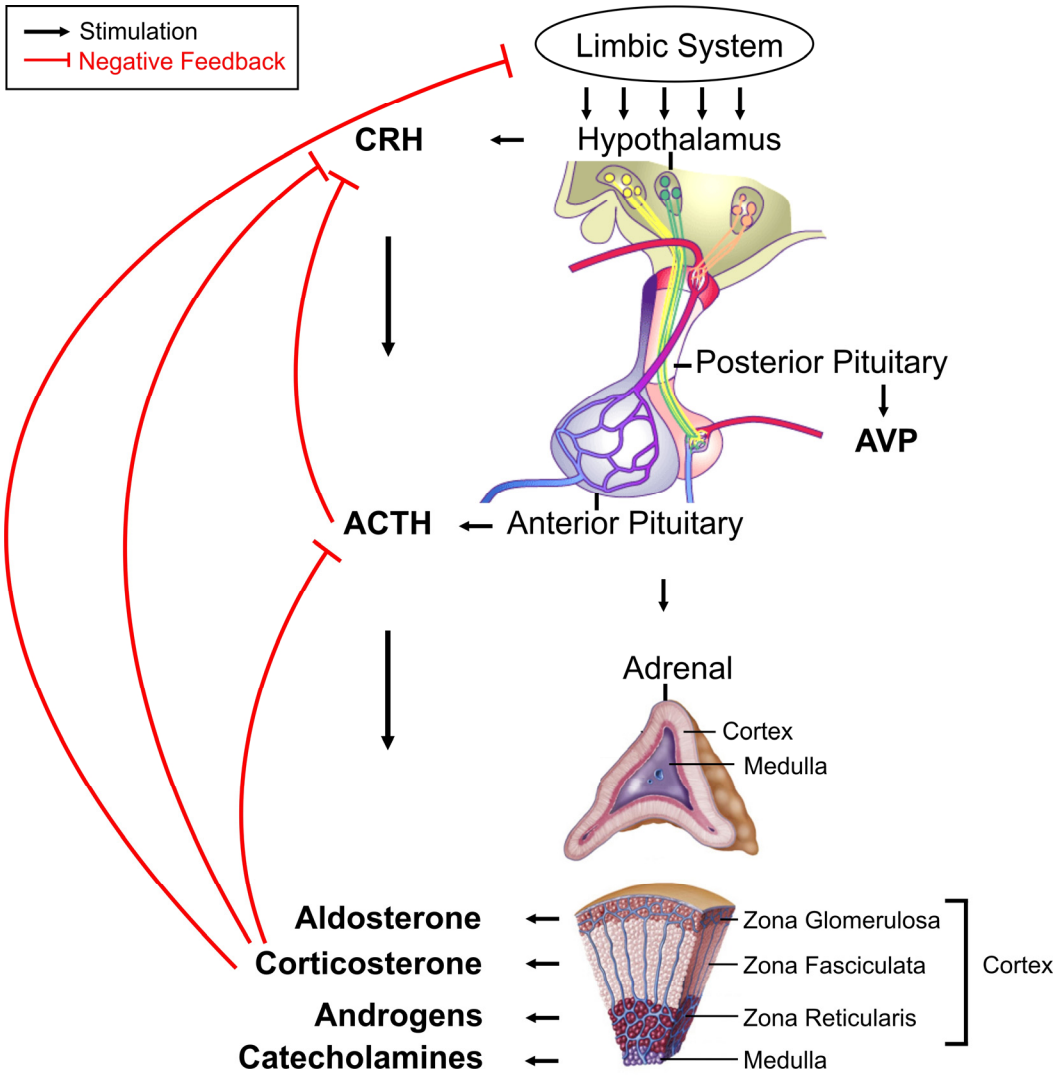

Figure 7: The HPA Axis – A Crucial Hormonal Mediator of Stress Response and Body Homeostasis
Triggered by the limbic system, CRH is released from the PVN of the hypothalamus, which in turn stimulates the secretion of ACTH from anterior pituitary. ACTH mainly triggers the release of glucocorticoids like cortisol or corticosterone from the zona fasciculata of the adrenal cortex. ACTH is also involved in the release of mineralocorticoids like aldosterone from the adrenal zona glomerulosa and of androgens from the adrenal zona reticularis and further influences the secretion of catecholamines from the adrenal medulla. AVP is mainly secreted by the posterior pituitary. Negative feedback regulation is exerted by glucocorticoids, which can inhibit both ACTH and CRH release and directly the limbic system. ACTH can further feed back on CRH secretion.
Figure in part reprinted from http://histoblog.viabloga.com/images/hypophyse_1_t.800.jpg and from http://www.gru.edu/mcg/phy/raineylab/images/webfigure2.jpg.

3.4.1.1. The Hypothalamus – Neural Stimuli Trigger the Release of CRH and AVP

The hypothalamus is a part of the brain located between thalamus and brain stem and contains a number of small nuclei with a variety of functions. It links the nervous system to the endocrine system by the secretion of hypothalamic releasing hormones, e.g. corticotropin-releasing hormone (CRH), thyrotropin-releasing hormone (TRH), gonadotropin-releasing hormone

(GnRH), and growth hormone-releasing hormone (GHRH) and by secretion of release-inhibiting hormones, e.g. somatostatin and dopamine. Triggered by the autonomic nervous system, the release of these liberins and statins controls body temperature, hunger, thirst, fatigue, sleep, and circadian cycles (McCann and Porter, 1969).

The hypothalamic nucleus responsible for the release of CRH is the paraventricular nucleus (PVN). CRH neurosecretory cells are parvocellular neurons within this PVN that project to the median eminence, which connects the hypothalamus with the pituitary gland (Alonso et al., 1986). From there, CRH and other releasing hormones are secreted into the pituitary portal circulation, diffuse to the anterior pituitary, and in turn stimulate or inhibit the secretion of pituitary hormones, e.g. ACTH (Rivier et al., 1982; Zimmerman et al., 1977).

CRH, a 41-amino acid peptide that is cleaved from the C-terminus of a 196-amino-acid pre-prohormone precursor by PC1 and PC2 (prohormone convertases 1 and 2), is the main activator of the HPA axis (Vale et al., 1981). Stress causes rapid activation of CRH neurons by activation of neural pathways afferent to the PVN, resulting in rapid CRH release followed by increases in CRH transcription and *de novo* synthesis of the peptide. Systemic physical and metabolic stressors, such as loss of blood volume, immune challenge, pain, and hypoglycemia, require an immediate response. They utilize monosynaptic ascending pathways from the brain stem and spinal cord with direct projections to the PVN (Aguilera and Liu, 2012; Herman et al., 2003). These direct pathways to the CRH neuron are mostly noradrenergic and adrenergic and stimulate CRH neurons by acting via α-adrenergic receptors in the CRH neuron. Psychogenic stressors utilize complex polysynaptic pathways, projecting from sensory organs and brain stem to limbic structures, the most important being the medial prefrontal cortex, hippocampus, and amygdala (Aguilera and Liu, 2012; Herman et al., 2003). These pathways interact with the CRH neuron indirectly through glutamatergic and GABAergic neurons (GABA=γ-aminobutyric acid) in the peri-PVN area, which form direct synapses with the CRH neuron. Under basal conditions, the CRH neuron is under inhibitory influence of GABAergic interneurons located in the periventricular region of the hypothalamus (Cullinan et al., 2008).

Acute stress induces Ca^{2+}-dependent rapid release of CRH, which is followed by rapid increases in gene transcription in order to restore releasable pools, resulting in an elevation of steady-state mRNA levels detectable about 2 h after acute stress (Ma et al., 1997). During chronic stress, changes in CRH expression in parvicellular neurons depend on the nature of the stress. Whereas psychogenic stressors induce transient increases in mRNA levels, returning to basal after the first few exposures to the stimulus, systemic paradigms cause elevations in mRNA levels up to 14 or more days after each stress exposure (Aguilera, 1998).

AVP, a nine-amino acid peptide derived from a preprohormone precursor, is not essential for activation of the HPA axis and has only a weak effect on ACTH release. However, AVP clearly

potentiates the stimulatory effect of CRH on ACTH release in the pituitary corticotrope cells (Gillies et al., 1982; Rivier and Vale, 1983). Like CRH, AVP responsible for ACTH secretion is produced in the parvocellular neurons of the PVN and released into pituitary portal capillaries from axon terminals of the median eminence (Sawchenko et al., 1984; Zimmerman et al., 1977). In analogy to CRH, the synergistic hypothalamic AVP release is stress-stimulated and also involves an increase in AVP transcription (Aguilera et al., 2008; Ma et al., 1997).

In order to exert it effects, CRH binds to CRH receptors 1 and 2 (CRH-R1/2) (Chen et al., 1993; Lovenberg et al., 1995), which are mainly coupled to G_s proteins (Grammatopoulos and Chrousos, 2002). Whereas CRH-R1 has been implicated in mediating normal responses to stress, CRH-R2 seems to be more responsible for fine tuning and counterregulation (Timpl et al., 1998). For stress-induced activation of the HPA axis and the initiation of biosynthesis and secretion of ACTH from cellular stores, CRH acts exclusively on CRH-R1 receptors. The synergistic action of AVP on ACTH release is mediated by G_q protein-coupled vasopressin 1b receptors (V1bR) in the anterior pituitary (Birnbaumer, 2000; Sugimoto et al., 1994). Both the resulting increase in cyclic adenosine monophosphate (cAMP) and intracellular Ca^{2+} lead to a stimulation of pro-opiomelanocortin (POMC) transcription and ACTH production (Jenks, 2009).

3.4.1.2. The Pituitary – CRH/AVP-mediated ACTH Release from Anterior Lobe and Osmolality/Volume-mediated AVP Release from Posterior Lobe

The pituitary is an endocrine gland at the base of the brain, resting in a small, bony cavity and covered by a dural fold. It is not a part of the brain but a protrusion of the hypothalamus with whom it is functionally connected by the median eminence. The pituitary gland consists of two components: the anterior pituitary or adenohypophysis and the posterior pituitary or neurohypophysis. Regulated by the hypothalamic liberins and statins, the anterior pituitary synthesizes and secretes tropic hormones that target other endocrine glands to release further downstream hormones, e.g. adrenocorticotropic hormone (ACTH or corticotropin), growth hormone (GH), thyroid-stimulating hormone (TSH or thyrotropin), luteinizing hormone (LH), follicle-stimulating hormone (FSH), prolactin (PRL), and melanocyte-stimulating hormone (MSH) (McCann et al., 1968). The posterior pituitary stores and secretes AVP, the majority of which is produced in the supraoptic nucleus (SON) of the hypothalamus and oxytocin, most of which is generated in the hypothalamic PVN (Hayward, 1975).

In contrast to the parvocellular CRH neurons in the hypothalamic PVN, which also produce and release small amounts of AVP (Sawchenko et al., 1984; Zimmerman et al., 1977), the main source of AVP are magnocellular neurons of the hypothalamic SON and PVN, which are also responsible for oxytocin release (Taniguchi et al., 1988). AVP is transported to the posterior

pituitary along these magnocellular neurons, where it is stored in vesicles and from where it is released to the peripheral circulation. AVP of magnocellular origin exerts the major AVP-hormone function, i.e. the regulation of body fluid homeostasis by mediating water retention in the kidney. Osmotic stressors like hyperosmolality or hypovolemia activate vasopressinergic neurons leading to opening of voltage-gated Ca^{2+} channels in these nerve terminals, transient Ca^{2+} influx, and the fusion of the AVP-containing neurosecretory granules with the nerve terminal membrane (Benetos et al., 1987; Dunn et al., 1973; Ishikawa and Schrier, 1983).

AVP exerts its antidiuretic, water-retaining effect by binding to V2Rs, expressed in the kidney in cells of the distal convoluted tubule and in principle cells of the collecting duct (Lolait et al., 1992). V2Rs in the basolateral membrane of these cells are associated with G_s proteins, which trigger the insertion of aquaporin-2 (AQP2) water channels into the apical cell membranes, involving cAMP increase and protein kinase A (PKA) activation. Aquaporins allow water to follow its osmotic gradient, leading to water re-absorption from the nephron back into the circulation (Nielsen et al., 1996). Besides the regulation of body fluid homeostasis, circulating AVP at high concentrations also elicits vasoconstriction and raises blood pressure. This effect is mediated by V1aR and Ca^{2+}, similar to V1bR a G_q protein-coupled receptor (Koshimizu et al., 2012; Morel et al., 1992).

In the anterior pituitary, the neurohormones CRH and AVP act synergistically via their specific CRH-R1 and V1bRs, respectively, to trigger the release of ACTH from corticotrope cells into the systemic circulation (Sawchenko et al., 1984; Zimmerman et al., 1977). ACTH is a 39-amino acid peptide but is synthesized as part of the 241-amino acid polypeptide POMC. POMC is synthesized primarily in the CNS by corticotrope cells of the anterior pituitary, by melanotrope cells of the intermediate lobe of the pituitary, and in the arcuate nucleus of the hypothalamus. It is also present in several peripheral tissues, e.g. in melanocytes in the skin, in adrenals, lung, spleen, in genitourinary- and gastrointestinal tracts, and in thyroid and immune cells (Eberle, 1988; Wikberg et al., 2000). The polypeptide hormone precursor POMC undergoes extensive, tissue-specific, post-translational processing via cleavage by endopeptidases, mainly PC1 and PC2. Further processing by phosphorylation, acetylation, amidation, and glycosylation contributes to the production of various polypeptide fragments by different cell types with varying physiological activity (Smith and Funder, 1988). In the anterior pituitary, POMC is cleaved to γ-melanocyte-stimulating hormone (γ-MSH), ACTH, and β-lipotropin (β-LPH). ACTH can further be processed to α-MSH and corticotropin-like intermediate lobe peptide (CLIP), whereas β-LPH can further be cleaved to γ-LPH and β-endorphin. From γ-LPH, even more β-MSH can be generated. Each of these peptides is packaged in large dense-core vesicles that are released by exocytosis in response to CRH/AVP-mediated stimulation (Smith and Funder, 1988).

ACTH and the other POMC cleavage products exert their numerous biological effects by activating melanocortin receptors, a family of five G_s-protein coupled receptors (MC1-5R) (Mountjoy et al., 1992). The MCRs are mainly expressed in melanocytes, endothelial cells, fibroblasts, immune cells, CNS, and brain and therefore play important functional roles in the regulation of behavior, skin pigmentation, energy homeostasis, feeding, immune system, cardiovascular system, and sexual function. The main ligands of the MCRs are the melanocortins, especially α-MSH, which has the highest receptor affinity in most cases. ACTH is able to bind to all five MCRs but in most cases with a profoundly lower affinity in comparison to the melanocortins. One exception is MC2R, which is exclusively responsive to ACTH and not to the MSHs (Gantz and Fong, 2003; Getting, 2006). MC2R is located in the adrenal zona glomerulosa and zona fasciculata, where it regulates steroidogenesis upon ACTH binding (Liakos et al., 1998).

3.4.1.3. The Adrenal – ACTH Regulates the Release of Glucocorticoids and Mineralocorticoids

The adrenal glands are endocrine glands sitting at the top of the kidneys. Each adrenal gland has two distinct areas, the outer adrenal cortex and the inner medulla (Figure 7). The adrenal cortex comprises three zones that differ anatomically and functionally: an outer zona glomerulosa, a central zona fasciculata, and an inner zona reticularis. Whereas the zona glomerulosa is the major site for production of mineralocorticoids, mainly aldosterone, which is largely responsible for regulation of salt and water homeostasis and blood pressure, the zona reticularis produces androgens, mainly dehydroepiandrosterone (DHEA) and androstenedione, the precursor of testosterone and estradiol in humans. Both the zona fasciculata and the medulla respond to stress, the former by the synthesis of corticosteroids such as cortisol and the latter by the release of catecholamines such as epinephrine or norepinephrine. Whereas the medullary release of catecholamines developed from tyrosine is triggered mainly and directly by the sympathetic nervous system, the release of cortical hormones developed from cholesterol is regulated by hormones itself, of which ACTH plays a major role.

Human steroidogenesis of mineralocorticoids, glucocorticoids, and androgens starts with the conversion of the common precursor cholesterol to pregnenolone by cholesterol side chain cleavage monooxygenase, also called P450scc and encoded by the CYP11A1 gene (Figure 8). For glucocorticoid synthesis, which takes place in the adrenal zona fasciculata, pregnenolone is converted to 17α-hydroxypregnenolone by 17α-hydroxylase (P450c17/CYP17A1). Consecutive catalytic activity of 3β-hydroxysteroid dehydrogenase (3β-HSD/HSD3B), 21α-hydroxylase (P450c21/CYP21A2), and 11β-hydroxylase (P450c11/CYP11B1) leads via 17α-

hydroxyprogesterone and 11-deoxycortisol to the generation of the glucocorticoid cortisol. Mineralocorticoid synthesis takes place accordingly in the zona glomerulosa using almost the same steroidogenic enzymes with the exception of 17α-hydroxylase and 11β-hydroxylase, which are not expressed there. Via pregnenolone and progesterone, cholesterol is converted to 11-deoxycorticosterone, mediated by consecutive action of P450scc, 3 β-HSD and P450c21. The last step in aldosterone synthesis is mediated by aldosterone synthase (P450aldo/CYP11B2), which catalyzes the 11β-hydroxylation to corticosterone, the 18-hydroxylation to 18-hydroxy-corticosterone, and the 18-oxidation to aldosterone. The generation of adrenal androgens is also catalyzed by 17α-hydroxylase, which converts 17α-hydroxypregnenolone to dehydroepiandrosterone and 17α-hydroxyprogesterone to androstenedione. These steroids are precursors of testosterone and estradiol (for review of steroidogenesis see (Hattangady et al., 2012; Sewer and Waterman, 2003)).

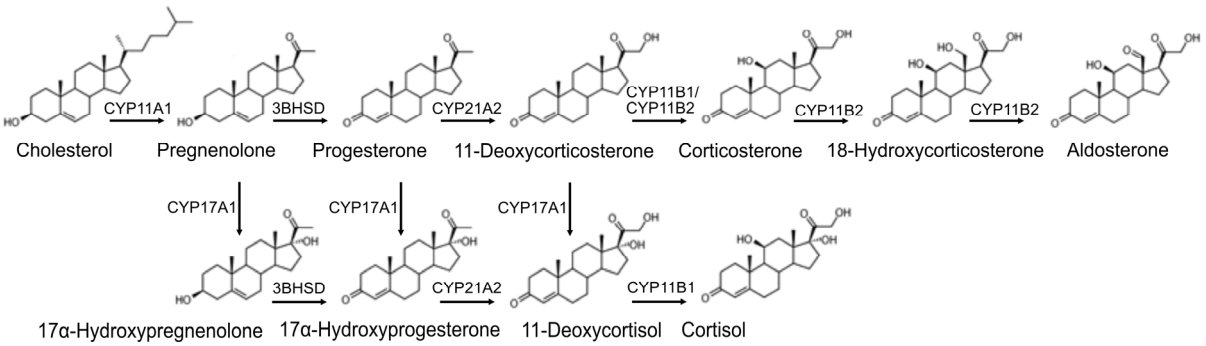

Figure 8: Adrenal Synthesis of Human Cortisol and Aldosterone
Mineralocorticoids in the adrenal zona glomerulosa and glucocorticoids in the zona fasciculata are generated from their common precursor cholesterol mediated by partially identical steroidogenic enzymes. The reactions catalyzed by CYP11A1 (cholesterol side chain cleavage monooxygenase), CYP11B1 (11β-hydroxylase), and CYP11B2 (aldosterone synthase) occur in the mitochondria, all other reactions take place in the endoplasmic reticulum. Enzymes specifically present in the zona fasciculata are CYP17A1 (17α-hydroxylase) and CYP11B1, while CYP11B2 is exclusively expressed in the zona glomerulosa. *Figure based on (Morohashi et al., 2013).*

In contrast to the human steroidogenesis described above, murine adrenal glands are not able to produce cortisol and androgens due to the lack of CYP17A1 expression (Figure 9). Therefore, in mice corticosterone and not cortisol is the predominant steroid of the adrenal cortex (Keegan and Hammer, 2002). 11-deoxycorticosterone is the common precursor for the production both aldosterone in the zona glomerulosa and corticosterone in the zona fasciculata. After binding to MC2R, ACTH regulates steroidogenesis by adenylate cyclase stimulation and PKA activation (Penhoat et al., 1989). Acutely, PKA phosphorylates steroidogenic acute regulatory protein (StAR), which mediates the delivery of the initial substrate cholesterol from

cellular stores to mitochondrial P450scc and therefore leads to a rapid cholesterol mobilization (Clark et al., 2000). Chronically, ACTH-dependent PKA activation stimulates the transcription of all steroidogenic CYP enzymes (CYP11A1, CYP17, CYP21A2, CYP11B1) with the exception of CYP11B2 (Holland and Carr, 1993; Sewer and Waterman, 2002, 2003). Because ACTH is able to stimulate especially 11β-hydroxylase transcription but has no influence on aldosterone synthase expression, ACTH has a greater impact on glucocorticoid than on mineralocorticoid regulation (Kramer et al., 1983).

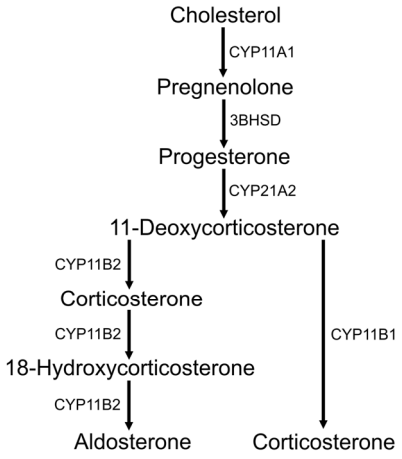

Figure 9: Synthesis of Corticosterone and Aldosterone in Mice

In contrast to humans, rodents are not able to synthesize cortisol and steroidogenesis of mineralocorticoids and glucocorticoids is equal up to 11-deoxycorticosterone. In the zona fasciculata, 11-deoxycorticosterone is converted exclusively to corticosterone by 11β-hydroxylase. In the zona glomerulosa, 11-deoxycorticosterone is also converted to corticosterone, in this zone mediated by aldosterone synthase, which is exclusively expressed there and which in a further two-step reaction generates aldosterone from corticosterone.
Figure based on http://upload.wikimedia.org/wikipedia/commons/8/89/Corticosteroid-biosynthetic-pathway-rat.png.

Glucocorticoids are a class of steroid hormones that are released in response to stress. Both cortisol and corticosterone respond to psychological but also physiological stress by enabling the mobilization of energy reserves. They exert effects on glucose, protein, and fat metabolism. Glucocorticoids stimulate gluconeogenesis by simultaneous inhibition of enteral glucose reabsorption and glucose uptake in muscles and adipose tissue, by proteolysis and mobilization of amino acids from peripheral tissues, and by lipolysis and the release of fatty acids, the latter two mechanisms providing substrates for gluconeogenesis. They have an immune-suppressive function by upregulating the expression of anti-inflammatory proteins and downregulating the expression of pro-inflammatory proteins. Together with catecholamines, glucocorticoids enhance cardiac power and blood pressure and cooperate in memory formation, e.g. of events associated with strong emotions, both positive and negative.

Whereas both CRH-R and MC2-R are membrane-bound G_s-protein-coupled receptors linked to the adenylate cyclase - cAMP - PKA pathway, glucocorticoid receptors are cytosolic steroid receptors. In the absence of hormones, the glucocorticoid receptor resides in the cytosol and forms a complex with a variety of proteins including heat shock proteins (Pratt et al., 2006). The

glucocorticoid hormone cortisol diffuses through the cell membrane into the cytoplasm and binds to the glucocorticoid receptor (GR) resulting in release of the heat shock proteins. The resulting activated GR complex has two principal mechanisms of action: Transactivation involves receptor homodimerization upon ligand binding, translocation into the cell nucleus, and interaction with specific glucocorticoid response elements (GRE) in the promoter region of the target genes, thus activating gene transcription (Mangelsdorf et al., 1995). Via transrepression, activated glucocorticoid receptors can complex with other transcription factors, such as NF-κB (Ray and Prefontaine, 1994) or AP-1 (Jonat et al., 1990), prevent them from binding their target genes, and repress gene expression normally upregulated by these factors.

3.4.1.4. Feedback Regulation and Circadian Rhythm of the HPA Axis

The activity of the HPA axis is determined by endogenous inputs clocked by the circadian rhythm and by exogenous inputs elicited by stress, both mediated by neural modulation and by glucocorticoid feedback control.

Glucocorticoids exert a negative feedback on the HPA axis at the level of pituitary, hypothalamus, and centrally at the level of the limbic system (Figure 7). Feedback inhibition is mediated via the GR and involves fast and slow feedback loops (Dallman et al., 1994; Keller-Wood and Dallman, 1984; Papadimitriou and Priftis, 2009). Slow feedback is mediated by glucocorticoid binding to cytosolic GRs and involves genomic regulation. In this manner, glucocorticoid production by HPA axis activation leads to a consecutive downregulation of CRH and AVP mRNA synthesis in the hypothalamus and of POMC gene transcription in the anterior pituitary (Birnberg et al., 1983; Kovacs et al., 2000; Kretz et al., 1999). Fast feedback regulation of the HPA axis occurs by acute inhibition of CRH and ACTH release. The rapidity of action from seconds to minutes suggests that this effect is not compatible with genomic regulation. Furthermore, rapid effects seem to be mediated by binding of glucocorticoids to membrane-associated glucocorticoid receptors instead of to the classical cytosolic ones (Tasker et al., 2006). Glucocorticoid binding to these membrane-bound receptors leads to the release of endocannabinoids, which exert acute, fast feedback by inhibition of glutamatergic stimulation of the PVN neurons (Di et al., 2003). In the absence of negative feedback control of ACTH secretion by glucocorticoids, ACTH can regulate its secretion by inhibition of hypothalamic CRH release, which also represents a fast feedback loop (Suda et al., 1987) (Figure 7).

Furthermore, the release of the HPA hormones underlies a circadian rhythm. This circadian rhythmicity is generated by the hypothalamic suprachiasmatic nucleus (SCN) dependent on the sleep-wake cycle of the organism (Ralph et al., 1990; Rusak and Zucker, 1979). The SCN triggers the rhythmic release of CRH, which in turn mediates the secretion of ACTH in a

pulsatile fashion. Under basal conditions, approximately 18 - 25 pulses of ACTH with various amplitudes are observed over 24 h. Depending on the light-dark cycle, maximum levels of ACTH are reached at a 2 - 4 h window around waking and subsequently decrease to a minimum at a 2 - 4 h window around sleeping. Corticosterone concentration profiles follow those of ACTH with approximately 2 h delay (Oster et al., 2006).

Dysregulation of the HPA axis, both up- or downregulation, plays a fundamental role in various stress-associated and psychiatric (Stokes and Sikes, 1991), neurodegenerative (Bao et al., 2008), metabolic (Williams, 1979), and chronic pain and inflammatory diseases (Bomholt et al., 2004). Increased activity of the HPA axis is associated with mood disorders, including e.g. obsessive-compulsive disorder, anxiety disorder, eat disorders, insomnia, major depressive disorder, and alcoholism (Arborelius et al., 1999; Kluge et al., 2007; Pariante, 2003; Stokes and Sikes, 1991). A metabolic consequence of HPA axis overactivation is hypercortisolism and the thereof resulting Cushing´s syndrome (Williams, 1979). The most common consequence of decreased HPA activity is adrenal insufficiency, also called Addison´s disease, and hypocortisolism (Williams, 1979), but it can also be associated with mood disorders like chronic fatigue syndrome (Papadopoulos and Cleare, 2012).

3.4.2. The Renin-Angiotensin-Aldosterone Axis

The Renin-Angiotensin-aldosterone-axis is a major regulator of extracellular fluid and salt balance and therefore the most important cascade for blood pressure regulation. It comprises a well-characterized cascade of proteases and hormones, of which the sequentially activated peptidase Renin and the octapeptide Angotensin II are the most important and physiologically active components. Angotensin II acts on the adrenal gland to release the mineralocorticoid aldosterone (Figure 10).

3.4.2.1. The Renin-Angiotensin System (RAS)

Renin is the initiator of the RAS and is derived from a Prorenin precursor by proteolytic cleavage (Galen et al., 1984). It is synthesized and stored in juxtaglomerular cells of the kidney, a specialized form of granulated smooth muscle cells located in the wall of the afferent arteriole of a nephron (Tobian, 1962). The peptidase is released from the juxtaglomerular apparatus into the blood circulation and generates Angiotensin I (Ang I) from its substrate angiotensinogen by proteolytic cleavage. Angiotensinogen is mainly produced by the liver (Nasjetti and Masson, 1971) and contains more than 400 amino acids. However, only the first ten amino acids represent Ang I (Tewksbury et al., 1981). The decapeptide Ang I is biologically mostly inactive

and serves as a precursor for the physiologically active Ang II. Ang II, an octapeptide, contains the first eight amino acids of Ang I and is generated by angiotensinogen-converting-enzyme (ACE) (Ng and Vane, 1967). The exopeptidase ACE is secreted by pulmonary and renal endothelial cells and removes the two C-terminal residues of Ang I (for reviews of the RAS see (Bottari et al., 1993; Fyhrquist and Saijonmaa, 2008)).

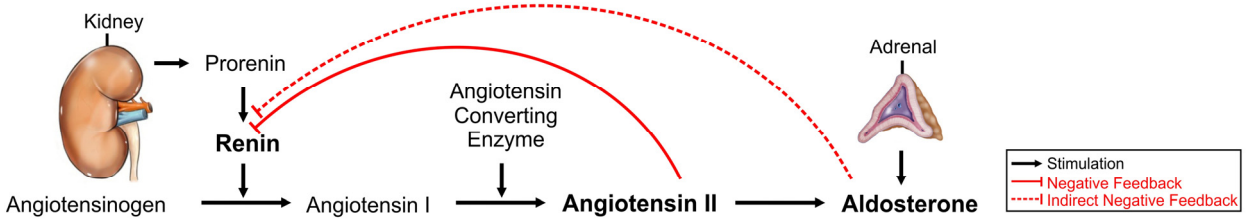

Figure 10: The Renin-Angiotensin System – The Main Stimulator of Aldosterone Release
Renin, derived from its precursor Prorenin, is secreted by juxtaglomerular cells in the kidney and generates Ang I from angiotensinogen by proteolytic cleavage. By Angiotensin converting enzyme, Ang I is further processed to Ang II, which stimulates the release of aldosterone from the adrenal cortex. Ang II can directly inhibit the RAS by suppressing renal Renin release, while aldosterone indirectly signals back to Renin release by aldosterone-induced volume expansion. *Figure in part reproduced from http://www.paradisi.de/images_artikel/1/12556_0.jpg and from http://www.gru.edu/mcg/phy/raineylab/images/webfigure2.jpg.*

The secretion of Renin and the initiation of the RAS is mainly provoked by three situations: First, by a decrease in arterial blood pressure and a decrease in blood volume, respectively, which is detected by renal baroreceptors (Blaine and Davis, 1971). Second, by the sympathetic nervous system, which innervates juxtaglomerular cells and activates the RAS in case of hypotension by acting through adrenaline-binding to β_1-adrenergic receptors (Gordon et al., 1967; Vander, 1965). Third, by a decrease in the glomerular filtration rate (GFR) and by thereof dependent reduced Na^+ levels in the ultra-filtrate of the nephron. The NaCl content and the renal blood flow is sensed indirectly by a Na^+ K^+ $2Cl^-$ symporter, which measures the speed of ion transport in the macula densa, a collection of densely packed epithelial cells in the distal tubule of the nephron (Skott and Briggs, 1987).

The RAS has a number of physiological effects, all contributing to blood pressure and fluid-salt balance regulation. Ang II, the main effector of the RAS, is a potent vasoconstrictor of arterioles throughout the whole body and thus has the potential to raise systemic arterial blood pressure (Basso and Terragno, 2001). In the kidney, Ang II maintains renal blood flow and GFR independently of arterial blood pressure changes. In this manner, Ang II provokes vasoconstriction of renal efferent arterioles in case of hypotension and of afferent arterioles in case of hypertension (Davalos et al., 1978; Heyeraas and Aukland, 1987). In the CNS, Ang II increases thirst sensation and the desire for salt (Avrith and Fitzsimons, 1978; Epstein et al.,

1969). Accordingly, it influences salt and water homeostasis by supporting the release of AVP from the posterior pituitary and by acting on the adrenal cortex to release aldosterone (Carpenter et al., 1961; Shimizu et al., 1973).

Ang II exerts its effects via two Ang II receptors mediating different physiological effects and exerting different mechanisms of action (Gunther, 1984). The Ang II receptor type 1 (AT1), mainly G_q- and sometimes G_i-protein-coupled, is involved in most of the well-established physiological effects of Ang II. It regulates vasoconstriction, aldosterone and ADH secretion but also cell proliferation and cellular growth, generation of reactive oxygen species, and inflammation (Fyhrquist and Saijonmaa, 2008). Thus, the AT1 receptor also mediates actions with potentially harmful consequences, i.e. hypertension, cardiac hypertrophy, and fibrosis. The G_i-protein-coupled Ang II receptor type 2 (AT2) was shown to counterbalance some effects of the AT1 receptor by mediating vasodilatation and inhibition of proliferation and growth (de Gasparo et al., 2000; Kaschina and Unger, 2003).

3.4.2.2. Aldosterone

Aldosterone, like corticosterone and cortisol a steroid hormone, is the primary human mineralocorticoid and is produced in the zona glomerulosa of the adrenal gland cortex (Giroud et al., 1956). Steroidogenesis of aldosterone starts with cholesterol and is carried out by nearly the same enzymes required for steroidogenesis of cortisol (3.4.1.3., Figure 8) (Hattangady et al., 2012). In contrast to cortisol biosynthesis, aldosterone biosynthesis lacks 17-hydroxylation of pregnenolone and progesterone, respectively, because the zona glomerulosa is not able to express P450c17 (Narasaka et al., 2001). In mice, where corticosterone is the main glucocorticoid, sterodogenesis of mineralocorticoids and glucocorticoids is equal up to 11-deoxycorticosterone (Figure 9). The last steps from 11-deoxycorticosterone to aldosterone are mediated by aldosterone synthase, which is exclusively expressed in the zona glomerulosa (Domalik et al., 1991; Ogishima et al., 1992). This zone-specific expression of P450aldo and the lack of P450c17 and P450c11, which are required for glucocorticoid synthesis, help to maintain the functional specificity of the adrenocortical zones and restrict aldosterone production to the zona glomerulosa.

Aldosterone biosynthesis is, similar to that of cortisol, regulated acutely by the StAR-mediated movement of cholesterol to P450scc in the mitochondria and chronically by aldosterone synthase expression. The main initiators of aldosterone release are Ang II, K^+, and ACTH. For acute regulation, all three stimulators mainly exert their effects by increasing cytosolic Ca^{2+} concentrations, by stimulating Ca^{2+}/calmodulin-dependent protein kinases (CaMK) or PKA, and at last by activating CREB (cAMP responsive element binding protein) and StAR (Cherradi et

al., 1998; Clem et al., 2005; Manna et al., 2003; Pezzi et al., 1996; Stocco, 2001). Chronic regulation is mainly exerted by the expression of aldosterone synthase, which is primarily induced by Ang II- and K^+-stimulated increase in intracellular Ca^{2+} and activation of CaMK (Condon et al., 2002; Holland and Carr, 1993; Tremblay et al., 1992). Aldosterone synthase expression is regulated directly by transcription factors like NURR1 (nuclear receptor related 1), NGF1B (nerve growth factor 1 B), ATF1 (cyclic AMP-dependent transcription factor), and CREB, which can be activated and phosphorylated by CaMKs (Bassett et al., 2004; Matthews et al., 1994). In contrast to chronic Ang II and K^+ effects, chronic ACTH release, however, rather decreases aldosterone secretion by decreasing CYP11B2 expression (Holland and Carr, 1993).

The effects of aldosterone are mediated by the mineralocorticoid receptor (MR), whose structure and mode of action is very similar to the GR (3.4.1.3.) (Arriza et al., 1987).

Because of its molecular similarity to aldosterone, glucocorticoids can also bind to the mineralocorticoid receptor with almost equal affinity (Arriza et al., 1987; Beaumont and Fanestil, 1983). Although glucocorticoids circulate at much higher concentrations than mineralocorticoids, a specific mineralocorticoid effect is generated by 11β-hydroxysteroid dehydrogenase type II (HSD11B2), existing in mineralocorticoid target tissues, e.g. epithelial cells in kidney and colon or vascular cells. It catalyzes the deactivation of glucocorticoids, i.e. the conversion of cortisol to the inactive metabolite cortisone in man or of corticosterone to 11-dehydrocorticosterone in rat, in order to prevent overstimulation by glucocorticoids and to allow selective mineralocorticoid action (Funder et al., 1988).

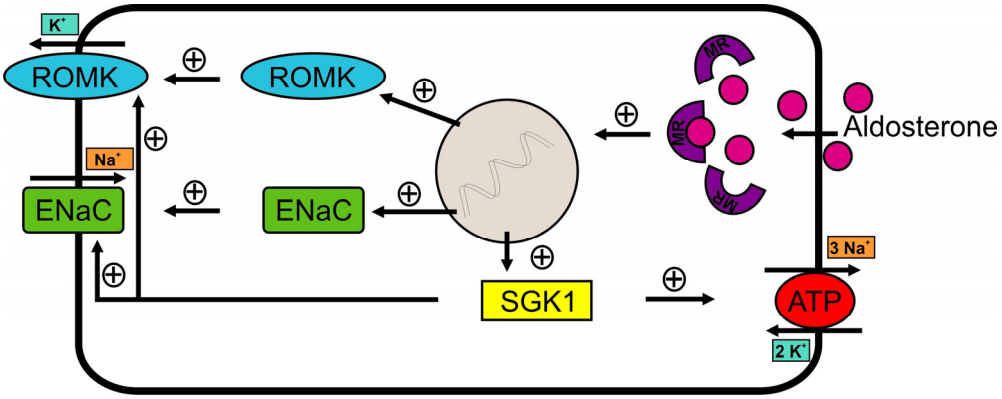

Figure 11: Aldosterone and the Regulation of Salt and Water Balance
By binding to MRs within distal convoluted tubule cells, connecting tubule cells, and principal cells of the collecting duct, aldosterone modulates directly the transcription of ENaC, ROMK, and SGK1 in the kidney nephron. SGK1 in turn indirectly stimulates the activity of the apical ENaC and ROMK but also of the basolateral Na^+-K^+-ATPase. Because the latter exchanges 3 Na^+ from the tubular cell into the blood and 2 K^+ from the blood into the tubular cell, a Na^+ gradient develops. This gradient consequently induces the entry of Na^+ into the tubular cell at the apical membrane through ENaC, while K^+ diffuses into the tubular lumen through apical ROMK. This aldosterone-triggered reabsorption of Na^+ and subsequent secretion of K^+ controls electrolyte and water levels in the entire body. *Figure based on (Kiryluk and Isom, 2007).*

The main function of aldosterone is the regulation of extracellular fluid and salt balance. Therefore, aldosterone binds to MRs within distal convoluted tubule cells, connecting tubule cells, and principal cells of the collecting duct in the kidney nephron. Activation of MRs modulates the transcription and/or the activity of several target genes, e.g. epithelial sodium channel (ENaC) (Chen et al., 1999b; Kemendy et al., 1992), renal outer medullary potassium channel (ROMK) (Beesley et al., 1998), Na^+-K^+-ATPase (Jorgensen, 1972), and serum and glucocorticoid-inducible kinase 1 (SGK1) (Bhargava et al., 2001). Aldosterone seems to be able to directly stimulate ENaC, ROMK, and Na^+-K^+-ATPase activity in the cell membrane of distal convoluted tubule and collecting duct principal cells by upregulating their mRNA levels (Figure 11). Indirectly, aldosterone induces the transcription of SGK1, which in turn can stimulate the activity of these channels (Kiryluk and Isom, 2007). The basolateral Na^+-K^+-ATPase exchanges 3 Na^+ from the cytosol of the tubular cell into the blood and 2 K^+ from the blood into the tubular cell, thereby providing a Na^+ gradient into the cell. Consequently, at the apical membrane, Na^+ follows this gradient and enters the tubular cell through ENaC, whereas K^+ diffuses into the tubular lumen. With this mechanism, aldosterone triggers the reabsorption of Na^+ and water into the blood and the subsequent secretion of K^+ into the urine. The salt and water retention leads to an increase in blood volume and therefore also in blood pressure.

3.4.2.3. RAS Feedback Regulation, Dysregulation, Antagonists, and Associated Diseases

For the maintenance of salt and water homeostasis, both the RAS and the thereof dependent aldosterone synthesis have to be regulated properly. Renin secretion and RAS activity is terminated through negative feedback loops, which can be induced by physiological stimuli like high arterial blood pressure, subsequently increased renal perfusion pressure, hypervolemia, increased Na^+ retention, increased K^+ load, and by α-adrenergic activation of the sympathetic nervous system (Williams, 2005). A hormonal feedback regulation is triggered by Ang II itself, which inhibits expression and release of Renin from juxtaglomerular cells (Johns et al., 1990; Vander and Geelhoed, 1965). Aldosterone exerts an indirect negative feedback because aldosterone-mediated salt and water retention leads to volume expansion, which also inhibits Renin release from the juxtaglomerular apparatus (Kaufman et al., 1980) (Figure 10). An endogenous antagonist of the RAS and aldosterone is the atrial natriuretic peptide (ANP), a peptide hormone secreted from cardiac myocytes in the atria of the heart in response to hypervolemia and hypernatremia (Anderson et al., 1986; de Bold, 1985). ANP mediates natriuresis and diuresis and thus is able to downregulate plasma volume and blood pressure (Brenner et al., 1990).

Dysregulation of the Renin-Angiotensin-aldosterone axis plays an important role in the pathogenesis of cardiovascular and renal disorders. Hyperaldosteronism, defined as a pathological increase in aldosterone production and release, may be caused by RAS overactivation (secondary hyperaldosteronism) or may develop independently of the RAS, e.g. due to adrenal adenoma (Conn's Syndrome) or due to adrenal hyperplasia (primary hyperaldosteronism). It is characterized by arterial hypertension, hypernatremia, hypokalemia, and metabolic alkalosis. Hypoaldosteronism accompanied by hypotension, hyponatremia, hyperkalemia, and metabolic acidosis can be provoked by adrenal insufficiency, mutations of steroidogenic genes, e.g. of CYP21A2, aldosterone synthase deficiency, and decreased RAS activity (Torpy et al., 1999).

Aldosterone/MR signaling as well as Ang II/AT1 receptor signaling can mediate further actions with harmful potential associated with their designated physiological effects. Common consequences due to or accompanied by overactivation of the Renin-Angiotensin-aldosterone axis are hypertension, thrombosis, hypertrophy, fibrosis, endothelial dysfunction, inflammation, and oxidative stress in cardiac, vascular, and renal tissues. Possible underlying molecular mechanisms are e.g. the stimulation of proliferative and hypertrophic signaling pathways, increased production or decreased degradation of extracellular matrix, and increased reactive oxygen species production (Atlas, 2007; Gekle and Grossmann, 2009; Marney and Brown, 2007; Weir and Dzau, 1999).

Due to these unwanted effects, also pharmacological antagonists of the Renin-Angiotensin-aldosterone axis have been developed, e.g. ACE inhibitors, AT1 receptor blockers, β-blockers, and aldosterone antagonists. They are used as therapeutic strategy to treat hypertension and associated cardiovascular and renal disorders. The combination of RAS inhibition and downregulation of AT1 receptor and MR activity, achieved by the simultaneous treatment with two or more of the above mentioned pharmacological antagonists, significantly reduces hypertension, cardiovascular and renal comorbidities, and mortality in patients (Atlas, 2007; Gekle and Grossmann, 2009; Marney and Brown, 2007; Weir and Dzau, 1999).

3.5. Aim of Thesis

In order to investigate physiological functions of the SPRED protein family, first detected and described in 2001 (Wakioka et al., 2001), we generated SPRED2 KO mice by a gene trap approach (Bundschu et al., 2005). SPREDs were identified as inhibitors of exclusively Ras/ERK/MAPK signaling (King et al., 2006; King et al., 2005; Miyoshi et al., 2004; Nobuhisa et

al., 2004; Nonami et al., 2004; Sivak et al., 2005; Wakioka et al., 2001), a cascade, which regulates cell proliferation and differentiation in almost every cell in almost every species. Thus, the suppressive effect of SPREDs on the Ras/ERK/MAPK pathway is thought to have widespread regulatory functions throughout the whole body.

In a first study, phenotypical characterization of SPRED2-deficient mice up to the age of five months demonstrated that loss of SPRED2 causes dwarfism due to consecutively upregulated ERK activity and thus identified SPRED2 as a novel regulator of chondrocyte differentiation and bone growth (Bundschu et al., 2005). Long term observations of SPRED2 KOs revealed an excessive grooming behavior, an abnormal high water uptake, and a reduced survival due to sudden death. Dissections of older mice or cadavers further disclosed clear signs of kidney deterioration. Therefore, I continued phenotypical characterization of SPRED2 KO mice to unravel these effects of SPRED2 deficiency in adult mice and to discover a common reason causing this versatile phenotype.

Due to the complex phenotype and the generally bad health state of SPRED2 KOs, we performed a broad analysis of serum parameters. Because this revealed profound salt and water imbalances, we considered a dysregulation of hormonal homeostasis as a possible cause. The accordingly performed systematic analysis of possibly contributing hormone axes showed that the disequilibrium in fluid and electrolyte balance was associated with hyperaldosteronism but did not affect AVP release. The detection of significantly lowered Ang II levels demonstrated that hyperaldosteronism developed independently of RAS activity. However, it was accompanied by increased aldosterone synthase expression. Aldosterone is together with corticosterone secreted by the adrenal gland, and both are under control of pituitary ACTH and of further upstream hypothalamic CRH. Therefore, we also investigated stress hormone release from the HPA axis, which was completely upregulated at all levels. According to current knowledge, HPA hormone actions are mainly mediated by G protein-coupled receptor pathways and steroid receptor-regulated gene expression. To date, only first insights were obtained how RTKs and MAPK pathways may participate in the regulation of the HPA axis-triggered stress hormone release (Blume et al., 2009; Gerrits et al., 2006; Khan and Watts, 2004; Singru et al., 2008). Thus, we aimed to discover a link between SPRED-mediated inhibition of Ras/ERK/MAPK signaling and HPA axis regulation.

Indeed, we detected that SPREDs, by suppressing Ras/ERK/MAPK-mediated activation of Ets transcription factors, can downregulate CRH transcription and release. This explained the hyperactivated HPA axis and the increased endogenous stress response in SPRED2 KO mice, both being reflected in the excessive grooming behavior. The hyperaldosteronism is in part a second consequence of enhanced HPA axis activity but mainly triggered by elevated adrenal aldosterone synthase expression. In SPRED2-deficient mice, this hyperaldosteronism elicits

hyperosmolality and polydipsia, the latter further contributing to hydronephrosis, kidney atrophy, and renal apotosis.

As a consequence of the gene trapping strategy, a truncated SPRED2 representing a functional EVH1 domain was expressed in our SPRED2 KO mice. Because the EVH1-β-geo expression might be reasonable for the severe and complex phenotype of our SPRED2 KOs, the exploration of its function was of special interest for us, too. In fact, our studies indicated a possible dominant negative effect of the fusion protein on the remaining SPRED1 expression and on Ras/ERK/MAPK signaling.

Although this study undoubtedly provided very valuable and interesting insights in phenotypical effects of SPRED2 deficiency, two follow-up studies investigating especially SPRED2 function in heart, and brain and a genetic screen to identify SPRED2-deficient humans are already in progress. Hereby, we aim to further enlighten and compare consequences of SPRED2 deficiency in mice and in humans.

Materials and Methods 4

4.1. Mouse Handling

4.1.1. Generation of SPRED2 KO Mice

The detailed procedure for the generation of SPRED2 KO mice has already been described previously (Bundschu, 2005; Bundschu et al., 2005; Ullrich and Schuh, 2009). In brief, SPRED2 KO mice were generated from the embryonic stem cell line XB228, which was obtained from BayGenomics, nowadays part of the IGTC. XB228 embryonic stem cells originated from 129P2/OlaHsd mice and contained the pGT0 gene trap vector, which inserted between exons 4 and 5 in the *Spred2* gene. XB228 cells with the trapped *Spred2* were injected into isolated blastocysts of super-ovulated and fertilized C57BL/6 female mice. Pseudo-pregnant foster mothers that have been mated with vasectomized male mice were used for reimplantation of blastocysts. To establish the SPRED2 KO mouse line, chimeric male offspring were mated to female C57BL/6 WT mice in order to test for germline transmission and to obtain first SPRED2 HET mice.

4.1.2. Mouse Raising and Breeding

Mice were housed in standard plastic cages, either individually or in groups of up to four mice, depending on their gender and the number of littermates. They were kept at a daily constant 12 h light and 12 h dark cycle, 25°C, and at a humidity of 50%. Tap water and standard mouse chow were available *ad libitum* unless stated otherwise.

In order to obtain offspring of all genotypes, i.e. SPRED2 WT, KO, and HET mice with equal ages in the same litter, usually one SPRED2 HET male mouse was mated with two SPRED2

HET female mice. To minimize possible inbred effects, mice were bred on a mixed 129P2/OlaHsd x C57Bl/6 genetic background.

4.1.3. Genotyping of SPRED2-deficient Mice

Mouse offspring was genotyped by PCR analysis using the REDExtract-N-Amp^{TM} Tissue PCR Kit from Sigma-Aldrich (Cat. No. XNATR). According to the protocol, genomic DNA was isolated from mouse tail tip biopsies of approximately 0.5 cm of length by incubating biopsies with a mixture of 100 µl Extraction Solution and 25 µl of Tissue Preparation Solution. Tail tips within the solution were incubated for 12 min at 55°C and boiled for 3 min at 95°C. After addition of 100 µl Neutralization Solution B, tissue extracts were ready for PCR amplification. The PCR reaction mix was set up with a 20 µl final volume and contained the following components for each sample:

Component	Volume	Final Concentration
REDExtract-N-Amp PCR Reaction Mix (2x)	10 µl	1x
SPR2-Geno-WT/KO-Forward Primer; Pr. 1 (10 mM)	0.8 µl	400 nM
SPR2-Geno-WT-Reverse Primer; Pr. 2 (10 mM)	0.8 µl	400 nM
SPR2-Geno-KO-Reverse Primer; Pr. 3 (10 mM)	0.8 µl	400 nM
Tissue Extract	4 µl	
Sterile Water	3.6 µl	
Final Volume	20 µl	

WT and KO PCRs were performed in the same tube using the following primers (Figure 13 A, Appendix 9.1.):

Primer	Sequence
SPR2-Geno-WT/KO-Forward Primer, Pr. 1	5` - GCTTGACCGGCACCCCGGTGAG - 3`
SPR2-Geno-WT-Reverse Primer, Pr. 2:	5` - GGGCACTGGATCCCTTGGAGC – 3`
SPR2-Geno-KO-Reverse Primer: Pr. 3:	5` - CGGATCTCAAACTCTCCTCC - 3`

The REDExtract-N-Amp PCR Reaction Mix already contains buffer, salts, dNTPs, Taq polymerase, JumpStart Taq antibody for hot start, and REDTaq loading dye. WT and KO fragments differing in size were amplified from the isolated DNA using the following cycling program:

Step	Temperature	Time	Number of Cycles
Initial Denaturation	94°C	3 min	1
Denaturation	94°C	1 min	
Annealing	59°C	1 min	30
Extension	72°C	1 min	
Final Extension	72°C	10 min	1

The resulting 803 bp WT fragment and the 452 bp KO fragment were separated on an agarose gel containing 1% agarose in 1 x TAE buffer (1 x Tris-Acetate-EDTA buffer: 40mM Tris, 20mM acetic acid, 1mM EDTA = ethylenediaminetetraacetic acid) and ethidium bromide at a final concentration of 0.5 µg/ml. PCR products were visualized, identified, and photographed by putting the gel on a UV-transilluminator (Gel Logic 100 Imaging System, Kodak) and by comparing the sizes of the PCR products with a DNA ladder (GeneRuler™ DNA Ladder Mix, Thermo Scientific; Cat. No. SM0331).

4.2. Mouse Experiments

In this study, all mouse experiments were conducted using at least seven SPRED2 KO mice and seven WT littermates as control. The WT and KO mouse groups always contained mice of comparable ages and comparable amounts of female and male littermates. The ages of mice used for the studies ranged between four and 24 months. The exact numbers and average ages of the mice used in the respective experiments are indicated in the “Results” section. All experiments have been approved by the local councils for animal care and were performed in accordance to the European law for animal care and use.

4.2.1. Examination of Water Uptake

Mice were kept in separate cages under standard conditions and were habituated to the new environment for 48 h. Water bottles were weighed every day for the period of one month and the volumes of consumed water were noted. The sum of the daily water volumes divided by the number of days revealed the average daily water uptake. Due to the hypochondroplasia-like dwarfism and the thereof dependent significantly reduced body weight in the SPRED2 KOs, the daily water consumption was further calculated in relation to body weight. Therefore, average daily water uptakes were divided by the respective body weight.

4.2.2. Experimental Water Deprivation

Mice were kept in standard cages individually or in groups according to their habitual environment. Water deprivation was carried out for 48 h, while mice had free access to mouse chow. A control group of animals was kept having free access to mouse chow and water. After 48 h both water-starved and control mice were weighed, trunk blood was taken, and serum was prepared as described below (4.2.3). Serum osmolalities were determined via freezing-point depression (Osmomat 030, Gonotec). For calculation of organ/body weight ratios of brain, adrenal gland, and kidney, total weights of tissues were measured and divided by the corresponding body weights.

4.2.3. Blood Collection and Serum Preparation

For routine laboratory measurements and most hormone determinations, blood was collected from the retro-orbital plexus. Therefore, mice were anesthetized by intraperitoneal injection of avertin (250 mg/kg body weight). Capillaries were generated by cutting the tips of Pasteur pipettes into pieces of 1 cm length with a glass knife. They were stored in PlusOne Repel-Silane ES (GE Healthcare; Cat. No. 17-1332-01), which prevents blood clotting within the capillary. For determination of serum AVP, trunk blood was collected in serum tubes after slight anesthetization with isoflurane (Isofluran CP, CP Pharma, Cat. No. 798-932). Blood was clotted in the serum tubes for 1 h. Coagulated blood was centrifuged at 3.000 x g for 15 min. The serum in the supernatant was stabilized by protease inhibitors (Complete EDTA-free Protease Inhibitor Cocktail Tablets, Roche, Cat. No. 04693132001), aliquoted, and stored at -80°C. Serum samples were used for determination of all in “Table 1” indicated routine serum parameters and for all hormone determinations except of CRH.

Preparation of Avertin	
Stock Solution (1g/ml)	1.25 g 2,2,2 tribromethanol (Cat. No. T48402) 1.25 ml tert-amyl alcohol (2-methyl-2-butanol, Cat. No. 152463)
Working Solution (25 mg/ml)	0.25 ml Stock Solution 9.75 ml 0.9% saline

4.2.4. Determination of Routine Laboratory Serum Parameters

Serum analysis of routine laboratory parameters was conducted in the Central Core Laboratory of the University Hospital Wuerzburg by standard automated laboratory analyzers using well-established and quality-controlled methods.

4.2.5. Determination of Hormone Levels

For detection of serum ACTH, aldosterone, corticosterone Ang II, GH, and IGF-1 blood was collected from the retro-orbital plexus between 9 and 12 a.m. For determination of serum AVP trunk blood was collected from water-starved and non-starved mice between 1 and 4 p.m. Serum was prepared as described above (4.2.3) and hormonal measurements were performed by EIA (enzyme immunoassay) or ELISA (enzyme-linked immunosorbent assay) using commercially available assays according to the manufacturer's instructions.

CRH was measured in brain lysates and in cell culture supernatants mHypoE-44 cells. For tissue lysates, mouse brains were prepared, the hypothalamic region containing the PVN was punched with a mold, and tissue was homogenized according to the manufacturer's instructions of the CRH ELISA kit. Hypothalamic lysates were stabilized with protease inhibitors (Complete EDTA-free Protease Inhibitor Cocktail Tablets, Roche, Cat. No. 04693132001), aliquoted, and stored at -80°C. For cell lysates, mHypoE-44 cells were seeded on 96-well plates and transfected with either SPRED1 or SPRED2 expression plasmids or empty vector (4.4.3). After starvation in low glucose DMEM without FBS for 48 h (4.4.5.), cell culture supernatants of mHypoE-44 cells were pipetted off and 50 µl of supernatants was used for CRH determination.

In each assay, determination of hormone levels in both provided standard reagents and mouse samples were performed in duplicate. The optical absorbance, which reflects the amount of hormone contained in the sample, was measured on a microplate reader (Wallac Victor^2 1420 Multilabel Counter, Perkin Elmer) at a wavelength of 450 nm. The mean values of duplicate readings were calculated for each standard and sample. A standard curve was generated by plotting the standard concentrations on the x-axis and the corresponding mean absorbance at

450 nm on the y-axis. For generation of the standard curve and for calculation of the unknown concentrations from the standard curve based on the measured absorptions, a four-parameter curve fitting software was used (Prism 4, GraphPad Software).

Hormone	Assay	Company
Aldosterone	ELISA	ALPCO Diagnostics, Cat. No. 11-ALDHU-E01
Corticosterone	EIA	Diagnostic Systems Laboratories, Inc., Cat. No. DSL-10-81100
ACTH	EIA	Peninsula Laboratories, LLC, Cat. No. S-1130
Ang II	EIA	Peninsula Laboratories, LLC, Cat. No. S-1133
GH	ELISA	Millipore, Cat. No. EZRMGH-45K
IGF-1	ELISA	Assay Pro, Cat. No. EMI1001-1
AVP	EIA	Assay Designs, Cat. No. 900-017
CRH	ELISA	Yanaihara Institute Inc., Cat. No. YK131

4.2.6. Wound Control and Monitoring

Mice that developed bloody and purulent wounds in facial and neck areas due to the excessive grooming behavior were controlled twice a week. Mice showing severe wounds, which extended the size of 1 cm^2 and did not improve within two weeks, were euthanatized or immediately used for experiments. In order to be able to monitor wound development, lesions were photographed by a digital camera (Coolpix 995, Nikon) once in a week.

4.3. Cloning of cDNAs and Expression Plasmids

4.3.1. pcDNA3.1-EVH1-β-geo and pcDNA3.1-β-geo

EVH1-β-geo, a fusion protein comprising a truncated form of SPRED2 and the gene trap vector-included reporter gene β-geo (fusion gene composed of β-galactosidase gene (lacZ) and neomycin resistance gene (neoR)), is still expressed in our SPRED2 KO mice. EVH1-β-geo contains a functional EVH1 domain but is without any attributed function yet. Both the EVH1-β-geo fusion protein and the β-geo reporter, the latter acting as a negative control for further

experiments, were cloned directly from RNA of SPRED2 KO mice (Appendix 9.2.). Because SPRED2 is highly expressed in brain and neural tissues, we used whole brain for RNA extraction. 1 ml of Trizol (Invitrogen, Cat. No. 10296-010) was added to 100 mg of brain tissue, and RNA was extracted from brain according to the manufacturer's instructions. For RT-PCR, 2 µg of total RNA and the following primers, which included the required restriction sites for cloning into pcDNA3.1/*myc*-His(-) B (NotI/HindIII), were used. Reverse transcription and amplification were performed using the Verso 1-Step RT-PCR Kit (Thermo Scientific, Cat. No. AB-1454/A) and a standard PCR protocol suggested by the manufacturer.

Primer	**Sequence**
NotI-S2/EVH1-β-geo -Forward, Pr. 4	5´-TAGCGGCCGC**ATG**ACCGAAGAAACACACCCGG-3´
NotI-β-geo-Forward, Pr. 5:	5´-TAGCGGCCGCGTCCCAGGTCCCGAAAACCAAA-3´
HindIII-Reverse (for both), Pr. 6:	5´-ATAAGCTT**TCA**GAAGAACTCGTCAAGAAGG-3´

After separation of PCR products by agarose gel electrophoresis (4.1.3.), DNA fragments of the predicted sizes, i.e. 4,422 bp for EVH1-β-geo and 3,984 bp for β-geo, were identified on a UV-transilluminator, cut out of the gel, and eluted using the NucleoSpin® Gel and PCR Clean-up Kit (Macherey-Nagel, Cat No. 740609.50). The purified cDNAs were cloned into the pCR-XL-TOPO® cloning vector via T/A cloning, which was enabled by their A-overhangs on 3´DNA ends produced by Taq polymerase and via the T-overhangs provided on 3´DNA ends of the pCR-XL-TOPO® cloning vector (TOPO® XL PCR Cloning Kit, Invitrogen, Cat No. K4700-10). After transformation of pCR-XL-TOPO®-EVH1-β-geo and pCR-XL-TOPO®-β-geo plasmids into One Shot® TOP10 Electrocomp™ E. coli (Invitrogen, included in TOPO® XL PCR Cloning Kit, Invitrogen, Cat No. K4700-10) and low scale plasmid preparation from bacteria cultures supplemented with suitable antibiotics (NucleoSpin® Plasmid Kit, Macherey-Nagel, Cat. No. 740588.250), the integrity and sequence of the EVH1-β-geo and β-geo inserts were checked by appropriate analytical restriction digests and custom DNA sequencing (Eurofins MWG; Ebersberg). Consecutively, pcDNA3.1/*myc*-His(-) B vector (Invitrogen, Cat. No. V855-20), a plasmid designed for overproduction of proteins in mammalian cell lines, pCR-XL-TOPO®-EVH1-β-geo and pCR-XL-TOPO®-β-geo plasmids were cut with NotI and HindIII in a preparative restriction digest (Fermentas). The desired DNA fragments, i.e. the digested backbone of pcDNA3.1/*myc*-His(-) B cloning vector and the digested inserts EVH1-β-geo and β-geo, were again eluted from an agarose gel after gel electrophoresis. Via ligation of sticky ends (Quick Ligation™ Kit, New England Biolabs, Cat. No. M2200S), EVH1-β-geo and β-geo were cloned into the NotI/HindIII sites of pcDNA3.1/*myc*-His(-) B. Both pcDNA3.1-EVH1-β-geo and

pcDNA3.1-β-geo expression plasmids were amplified in and re-isolated from bacterial cultures supplemented with appropriate antibiotics. Repeated analytical restriction digests and custom DNA sequencing verified the integrity of pcDNA3.1-EVH1-β-geo and pcDNA3.1-β-geo plasmids so that they were produced in large scale (NucleoBond® PC 500 Kit, Macherey-Nagel, Cat. No. 740574) for the transfection and expression in eukaryotic cells.

4.3.2. pGL3-CRH$_{Prom-RE}$ and pGL3-CRH$_{Prom}$

In order to perform *in vitro* assays to monitor the activity of the CRH promoter, we cloned a 5.7 kb region of the CRH promoter, which contained exon 1, critical regulatory elements, and transcription factor binding sites (Appendix 9.3.). In particular, the CRH gene contains a repressor element-1/neuron-restrictive silencing element (RE-1/NRSE) in the intron between CRH exons 1 and 2, a critical regulatory element, which is able to silence CRH transcription (Seth and Majzoub, 2001). In order to exclude possible suppressive effects of RE-1/NRSE on CRH transcription in general, we cloned both the CRH promoter region with and without the RE-1/NRSE repressor element (Figure 30 A and B). We amplified the 5.7 kb CRH promoter sequence including the RE-1/NRSE repressor (Figure 30 A) by PCR from genomic mouse DNA. DNA was isolated from thymus of a WT mouse using the DNeasy Blood & Tissue Kit (Qiagen, Cat. No. 69506). For PCR, 150 ng of isolated genomic DNA and the following primers including required restriction sites for cloning into pGL3-Basic vector (XhoI) were used. Amplification was conducted via Phusion High-Fidelity DNA Polymerase (Thermo Scientific, Cat. No. F-530S) according to a standard PCR protocol suggested by the manufacturer.

Primer	**Sequence**
XhoI-CRH-RE-1/NRSE-Forward, Pr. 7	5´-CCGCTCGAGATGGCCTTTCCAAGGGTAATTC-3´,
XhoI-CRH-RE-1/NRSE-Reverse, Pr. 8:	5´-CCGCTCGAGAGAAGGTGGGGGAGAAAGGTAA-3´

The DNA fragment representing the CRH promoter sequence including the RE-1/NRSE element with the predicted size of 5,834 bp was first cloned into the pCR-XL-TOPO® cloning vector in analogy to the cloning procedure indicated above in 4.3.1. Because the Phusion High-Fidelity DNA Polymerase does not produce A-overhangs on 3´DNA ends, A-tailing was performed using the PCR product purified from the agarose gel. After incubating with DreamTaq DNA Polymerase (Thermo Scientific, Cat. No. EP0703) for 20 min at 72°C, the A-tailed cDNA was again purified from an agarose gel. From pCR-XL-TOPO®-CRH$_{Prom-RE}$, the cloned CRH promoter region was transferred into the pGL3-Basic vector, which contains a firefly luciferase

reporter gene (Promega, Cat. No. E1751). Both pCR-XL-TOPO®-$CRH_{Prom-RE}$ and pGL3-Basic were cut with XhoI (Fermentas). pGL3-Basic was further dephosphorylated on 5`ends using Antarctic Phosphatase (New England Biolabs, Cat.No. M0289S) in order to avoid vector re-ligation. Via ligation of sticky ends, $CRH_{Prom-RE}$ was cloned in front of the luciferase reporter gene in the pGL3-Basic vector, which allows the monitoring of reporter gene expression under control of the CRH promoter after transfection into eukaryotic cell lines.

To be able to study CRH promoter activity also in the absence of the RE-1/NRSE repressor, we generated a second CRH promoter reporter without the RE-1/NRSE element (Figure 30 B). Because we were not able to amplify and to clone the shortened CRH promoter region directly from genomic mouse DNA, the RE-1/NRSE silencer was removed retroactively, resulting in a CRH promoter sequence with a predicted size of 5,669 bp. The only endonuclease with the property to cut once between exon 1 and RE-1/NRSE in the CRH promoter and to not cut in the pGL3-Basic vector was the restriction endonuclease Eco91I (Fermentas). Eco91I further fitted in a double digest with BglII or HindIII, the only usable restriction sites in the pGL3-Basic vector for our purpose. Because the double digest of pGL3-$CRH_{Prom-RE}$ with Eco91I and BglII produced sticky ends that did not fit to each other, T4 DNA Polymerase (Thermo Scientific, Cat. No. EP0061) was used to blunt DNA ends due to its ability to fill-in 5' DNA-overhangs and to remove 3' DNA-overhangs. After incubation with T4 DNA Polymerase according to the manufacturer's instructions, quick ligation of blunt ends was performed, revealing at least a pGL3-Basic-CRH promoter reporter vector lacking the RE-1/NRSE repressor (pGL3-CRH_{Prom}).

4.4. Cell Culture, Transfection, and *in vitro* Assays

4.4.1. Cultivation of HEK 293 T cells

Cells of the adherent HEK 293 T cell line (Human Embryonic Kidney Cells) were grown in high glucose Dulbeccos modified Eagle´s medium (DMEM, Invitrogen, Cat. No. 31966047), which already contained 25 mM glucose, 5.67 mM L-glutamine, and 1 mM sodium pyruvate. Culture medium was further supplemented with 10% fetal bovine serum (FBS, Invitrogen, Cat. No. 10500-064). To maintain the cell line, cells were kept on 10 cm plates at 37°C and 5% CO_2 and grown in a monolayer to a confluency of 80-90%. Every 3 to 4 days, cells were rinsed in sterile phosphate buffered saline (1xPBS: 137 mM NaCl, 2,7 mM KCl, 10 mM Na_2HPO_4, 2mM

KH_2PO_4, pH 7.4), detached with 0.05% trypsin-EDTA (Invitrogen, Cat. No. 15400054), and replated at a ratio of 1:10 or 1:20 after resuspension in fresh culture medium.

4.4.2. Cultivation of mHypoE-44 cells

Cells of the embryonic mouse hypothalamic cell line mHypoE-44 also grew in monolayer cultures attached to the tissue culture plate. They were maintained in high glucose DMEM (Invitrogen, Cat. No. 61965059), which already included 25 mM glucose and 3.97 mM L-glutamine and which was supplemented with 10% FBS. For cultivation, mHypoE-44 cells were kept on 10 cm plates at 37°C and 5% CO_2 until the adherent monolayer reached a confluency of 70-90%. Every 2 to 4 days, cells were rinsed with 1xPBS, detached with 0.05% trypsin-EDTA, and splitted with a plate ratio of 1:4 to 1:10 in fresh culture medium.

4.4.3. Transfection of HEK 293 T and mHypoE-44 cells

24 h before transfection, HEK 293 T and mHypoE-44 cells, respectively, were splitted in an appropriate ratio and seeded in the appropriate culture medium to reach 90% confluency overnight. Cells were transiently transfected with Lipofectamine® 2000 Reagent (Invitrogen, Cat. No. 11668-027). The used amount of DNA, culture medium, and transfection reagent depended on the size of culture plates, as also indicated in the manufacturer's instructions. Transfection of HEK 293 T and mHypoE-44 cells was performed with the appropriate culture media without FBS. Dependent on the experimental design, cells were single or cotransfected with the expression plasmids listed below (Appendix 9.4., Vector Cards):

Name of Plasmid	Vector Backbone	cDNA
Mock	pcDNA3.1/*myc*-His(-) A	-
Mock	pcDNA3.1/*myc*-His(-) B	-
Mock	pGL3-Basic	-
pcDNA3.1-SPRED1	pcDNA3.1/*myc*-His(-) A	*Spred1*
pcDNA3.1-SPRED2	pcDNA3.1/*myc*-His(-) A	*Spred2*
pcDNA3.1-EVH1-β-geo	pcDNA3.1/*myc*-His(-) B	*EVH1-β-geo*
pcDNA3.1-β-geo	pcDNA3.1/*myc*-His(-) B	*β-geo*
pRL-TK	pTK	*Renilla Luciferase*

pGL3-$CRH_{Prom\text{-}RE}$	pGL3-Basic	*$CRH_{Prom\text{-}RE}$*
pGL3-CRH_{Prom}	pGL3-Basic	*CRH_{Prom}*
pGL2-4xEts1	pGL2-Basic	HSV-TK-*4xEts1*

6 h after transfection, serum-free medium was replaced by normal culture medium containing FBS. 18 - 48 h after transfection, cells were prepared for Western Blot, ERK activity assay, luciferase assay, ELISA, or X-Gal (5-bromo-4-chloro-3-indolyl-beta-D-galactopyranoside) staining.

4.4.4. *In vitro* ERK Activity Assay

24 h before transfection, HEK 293 T cells were seeded on 6-well plates coated with 0.1% gelatin in PBS. Cells were transiently transfected with pcDNA3.1 expression plasmids for SPRED1, EVH1-β-geo, β-geo, or empty vector as described above (4.4.3). After transfection, serum-free medium was not replaced as usual but cells were serum-starved for 36 h in order to downregulate GF-dependent pathways. In order to re-activate especially the Ras/ERK/MAPK cascade in the starved cells, serum-free medium was removed and transfected HEK 293 T cells were stimulated for 3 min with 10 ng/ml EGF (Cell Signaling, Cat. No. 8916). EGF was dissolved in Krebs-Ringer-HEPES buffer (122.5 mM NaCl, 5.4 mM KCl, 0.8 mM $MgCl_2$, 1.2 mM $CaCl_2$, 1.0 mM NaH_2PO_4, 10 mM HEPES (4-(2-hydroxyethyl)-1-piperazineethanesulfonic acid), 6 mM Glucose), which was pre-warmed to 37°C. After EGF-dependent stimulation of ERK phosphorylation and activity, cells were homogenized for Western blot analyses.

4.4.5. *In vitro* CRH Promoter Reporter Assay

24 h before transfection, mHypoE-44 cells were seeded on 96-well plates. Cells were either transfected (4.4.3) with the CRH promoter luciferase reporter vector containing the RE-1/NRSE repressor (pGL3-$CRH_{Prom\text{-}RE}$) or lacking it (pGL3-CRH_{Prom}). Additionally, cells were cotransfected with the *Renilla* luciferase control reporter vector (pRL-TK, Promega, Cat. No. E2241). CRH promoter activity was either monitored in the presence of cotransfected SPRED1 and SPRED2, respectively, and in each case both in the presence or absence of EVH1-β-geo. In order to stimulate CRH promoter activity, which is normally induced in response to stress, mHypoE-44 cells were starved for glucose and FBS after transfection. Thus, the serum-free but high glucose DMEM was replaced by low glucose DMEM without FBS (5.56 mM glucose, 3.97 mM L-glutamine, Invitrogen, Cat. No. 21885108) for 24 - 30 h after transfection. Firefly and

Renilla luciferase activity were determined using the Dual-Glo System (Promega, Cat No. E2920) and detecting the luminescence by a microplate reader (Wallac Victor^2 1420 Multilabel Counter, Perkin Elmer). For each sample, firefly luciferase signals were normalized to *Renilla* luciferase activity. Because each of the various combinations of plasmid transfections were performed at least twelve times, mean values were calculated from the firefly/*Renilla* luciferase signal ratios for each experimental approach. The mean value of samples only transfected with CRH promoter luciferase reporter and *Renilla* luciferase control vector was set to 1 and mean values of all other cotransfected samples were expressed as x-fold of 1.

4.4.6. *In vitro* Ets Transcription Factor Reporter Assay

According to the CRH promoter reporter assay, an Ets transcription factor reporter assay was performed. Instead of the CRH promoter luciferase reporter (pGL3-CRH_{Prom}), a luciferase reporter vector containing 4 Ets1 transcription factor binding sites (pGL2-4xEts1) was used (Appendix 9.5., 4.4.3., (Hoffmeyer et al., 1998)). mHypoE-44 cells were prepared for transfection and transfected as described above (4.4.3., 4.4.5.) with the exception that cells were only starved for FBS but not for glucose 24 - 30 h after transfection. Luciferase activity determination and data analyses were also performed in accordance to the CRH promoter reporter assay (4.4.5.).

4.5. Analysis and Quantification of Protein and mRNA Expression

4.5.1. Western Blot

For analysis of protein expression in cell lysates by Western Blot, cells were seeded on 6-well plates 24 h prior to transfection and transfected with the desired plasmids as described in 4.4.3. 18 - 48 h past transfection or after termination of ERK activity assay, cells were scratched from culture wells and lysed in 2% SDS (sodium dodecyl sulphate) in PBS. Lysis buffer was supplemented with Complete EDTA-free Protease Inhibitor Cocktail Tablets and PhosSTOP Phosphatase Inhibitor Cocktail Tablets (Roche, Cat. No. 04906837001) to prevent degradation and de-phosphorylation of proteins, in our case especially the de-phosporylation of ERK. For

analysis of mouse tissue lysates, 50 mg of the desired tissue was homogenized with a homogenizer (Polytron PT 3100) in 1 ml of 2% SDS/PBS sample buffer containing protease and phosphatase inhibitors as described above. If cell or tissue samples appeared very viscous due to DNA released from the nucleus, lysates were sonified for 10 s at 50% duty cycle and 50% power (Sonopuls HD 2070, Bandelin). Protein concentrations were estimated via UV-spectroscopy by inserting the measured absorptions into the following formula: protein concentration (mg/ml) = 1.55 x (A_{280}-A_{320}) - 0.76 x (A_{260}-A_{320}). Protein samples that were not immediately used for Western blot were stored at -80°C. Before loading on 6 - 12% polyacrylamide gels, probes were supplemented with Laemmli buffer. Protein samples (cell lysates: 5 - 20 µg, mouse tissue lysates: 30 - 50 µg of total protein) and a marker containing proteins with defined sizes (PageRuler Prestained Protein Ladder, Fermentas, Cat. No. 26616) were separated by SDS-PAGE (sodium dodecyl sulphate-polyacrylamide gel electrophoresis) under reducing conditions according to their size. The separated proteins were electrotransferred from the gel to nitrocellulose membranes (Protran BA38, Whatman, Cat. No. 10401396) using semi-dry blotters (Fastblot B44, Biometra, 015-200). Protein transfer and loading amount were verified by Ponceau S staining of the nitrocellulose membranes.

Solution/Buffer	**Contents**
Resolving Gel (10 ml), depending on percentage (6 - 12%):	5.3 - 3.3 ml H_2O, 2 - 4 ml 30% acrylamide mix (Rotiphorese®Gel 30, Roth, Cat. No. 3029.1), 2.5 ml 1.5 M Tris (pH 8.8), 100 µl 10% SDS, 100µl 10% ammonium persulfate (APS), 8 - 4 µl tetramethylethylendiamin (TEMED)
Stacking Gel (10 ml, 5%)	6.8 ml H_2O, 1.7 ml 30% acrylamide mix, 1.25 ml 1.0 M Tris (pH 6.8), 100 µl 10% SDS, 100µl 10% APS, 10 µl TEMED)
5 x Laemmli Buffer	(250 mM Tris pH 6.8, 10% SDS, 40% glycerol, 0.05% bromphenolblue, 5% β-mercaptoethanol)
1 x SDS-PAGE Running Buffer	25 mM Tris base, 192 mM glycine, 0.1% SDS
1 x Western Blot Transfer Buffer	25 mM Tris base, 192 mM glycine, 0.1% SDS, 20% methanol
Ponceau S Staining Solution	2% Ponceau S, 30% trichloracetic acid, 30% sulfosalicylic acid
Wash Solution	0.05% Tween 20 in PBS
Blocking/Antibody Incubation Solution	4% non-fat dry milk powder in 0.05% PBS-Tween 20

To reduce unspecific antibody binding, membranes were blocked with 4% milk in 0.05% PBS-Tween for at least 1 h. Membranes were incubated with primary antibodies diluted in blocking

solution at 4°C overnight and washed 4 times for 5 min with 0.05% PBS-Tween. Incubation with the secondary antibodies was performed at room temperature for 1 - 2 h before blots were washed again. For signal detection, the ECL (Enhanced Chemoluminescence) Plus Western Blotting Substrate Kit was used according to the manufacturer's instructions (Pierce, Cat. No. PI80196).

Antibody	Dilution	Company/Reference
SPRED2	1:500	(Bundschu, 2005; Bundschu et al., 2005)
β-galactosidase (β-gal)	1:5,000	Abcam, Cat. No. ab616
p44/42 MAPK (ERK)	1:2,000	Cell Signaling, Cat. No. 9102
Phospho-p44/42 MAPK (P-ERK)	1:1,000	Cell Signaling, Cat. No. 9101
Peroxidase-AffiniPure Goat Anti-Rabbit IgG (Immunoglobulin G)	1:10,000	Jackson ImmunoResearch, Cat. No. 111-035-144)

4.5.2. Northern Blot

Northern blot analysis was performed in order to examine the levels of CRH mRNA in SPRED2 KO mice and WT controls. Mice were decapitated, brains were removed, and the hypothalamic PVN region was prepared by punching with a mold. RNA was isolated using Trizol (Invitrogen, Cat. No. 10296-010) and re-suspended in RNase-free DEPC water. 20 µg of each total RNA sample were supplemented with RNA loading dye (Thermo Scientific, Cat. No. R0641) and size-separated in a formaldehyde-agarose gel. The separated RNA was transferred onto a nylon membrane (Hybond™-N+, GE Healthcare, Cat. No. 45-000-932) by a capillary blot using 20 x SSC and was fixed to the membrane by UV crosslinking for 3 min at 312 nm. To generate a CRH-specific probe, a 357 bp cDNA sequence of CRH located in exon 2 was amplified by RT-PCR (Appendix 9.7., Verso 1-Step RT-PCR Kit, Thermo Scientific, Cat. No. AB-1454/A). Therefore, RNA isolated from a WT mouse brain, the following primers, and a standard RT-PCR protocol suggested by the manufacturer were used.

Primer	Sequence
CRH-Ex2-Forward, Pr. 9	5´-AGCCCTTGAATTTCTTGCAG-3´
CRH-Ex2-Reverse, Pr. 10:	5´-GGTGGAAGGTGAGATCCAGA-3´

The probe was labeled radioactively with ^{32}P using the Prime-It II Random Primer Labeling Kit (Stratagene, Cat. No. 300385) according to the manufacturer's instructions. In order to block unspecific binding of nucleic acids to the membrane, the membrane was pre-hybridized in hybridisation buffer for 1 h at 42°C. After purification of the radioactively labeled probe using a Sephadex column (PD MiniTrap G-10, GE Healtcare), the probe was added to the hybridisation solution and incubated on the membrane for 24 h at 42°C. The membrane was washed twice with low stringency wash buffer at 42°C first and then twice with high stringency wash buffer at 55°C. Radiographic signals resulting from the amount of radioactive ^{32}P bound to the Northern blot membrane and representing the expression level of CRH mRNA were detected by a Phosphoimager (BAS-1500, FujiFilm) and quantified as described below (4.5.3.).

Solution/Buffer	**Contents**
DEPC-H_2O	0.1% diethylpyrocarbonate (DEPC) in H_2O, stirred for at least 2 h at 37°C, then autoclaved to inactivate DEPC
Running Buffer (1 x MOPS)	20 mM MOPS (3-(N-morpholino)propanesulfonic acid), 5 mM sodium acetate, 1 mM EDTA
RNA Gel	1% RNA agarose in 1 x MOPS
20 x SSC (Saline-Sodium Citrate)	3 M NaCl, 0.3 M trisodium citrate
100 x Denhard´s Solution	2% bovine serum albumin (BSA), 2% Ficoll, 2% polyvinylpyrolidone
Hybridisation Buffer	50% formamide, 25% 20 x SSC, 5% 100 x Denhard´s Solution, 5% 10% SDS, 500 µg salmon sperm DNA (Applichem, Cat. No. A2160)
Low Stringency Wash Buffer	2 x SSC, 0.1% SDS
High Stringency Wash Buffer	0.2 x SSC, 0.1% SDS

4.5.3. Quantification of ERK Phosphorylation and of CRH mRNA Levels in Brain

For quantification of ERK activity, Western blots demonstrating the levels of ERK and P-ERK in WT and SPRED2 KO mice were scanned and converted to TIFF files. Band intensities were quantified using ImageJ software (National Institutes of Health) and expressed as arbitrary densitometric units. For every mouse sample, the ratio of P-ERK to total ERK was calculated. Mean value of all WT samples was set to 1 and mean value of KO samples was expressed as x-fold of WT.

For quantification of CRH mRNA levels, band intensities were also quantified using ImageJ. For every mouse sample, the ratio of CRH mRNA band intensities to total RNA was calculated, the mean ratio of WT was normalized to 1, and mean value of KO samples was expressed as x-fold of WT.

4.6. Histology and Immunohistochemistry

4.6.1. Hematoxylin and Eosin Staining (H&E Staining)

To investigate morphology, kidneys were dissected from sacrificed mice, fixed in 4% paraformaldehyde (PFA)/PBS for 24 h, and embedded in paraffin. 7 µm sections were collected on SuperFrost Plus microscope slides (Thermo Scientific, Cat No. 10149870). According to a standard protocol (http://web.uni-frankfurt.de/fb15/nrp/br/script/node18.html), sections were deparaffinized, rehydrated, stained with haematoxylin and eosin, dehydrated, and mounted with Entellan (Merck Millipore, Cat. No. 107960). Overview photos were taken by an Axiophot 2 microscope equipped with a 2.5-fold plan objective and an AxioCam MRc Rev.3 FireWire camera (Zeiss). Detailed photos were taken by an Eclipse E600 microscope (Nikon) equipped with 10-, 60-, and 100-fold objectives and a DXM1200F camera (Nikon).

4.6.2. TUNEL Assay

Apoptotic processes in kidneys were investigated by a TUNEL (Terminal deoxynucleotidyl transferase dUTP nick end labeling) assay, which was based on the breakdown of DNA especially in apoptotic cells. Dissected kidneys were embedded in Tissue-Tek OCT-compound (Sakura, Cat. No. 4583) in compatible plastic tubes and snap-frozen in liquid nitrogen. 5 µm cryosections were cut using a CM1950 cryostat (Leica) equipped with C35 carbon steel microtome blades (Feather/PFM medical, Cat. No. 207500003) and collected on SuperFrost Plus microscope slides. Slices were fixed, permeabilized, and fragmented DNA of apoptotic cells was labeled with flourescein-12-dUTP at 3´-OH DNA ends using the enzyme terminal deoxynucleotidyl transferase according to the manufacturer's instructions (DeadEnd™ Flourometric TUNEL System, Promega, Cat. No. TB235). Thus, apoptotic cells in the kidney could be identified by green fluorescence. Nuclei of all renal cells were counterstained with 0.1µg/ml DAPI (4',6-diamidino-2-phenylindole) in PBS. All stained sections were mounted with

Mowiol 4-88 (Roth, Cat. No. 9002-89-5) and investigated by a BX41 microscope (Olympus) equipped with 20- and 60-fold objectives and a CCD-FV2T camera (Olympus). Photos were pseudo-colored using the computer-assisted image analysis system Cell-D (Olympus).

4.6.3. Immunohistochemistry

Dissected brains, pituitary glands, adrenal glands, and kidneys were embedded in Tissue-Tek, and 10 µm cryosections were prepared as described above (4.6.2.). Tissue slices were fixed in 4% PFA/PBS for 10 min, permeabilized with 0.2% Triton X-100 in PBS for 20 min, and blocked in 10% goat serum/PBS for at least 1 h. Primary antibodies were incubated overnight, secondary antibodies for 2 h, both in 10% goat serum/PBS and in a humidified chamber in the dark. After incubation with antibodies, slides were washed 4 times with PBS. Stained sections were investigated and photographed using an Eclipse E600 microscope equipped with a C1 confocal scanning head and 10-, 60-, and 100-fold objectives (Nikon).

Antibody	Dilution	Company/Reference
SPRED2	1:50	(Bundschu, 2005; Bundschu et al., 2005)
Aldosterone Synthase	1:50	(Wotus et al., 1998)
Alexa Fluor® 488 Goat Anti-Rabbit IgG	1:1,000	Invitrogen, Cat. No. A11008
Alexa Fluor® 594 Goat Anti-Rabbit IgG	1:1,000	Invitrogen, Cat. No. A11012

4.6.4. X-Gal Staining

X-Gal stainings were performed as previously described (Ullrich and Schuh, 2009). In brief, HEK 293 T cells were stained upon removal of culture medium and washing with PBS. For staining of tissue sections, 5 µm cryosections were prepared as described above (4.6.2) and slices were mounted with glycerol after staining. Whole organs were washed with PBS and stained directly after dissection. All specimens were fixed in X-Gal Fixation Buffer. Cells and tissue sections were fixed for 15 min, organs for 15 min up to 1 h depending on size. After washing of cells and slices with X-Gal Wash Buffer 2 times for 5 min, and of whole organs 3 times for 15 - 30 min, specimens were stained overnight with X-Gal Staining Buffer in a humidified chamber at 37°C. For better permeabilization of organs, 0.01% deoxycholate and 0.02% Nonidet P-40 were included in both wash and staining buffers. Whole organs were photographed by a digital camera (Coolpix 995, Nikon), cells and tissue sections by an Eclipse

E600 microscope equipped with 10-, 60-, and 100-fold objectives and a DXM1200F camera (Nikon).

Solution/Buffer	Contents
0.1 M Phosphate Buffer	27 mM NaH_2PO_4, 73 mM Na_2HPO_4
X-Gal Fixation Buffer	0.1 M Phosphate Buffer supplemented with 5 mM EGTA (ethylene glycol tetraacetic acid, pH 8), 2 mM $MgCl_2$, and 0.2% glutaraldehyde
X-Gal Wash Buffer	0.1 M Phosphate Buffer supplemented with 2 mM $MgCl_2$
X-Gal Stock Solution (50 mg/ml)	500 mg X-Gal in 10 ml dimethylformamide
X-Gal Staining Buffer	0.1 M Phosphate Buffer supplemented with 2 mM $MgCl_2$, 5 mM $K_4Fe(CN)_6$, 5 mM $K_3Fe(CN)_6$, and 1mg/ml X-Gal

4.7. Statistics

All results included in this study are expressed as mean ± standard deviation. Values of $p<0.05$ were considered as statistically significant and degrees of statistical significance were defined as $*p<0.05$, $**p<0.01$, and $***p<0.001$.

4.7.1. Basic Statistics

All data sets were analyzed by comparing the different sample groups in each experiment using unpaired two-sample *t*-tests or Welch´s tests depending on their homogeneity of variances. Normal distribution of data was ensured using graphical analysis tools provided by Statistica (StatSoft), such as box plot and quantile-quantile plot.

4.7.2. Kaplan-Meier Survival Analysis

To determine the survival probability of SPRED2 KO mice in comparison to WT littermates, we observed 20 SPRED2 KO mice and 20 WT littermate controls starting from their date of birth until the age of 18 months and documented, if applicable, the age of death. Kaplan-Meier

survival curves were generated using WinSTAT (Statistics Software Add-In for Microsoft Excel). This software included the generation of survival curves and life tables of WT and KO mice, and the calculation of statistical differences between the survival rates of WT and KO groups by computation of logrank test, chi-square, and *p* values.

Results 5

5.1. Generation of SPRED2 KO Mice

The family of SPRED proteins was detected by a yeast two hybrid screen and was described by a Japanese group due to their sequence homology to Sprouty proteins (Wakioka et al., 2001). In parallel, our group discovered the SPREDs because of their sequential homology to the EVH1 domain of VASP. To investigate physiological consequences of SPRED deficiency, we started to generate SPRED2 KO mice by a gene trap approach in 2003 (Bundschu, 2005; Bundschu et al., 2005). In brief, the embryonic stem cell clone XB228 originating from 129P2/OlaHsd mice was injected into isolated blastocysts of super-ovulated and fertilized C57BL/6 female mice. The blastocysts were reimplanted into pseudo-pregnant foster mothers that have been mated with vasectomized male mice. Chimeric male offspring were mated to female C57BL/6 WT mice to test for germline transmission and to obtain first SPRED2 HET mice to establish the SPRED2 KO mouse line (Figure 6).

The XB228 cell line comprises a disrupted *Spred2* gene resulting from the random insertion of the pGT0pfs gene trap vector between exons 4 and 5 of *Spred2* (Figure 12 A). This gene trap vector includes a promoterless fusion gene (*β-geo*). It is composed of a reporter gene (*lacZ*) allowing profiling of endogenous promoter activity and of an antibiotic resistance gene (*neoR*) enabling the positive selection of gene trap vector integration. This fusion gene is flanked by an upstream splice acceptor (SA) and a further upstream intronic sequence of the *Engrailed2* gene (En2 intron 1). Both the splice branch site included in En2 intron 1 and the SA are required for proper vector integration and splicing. *β-geo* is flanked downstream by a transcriptional termination sequence (Simian virus 40 polyadenylation site, pA) and by a part of the pUC vector backbone (pUC), which is needed for proper gene trap vector amplification before integration into the mouse genome.

Prior to blastocyst injection of the ES cell clone, gene trap vector insertion and expression of the reporter protein β-gal was confirmed by X-Gal staining of ES cells (Figure 12 B). The enzyme β-

gal converts X-Gal to 5,5'-dibromo-4,4'-dichloro-indigo, an intensely blue and insoluble product, which stains cells and tissues and thus monitors *Spred2* promoter-driven expression of the reporter instead of *Spred2*.

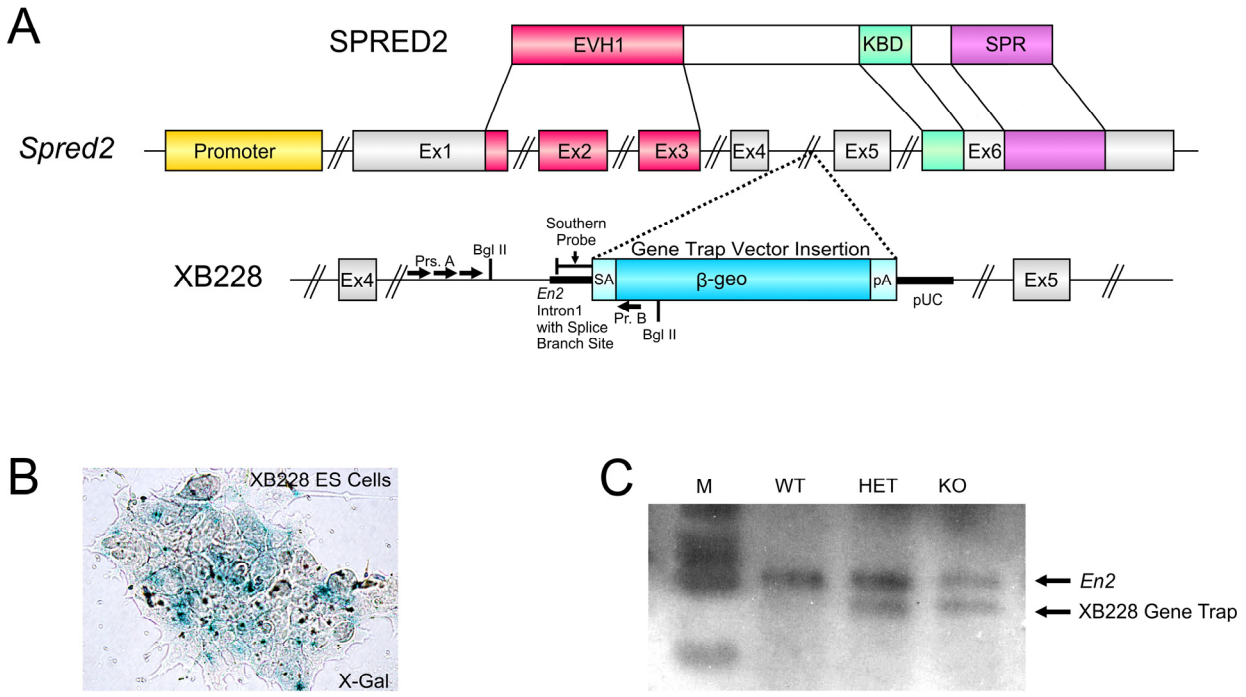

Figure 12: Generation of SPRED2 KO Mice - Localization and Verification of Gene Trap Vector Insertion
A) The pGT0pfs gene trap vector disrupts the *Spred2* gene by random insertion between exons (Ex) 4 and 5. It comprises a part of the *Engrailed2* intron 1 structure (*En2* intron 1), a splice acceptor site (SA), a promoterless β-galactosidase (*lacZ*)/neomycin resistance (*neoR*) fusion gene (*β-geo*), a Simian virus 40 polyadenylation sequence (pA), and a pUC backbone sequence. A reverse primer located in the gene trap vector (Pr. B) and different forward primers (Prs. A) covering the complete intron 4 of *Spred2* were used for definition of the exact gene trap vector insertion point in *Spred2* by PCR. For verification of single gene trap vector integration by Southern Blotting, genomic mouse DNA was digested with Bgl II, as indicated cutting only once at the 5´end of the gene trap vector and just upstream of it. Digested DNA samples were labeled using a part of the *En2* intron 1 sequence as a probe. *Figure based on (Bundschu et al., 2005).* **B)** X-Gal staining of cultured XB228 ES cells demonstrating by blue color the gene trap vector integration in *Spred2* and the ability to monitor *Spred2* promoter-driven expression of the *β-geo* reporter gene instead of *Spred2. Figure in part reproduced from (Bundschu et al., 2006a) with permission from Elsevier.* **C)** Southern blot with DNA of SPRED2 WT, HET, and KO mice. The upper band, which is present in all samples, corresponds to the endogenous *En2* gene. The lower band was only seen in HET and KO mouse DNA and represents the single insertion of the gene trap vector (M: DNA-Marker). *Figure in part reprinted from (Bundschu et al., 2005).*

The exact gene trap vector insertion point in *Spred2* was defined by PCR using a reverse primer located in the gene trap vector and different forward primers covering the complete intron 4 of the *Spred2* gene (Prs. A and B, Figure 12 A). Subsequent sequencing of PCR products, which were only obtained with forward primers very near by the insertion point, identified the latter. Single integration was verified by Southern blot with genomic DNA digested with BglII,

cutting just upstream of the gene trap vector and only once at its 5´end. A part of the pGT0pfs vector downstream of the BglII cutting site, representing a part of the *En2* intron 1 sequence, was used as a radioactive probe (Figure 12 C).

The successful disruption of the *Spred2* gene in the SPRED2 KO mice was confirmed on RNA level by RT-PCR and Northern blot and on protein levels by Western blot. Hence, we could monitor SPRED2 expression in a great variety of organs isolated from SPRED2 KO mice and WT littermates (Bundschu et al., 2005).

5.2. Breeding and Genotyping of SPRED2 KO Mice

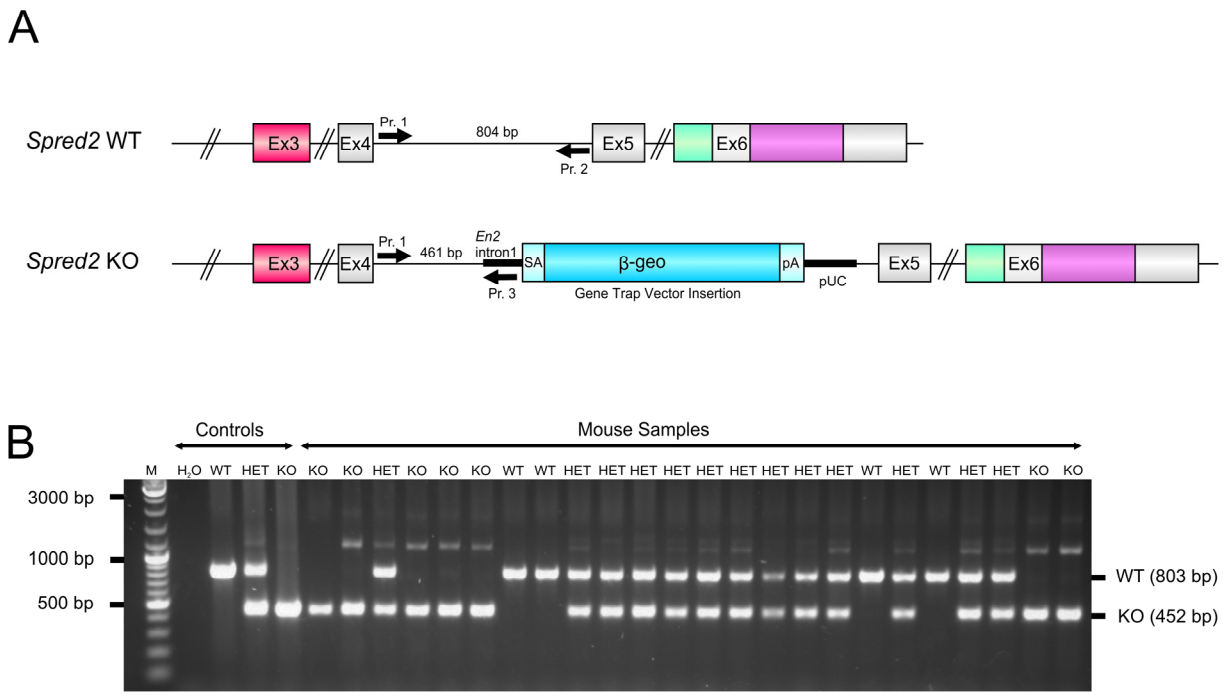

Figure 13: Genotyping of SPRED2 KO Mice

A) Genomic exon/intron organization of the murine WT *Spred2* gene and of the "trapped" *Spred2* gene in SPRED2 KO mice. Offspring was genotyped by PCR using a common forward primer located upstream of the gene trap vector insertion point in intron 4 (SPR2-Geno-WT/KO-Forward Primer; Pr. 1). The WT allele was specifically amplified by combining the forward primer with a reverse primer located downstream of the insertion at the end of intron 4 (SPR2-Geno-WT-Reverse Primer; Pr. 2). For amplification of the KO allele, a reverse primer (SPR2-Geno-KO-Reverse Primer, Pr. 3) located at the beginning of the gene trap vector was used (Ex= Exon, *En2* intron 1 = *Engrailed2* intron 1 structure, SA = splice acceptor site, β-geo = β-galactosidase (lacZ)/neomycin resistance (neoR) fusion gene, pA = Simian virus 40 polyadenylation sequence, pUC = pUC vector backbone sequence). *Figure based on (Bundschu et al., 2005).* **B)** Exemplary picture of a genotyping PCR after agarose gel electrophoresis. According to the primers used for genotyping, WT mice were identified by the amplification of a 803 bp DNA fragment, SPRED2 KOs by the amplification of a 452 bp fragment, and HETs by containing both the WT and KO amplicons (M=Marker).

To maintain the SPRED2 KO mouse line, usually one SPRED2 HET male mouse was mated with two SPRED2 HET female mice. Thus, the offspring contained littermates of all genotypes, i.e. SPRED2 WT, KO, and HET mice with equal ages. Mating of SPRED2 KO mice among each other was also possible, but offspring was obtained in only about 50% of the breeding pairs. To minimize possible inbred effects, mice were kept on a mixed 129P2/OlaHsd × C57Bl/6 genetic background.

Offspring were genotyped by PCR analysis with a modified and renewed protocol, which allows the amplification of WT and KO alleles together in one reaction and which produces considerably shorter amplicons, thus enabling fast and easy genotyping. For PCR, a common forward primer located upstream of the gene trap vector insertion point in intron 4 (SPR2-Geno-WT/KO-Forward Primer; Pr. 1) was used. In combination with a WT allele-specific reverse primer (SPR2-Geno-WT-Reverse Primer; Pr. 2) located downstream of the insertion at the end of intron 4 and with a KO allele-specific reverse primer (SPR2-Geno-KO-Reverse Primer, Pr. 3) located within the gene trap vector (Figure 13 A, Appendix 9.1.), characteristic WT and KO fragments were amplified. This genotyping PCR results in the generation of an 803 bp WT amplicon and of a 452 bp SPRED2 KO amplicon (Figure 13 B).

5.3. The EVH1-β-geo Fusion Protein Expressed in SPRED2 KO Mice May Act Dominant Negative

In our KO mice, the *Spred2* gene was disrupted by insertion of a gene trap vector between exons 4 and 5 of *Spred2* (Figure 12 and 13). Although the *Spred2* gene was interrupted by gene trap vector insertion, the first 4 exons of *Spred2* remained intact. Because of the SA and the splice branch site provided by the gene trap vector and due to the SD in upstream exon 4, β-geo is spliced to the end of *Spred2* exon 4 after transcription of the trapped *Spred2* allele. Upon translation of the "trapped" *Spred2* gene, either the sole β-geo reporter is expressed if the internal start codon of β-geo is used or a fusion protein harboring *Spred2* exon 1-4 and β-geo if the start codon of *Spred2* is used (Figure 14). Thus, a potentially expressed fusion protein would then comprise a complete and functional EVH1 domain encoded by exons 1-3, while KBD and SPR domains, both encoded by exon 6, would be deleted.

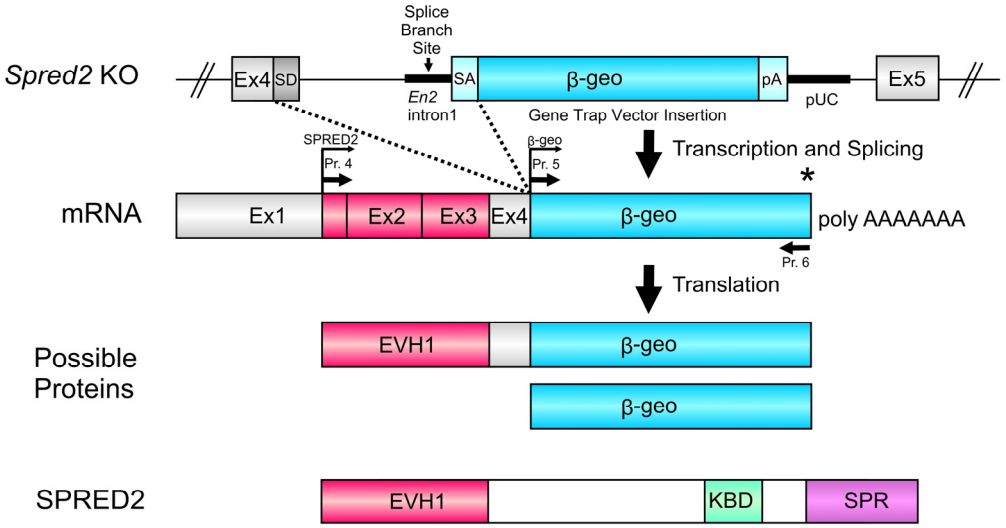

Figure 14: Schematic Illustration of Possible Forms of *β-geo* Reporter Gene Expression in SPRED2 KO Mice
In our SPRED2 KO mice, *Spred2* was disrupted by insertion of the gene trap vector pGT0pfs in sense orientation into intron 4 between *Spred2* exons 4 and 5. The gene trap vector provides a splice branch site and a SA for the next upstream located exon 4, which itself carries a splice donor site (SD). After transcription, *β-geo* is spliced to the end of *Spred2* exon 4. If protein translation starts at the start codon of *Spred2* exon 1 (first bent arrow), a fusion protein of a truncated SPRED2 comprising exons 1-4 and the β-geo reporter is expressed in the SPRED2 KO mice. If protein translation starts at the start codon of the *β-geo* gene (second bent arrow), only the β-geo reporter is expressed. Independent of translational start, translation stops at the stop codon of β-geo (*). Expression of the fusion protein is inevitably associated with the expression of the complete SPRED2-EVH1 domain in the SPRED2 KOs. For the conduction of *in vitro* studies, *EVH1-β-geo* and *β-geo,* respectively, were subcloned using the indicated primers (Pr. 4, 5, and 6, arrows, Ex = Exon, *En2* intron 1 = *Engrailed2* intron 1 structure, SA = splice acceptor site, β-geo = β-galactosidase (lacZ)/neomycin resistance (neoR) fusion gene, pA = Simian virus 40 polyadenylation sequence, pUC = pUC vector backbone sequence). *Figure modified from (Ullrich et al., 2011).*

5.3.1. Deletion of SPRED2 but Expression of an EVH1-β-geo Fusion Protein

In order to examine if the EVH1-β-geo fusion protein was present in our SPRED2-deficient mice, we performed Western blot analyzes with brain and kidney lysates, both tissues with confirmed high SPRED2 expression. For protein detection, we used either an anti-SPRED2 antibody or an anti-β-gal antibody. The anti-SPRED2 antibody recognizes an epitope in the coding sequence of exon 4 and hence is able to detect the common SPRED2 isoform but also the EVH1-β-geo fusion protein (Bundschu et al., 2005). The anti-β-gal antibody recognizes the β-geo reporter but also the fusion protein (Figure 15 A).

Expression of the common 46 kDa SPRED2 isoform was confirmed by SPRED2-specific antibodies in lysates of WT brain, whereas a prominent 30 kDa band was observed in WT kidney lysates, most likely representing a *Spred2* splice variant. Both proteins were absent in the corresponding KO lysates (Figure 15 A, middle panel). Instead, anti-SPRED2 antibodies recognized a 150 kDa protein in the KO lysates. This migrated with the calculated molecular mass of the EHV1-β-geo fusion protein (134 kDa β-geo and 16 kDa N-terminal SPRED2; Figure

15 A, upper panel) and was absent in WT lysates. Mock and *Spred2* transfected HEK 293 T cells saved as negative and SPRED2 positive controls, respectively. Anti-β-gal antibodies also detected the 150 kDa band, thereby confirming the expression of the EVH1-β-geo fusion protein in KO mouse organs. In the SPRED2 KO lysates, they additionally recognized a second protein with apparent molecular weight of about 135 kDa, which is consistent with the calculated mass of the β-geo protein and was absent in blots probed with anti-SPRED2 antibodies (Figure 15 A, lower panel).

In sum, we could show that translation took place *in vivo* from both possible start codons, leading to an expression of both the β-geo reporter and the EVH1-β-geo fusion protein in our SPRED2 KO mice.

5.3.2. Functional Expression of Subcloned EVH1-β-geo in Eukaryotic Cells

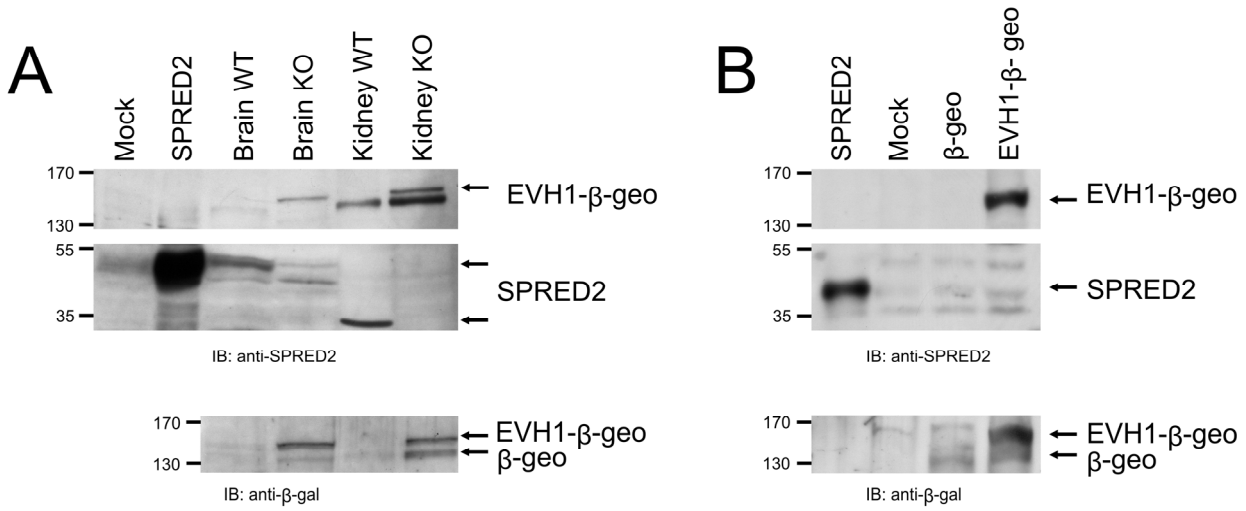

Figure 15: Verification of EVH1-β-geo and β-geo Protein Expression *in vivo* and *in vitro*
A) Western blot analysis with brain and kidney lysates of SPRED2 KO mice and WT controls. Blots were probed with anti-SPRED2 (upper and middle panel) and with anti-β-gal antibodies (lower panel). In WT tissues, the common 46 kDa isoform of SPRED2 was expressed in brain, while a shortened 30 kDa isoform was expressed in the kidney (middle panel). In KO tissues, both SPRED2 protein isoforms were absent (middle panel); however, the expression of the EVH1-β-geo fusion protein was detected by both anti-SPRED2 and anti-β-gal antibodies (upper and lower panel). Anti-β-gal further detected the expression of the sole β-geo reporter, which was absent in WT tissues and not recognized by anti-SPRED2 antibodies in SPRED2 KO tissues (upper and lower panel). SPRED2 and mock-transfected cells served as positive and negative controls, respectively. **B)** Western blot analysis with subcloned EVH1-β-geo and β-geo in transfected HEK 293 T cells also demonstrated the expression of both proteins. Anti-SPRED2 antibodies detected specifically the expression of EVH1-β-geo (upper panel), anti-β-gal antibodies both the EVH1-β-geo fusion protein and the β-geo reporter (lower panel). SPRED2 and mock-transfected cells served as positive and negative controls, respectively (middle panel). *Figure modified from (Ullrich et al., 2011).*

To get an impression if the expression of the EVH1-β-geo fusion protein or if sole β-geo exerts any effect *in vivo* and in order to be able to investigate possible effects *in vitro*, we subcloned both genes from our SPRED2 KO mice (Appendix 9.2.). Therefore, we amplified *EVH1-β-geo* and *β-geo* by RT-PCR using RNA isolated from brain of a SPRED2 KO mouse. Forward primers contained the start sequences of *Spred2* (Pr.4) and *β-geo* (Pr.5), respectively, together with an upstream HindIII site for cloning. The common reverse primer (Pr.6) comprised the end of the *β-geo* sequence with the stop codon and a downstream NotI cloning site (Figure 14). The received cDNAs were subcloned into NotI/HindIII sites of pcDNA3.1/*myc*-His(-) B vector and transfected in HEK 293 T cells.

Expression of both proteins was shown by Western blot using anti-SPRED2 and anti-β-gal antibodies. While anti-SPRED2 incubation revealed only EVH1-β-geo expression (Figure 15 B, upper panel), the anti-β-gal antibody again detected both EVH1-β-geo and β-geo (lower panel). Mock and *Spred2* transfected HEK 293 T cells were used as negative and SPRED2 positive controls, respectively (middle and lower panel).

To confirm the enzymatic activity of EVH1-β-geo and β-geo (Figure 16 A and B), HEK 293 T cells were transfected with each expression plasmid and stained with X-Gal. In contrast to the mock-transfected control (Figure 16 C), the conversion of X-Gal to its indigo derivative by both proteins was seen by blue staining.

Taken together, both the proper expression and the enzymatic functionality of EVH1-β-geo and β-geo proteins could be verified.

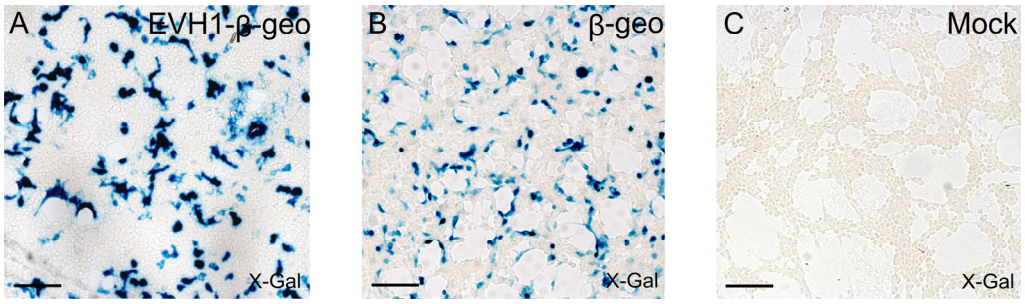

Figure 16: Validation of Enzymatic Functionality of Subcloned EVH1-β-geo/β-geo by X-Gal Stainings
X-Gal stainings of transfected HEK 293 T cells confirmed the enzymatic activity of **A)** the EVH1-β-geo fusion protein and **B)** the β-geo reporter as seen by intense blue staining of cells. **C)** Mock-transfected cells served as negative control. Scale bars: 100 µm. *Figure in part adopted from (Ullrich et al., 2011).*

5.3.3. Putative Dominant Negative Effect of EVH1-β-geo on SPRED1 and Ras/ERK/MAPK Signaling in SPRED2 KO Mice

Because SPREDs have been described as MAPK pathway inhibitors, we aimed to examine if EVH1-β-geo or β-geo in our SPRED2 KO mice exerts any effect on function or expression of the remaining SPRED1 and hence on MAPK signaling. Due to the cloning of EVH1-β-geo and β-geo expression constructs, we were able to *in vitro* reconstitute the *in vivo* situation of our SPRED2 KO mice, which lack SPRED2 expression but are still capable to express SPRED1. Therefore, we transfected HEK 293 T cells with different expression plasmids in the following manner (Figure 17): either with SPRED1 or with SPRED1 and EVH1-β-geo or with SPRED1 and β-geo. We tested two different ratios of SPRED1 and EVH1-β-geo and β-geo, respectively: EVH1-β-geo/β-geo were either expressed in deficit (3 µg pcDNA3.1-SPRED1 + 3 µg pcDNA3.1-EVH1-β-geo or 3 µg pcDNA3.1-β-geo) or in approximately twofold excess (3 µg pcDNA3.1-SPRED1 + 7 µg pcDNA3.1-EVH1-β-geo or 7 µg pcDNA3.1-β-geo). In order to induce Ras/ERK/MAPK pathway activation, cells were stimulated with 10ng/ml EGF after transfection. After cell lysis, we examined ERK phosphorylation by Western blot analysis.

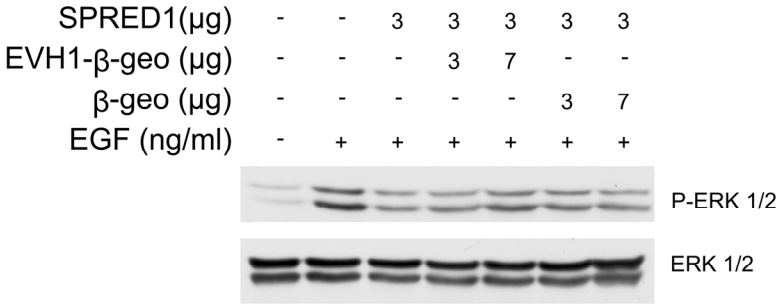

Figure 17: Putative Dominant Negative Effect of EVH1-β-geo on Ras/ERK/MAPK Signaling
HEK 293 T cells were transfected either with SPRED1 or in combination with EVH1-β-geo or β-geo expression plasmids, stimulated with 10 ng/ml EGF, and cell lysates were immunoblotted with anti-ERK and anti-P-ERK antibodies. SPRED1 was able to inhibit the EGF-induced ERK phosphorylation, while coexpression of EVH1-β-geo in deficit (3 µg SPRED1 + 3 µg EVH1-β-geo) did not exert any further effect on Ras/ERK/MAPK activity. However, expression of SPRED1 and EVH1-β-geo, the latter in approximately twofold excess (3 µg SPRED1 + 7 µg EVH1-β-geo), revealed an increased ERK phosphorylation in HEK 293 T cells in comparison to cells expressing solely SPRED1. This suggests a possible dominant negative effect of the EVH1-β-geo fusion protein on Ras/ERK/MAPK signaling. Coexpression of sole β-geo without the EVH1 domain had no effect on SPRED1-mediated inhibition of ERK phosphorylation. Unstimulated mock-transfected cells served as negative control.

In comparison to the unstimulated mock-transfected control, stimulation of mock-transfected cells with EGF led to a substantial increase in ERK phosphorylation, which could be considerably inhibited by SPRED1. In cells cotransfected with SPRED1 and EVH1-β-geo in deficit, ERK phosphorylation was reduced comparably to cells transfected only with SPRED1. However, expression of SPRED1 and of EVH1-β-geo in double amount revealed increased

ERK phosphorylation in comparison to cells expressing just SPRED1 or SPRED1 and EVH1-β-geo in deficit. ERK phosphorylation in cells transfected with SPRED1 and β-geo, either in deficit or excess, was comparable to that in cells expressing solely SPRED1 or SPRED1 and EVH1-β-geo in deficit.

This analysis showed that β-geo alone has no effect on SPRED1-mediated inhibition of MAPK signaling, while EVH1-β-geo, at least when expressed in excess, seemed to cause an impaired reduction of ERK phosphorylation by SPRED1. Thus, the EVH1 domain in the EVH1-β-geo fusion protein may exert a dominant negative effect on the SPRED1-mediated inhibition of ERK activity in our SPRED2 KO mice, leading to a more active Ras/ERK/MAPK pathway and to an aggravated phenotype.

5.4. Obvious and Versatile Phenotype in SPRED2 KO Mice

From birth on, SPRED2-deficient mice are viable but already significantly smaller as compared to their WT littermates. Hence, we could publish previously that loss of SPRED2 causes dwarfism (Figure 5) and we thereby identified SPRED2 as a novel regulator of chondrocyte differentiation and bone growth ((Bundschu et al., 2005), 3.2.6.1). Till that time I continued the SPRED2 KO mouse project in 2005, no long term observations have been conducted in order to investigate further effects of SPRED2 deficiency in adult mice. However, the breeding and comprehensive investigation of SPRED2 KO mice older than three months showed multiple affections in addition to the dwarf phenotype, such as an increasing deterioration of health state, sudden death due to unknown reasons, and multiple behavioral abnormalities, e.g. excessive drinking and obsessive grooming. To clarify if these phenotypical effects were caused by organ defects, mice at different ages were examined for pathological alterations.

5.5. SPRED2 Deficiency in Mice Leads to Hydronephrosis, Renal Atrophy, and Kidney Deterioration

In fact, dissections of mice older than three months, either died of unknown reasons or sacrificed for tissue sampling, revealed various degrees of renal pathological incidents. Extreme examples were characterized by severely distended kidneys filling large parts of the abdomen

(Figure 18 A). Kidneys were merely composed of a transparent capsule filled with a huge amount of liquid. Simultaneously, progressive atrophy of cortex and medullar zones led to a complete destruction of renal tissue, which clearly reflected a hydronephrosis-like disease pattern. Comparison of whole dissected organs demonstrated that affected kidneys of KO mice appeared pale and not sufficiently supplied with blood (Figure 18 B). In the course of affection, kidneys became deformed due to the fluid-inflated renal pelvis and the developing atrophy. They easily collapsed, especially after artificially induced effluence of liquid. Whereas the left kidney in Figure 18 B was severely damaged by hydronephrosis, which commonly developed unilateral, the right kidney seemed to act compensatory at this stage of disease.

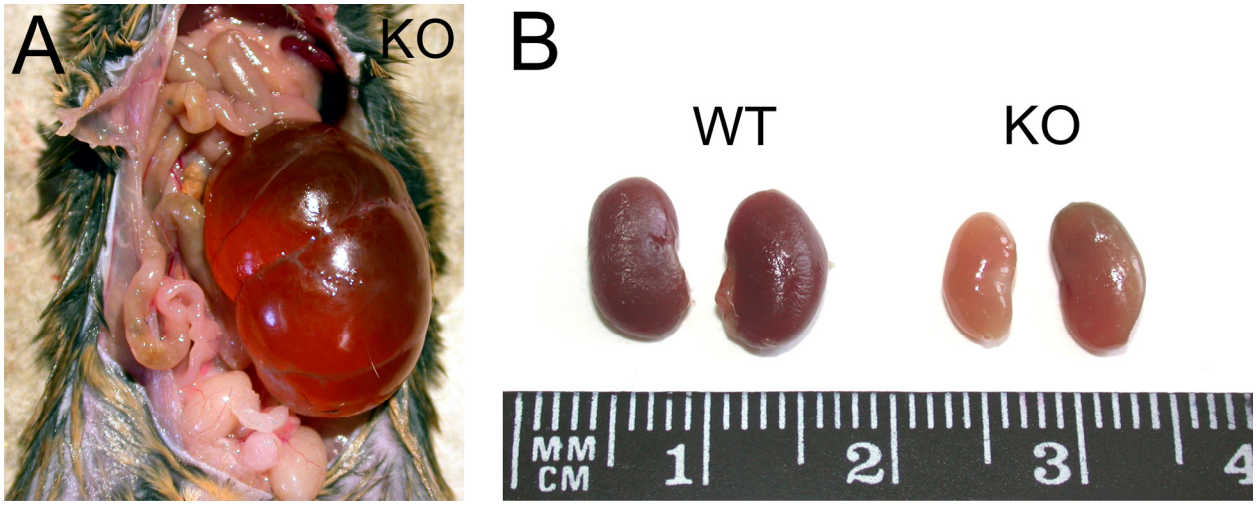

Figure 18: Hydronephrosis and Kidney Damage in SPRED2 KO Mice
A) Exterior view of a heavily affected and inflated left kidney, characterized by an extreme accumulation of liquid and a parallel decline of renal cortex and medulla, both common consequences of hydronephrosis. **B)** As a result of hydronephrosis and renal atrophy, affected isolated and liquid-drained kidneys of SPRED2 KO mice (left KO kidney) appeared flabby, exsanguinous, and morphologically altered. Because the hydronephrosis developed usually unilateral, the contralateral KO kidney (right KO kidney) seemed to act compensatory.

For detailed analysis of renal morphology, paraformaldehyde-fixed WT and KO kidneys were embedded in paraffin, cross- and longitudinal sections were prepared, and stained with H&E. In comparison to the WT kidney (Figure 19 A) showing normal kidney morphology, histological analysis of sections confirmed hydronephrosis in KO kidneys (Figure19 B-D). In particular, strongly dilated renal pelves (Figure 19 B-D, asterisks) and Bowman´s capsules (Figure 19 B-F, arrowheads) were indicative for hydronephrosis-associated fluid retentions. Completely destroyed lateral cortex and mark regions due to massive lymphocytic infiltration (Figure 19 B-F, arrows) further emphasized atrophy of renal tissue in KO kidneys, which is also a common consequence of hydronephrosis.

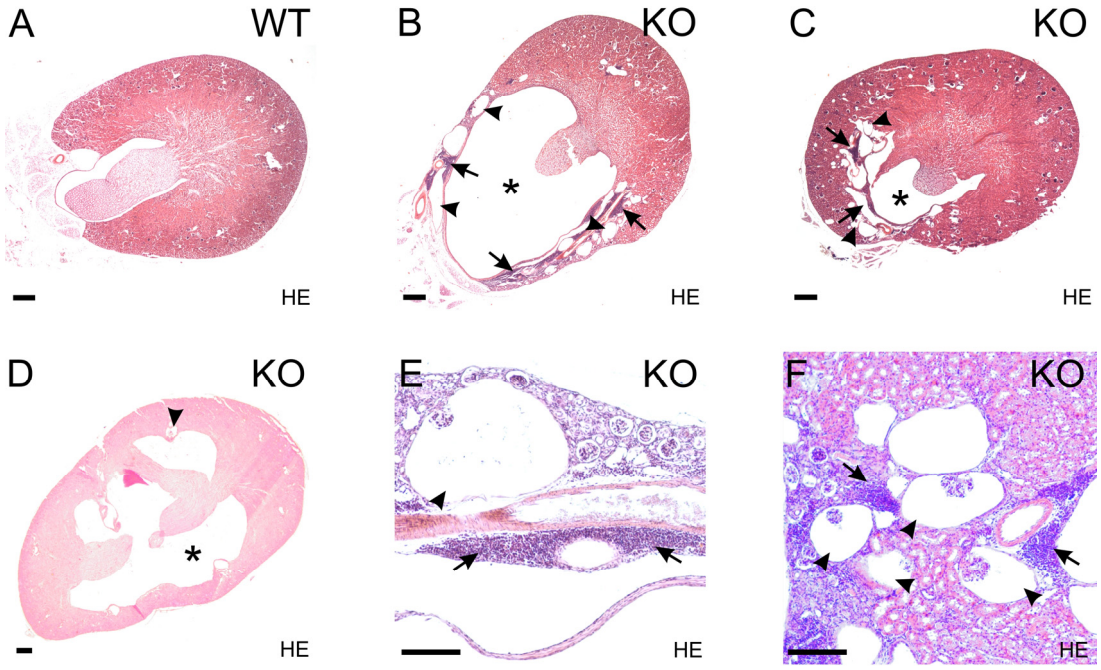

Figure 19: Progressive Atrophy and Severe Lymphocytic Infiltration in Kidneys of SPRED2 KO Mice
H&E-stained cross sections of **A)** WT and **B) C)** SPRED2 KO kidneys and **D)** H&E-stained longitudinal section of SPRED2 KO kidneys supported the diagnosis of hydronephrosis. Especially KO kidneys displayed extremely dilated renal pelves (asterisks) and Bowman´s capsules (arrowheads) caused by the accumulated liquid. This was accompanied by severe atrophy of cortex and medullar zones and by prominent invasion of lymphocytes (arrows). **E) F)** Detailed view of strongly inflated Bowman´s capsules (arrowheads) and lymphocytic infiltration (arrows) in SPRED2 KO kidneys. Scale bars: 500 µm.

5.6. Hydronephrosis Is Associated with Tubular Breakdown and Apoptosis in SPRED2 KO Mice

In order to investigate if apoptotic processes contribute to the observed kidney degeneration, we examined kidney morphology on cellular level by H&E-stained paraffin kidney sections. KO kidneys displayed degeneration and atrophy of renal cells, especially in tubular cells (Figure 20 A and B, arrows), whereas glomeruli seemed to remain morphologically intact (asterisks). Since atrophy is a general process of reabsorption and breakdown of tissues and involves apoptosis on a cellular level, we performed TUNEL assays. Apoptotic cells in cryosections of WT and KO kidneys were stained by labeling fragmented DNA at 3´-OH ends with flourescein-12-dUTP using the enzyme terminal deoxynucleotidyl transferase. Compared to WT kidneys (Figure 20 C), the number of TUNEL-positive cells was clearly elevated in KO kidneys, with the majority detected in kidney cortex (Figure 20 D). This was also attested by a higher magnification of WT and KO kidney sections (Figure 20 G and H). To gain an impression of the apoptotic cell rate, cell nuclei were counterstained with DAPI in both overviews (Figure 20 E and F) and magnified

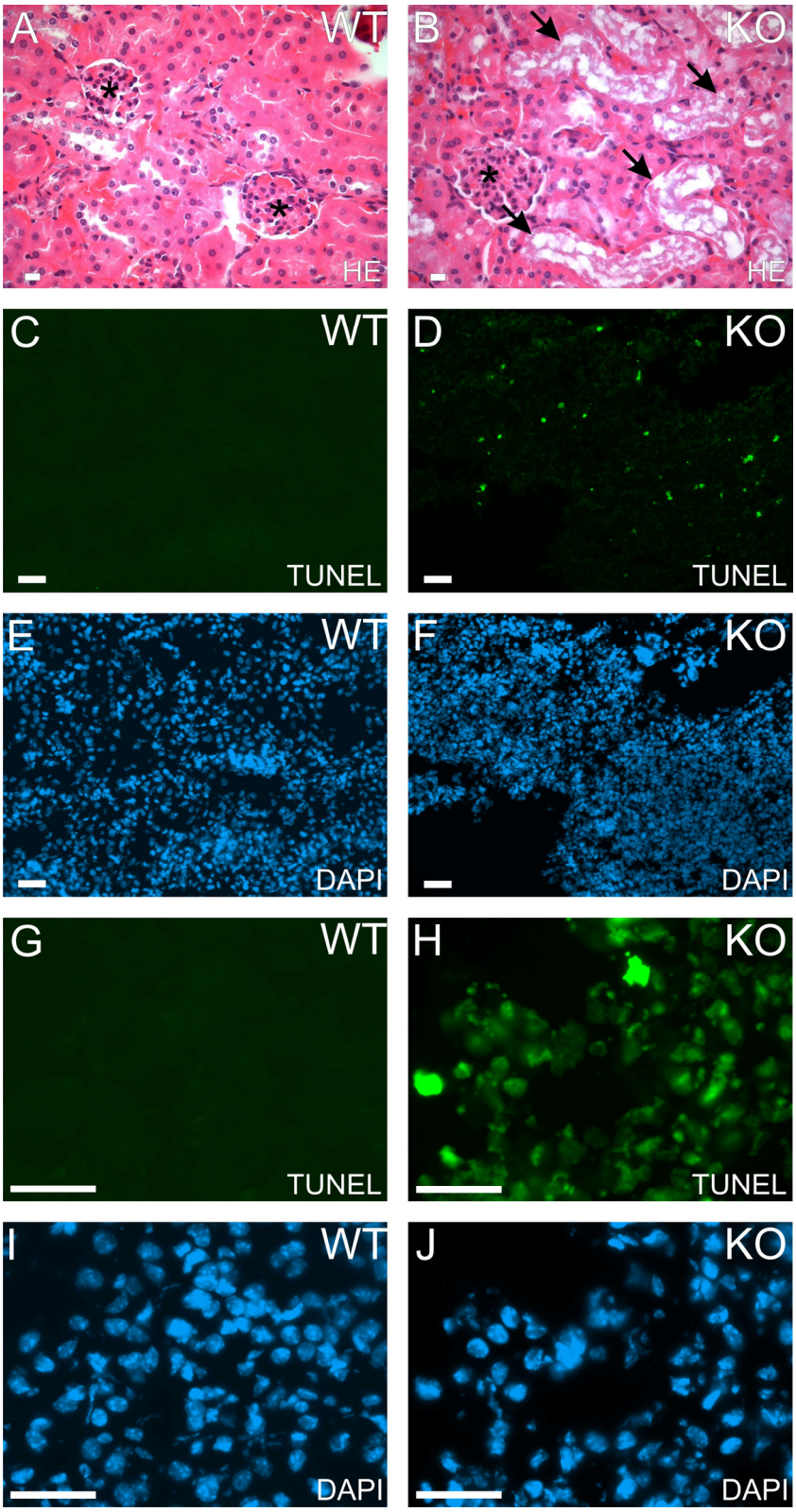

Figure 20: Tubular Breakdown and Apoptosis Contribute to Kidney Degeneration SPRED2 KO Mice
H&E-stained paraffin sections of **A)** WT and **B)** KO kidneys disclosed the decline of renal tubules (arrows), while glomeruli were unaffected in SPRED2-deficient mice. TUNEL assays with cryosections of **C) G)** WT and **D) H)** SPRED2 KO kidneys labeling apoptotic cells by green fluorescence further demonstrated an increase of apoptosis in renal cells of KO kidneys. **C) D)** Overviews containing kidney cortex and outer medulla regions. **G) H)** Detailed views of the cortex. **E) F)** Overviews and **I) J)** detailed views of DAPI-counterstainings marking cell nuclei in kidney sections of **E) I)** WT and **F) J)** KO mice. Scale bars: 50 µm.

views (Figure 20 I and J), confirming that a substantially higher number of cells underwent apoptosis in KO kidneys.

Thus, renal atrophy in SPRED2 KO mice seemed to be caused by apoptotic processes especially in the tubules, which might either be causative for or a consequence of hydronephrosis.

5.7. Kidney Damage in SPRED2 KOs Is Accompanied by Polydipsia, Hyperosmolality, and Higher Serum Salt Load

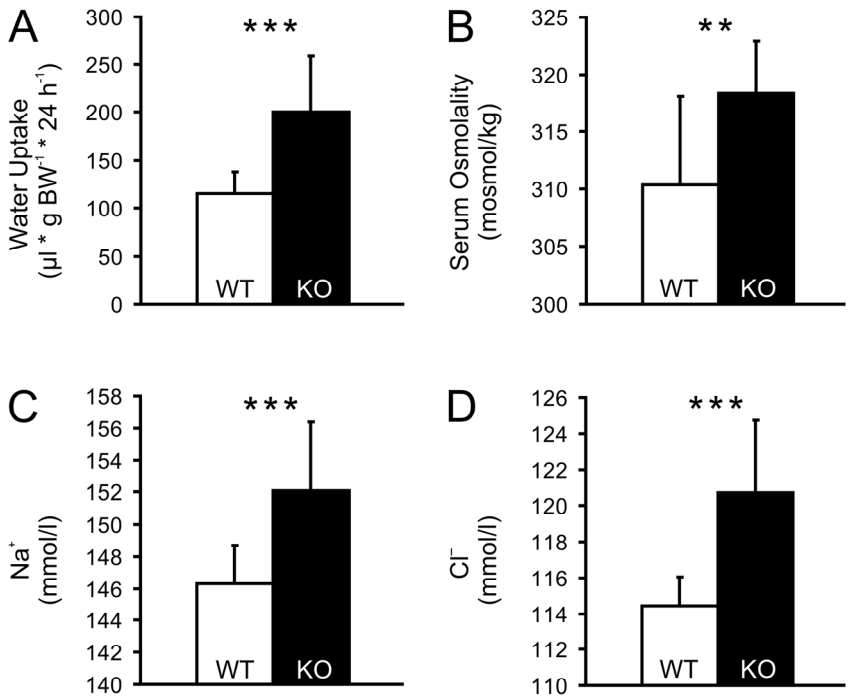

Figure 21: Excessive Water Uptake Correlates with Increased Serum Osmolality and Elevated Serum NaCl
A) Daily water consumption was nearly doubled in SPRED2 KO mice (n(WT/KO)=12; ****p*<0.001). **B)** Polydipsia was provoked by a significantly increased serum osmolality (n(WT/KO)=12; ***p*<0.01). Hyperosmolality was caused by an augmented serum salt load as demonstrated by significantly elevated **C)** Na^+ and **D)** Cl^- levels (n(WT/ KO)≥12; ****p*<0.001). *Results are expressed as mean ± SD. Figure reprinted from (Ullrich et al., 2011).*

Since renal disorders are often accompanied by changes in salt and water homeostasis, we first analyzed the drinking behavior of WT and KO animals aged six to 24 months over a period of one month. Water bottles were weighed each day, and the daily water uptake was noted.

Calculation of average daily water consumption in relation to body weight (BW) revealed a nearly doubled water uptake in SPRED2 KO mice (114.7 ± 23.3 µl * g BW^{-1} * 24 h^{-1} (WT) vs. 200.0 ± 58.4 µl * g BW^{-1} * 24 h^{-1} (KO); n(WT/KO)=12; ****p* <0.001; Figure 21 A). Enhanced thirst and increased water consumption are physiological consequences of a decreased blood volume and/or an increase in blood osmolality. Determination of blood osmolality via freezing-point depression in serum of WT and KO mice at the average age of ten months revealed that polydipsia correlated with a significantly elevated serum osmolality in SPRED2 KO mice (310.3 ± 7.8 mosmol/kg (WT) vs. 318.3 ± 4.6 mosmol/kg (KO); n(WT/KO)≥10; ***p* <0.01; Figure 21 B). In order to elucidate hyperosmolality, we measured the levels of various osmolytes in the same serum samples of WT and KO mice used for the determination of hyperosmolality. Except for increased Na^+ (146.3 ± 2.3 mmol/l (WT) vs. 152.1 ± 4.2 mmol/l (KO); n(WT/KO)≥10; ****p* <0.001; Figure 21 C) and Cl^- (114.4 ± 1.6 mmol/l (WT) vs.120.7 ± 4.1 mmol/l (KO); n(WT/KO)≥10; ****p* <0.001; Figure 21 D), the levels of all other measured osmolytes were unchanged or reduced (Table 1).

Therefore, in our SPRED2 KO mice the elevated bold salt load seems to be causative for hyperosmolality, which further results in excessive drinking.

5.8. Serum Parameter Analyses Underline Kidney Damage and Indicate SPRED2 Deficiency-Provoked Homeostatic Imbalance

In order to further examine the kidney phenotype and the generally bad state of health of our SPRED2 KO mice, we determined in addition to salt and osmolality parameters a variety of common routine serum parameters in WT and KO mice aged ten months at average (Table 1, survey of analyzed parameters).

Within the measured ion parameters Na^+, Cl^-, Ca^{2+}, PO_4^{3-}, and K^+, no significant changes could be detected apart from Na^+ and Cl^- (Figure 21 C and D, Table 1). However, K^+ levels (5.2 ± 1.1 mmol/l (WT) vs. 4.9 ± 0.5 mmol/l (KO); n(WT/KO)≥10; n.s.) were obviously but not significantly decreased in the KOs. Together with the observed hypernatremia, we considered this as a possible indication for hyperaldosteronism.

While the kidney parameters creatinin and uric acid were unchanged, urea levels (38.4 ± 11.1 mg/dl (WT) vs. 51.9 ± 26.3 mg/dl (KO); (WT/KO)≥10; n.s.) were apparently but not significantly increased in KOs, corroborating a functional renal disorder, a post-renal blockage of urine flow, or both.

Parameter	WT	KO
Osmolality (mosmol/kg)	310.3 ± 7.8	318.3 ± 4.6**
Na^+ (mmol/l)	146.3 ± 2.3	152.1 ± 4.2***
Cl^- (mmol/l)	114.4 ± 1.6	120.7 ± 4.1***
K^+ (mmol/l)	5.2 ± 1.1	4.9 ± 0.5
Ca^+ (mmol/l)	2.2 ± 0.1	2.2 ± 0.2
PO_4^{3-} (mmol/l)	2.4 ± 0.2	2.4 ± 0.4
Urea (mg/dl)	38.4 ± 11.1	51.9 ± 26.3
Creatinine (mg/dl)	0.12 ± 0.04	0.10 ± 0.00
Uric Acid (mg/dl)	0.88 ± 0.47	0.81 ± 0.36
Glucose (mg/dl)	216.6 ± 52.7	140.6 ± 28.3***
Triglyceride (mg/dl)	72.8 ± 10.7	51.5 ± 18.3*
Cholesterol (mg/dl)	154.4 ± 32.6	109.0 ± 24.1**
Alkaline Phosphatase (U/l)	69.4 ± 27.3	48.8 ± 13.3*
GOT/AST (U/l)	145.5 ± 71.2	69.2 ± 18.6*
GPT/ALT (U/l)	73.1 ± 35.5	34.4 ± 9.4*
GGT (U/l)	0.10 ± 0.00	0.10 ± 0.00
Bilirubin (mg/dl)	0.10 ± 0.00	0.12 ± 0.04
Iron (µg/dl)	150.8 ± 25.8	146.9 ± 30.7
Lactat Dehydrogenase (U/l)	363.8 ± 120.9	279.7 ± 179.4
Cholinesterase (U/l)	7985 ± 1178	6354 ± 2239
Total CK (U/l)	636.2 ± 242.3	101.2 ± 42.1**
Albumin (g/dl)	2.9 ± 0.3	2.7 ± 0.3
Total Protein (g/dl)	4.9 ± 0.3	4.9 ± 0.7
Amylase (U/l)	2870 ± 522	2954 ± 757
Lipase (U/l)	26.7 ± 12.1	18.7 ± 5.2

Table 1: Examination of Standard Parameters in Serum of WT and SPRED2 KO Mice
GOT/AST = Glutamate Oxaloacetate Transaminase/Aspartate Aminotransferase; GPT/ALT = Glutamate Pyruvate Transaminase/Alanine Aminotransferase; GGT = γ-Glutamyltransferase; CK = Creatine Kinase; n(WT/KO) ≥10 for all parameters; *p<0.05; **p<0.01; ***p<0.001; results are expressed as mean ± SD. *Table modified from (Ullrich et al., 2011).*

Based on polydipsia, renal damage, decreased body weight, and adynamia, we considered diabetes mellitus as a possible underlying disease in our SPRED2 KOs. Lack of insulin or a decreased insulin effect leads to an increase in serum glucose and lipolysis in diabetes mellitus patients. However, because of a 35% reduction in serum glucose (216.6 ± 52.7 mg/dl (WT) vs. 140.6 ± 28.3 mg/dl (KO); n(WT/KO)≥10; ***p <0.001) and of a nearly 30% reduction in triglycerides (72.8 ± 10.7 mg/dl (WT) vs. 51.5 ± 18.3 mg/dl (KO); n(WT/KO)≥10; *p <0.05) and in cholesterol (154.4 ± 32.6 mg/dl (WT) vs. 109.0 ± 24.1 mg/dl (KO); n(WT/KO)≥10; **p <0.01), we could exclude diabetes mellitus as reason for the bad health state in the KO mice.

In line with the dwarf phenotype of SPRED2-deficient mice (Bundschu et al., 2005), alkaline phosphatase (69.4 ± 27.3 U/l (WT) vs. 48.8 ± 23.3 U/l (KO); n(WT/KO)≥10; *p <0.05) was decreased by 30%, which is indicative for bone diseases, hereunder achondroplasia.

The liver parameters GOT/AST (145.5 U/l ± 71.2 (WT) vs. 69.2 ± 18.6 U/l (KO); n(WT/KO)≥10; *p <0.05) and GPT/ALT (73.1 ± 35.5 U/l (WT) vs. 34.4 ± 9.4 U/l (KO); n(WT/KO)≥10; *p <0.05), when elevated very important and specific indicators for severe liver diseases, were dramatically reduced in SPRED2 KO mice. However, a diagnostic relevance of a decrease in these parameters is not known. Liver-specific GGT levels were unchanged, as well as the liver-associated parameters bilirubin, iron, lactate dehydrogenase, and cholinesterase. While level changes of bilirubin, iron, and lactate dehydrogenase besides liver function can further affect blood cell formation, changes in lactate dehydrogenase and cholinesterase can also be indicative for heart and skeletal muscle diseases. A very specific indicator for heart muscle damage is the elevation of total CK. H owever, this parameter was substantially decreased in the SPRED2 KOs (636.2 ± 242.3 U/l (WT) vs. 101.2 ± 42.1 U/l (KO); n(WT/KO)≥10; **p <0.01). Again, no physiological relevance has been assigned to a CK reduction.

At least, the levels for albumin and total protein, general parameters of metabolism and nutrition, and amylase and lipase, when upregulated clear indicators for pancreatitis, did not differ between WT and SPRED2 KO mice.

Taken together, this routine serum parameter analysis of WT and SPRED2 KO mice clearly reflected a water-electrolyte imbalance associated with kidney dysfunction. Furthermore, it mirrored the recently published hypochondroplasia-like bone disorder. The decrease in numerous of the estimated metabolites (e.g. glucose, triglycerides, cholesterol) and enzyme levels (e.g. GOT/AST, GPT/ALT, total CK) suggested a disorder in body homeostasis and energy balance of SPRED2 KO mice.

5.9. Loss of SPRED2 Leads to Dysregulation of Salt and Water Homeostasis-Controlling Hormones

5.9.1. Augmented Aldosterone Secretion Is Accompanied by Elevated Expression of Aldosterone-Synthase

Aldosterone is one potent regulator of fluid and salt homeostasis by stimulating the reabsorption of Na^+ and water and the secretion of K^+ in the kidneys.To clarify whether hyperosmolality, hypernatremia, and the tendency to hypokalemia in SPRED2 KO mice were associated with an elevated aldosterone release, we estimated aldosterone in serum of WT and KO mice at the average age of eight months by EIA. Indeed, serum aldosterone (365.6 ± 146.9 pg/ml (WT) vs. 600.1 ± 289.2 pg/ml (KO); n(WT/KO)=14; $^{**}p$ <0.01) was almost doubled in SPRED2 KO mice (Figure 22 A).

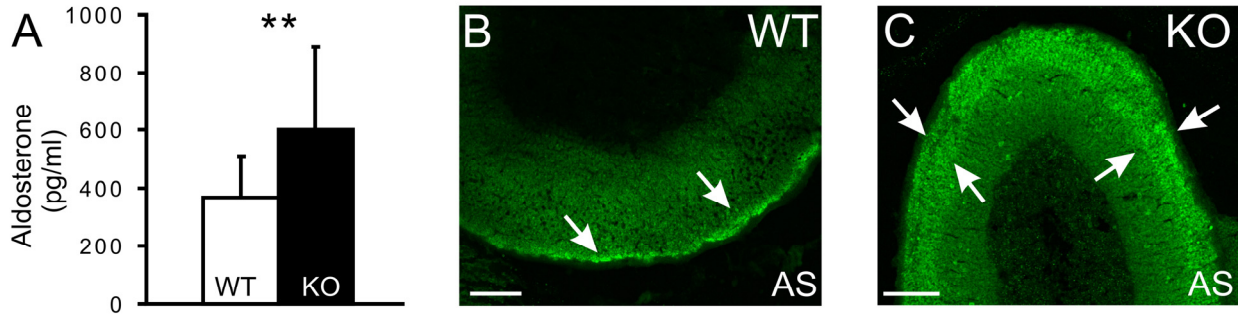

Figure 22: Increased Adrenal Aldosterone Synthase Expression Elicits Elevated Aldosterone Secretion
A) The observed hyperosmolality and hypernatremia in our SPRED2-deficient mice were provoked by almost doubled serum aldosterone levels (n(WT/KO)=14; $^{**}p$<0.01). **B)** Immunohistochemistry of aldosterone synthase in adrenal glands of WTs showed the common expression pattern restricted to the zona glomerulosa (arrows). **C)** In SPRED2 KO mice, the amount of adrenal aldosterone synthase was increased and the site of expression was obviously broadened (arrows). AS = aldosterone synthase; scale bars: 200 µm; results are expressed as mean ± SD. *Figure modified from (Ullrich et al., 2011).*

The production of aldosterone from 11-deoxycorticosterone is catalyzed by the aldosterone synthase, which is primarily expressed in aldosterone-producing cells in the zona glomerulosa of the adrenal cortex. To clarify if the hyperaldosteronism in SPRED2 KO mice was accompanied by an increase in aldosterone synthase expression, we performed immunohistochemistry with aldosterone synthase-specific antibodies. In WT adrenal glands, aldosterone synthase staining showed its regular expression pattern restricted to the zona

glomerulosa, a thin layer at the border of the adrenal cortex (Figure 22 B). In contrast, in adrenals of SPRED2 KO mice aldosterone synthase expression was obviously elevated and the site of expression was expanded. The resulting altered adrenocortical zonation may be provoked either by a broadening of the zona glomerulosa itself, by a repression of the adjacent zona fasiculata or by a mislocalization of zona glomerulosa cells in the zona fasciculata (Figure 22 C).

However, this study demonstrated a substantial increase in aldosterone synthase expression, which resulted in enhanced aldosterone production in SPRED2 KO mice.

5.9.2. Hyperaldosteronism Develops Independently of Renin-Angiotensin System Activity

Aldosterone production and aldosterone synthase expression is mainly controlled by K^+ and the RAS since Ang II potently stimulates the secretion of aldosterone from the adrenal cortex. Because K^+ was rather decreased in the SPRED2 KO mice, we investigated if elevated aldosterone release was accompanied by overactivation of the RAS. Therefore, we measured Ang II in serum of WT and KO mice at the average age of ten months by EIA. Unexpectedly, serum Ang II concentration (1.17 ± 0.53 ng/ml (WT) vs. 0.49 ± 0.19 ng/ml (KO); n(WT/KO)≥10; $^{**}p$ <0.01) in the KO mice was reduced by over 50% as compared to WT controls (Figure 23). This suggests that increased aldosterone biosynthesis and secretion was not mediated by the RAS in our SPRED2-deficient mice.

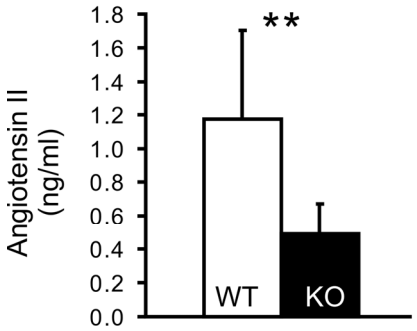

Figure 23: Reduced Ang II Release despite Hyperaldosteronism in SPRED2 KO Mice

Although Ang II is known as a primary stimulator of aldosterone release, serum levels were only halved in SPRED2-deficient KO mice (n(WT/KO)≥12); $^{**}p$<0.01) indicating a RAS-independent development of hyperaldosteronism. Results are expressed as mean ± SD. *Figure in part reproduced from (Ullrich et al., 2011).*

5.9.3. Water Deprivation Causes Elevated Loss of Body Fluid in SPRED2 KO Mice

Based on hyperaldosteronism, increased blood salt load, and polydipsia (Figure 21), we analyzed the ability for water retention in SPRED2 KO mice. Therefore, we first determined body weights in SPRED2-deficient mice and WT controls at the average age of ten months before and after experimental water deprivation for 48 h (non-water deprived/basal = (B); water deprived = (WD); Table 2).

Because loss of SPRED2 causes hypochondroplasia-like dwarfism (Bundschu et al., 2005), the body weight in the KOs was reduced already before water deprivation (36.6 ± 7.1 g (WT $^{(B)}$) vs. 23.9 ± 4.0 g (KO $^{(B)}$); n(WT/KO$^{(B)}$)≥10; ***p <0.001). It further decreased after withdrawal of water (32.2 ± 7.0 g (WT $^{(WD)}$) vs. 19.3 ± 3.7 g (KO $^{(WD)}$); n(WT/KO$^{(WD)}$)≥10; ***p <0.001; Table 2). However, while water starvation had no significant effect on body weight within the WT group (36.6 ± 7.1 g 8WT$^{(B)}$) vs. 32.2 ± 7.0 g (WT$^{(WD)}$); n(WT$^{(B)/(WD)}$)=10; n.s.), it significantly reduced body weight within the KO group (23.9 ± 4.0 g (KO$^{(B)}$) vs. 19.3 ± 3.7 g (KO$^{(WD)}$); n(KO$^{(B)/(WD)}$)≥10; **p <0.01). Accordingly, the relative percental body weight reduction was about 12% in WT but with approximately 19% notably higher in SPRED2 KO mice (Table 2).

	Basal (B)		Water Deprivation (WD)		
Parameter	**WT**	**KO**	**WT**	**KO**	**Significance**
Body Weight (BW, g)	36.6 ± 7.1	23.9 ± 4.0	32.2 ± 7.0	19.3 ± 3.7	A***; B***; D**
BW Reduction (%)			12.02	19.25	

Table 2: Effect of Water Deprivation on Body Weights of WT and SPRED2 KO Mice

Body weights of SPRED2 KO mice and corresponding WT littermates were determined before and after 48 h of water deprivation, revealing a loss of body fluid in both WT and SPRED2 KO mice, but an obviously higher body weight reduction in the SPRED2 KOs. A: WT non-deprived vs. KO non-deprived; B: WT deprived vs. KO deprived; C: WT non-deprived vs. WT deprived; D: KO non-deprived vs. KO deprived; for all parameters: n(WT/KO)≥10; *p<0.05; **p<0.01; ***p<0.001; results are expressed as mean ± SD. *Table in part taken from (Ullrich et al., 2011).*

In a further experiment, we additionally determined absolute weights of adrenals, kidneys, and brains, the corresponding organ/body weight ratios, and serum osmolalites. Determinations were performed in both the water-starved group of WT and SPRED2 KO mice after 48 h of water deprivation and in a second untreated group under basal conditions (Table 3). Despite the dwarf phenotype of SPRED2-deficient mice, absolute organ weights of brain and kidney were unaltered comparing WTs and KOs, and water deprivation had no considerable effect, too. Although not significant, absolute weights of adrenals even tended to be higher in dwarf SPRED2 KOs under basal conditions and further increased after water starvation. (*Adrenals:* 4.16 ± 0.99 mg ($WT^{(B)}$) vs. 4.36 ± 1.39 mg ($KO^{(B)}$) vs. 4.57 ± 0.76 mg ($WT^{(WD)}$) vs. 5.21 ± 0.67 mg ($KO^{(WD)}$) ;n($WT/KO^{(B)/(WD)}$)≥10; n.s); *Kidneys:* 352.3 ± 90.3 mg ($WT^{(B)}$) vs. 320.7 ± 41.2 mg ($KO^{(B)}$) vs. 362.7 ± 83.0 mg ($WT^{(WD)}$) vs. 323.8 ± 81.6 mg ($KO^{(WD)}$) ;n($WT/KO^{(B)/(WD)}$)≥10; n.s); *Brains:* 493.7 ± 26.3 mg ($WT^{(B)}$) vs. 506.2 ± 36.9 mg ($KO^{(B)}$) vs. 517.6 ± 29.6 mg ($WT^{(WD)}$) vs. 514.2 ± 35.5 mg ($KO^{(WD)}$); ;n($WT/KO^{(B)/(WD)}$)≥10; n.s).

Due to hypochondroplasia-like dwarfism and the reduced body weights in SPRED2 KO mice already under basal conditions, we focused on relative organ weight changes. Both within the water-starved group and within the basal group, all determined organ/body weight ratios were significantly elevated in the KO mice as compared to the WTs. (Basal group*: Adrenals:* 0.014 ± 0.005% ($WT^{(B)}$) vs. 0.019 ± 0.006% ($KO^{(B)}$); n($WT/KO^{(B)}$)≥10; **p* <0.05; *Kidneys:* 1.1 ± 0.2% ($WT^{(B)}$) vs. 1.3 ± 0.1% ($KO^{(B)}$); n($WT/KO^{(B)}$)≥10; ***p* <0.01; *Brains:* 1.6 ± 0.4% ($WT^{(B)}$) vs. 2.1 ± 0.2% ($KO^{(B)}$); n($WT/KO^{(B)}$)≥10; ***p* <0.01; Water deprived group: *Adrenals:* 0.016 ± 0.006% ($WT^{(WD)}$) vs. 0.028 ± 0.007% ($KO^{(WD)}$); n($WT/KO^{(WD)}$)≥10; ***p* <0.01; *Kidneys:* 1.2 ± 0.3% ($WT^{(WD)}$) vs. 1.7 ± 0.2% ($KO^{(WD)}$); n($WT/KO^{(WD)}$)≥10; ****p* <0.001; *Brains:* 1.7 ± 0.3% ($WT^{(WD)}$) vs. 2.7 ± 0.5% ($KO^{(WD)}$); n($WT/KO^{(WD)}$)≥10; ****p* <0.001). This phenotype-dependent increase in organ weight/body weight ratios could be explained by the hypochondroplasia of SPRED2 KO mice, which is a disproportionate form of dwarfism. Comparing organ/body weight ratios of SPRED2-deficient mice before and after water deprivation, a dramatic increase in ratios was detected for adrenal glands (0.019 ± 0.006% ($KO^{(B)}$) vs. 0.028 ± 0.007% ($KO^{(WD)}$); n($KO^{(B)/(WD)}$)≥13; ****p* <0.001), kidneys (1.3 ± 0.1% ($KO^{(B)}$) vs. 1.7 ± 0.2% ($KO^{(WD)}$); n($KO^{(B)/(WD)}$)≥13; ****p* <0.001), and brains (2.1 ± 0.2% ($KO^{(B)}$) vs. 2.7 ± 0.5% ($KO^{(WD)}$); n($KO^{(B)/(WD)}$)≥13; ****p* <0.001. Contrarily, within the WT group again no significant changes in organ/body weight ratios could be seen (*Adrenals:* 0.014 ± 0.005% ($WT^{(B)}$) vs. 0.016 ± 0.006% ($WT^{(WD)}$); n($WT^{(B)/(WD)}$)=10; n.s.; *Kidneys:* 1.1 ± 0.2% ($WT^{(B)}$) vs. 1.2 ± 0.3% ($WT^{(WD)}$); n($WT^{(B)/(WD)}$)=10; n.s.; *Brains:* 1.6 ± 0.4% ($WT^{(B)}$) vs. 1.7 ± 0.3% ($WT^{(WD)}$); n($WT^{(B)/(WD)}$)=10; n.s.). Correspondingly, in WT mice, water deprivation led to an organ/body weight ratio increase of nearly 15% in adrenals, 9% in kidneys, and 6% in brains. However, in SPRED2 KO mice, in which all organ/body weight ratios were significantly elevated after water starvation, withdrawal

	Basal (B)		Water Deprivation (WD)		
Parameter	**WT**	**KO**	**WT**	**KO**	**Significance**
Body Weight (BW, g)	32.1 ± 8.4	24.3 ± 2.1	32.2 ± 7.0	19.3 ± 3.7	A**; B***; D***
Adrenal Gland Weight (mg)	4.16 ± 0.99	4.63 ± 1.39	4.57 ± 0.76	5.21 ± 0.67	
Adrenal Gland Weight/BW Ratio (%)	0.014 ± 0.005	0.019 ± 0.006	0.016 ± 0.006	0.028 ± 0.007	A*; B**; D***
Adrenal Gland Weight/BW Ratio Increase (%)			14.29	47.37	
Kidney Weight (mg)	353.2 ± 90.3	320.7 ± 41.2	362.7 ± 83.0	323.8 ± 81.6	
Kidney Weight/BW Ratio (%)	1.1 ± 0.2	1.3 ± 0.1	1.2 ± 0.3	1.7 ± 0.2	A**; B***; D***
Kidney Weight/BW Ratio Increase (%)			9.09	30.77	
Brain Weight (mg)	493.7 ± 26.3	506.2 ± 36.9	517.6 ± 29.6	514.2 ± 35.5	
Brain Weight/BW Ratio (%)	1.6 ± 0.4	2.1 ± 0.2	1.7 ± 0.3	2.7 ± 0.5	A**; B***; D***
Brain Weight/BW Ratio Increase (%)			6.25	28.57	
Serum Osmolality (mosmol/kg)	310.3 ± 7.8	318.3 ± 4.6	331.8 ± 6.2	357.6 ± 23.3	A**; B***; C***; D***
Serum Osmolality Increase (%)			6.93	12.35	

Table 3: Effect of Water Starvation on Adrenal, Kidney, and Brain Weights, Corresponding Organ/Weight Ratios, and Serum Osmolalities of WT and SPRED2 KOs
Indicated organ weights, organ/body weight ratios, and serum osmolalities of SPRED2 KO mice and corresponding WT littermates were determined under basal conditions in one group of untreated mice and in a second water-starved mouse group after 48 h of water deprivation. While absolute organs weights did not differ significantly between the groups, both organ/body weight ratios and serum osmolalities showed an augmented increase in SPRED2 KOs in comparison to the WTs after water starvation, again indicating water imbalances and fluid loss especially in the KOs. A: WT non-deprived vs. KO non-deprived; B: WT deprived vs. KO deprived; C: WT non-deprived vs. WT deprived; D: KO non-deprived vs. KO deprived; for all parameters: n(WT/KO)≥10; *p<0.05; **p<0.01; ***p<0.001; results are expressed as mean ± SD. *Table in part adopted from (Ullrich et al., 2011).*

of water led to an organ/body weight ratio augmentation by overall 47% in adrenals, by 31% in kidneys, and by 29% in brains of SPRED2-deficient mice. Thus, the increase in organ/body weight ratios in SPRED2 KOs still rose by 20% in kidney/body weight and brain/body weight ratios, respectively, and even by over 30% in adrenal/body weight ratio.

As already demonstrated (see Figure 21 B and Table 1), serum osmolality of SPRED2 KO mice was significantly elevated as compared to WT controls even under basal conditions (310.3 ± 7.8 mosmol/kg ($WT^{(B)}$) vs. 318.3 ± 4.6 mosmol/kg ($KO^{(B)}$); n($WT/KO^{(B)}$)≥10; $^{**}p$ <0.01). Osmolality further increased after water starvation (331.8 ± 6.2 mosmol/kg ($WT^{(WD)}$) vs. 357.6 vs. ± 23.3 mosmol/kg ($KO^{(WD)}$); n($WT/KO^{(WD)}$)≥10; $^{***}p$ <0.001). Although the increase of serum osmolality after water deprivation was significant within WT (310.3 ± 7.8 mosmol/kg $WT^{(B)}$ vs. 331.8 ± 6.2 mosmol/kg $WT^{(WD)}$; n($WT^{(B)/(WD)}$)≥10; $^{***}p$ <0.001) and KO mice (331.8 ± 6.2 mosmol/kg $KO^{(B)}$ vs. 357.6 vs. ± 23.3 mosmol/kg $KO^{(WD)}$; n($KO^{(B)/(WD)}$)≥13; $^{***}p$ <0.001), the elevation was with 12% almost doubled in SPRED2 KO mice as compared to a 7% increase in WT animals.

Taken together, the water deprivation experiment clearly demonstrated impaired water retention and fluid loss in our SPRED2 KO mice, leading to a stronger decreased body weight, to more elevated organ/body weight ratios, and to a further increased serum osmolality after dehydration as compared to WT littermates.

5.9.4. Vasopressin Response Is Unaffected by Ablation of SPRED2

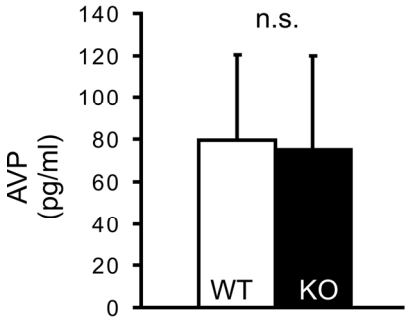

Figure 24: SPRED2 Deficiency Has no Influence on AVP Release after Water Deprivation
Despite basal polydipsia and the extreme loss of body fluid induced by water starvation, no significant differences in serum AVP could be detected after water deprivation (n(WT/KO)≥17; n.s.= not significant). Results are expressed as mean ± SD. *Figure in part reprinted from (Ullrich et al., 2011).*

Vasopressin is a multifunctional effector in the body, and one of its most important functions is the stimulation of water retention in the kidney. Upon serum hyperosmolality or hypovolemia, AVP induces the integration of aquaporin channels into the apical membrane of renal distal convoluted tubule and collecting duct cells. We wondered if the reduced ability of fluid retention after water deprivation in our SPRED2-deficient mice was caused by an AVP release disorder.

Therefore, we analyzed AVP levels in serum of WT and KO mice at the average age of ten months by EIA after 48 h of water starvation. Thirst and water deprivation have been shown to significantly increase serum vasopressin. However, unexpectedly, we could not detect any differences between WT and KO AVP levels after water deprivation (79.4 ± 40.7 ng/ml (WT) vs. 74.9 ± 44.9 ng/ml (KO); n(WT/KO)≥10; n.s.; Figure 24). Thus, we assumed that a dysregulation of AVP secretion might not be reasonable for polydipsia in our SPRED2 KO mice.

5.10. Increased Release of the Stress Hormones CRH, ACTH, and Corticosterone from the Hypothalamic-Pituitary-Adrenal Axis in SPRED2 KO Mice

In addition to the RAS and K^+, ACTH is another regulator of aldosterone release by generally stimulating steroidogenesis in the adrenal gland. Because of the reduced Ang II and K^+ levels, excluding an RAS- and K^+-dependent elevated alsosterone release, we investigated if ACTH might be involved in the development of hyperaldosteronism in SPRED2 KO mice. The production and release of ACTH was measured by EIA using serum samples of WT and KO mice at the average age of ten months. Indeed, we found serum ACTH elevated about 30% (0.90 ± 0,27 ng/ml (WT) vs. 1.27 ± 0,78 ng/ml (KO); n(WT/KO)≥17; **p* <0.05; Figure 25 B).

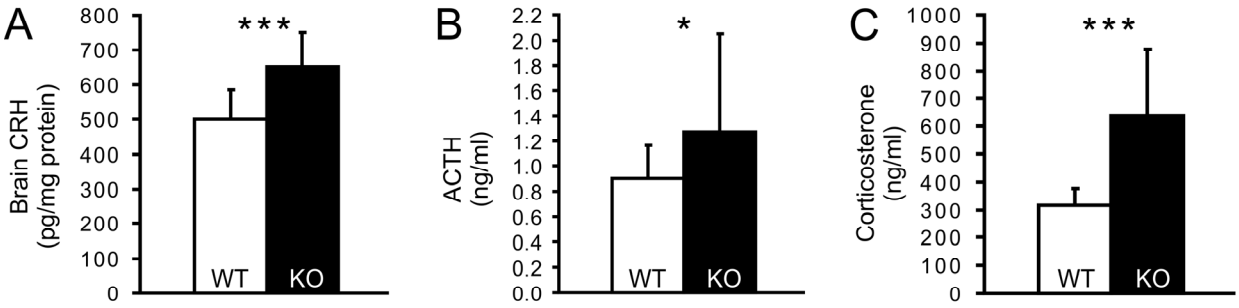

Figure 25: Increased Pituitary ACTH Release in SPRED2 KOs Is Stimulated by Augmented Hypothalamic CRH Secretion and Followed by Elevated Corticosterone Production
Upregulation of stress hormone secretion at all levels of the HPA axis in SPRED2-deficient mice was demonstrated by **A)** a 30% increase in CRH in PVN region-containing brain lysates (n(WT/KO)=20; *p****<0.001), **B)** a 30% increase in serum ACTH (n(WT/KO)≥22; **p*<0.05), and **C)** a more than doubled serum corticosterone level (n(WT/KO)=12; *p****<0.001). Results are expressed as mean ± SD. *Figure in part reproduced from (Ullrich et al., 2011).*

Together with CRH and corticosterone, ACTH is produced by tissues of the HPA axis and is, besides its function as a regulator of steroidogenesis, also a potent mediator of stress responses. Triggered by the limbic system, CRH is secreted by the PVN of the hypothalamus in response to stress. CRH stimulates the release of ACTH from corticotrope cells of the anterior pituitary into the systemic circulation. In turn, ACTH further induces the release of corticosterone from the zona fasciculata of the adrenal cortex. In order to investigate if the increased ACTH secretion is accompanied by consecutive upregulation also of the upstream acting CRH and the downstream corticosterone, we also determined CRH by ELISA and corticosterone by EIA. CRH released from hypothalamus and exerting its main action in the pituitary was measured in PVN region-containing brain lysates. Corticosterone, like ACTH released into the systemic circulation, was measured from serum samples of WT and KO mice aged ten months at average. With this analysis, we found CRH, the primary ACTH secretagogue, in line with ACTH significantly increased about 30% (499.0 ± 84.6 pg/mg protein (WT) vs. 652.6 ± 98.6 pg/mg protein (KO); n(WT/KO)=20; ***p <0.001) in brain lysates of SPRED2-deficient animals (Figure 25 A). Consistently, also corticosterone, released downstream of ACTH stimulation, was more than doubled in serum of SPRED2 KO mice (315.9 ± 60.3 ng/ml (WT) vs. 635.2 ± 242.0 ng/ml (KO); n(WT/KO)=12; ***p <0.001; Figure 25 C). Thus, we could show a clear upregulation of stress hormone release from all levels of the HPA axis.

5.11. Augmented Hypothalamic-Pituitary-Adrenal Stress Hormone Release Is Accompanied by Elevated Hypothalamic-Pituitary Growth Hormone Secretion in SPRED2 KO Mice

Bone development and bone growth can be regulated by a variety of signaling pathways, hereunder by FGF/FGFR3/MAPK/ERK signaling and by growth hormone (GH), which is released from the hypothalamic-pituitary-growth axis. Similar to ACTH from the HPA axis, GH is synthesized and stored in the anterior pituitary and secreted by somatotropic cells into the systemic circulation. GH release is stimulated by its liberin growth-hormone-releasing hormone (GHRH). GHRH is, similar to CRH, released from neurosecretory neurons of the hypothalamus, which are located in the arcuate nucleus. GH stimulates the production of insulin-like growth factor 1 (IGF-1) in the liver, which is comparable with ACTH-induced steroidogenesis in adrenal gland. Both GH itself and IGF-1 are able to regulate long bone growth by stimulating chondrocyte proliferation (Isaksson et al., 1982; Isgaard et al., 1988).

Because of the elevated stress hormone secretion from the HPA axis, and because SPRED2 deficiency leads to hypochondroplasia-like dwarfism (Bundschu et al., 2005), we wondered if hypothalamic-pituitary-growth hormone release was also dysregulated in the SPRED2 KO mice. We therefore analyzed levels of GH and IGF-1 by ELISA using serum samples of WT and KO mice at an average age of six months. We found both serum GH (2.9 ± 2.7 ng/ml (WT) vs. 8.1 ± 5.2 ng/ml (KO); n(WT/KO)≥15; $^{**}p$ <0.01; Figure 26 A) and IGF-1 (381.6 ± 104.9 ng/ml (WT) vs. 604.9 ± 212.1 ng/ml (KO); n(WT/KO)≥15; $^{***}p$ <0.001; Figure 26 B) elevated in SPRED2-deficient mice.

This finding was on the one hand consistent with a generalized upregulation of hypothalamic-pituitary hormone production; on the other hand it was in stark contrast to the dwarf phenotype of our SPRED2 KO mice.

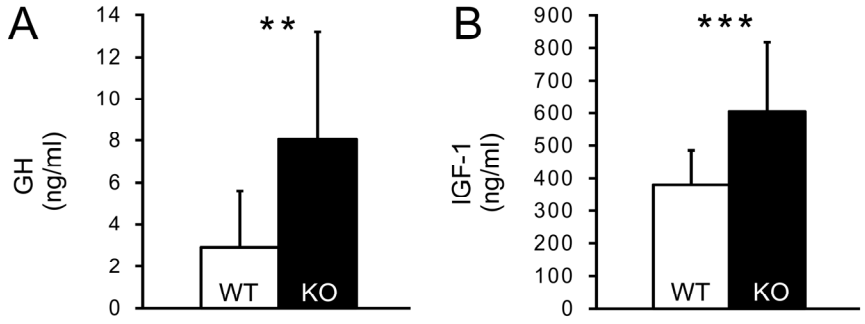

Figure 26: Elevated Growth Hormone Secretion from the Hypothalamic-Pituitary Axis in SPRED2 KO Mice
A) Augmented GH release from the pituitary, which was almost tripled in SPRED2 KOs n(WT/KO)≥15; $^{**}p$ <0.01), elicited **B)** a subsequent 60% increase in IGF-1 secretion from the liver (n(WT/KO)≥15; $^{***}p$ <0.001). Results are expressed as mean ± SD. *Figure based on (Ullrich et al., 2011).*

5.12. Overshooting Stress Hormone Release Is Associated with Obsessive Grooming and Self-Inflicted Skin Lesions in SPRED2 KO Mice

The HPA axis is a key mediator of stress and responds to neural inputs from the central and peripheral nervous system. Upregulation of HPA hormone secretion has been shown to be involved in a variety of stress-associated and mood disorders like depression, burnout syndrome, or bipolar, borderline, and compulsive disorders.

Very strikingly, SPRED2 KO mice older than four months developed severe skin lesions. They were usually first noticed as small wounds at the snout or cheek but evolved into uni- or bilateral lesions encompassing large parts of the neck or face (Figure 27). These lesions occurred in SPRED2 KO mice, regardless of whether they were housed individually or together with cage mates. No lesions were observed in WT littermates, even when kept in the same cage together with KO mice. SPRED2-deficient mice were never found behaving aggressively or being busy in grooming other cage mates. However, they were very often and very intensely seen engaged in self-grooming regardless if housed individually or in groups. Long-term observations and video monitoring of SPRED2 KO mice and WT littermates demonstrated that KOs spent clearly more time for grooming as WT controls. SPRED2-deficient mice performed excessive and injurious levels of self-grooming bouts regardless of day or night time, resulting in bloody wounds and purulent lesions.

The observed phenotype of our SPRED2 KO mice is reminiscent of a compulsive disorder, which affects regular grooming behavior and manifests as obsessive grooming. It is very likely a consequence of the excessive stress hormone release from the HPA system.

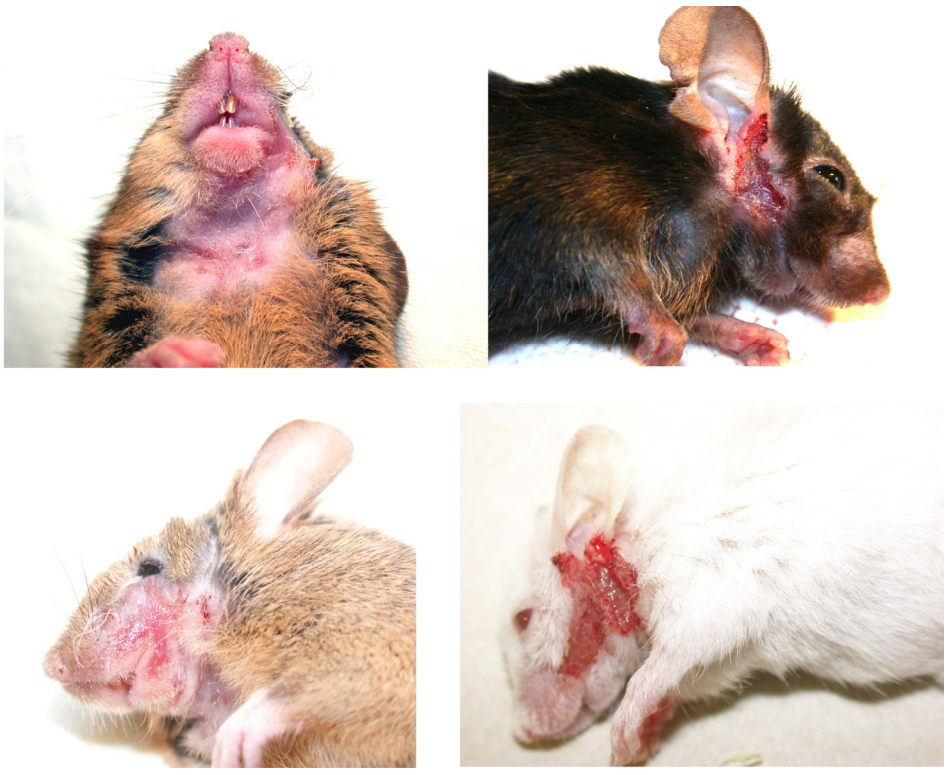

Figure 27: Obsessive Grooming of SPRED2 KO Mice Results in Self-Inflicted Skin Lesions
Mice older than four months developed oozing and bloody uni- or bilateral skin lesions, which resulted from excessive self-grooming. In combination with the upregulated stress hormone release from the HPA axis, this behavior might be indicative for an obsessive-compulsive disorder. *Figure in part reprinted from (Ullrich et al., 2011).*

5.13. SPRED2 Expression Profiling in Hypothalamic-Pituitary-Adrenal Tissues and Kidney

SPRED2 expression has been shown to be almost ubiquitous in mouse tissues as demonstrated previously on RNA and protein levels and by *Spred2* promoter activity assays (Bundschu et al., 2006a; Engelhardt et al., 2004). In order to monitor SPRED2 expression in organs involved in the phenotypical pathologies of SPRED2-deficient mice, we especially focused on tissues of the HPA axis and the kidney. We visualized on the one hand *Spred2* promoter activity by X-Gal-stainings using whole organs and tissue sections of HET mice; on the other hand, we analyzed the expression pattern of SPRED2 by immunohistochemistry using tissue sections of WT mice and a SPRED2-specific antibody for protein detection.

As demonstrated previously, both *Spred2* promoter activity and SPRED2 expression is very high in brain. Accordingly, the entire HET brain was blue colored upon X-Gal staining in comparison to the WT control (Figure 28 A). In particular in the hypothalamus, where CRH and AVP are synthesized in the PVN, the *Spred2* promoter was clearly active. Hypothalamic *Spred2* promoter activity was further confirmed by X-Gal stained brain sections of HET mice, demonstrating an evenly distributed blue staining in the entire organ (Figure 28 B). SPRED2 protein expression was comparable to endogenous promoter activity and also evenly distributed throughout the entire hypothalamus as shown by anti-SPRED2 staining of WT brain sections (Figure 28 C).

ACTH is released into the systemic circulation from the anterior, and AVP from the posterior part of the pituitary gland. *Spred2* promoter activity was also present in the whole organ (Figure 28 D), which was confirmed by tissue sections (Figure 28 E). SPRED2 protein expression was again detected throughout the whole pituitary but seemed to be especially high in the posterior tract (Figure 28 F).

The adrenal gland releases aldosterone from the zona glomerulosa and corticosterone from the zona fasciculata. X-Gal staining of adrenals as well indicated a strong endogenous *Spred2* promoter activity (Figure 28 G), which was further defined by sectional analysis. Predominantly a thin layer at the border of the adrenal cortex representing the zona glomerulosa was positive for both promoter activity and SPRED2 expression (Figure 28 H and I), indicating a role of SPRED2 especially in mineralocorticoid synthesis and/or release.

Finally, we could demonstrate *Spred2* promoter activity and SPRED2 expression in the kidney and thereby confirm our former data. The endogenous *Spred2* promoter activity was substantially higher in cortex and outer medulla as compared to inner medulla and papilla (Figure 28 J and K). Blue staining marked especially the zone in kidney cortex, where proximal

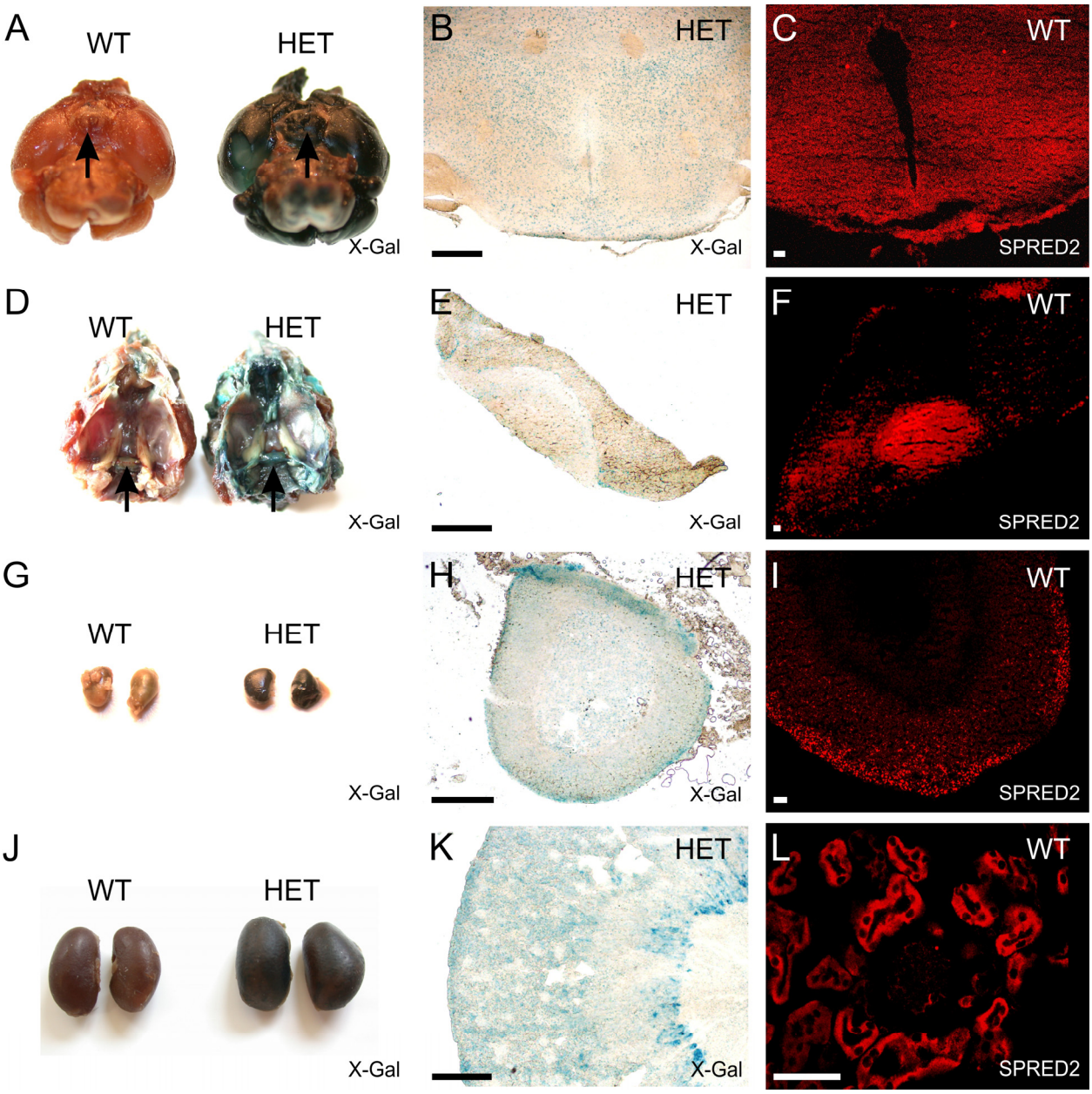

Figure 28: *Spred2* Expression Profiling in Tissues of the HPA Axis and in Kidney
Endogenous *Spred2* promoter activity of **A) D) G) J)** whole WT and HET organs (arrows) and **B) E) H) K)** tissue sections of SPRED2 HET mice was demonstrated by X-Gal stainings. **C) F) I) L)** SPRED2 protein expression was shown by immunohistochemistry with tissue sections of WT mice. **A) B) C)** Both *Spred2* promoter activity and SPRED2 expression were evenly distributed throughout the whole hypothalamus. **D) E) F)** Endogenous promoter activity was detected in the entire pituitary gland, but protein content seemed to be most pronounced in the posterior part. **G) H) I)** SPRED2 expression and *Spred2* promoter activity were especially high in the zona glomerulosa of the adrenal gland, which is the site of aldosterone release. Proximal and/or distal tubules but not the glomeruli were the sites of highest *Spred2* promoter activity and protein content in the kidney. **J) K) L)** Scale bars: B, E, H, K: 500 µm; C, F, I, L: 50 µm. *Figure modified from (Ullrich et al., 2011).*

and distal tubules are located. A tubules-restricted *Spred2* promoter activity was also indicated by the lack of blue staining in renal glomeruli. In line, substantial SPRED2 expression examined

by immunohistochemistry was also seen in cortex and in the cortico-medullary boundary, again showing intensely stained renal tubules, while glomeruli were devoid of SPRED2 (Figure 28 L). Taken together, expression profiling verified both profound endogenous *Spred2* promoter activity and SPRED2 expression in the tissues of the HPA axis and in the kidney.

5.14. SPRED2 Inhibits Hypothalamic CRH Production and Release by Downregulating CRH Promoter Activity in an ERK/MAPK/Ets1-Dependent Manner

5.14.1. Increased *in vivo* ERK Phosphorylation in Brains of SPRED2 KOs

A very important question we still had to address was the mechanism how SPRED2 could be involved in the dysregulation of the HPA axis. Because SPREDs have been shown to be negative regulators of exclusively Ras/ERK/MAPK signaling (King et al., 2005; Nonami et al., 2004; Wakioka et al., 2001), we first examined ERK expression and phosphorylation in six and twelve months old WT and SPRED2 KO animals. Since the hypothalamus is part of the limbic system, the site of CRH release from parvocellular neurons of the PVN, and thus the most upstream trigger of the HPA axis, we used the same brain lysates as for CRH ELISA because they mainly contained the hypothalamic PVN. ERK/MAPK activity in these brain lysates was investigated by Western blot analysis using anti-ERK and anti-P-ERK antibodies.

In both six and twelve months old animals, we detected an obviously increased ERK phosphorylation in the SPRED2 KOs as compared to WTs, while the unphosphorylated form of ERK was expressed equally (Figure 29 A). ERK phosphorylation was quantified by determination of signal strengths of ERK and P-ERK and expressing them as arbitrary units. For each sample, P-ERK signals were normalized to the corresponding ERK signals, i.e. the ratio of P-ERK to ERK was calculated and the mean of the WT ratios was set as 1. This quantification revealed an over 2.5-fold elevated P-ERK to ERK ratio in both age groups of SPRED2 KO mice as compared to the WT groups (Figure 29 B; *6 months old mice*: 1 ± 0.35 arbitrary units (WT) vs. 2.73 ± 0.73 arbitrary units (KO); n(WT/KO)≥8; ***p<0.001; *12 months old mice*: 1 ± 0.56 arbitrary units (WT) vs. 2.58 ± 0.42 arbitrary units (KO), n(WT/KO)≥7; ***p<0.001).

Due to the loss of SPRED2-mediated inhibition, ERK activation was upregulated in the PVN-containing hypothalamic region of SPRED2 KOs. Thus, we could confirm the suppressive effect of SPRED2 on Ras/ERK/MAPK signaling and demonstrate it initially *in vivo* in mouse brain.

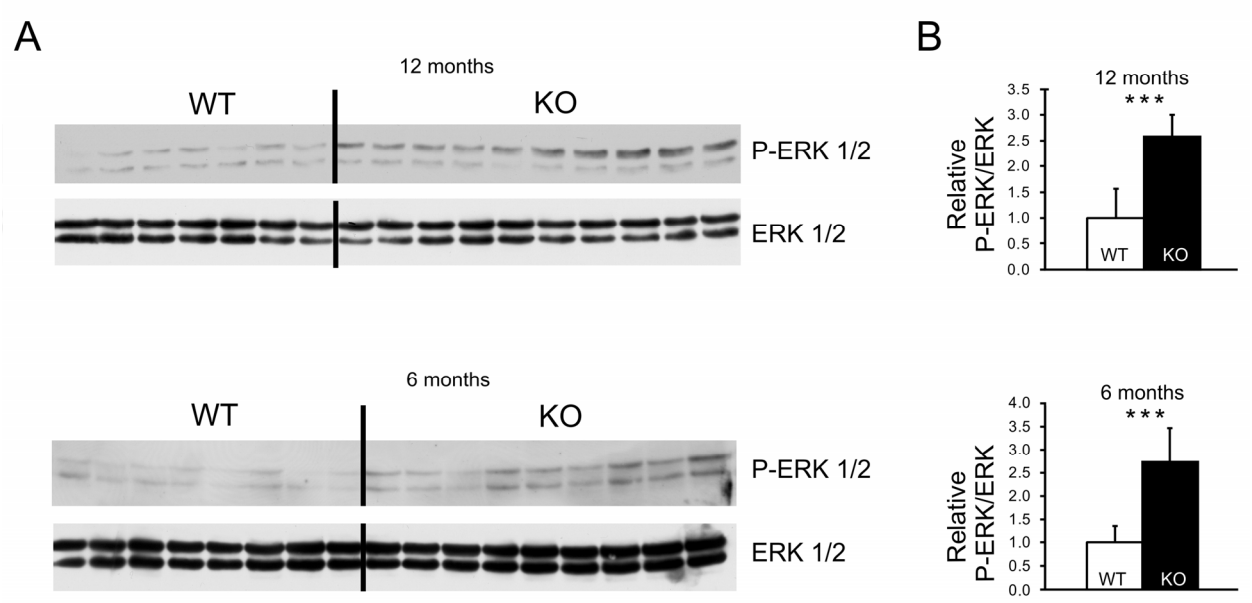

Figure 29: Increased Ras/ERK/MAPK Signaling in PVN-Containing Brain Regions of SPRED2-Deficent Mice
A) Western blot analysis with anti-ERK and anti-P-ERK antibodies using hypothalamus lysates of both six and twelve months old SPRED2 KOs revealed augmented ERK phosphorylation in both young and aged mice in comparison to WT controls. **B)** Quantification of ERK and P-ERK signals demonstrated a more than 2.5-fold increase of the P-ERK/ERK ratio both in young and aged SPRED2-deficient mice (n(WT/KO)≥7); ****p*<0.001). Results are expressed as mean ± SD. *Figure in part reprinted from (Ullrich et al., 2011).*

5.14.2. SPREDs Suppress CRH Transcription *in vitro*

Because SPRED2 downregulates MAPK signaling and ERK phosphorylation in the hypothalamus, we aimed to investigate if SPRED-mediated Ras/ERK/MAPK pathway regulation also has a direct impact on hypothalamic CRH production. To date, the only known functional cellular role of SPREDs is the exclusive inhibition of Ras/ERK/MAPK signaling, one of its main consequences is transcriptional regulation of target genes. Thus, we assumed that the most likely way how SPRED could influence CRH release is by regulating CRH transcription.

To be able to monitor possible SPRED effects on CRH transcription *in vitro*, we used a reporter vector containing a firefly luciferase reporter gene expressed under control of the CRH promoter. To generate this CRH promoter reporter we amplified a 5.7 kb region of the 5´ CRH promoter sequence including exon 1 by PCR from genomic mouse DNA and cloned it into the firefly luciferase reporter vector pGL3 (Appendix 9.3.). Due to the occurrence of RE-1/NRSE, a critical regulatory element in intron 1 of the CRH gene, which is able to silence CRH transcription (Seth and Majzoub, 2001), we cloned both the CRH promoter region with ($CRH_{Prom\text{-}RE}$) and without (CRH_{Prom}) the RE-1/NRSE repressor. The embryonic mouse hypothalamus cell line mHypoE-44 was transiently transfected with the CRH promoter firefly luciferase reporters and with an internal control vector containing the *Renilla* luciferase reporter

gene driven by a constitutive active promoter. The CRH promoter reporter containing the RE-1/NRSE between exon 1 and 2 (pGL3-CRH$_{Prom-RE}$) revealed no luciferase signal in mHypoE-44 cells, which underlined the repressive effect of RE-1/NRSE on CRH transcription (Figure 30 A). Thus, further reporter studies were conducted with the CRH promoter reporter construct lacking the RE-1/NRSE repressor (pGL3-CRH$_{Prom}$, Figure 30 B). mHypoE-44 cells were transfected with the CRH promoter firefly luciferase reporter pGL3-CRH$_{Prom}$, with the *Renilla* luciferase control vector, with SPRED1 and SPRED2, respectively, either with EVH1-β-geo in approximately trifold excess or without (Figure 30 C). Because CRH is released in response to stress *in vivo*, mHypoE-44 cells were normally cultured in high glucose and FBS-containing medium but were starved in low glucose medium without FBS for 24 - 30 h after transfection. Firefly and *Renilla* luciferase reporter activity were determined, luminescent signals of firefly luciferase activity were normalized to *Renilla* luciferase activity for all samples, and mean relative activity of cells expressing solely the CRH promoter reporter was set to 1.

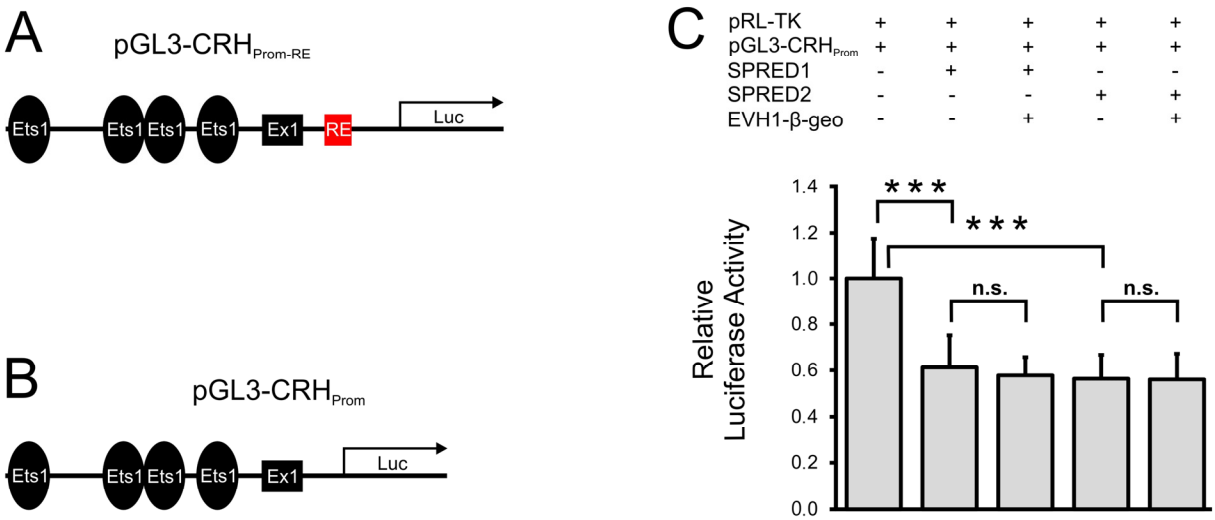

Figure 30: SPRED1 and SPRED2 Downregulate CRH Promoter Activity *in vitro*
A) Schematic depiction of the cloned CRH promoter luciferase reporter pGL3-CRH$_{Prom-RE}$ including the RE-1/NRSE repressor. Approximate positions of the predicted 4 Ets1 binding sites (Ets1), exon 1 (Ex1), the RE-1/NRSE repressive element (RE), and the firefly luciferase reporter gene (Luc) are indicated. **B)** Schematic depiction of the cloned CRH promoter luciferase reporter pGL3-CRH$_{Prom}$ lacking the RE-1/NRSE repressor. Approximate positions of the predicted 4 Ets1 binding sites, exon 1, and the firefly luciferase reporter gene are indicated. **C)** CRH promoter reporter assay in mHypoE-44 cells using pGL3-CRH$_{Prom}$, which comprises the CRH promoter region without the RE-1/NRSE repressive element. Both SPRED1 and SPRED2 were able to reduce firefly luciferase reporter gene expression and thus CRH promoter activity to 60%. No further effect on CRH promoter activity was detected by coexpression of EVH1-β-geo in about trifold excess (n=12; ***p<0.001; n.s.=not significant). Results are expressed as mean ± SD. *Figure modified from (Ullrich et al., 2011).*

These assays revealed that both SPRED1 and SPRED2 were able to suppress the relative luciferase activity of the CRH promoter reporter by about 40% (1 ± 0.18 arbitrary units (CRH$_{Prom}$)

vs. 0.61 ± 0.14 arbitrary units (SPRED1) vs. 0.58 ± 0.08 arbitrary units (SPRED1/EVH1-β-geo) vs. 0.56 ± 0.10 arbitrary units (SPRED2) vs. 0.56 ± 0.11 arbitrary units (SPRED2/EVH1-β-geo); n≥12; ***p<0.001). Cotransfection of EVH1-β-geo in excess did not exert any further effect on CRH promoter activity (Figure 30 C).

Hence, SPRED1 and SPRED2 can downregulate CRH transcription and expression explaining the elevated CRH production in SPRED2-deficient mice. In contrast to the putative dominant negative effect of EVH1-β-geo on ERK-phosphorylation detected by cotransfection studies in HEK 293 T cells (5.3.3.), the fusion protein seemed to have no effect on CRH promoter activity.

5.14.3. SPREDs Inhibitory Effect on CRH Promoter Activity is Dependent on ERK/MAPK-mediated Regulation of Ets Transcription Factors

The CRH promoter comprises a manifold set of transcription factor binding sites as predicted by Alibaba 2.1 TF Binding Prediction. Hereunder are a great variety of predicted binding sites for Ets transcription factor family members (Appendix 9.6.). In particular, the cloned CRH promoter reporter region lacking the RE-1/NRSE repressor (CRH_{Prom}) contains four binding sites for Ets1, four for PU.1, two for Erg1, and for one Elk1, Elf1, and PEA3 (Figure 30 B). Because transcription factors of the Ets family are favored targets of the Ras/ERK/MAPK cascade, they could provide the link between SPRED-mediated inhibition of Ras/ERK/MAPK signaling and SPRED-mediated suppression of CRH transcription.

To investigate if Ets binding sites in the CRH promoter are indeed critical for SPRED-dependent regulation of CRH transcription, we performed an Ets reporter assay. Therefore, we used a plasmid comprising 4 Ets1 transcription factor binding sites, which control the expression of a downstream firefly luciferase reporter gene (Figure 31 A, Appendix 9.5., (Hoffmeyer et al., 1998)). The experimental setup was based on the CRH promoter reporter study, i.e. mHypoE-44 cells were transfected with the 4xEts1 reporter, with a *Renilla* luciferase reporter vector as internal control, and with SPRED1 and SPRED2, respectively, either with about trifold amounts of EVH1-β-geo or without. In case of the Ets reporter assay, cells were only starved for FBS but not for glucose for 24 - 30 h after transfection. By this Ets reporter assay, we detected that again both SPRED1 and SPRED2 were able to reduce relative luciferase activity. SPRED expression led to an inhibition of Ets factor-dependent gene transcription by even 90% in mHypoE-44 cells (1 ± 0.47 arbitrary units (Ets1) vs. 0.097 ± 0.044 arbitrary units (SPRED1) vs. 0.071 ± 0.035 arbitrary units (SPRED1/EVH1-β-geo) vs. 0.066 ± 0.031 arbitrary units (SPRED2) vs. 0.055 ± 0.007 arbitrary units (SPRED2/EVH1-β-geo); n≥12; ***p<0.001). The SPRED function on Ets1-mediated transcription was unaffected by coexpression of EVH1-β-geo in excess (Figure 31 B).

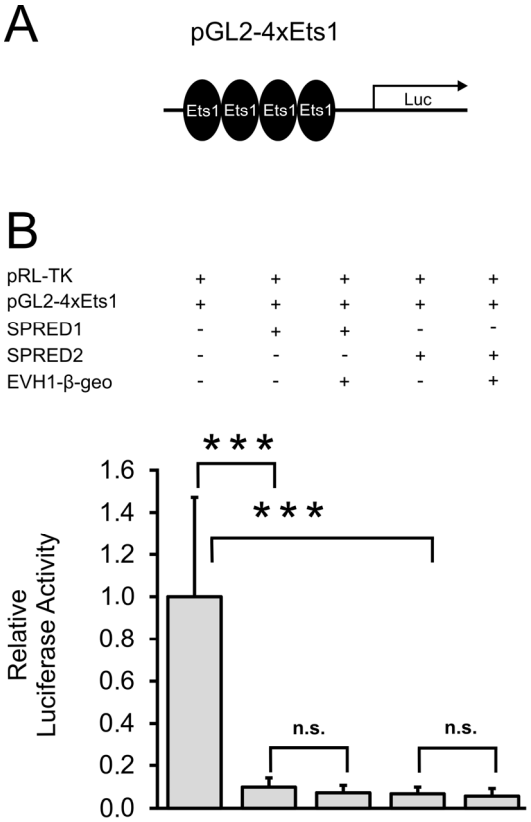

Figure 31: SPRED1 and SPRED2 Suppress Ets1-dependent Transcription
A) Schematic depiction of the 4xEts1 reporter pGL2-4xEts1 containing 4 binding sites for the transcription factor Ets1 (Ets1) and the firefly luciferase reporter gene (Luc). **B)** Both SPRED1 and SPRED2 were able to downregulate Ets1-dependent transcription of the luciferase reporter gene to approximately 10%. EVH1-β-geo coexpression in approximately trifold amounts did not exert any further effect on Ets1-dependent transcriptional activity (n=12; ****p*<0.001; n.s.=not significant). Results are expressed as mean ± SD. *Figure modified from (Ullrich et al., 2011).*

This Ets reporter study again gave no hint on any effect exerted by EVH1-β-geo on Ets-like factor mediated transcription. However, this study confirms that CRH transcription can be regulated by the activation of Ets binding sites, especially Ets1, which are present in the CRH promoter. Thus, it provides an explanation how inhibition of Ras/ERK/MAPK signaling and thereof dependent downregulation of Ets1-mediated transcription by SPREDs can suppress CRH transcription and production.

5.14.4. SPREDs Reduced CRH Release from mHypoE-44 Cells *in vitro*

In order to investigate if SPRED-mediated inhibition of CRH transcription also leads to a reduction of CRH release *in vitro*, we performed a CRH ELISA using the hypothalamic mHypoE-44 cell line (Figure 32). mHypoE-44 cells were transfected with SPRED1, SPRED2, or empty expression plasmid, starved for glucose and FBS for 36 h, and cell culture supernatants were used for determination of the secreted CRH. Indeed, SPRED1 reduced *in vitro* CRH secretion by 30% and SPRED2 by 40%, which was in line with the downregulation of CRH transcription (34.2 ± 8.9 pg/ml (Mock) vs. 25.4 ± 3.6 pg/ml (SPRED1) vs. 20.6 ± 2.9 pg/ml (SPRED2); n=9; Mock vs. SPRED1: **p* <0.05; Mock vs. SPRED2: ***p* <0.01).

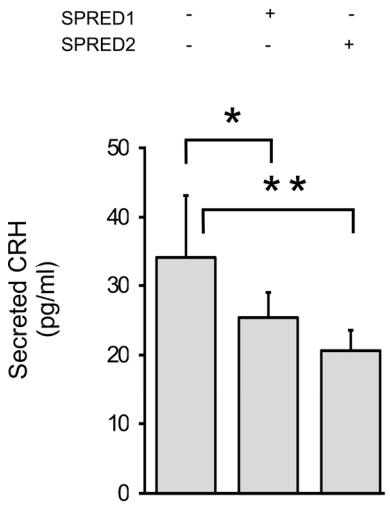

Figure 32: Reduction of CRH Release from mHypoE-44 Cells by SPRED1 and SPRED2 *in vitro*
ELISAs with cell culture supernatants of mHypoE-44 cells demonstrated a decrease of CRH secretion to 70% by SPRED1 and to 60% by SPRED2 (n=12; **p*<0.05 for SPRED1; ***p*<0.01 for SPRED2). Results are expressed as mean ± SD. *Figure in part reprinted from (Ullrich et al., 2011).*

5.14.5. Higher Content of CRH mRNA in Hypothalamic PVN-Containing Brain Regions of SPRED2-deficient Mice

In hypothalami of SPRED2 KO mice, we already detected increased ERK phosphorylation (5.14.1.) in combination with augmented CRH release (5.10.) *in vivo*. The downregulation of CRH promoter activity (5.14.2) mediated by Ets family transcription factors (5.14.3) and of CRH release (5.14.4) by SPREDs has been demonstrated *in vitro*. In order to ascertain if SPREDs are able to regulate MAPK/ERK-dependent CRH transcription not only *in vitro* but also *in vivo*, we quantified the levels of CRH mRNA in hypothalamic PVN regions of WT and SPRED2 KO mice. Therefore, we performed Northern blot analysis with RNA isolated from the PVN-containing region of the hypothalamus and using a part of the mouse CRH cDNA labeled with ^{32}P as a radioactive probe (Figure 33 A, Appendix 9.7.). CRH mRNA levels were quantified by imaging the ^{32}P comprised in the bound probe and by normalizing the signals to the corresponding total RNA content. Both the signal strengths of ^{32}P and total RNA were expressed as arbitrary units, the relative CRH mRNA contents of WT and KO samples were calculated, and WT was set to 1. This quantification revealed a 60% increase of CRH mRNA in the KO mice (Figure 33 B; 1 ± 0.58 arbitrary units (WT) vs. 1.62 ± 0.55 arbitrary units (KO); n(WT/KO)≥8; **p*<0.05), indicating a functional role of SPREDs in the regulation of CRH transcription and expression also *in vivo*.

Taken together, this study showed that SPREDs are suppressors of CRH promoter activity, transcription, and release both *in vivo* and *in vitro*. SPRED-mediated downregulation of CRH release was accompanied by SPRED-mediated inhibition of ERK/MAPK signaling and a reduced activation of Ets1 factor-dependent transcription, leading to a decreased ERK/MAPK/Ets1-dependent CRH promoter activity. *Vice versa*, in our SPRED2 KO mice,

ERK/MAPK activity, CRH mRNA levels, and hypothalamic CRH release were accordingly increased. Thus, our study provides a new link how SPRED can mediate the activity of the HPA axis by regulating ERK/MAPK/Ets1 signaling.

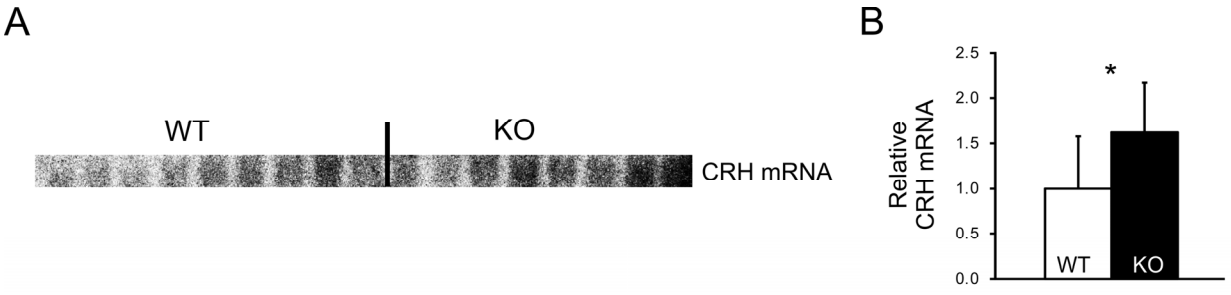

Figure 33: Elevated CRH mRNA Levels in Hypothalamic PVN-Containing Brain Regions of SPRED2 KOs
A) Northern blot analysis with RNA samples from the PVN-containing hypothalamus of WT and SPRED2 KO mice. Radioactive labeling of CRH mRNA with ^{32}P demonstrated a higher CRH mRNA content in the KOs. **B)** Quantification of CRH mRNA levels demonstrated a 60% increase in PVN-containing brain regions of SPRED2-deficient mice (n(WT/KO)≥8; *p<0.05). Results are expressed as mean ± SD. *Figure modified from (Ullrich et al., 2011).*

5.15. Reduced Survival Probability in SPRED2 KO Mice

Most likely associated with the various phenotypical affections and the generally poor health status, our SPRED2 KO mice died obviously earlier as compared to their WT littermates, while in most cases the cause of death was unknown.

We determined the survival probability of WT and SPRED2 KO mice by Kaplan-Meier survival analysis. Therefore, we observed 20 SPRED2 KO mice and 20 WT littermate controls over a period of 18 months and documented, if applicable, the age of death. Very strikingly, more than 50% of the SPRED2-deficient KO mice already died within the first five months of age (Figure 34). The outward health was still good in most mice at this age because obsessive grooming, wound development, and kidney degeneration usually begin at the earliest at the age of about four months. However, these comparatively young animals were suddenly found dead in their cages. Further 25% of KO mice died within the remaining 13 months, so that only 25% of KOs survived the whole period of 18 months. In contrast, 80% of all WT mice were still alive at the end of the 18 months (80 ± 8.9% (WT) vs. 25 ± 9.7% (KO); n(WT/KO)=20; ***p<0.001). This results in a 55% reduction of survival probability in SPRED2 KO mice KOs as compared to WTs.

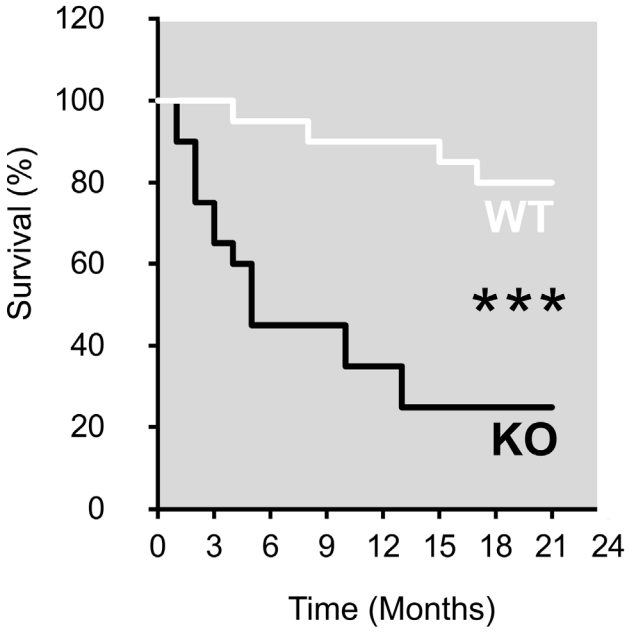

Figure 34: Kaplan-Meier Survival Analysis of SPRED2 KO Mice and WT Littermate Controls
In comparison to WT mice, of which 80% survived the investigated time period of 18 months, only 25% of SPRED2 KOs survived the whole time span, revealing a 55% reduction of survival probability in KOs (n(WT/KO)=20; ****p*<0.001).

Hence, we could show a significantly reduced life expectancy for SPRED2 KO mice. The unclear sudden death of especially younger animals does not necessarily have a causal relationship to the phenotypical affections described in this work. It rather points towards paroxysmal disorders that might either emanate from the cardiovascular system, e.g. myocardial infarction or stroke or from the nerve system e.g. epilepsia.

Two further studies have already been initiated to investigate the possible causes for the reduced survival probability of our SPRED2 KO mice and to further characterize phenotypical consequences provoked by SPRED2 deficiency: One study to explore the effects of SPRED2 deficiency on the cardiovascular system and another study to further unravel behavior and synaptic function in SPRED2-deficient mice.

6 Discussion

6.1. The SPRED2 Gene Trap Model – Possible Effects of the EVH1-β-geo Fusion Protein

In 2001, SPRED proteins were discovered by a yeast to hybrid screen, they were named after the related Sprouty proteins with whom they share a homologous C-terminus, and they were described as exclusive inhibitors of Ras/ERK/MAPK signaling (Wakioka et al., 2001). At the same time, our group also detected the SPREDs due to their homology to the EVH1 domain of VASP. In order to unravel the completely unknown *in vivo* function of SPRED proteins, we generated a KO mouse model lacking functional SPRED2 protein expression.

For disruption of the *Spred2* gene in mice, we used the very fast gene trap method, which allowed a functional knockout of the target gene in combination with gene expression profiling by X-Gal staining (Bundschu et al., 2006a; Bundschu et al., 2005; Ullrich and Schuh, 2009). With this study, we could show and confirm that gene trapping resulted in a loss of full-length SPRED2 in SPRED2-deficient mice, as demonstrated by Western blot. Surprisingly, in WT kidney lysates instead of the common 46 kDa SPRED2 isoform expressed for example in WT brain, we detected the expression of a substantially smaller isoform of about 30 kDa (5.3.1., Figure 15 A). By screening of human expressed sequence tag (EST) databases in an earlier experiment indicating that the *Spred2* gene generates at least three forms of transcripts (Engelhardt, 2004), we already got a hint for the appearance of SPRED splice variants. Furthermore Eve-3 has been described as a liver-specific splice variant of SPRED3, thus confirming the natural occurrence of SPRED splice variants (King et al., 2006).

The gene trap vector, which disrupts the endogenous *Spred2* gene in our mouse model, is inserted between exons 4 and 5. It was repeatedly described that exons upstream of the disruption point were still used as an RNA template regardless if the mouse models were generated by homologous recombination or by gene trapping. This may lead to the expression

of either a truncated protein or a truncated splice variant or of read-through products containing both exonic and vector information (Bula et al., 2005; Calfa et al., 2011; McClive et al., 1998). Because *Spred2* was interrupted downstream of exon 4, the expression of exons 1 - 4 primarily representing the EVH1 domain could not be excluded. Indeed, besides the sole β-geo reporter, we detected the expression of a fusion protein comprising the EVH1 domain and β-geo. This was in contrast to our recent studies, in which Northern and Western blot analysis using RNA or protein lysates prepared from SPRED2 KO brains failed to detect any expression of full-length-SPRED2, any truncated SPRED2, or any enlarged read-through product (Bundschu, 2005). However, in this present study, the detection of the EVH1-β-geo was possible by Western blot not only in brain lysates, one of the tissues with highest natural SPRED2 expression, but also in kidney and both by anti-SPRED2 and anti-β-gal antibodies. One reason for the now possible detection of EVH1-β-geo could be the affinity of the anti-β-gal antibody used exclusively in this study. It seemed to be higher for EVH1-β-geo as the affinity of the anti-SPRED2 antibody used in the former studies. Moreover, the anti-SPRED2 antibody used in the present study was freshly purified from serum of immunized rabbits, might have a better quality, and thus detect also lower amounts of protein. Too low levels of RNA or protein might be a further reason for the undetectable EVH1-β-geo in the former study.

In order to investigate possible effects, which EVH1-β-geo might exert on the remaining SPRED1 activity and thus on SPRED mediated Ras/ERK/MAPK signaling in our SPRED2 KO mice, we subcloned EVH1-β-geo and β-geo. Their expression and functionality was confirmed in transfected HEK 293 T cells by Western Blot and X-Gal stainings. Expression of SPRED1 and higher amounts of EVH1-β-geo in EGF-stimulated HEK 293 T cells showed a less reduced ERK phosphorylation in comparison to cells expressing only SPRED1. This obvious increase in ERK phosphorylation mediated by EVH1-β-geo led us to the assumption that the EVH1-β-geo fusion protein might exert a dominant negative effect on Ras/ERK/MAPK signaling.

Although both the EVH1 and the SPR domain of SPREDs have been shown to be required for appropriate function, the EVH1 domain rather seems to exert the biochemical inhibitory function on the Ras/ERK/MAPK pathway, while the SPR domain triggers the protein localization on cell membranes and association with interaction partners. The EVH1 domains of Ena/VASP, Homer/Vesl, and WASP protein families are also popular protein interaction modules (Fedorov et al., 1999). However, due to a narrower binding groove, a different mechanism of interaction and a binding to less proline-rich motifs is assumed for the SPRED proteins in comparison to the other EVH1 domain-containing proteins (Harmer et al., 2005; Zimmermann et al., 2004). Maybe associated with this predicted divergent binding modus, to date only two binding partners of the SPRED-EVH1 domain have been identified yet (Mardakheh et al., 2009; Stowe et al., 2012). Strikingly, interaction with both proteins indeed mediate inhibitory functions of SPREDs: Binding of SPRED2 to NBR1 targets the FGFR to lysosomal degradation and binding

of SPRED1 to the RasGAP NF1 inactivates Ras by inducing the hydrolysis of active Ras-GTP, both resulting in downregulation of Ras/ERK/MAPK signaling (Mardakheh et al., 2009; Stowe et al., 2012). Thus, in our SPRED2 KO mice, the functional EVH1 domain in the EVH1-β-geo fusion protein might intercept SPRED1 binding partners needed for proper SPRED-mediated Ras/ERK/MAPK pathway inhibition and therefore evoke a less reduced ERK activity.

A possible dominant negative effect of the EVH1-β-geo fusion protein is further supported by ΔC-SPRED1 and ΔC-SPRED2 mutants missing the SPR but still containing the EVH1 domain. These mutants also demonstrate dominant negative behavior in different cell types and after stimulation of Ras/ERK/MAPK signaling with different agonists (King et al., 2005; Nonami et al., 2004; Wakioka et al., 2001). Similarly, the EVH1 domain of the related VASP was also shown to act dominant negative when overexpressed in cardiac myocytes (Eigenthaler et al., 2003).

In contrast to the possible dominant negative effect of EVH1-β-geo on ERK activity, neither in the CRH promoter reporter assay nor in the Ets transcription factor reporter assay we could detect any effect of EVH1-β-geo on SPRED-mediated transcriptional regulation (5.14.2./5.14.3.) Although we suppose that SPRED-mediated inhibition of Ets factor-dependent CRH transcription is a downstream consequence of SPRED-mediated suppression of Ras/ERK/MAPK signaling, the two assays might not directly be comparable. While the ERK phosphorylation assay was performed in HEK 293 T cells, the transcriptional reporter assays were performed in the hypothalamic mHypoE-44 cell line. Furthermore, Ets-dependent CRH transcription is very likely activated by the Ras/ERK/MAPK cascade but maybe in part also coinfluenced by other pathways, which are not affected by SPREDs. Thus, the effect that EVH1-β-geo might exert on SPRED function might be dependent on cell type, tissue, and regulated process and on targeted and involved factors.

An indication that a dominant negative effect of EVH1-β-geo may at least partly play a role in the regulation of physiological processes in our SPRED2 KOs is the very complex and versatile phenotype including dwarfism (Bundschu et al., 2005), HPA axis dysregulation, salt and water imbalances, and cardiac, neuronal, behavioral, and mood disorders (see results 5.9.,5.10., 5.11., and 7.). In contrast, two further existing SPRED1 and SPRED2 KO mouse models have comparably mild phenotypes (Denayer et al., 2008; Inoue et al., 2005; Nobuhisa et al., 2004; Nonami et al., 2004; Phoenix and Temple, 2010). Therefore, the phenotype of SPRED2 KO mice generated in our group resembles most likely that of SPRED2 KO/SPRED1 HET mice but is less severe than that of the embryonic lethal SPRED1/2 double KO mouse model (Nobuhisa et al., 2004; Taniguchi et al., 2007). This may be caused by the additional dominant negative effect of EVH1-β-geo in our SPRED2 KO mice, leading to an impaired inhibitory effect of the remaining SPRED1 on the Ras/ERK/MAPK pathway.

6.2. Causes of Kidney Damage in SPRED2 KO Mice – An Interplay of Hydronephrosis, Atrophy, and Apoptosis

SPRED2 KO mice older than six months showed various stages of kidney degeneration, which was induced by hydronephrosis. Hydronephrosis is usually caused by obstruction of free urine flow out of the kidney leading to an upward transmission of uretral pressure and thus to distension and dilation of the renal pelvis. The causative obstruction may be partial or complete, unilateral or bilateral, and may develop acutely or chronically throughout the whole urinary system including kidneys, ureters, bladder, and urethra. Hence, hydronephrosis can result from various abnormal pathophysiological occurrences in the urinary tract already developing during fetal development, including congenital structural abnormalities of the junctions between the kidney, ureter, and bladder. Non-congenital and non-structural causes in adulthood leading to obstructions of the urinary tract comprise urinary stones, blood clots, retroperitoneal fibrosis within the urinary system, or external pressure on the urinary system e.g. by tumors or abnormally placed blood vessels. At last, hydronephrosis can also result from reflux of urine from the bladder back into the kidneys, which could be a consequence of prostatic enlargement, abnormal bladder muscle contraction, or abdominal tumors. Blocking of urine outflow or reflux will commonly result in infections and inflammatory reactions of the urinary tract, further leading to progressive renal atrophy and kidney failure.

Indeed, in our SPRED2 KO mice, hydronephrosis was accompanied by considerable atrophy of renal tissue and increased apoptosis of renal tubules. Characteristically, we observed mostly unilateral hydronephrosis associated with dramatic pelvis dilatations, parenchymal thinning, and loss of normal renal morphology. Affected and dilated kidneys further showed lymphocytic infiltration, which was indicative for inflammatory and infectious processes. In contrast, the contralateral kidneys were structurally and functionally still intact and seemed to compensate renal function.

Apoptosis, as also detected in kidneys of our SPRED2 KO mice, is considered to be the main process of cell death in renal parenchymal cell demise and atrophy and is often involved in the initiation and progression of a variety of renal disorders (Amore and Coppo, 2000; Ortiz, 2000). In our SPRED2 KO mouse model, hydronephrosis occurs in parallel to renal atrophy and apoptosis. However, the causal relationship, i.e. if apoptosis of kidney cells occurs first and may be causative for hydronephrosis and renal atrophy or, *vice versa*, if the occurrence of hydronephrosis may lead to apoptosis and renal atrophy remains to be elucidated.

Because kidney cells are armed with the genetic machinery to undergo apoptosis, this process is likely to play a physiological role in the kidney. In mature and healthy kidneys, an equilibrium

between cell proliferation and apoptosis keeps the turnover of renal cells very low, and apoptosis normally is a rare event (Mene and Amore, 1998; Savill, 1994; Savill et al., 1996). However, the deficiency of SPRED2, a critical Ras/ERK/MAPK pathway inhibitor, may result in a disequilibrium between ERK-regulated cell proliferation, differentiation, and apoptosis. In this manner, FGFR3 mutations leading to a constitutive active RTK and an upregulated Ras/ERK/MAPK signaling cause thanatophoric dysplasia. This skeletal disorder is a severe and lethal form of dwarfism similar to the milder hypochondroplasia, which we observed in SPRED2 KO mice (Bundschu et al., 2005; Legeai-Mallet et al., 1998). Interestingly, FGFR3 mutations in thanatophoric dysplasia do not hamper chondrocyte proliferation but rather alter their differentiation by triggering premature apoptosis of chondrocytes (Legeai-Mallet et al., 1998). Similarly, missing inhibition of ERK pathways and premature apoptosis contribute to the dwarfism but could also play a role in the observed cell death in kidneys of SPRED2-deficient mice. Cell debris could evoke occlusions of the urinary system leading to the disturbed urine outflow and further resulting in hydronephrosis and kidney atrophy.

Contrarily, hydronephrosis may also be the origin of apoptosis. The latter may occur in parallel to the hydronephrosis-provoked renal atrophy as described in several experimental rat studies using congenital and surgical hydronephrosis models (Gobe and Axelsen, 1987; Truong et al., 1996; Zhou et al., 2002). The demise of especially renal tubules rather than glomeruli, as also observed in SPRED2 KOs, seems to be a common consequence of hydronephrosis (Gobe and Axelsen, 1987; Truong et al., 1996; Zhou et al., 2002).

While in case of premature apoptosis, due to upregulated MAPK signaling, the hydronephrosis would presumably rather develop bilaterally starting already in early embryonic development, the hydronephrosis observed in SPRED2 KO mice was mostly unilateral and developed in adulthood. Thus, in our SPRED2 mouse model renal apoptosis might be, together with the extreme parenchymal atrophy, a consequence of hydronephrosis. By visual inspection and dissection, we could not detect any obvious stones within or tumors outside the urinary system. Accordingly, the blood test results did not provide any indication for urolith development because levels of Ca^{2+} and PO_4^{3-}, which may contribute to urinary stone formation, were normal (Table 1).

Taken together, the exact mechanisms of hydronephrosis development and the resulting kidney deterioration have to be investigated further. However, the profound polydipsia of SPRED2 KOs might play a role because psyochogenic or congenital polydipsia have been shown to lead to hydronephrosis both in men and mice (Blum and Friedland, 1983; Blum et al., 1983; McDill et al., 2006; Silverstein et al., 1961).

6.3. Polydipsia, Impaired Water Retention, and Hyperosmolality in SPRED2 KOs - No Effect of SPRED2 on AVP-Dependent Water Balance Regulation

The polydipsia observed in our SPRED2 KO mouse model was characterized by nearly doubled daily water uptake. A main cause of polydipsia and resulting polyuria is an impaired ability of the kidneys to concentrate urine. Most frequent reasons for polydipsia are Diabetes mellitus, Diabetes insipidus, and other osmotic disorders leading to diuresis, e.g. defects in renal transport carriers required for reabsorption of ions or glucose.

Diabetes mellitus is a well-known glucose metabolism disorder, which leads to osmotic diuresis due to increased glucose levels in serum and also in urine provoked by overload of renal glucose carriers required for glucose reabsorption. The elevation in serum glucose levels is caused by the lack of insulin or by an impaired cellular response to insulin, which normally regulates the glucose uptake from the blood into liver, skeletal muscle, and fat cells. In diabetes, blood glucose, usually the most readily available energy source in the body can not be used for metabolism. Instead, lipolysis takes place and fats are used as alternative energy source, which is accompanied by an increase in serum levels of cholesterol and triglycerides. However, because our SPRED2-deficient mice showed clearly reduced serum glucose, triglyceride, and cholesterol levels, we could exclude diabetes mellitus as cause of polydipsia.

Diabetes insipidus exists in two different types, each with a different etiology. The most prevalent form, diabetes insipidus centralis, is caused by AVP deficiency, while the second form, diabetes insipidus renalis, is elicited by an insensitivity of the kidney epithelia to respond to AVP. We wondered if a lacking or insufficient production of AVP is causative for the polydipsia in the SPRED2 KO mice. AVP, by binding to V2Rs in the basolateral membrane, increases water permeability of the kidney's distal convoluted tubule and collecting duct by triggering the insertion of AQP2 water channels into the apical cell membranes. Water deprivation is a common experiment to investigate disorders in AVP production and release because under normal physiological conditions thirst leads to an increase in AVP secretion and water reabsorption (Chatelain et al., 2003; Sebaai et al., 2002). However, experimental water starvation for 48 h revealed no differences in AVP release of SPRED2 KO mice in comparison to WT controls. Thus, diabetes insipidus centralis does not seem to be causative for the augmented water consumption of SPRED2 KOs. Furthermore, SPRED-mediated Ras/ERK/MAPK signaling seems to play a negligible role in the regulation of AVP secretion. If SPRED2 is able to impact the development of diabetes insipidus renalis, which can amongst

others be provoked by loss-of-function mutations of V2R (Yun et al., 2000) and AQP2 (Rojek et al., 2006; Yang et al., 2006), remains to be elucidated.

Nevertheless, compared to the already profound body weight loss in WT controls, the body weights of SPRED2 KO mice were even further reduced after water starvation indicating an extreme loss of body fluid especially in KOs. Accordingly, due to body weight reduction, adrenal, kidney, and brain weight/body weight ratios were increased after water starvation, a phenomenon that is commonly observed in water deprivation experiments (Chatelain et al., 2003; Sebaai et al., 2002; Ulrich-Lai et al., 2006). While the absolute weights of kidneys and brains were kept almost constant during water deprivation, the adrenal weights even increased due to hyperplastic and hypertrophic events representing also a common consequence of water starvation and chronic stress (Chatelain et al., 2003; Sebaai et al., 2002; Ulrich-Lai et al., 2006). Enhanced fluid loss and impaired water retention in SPRED KOs were further reinforced because water deprivation also increased serum osmolality to a greater extent that in WT littermates. Additionally, serum osmolality in KOs was already augmented under basal conditions and even despite the elevated water uptake. This basal hyperosmolality that could not be compensated by enhanced drinking in SPRED2-deficient mice pointed towards a disorder affecting renal salt reabsorption, eliciting an elevated serum salt load and thus causing osmotic diuresis and polydipsia.

6.4. Hyperaldosteronsim – The Elicitor of Hyperosmolality and Salt and Water Imbalances in SPRED2 KO Mice

Indeed, enhanced drinking was accompanied by significantly elevated serum Na^+ and Cl^- levels, which were very likely causative for serum hyperosmolality in SPRED2 KO mice because the levels of all other determined osmolytes were unchanged (Table 1). Nearly congruent phenotypes to that of our SPRED2 KO mice were described in mouse models carrying loss-of-function mutations of the renal Na^+-K^+-$2Cl^-$ cotransporter (Takahashi et al., 2000), the ROMK channel (Lorenz et al., 2002), the V2R (Yun et al., 2000), and of AQP2 (Rojek et al., 2006; Yang et al., 2006). All these KO mouse models display polydipsia and/or polyuria, hydronephrosis, dramatically impaired urine concentrating abilities, and growth retardation. Furthermore, the loss-of-function models of the renal salt transporters (Lorenz et al., 2002; Takahashi et al., 2000) and the V2R (Yun et al., 2000) additionally showed elevated serum Na^+ and Cl^- levels and hyperosmolality as it was seen in combination with all the other symptoms also in the

SPRED2 KOs. In these mouse models, hypernatremia, hyperchloremia, and the resulting hyperosmolality are regarded as secondary effects of dehydration due to an impaired salt reabsorption elicited by non-functional Na^+-K^+-$2Cl^-$ cotransporters (Takahashi et al., 2000) and ROMK channels, or due to an impaired water reabsorption elicited by non-functional V2Rs (Yun et al., 2000). However, in our SPRED2-deficient mice, elevated serum salt load does not seem to be a consequence of dysregulated salt and water transporters but instead caused by an imbalance in hormonal homeostasis. Hyperosmolality, elevated NaCl serum levels, and higher water uptake prompted us to estimate serum aldosterone and indeed, aldosterone levels were substantially increased in SPRED2 KOs. Hyperaldosteronism leads to Na^+ and fluid retention in the kidney and thus to volume overload. Hypervolemia further results in the activation of counter-regulatory mechanisms, e.g. inhibition of the RAS and ANP release. This further causes increased renal excretion of salt and water and therefore leads to polyuria and polydipsia. Taken together, in our SPRED2 KO mice, aldosterone supports an increased Na^+ reabsorption that can not be compensated by augmented water uptake. The resulting increased urinary sodium excretion additionally leads to osmotic diuresis and hence is the elicitor of the urinary concentrating defect, polyuria, and polydipsia. Thus, hyperaldosteronism seems to be causative for the disequilibrium of salt and water homeostasis in our SPRED2-deficient mice.

6.5. Increased Aldosterone-Synthase Expression and Elevated Serum ACTH – Causes of Renin-Angiotensin System-Independent Hyperaldosteronism

Hyperaldosteronism in our SPRED2 KO mice was characterized by nearly doubled serum aldosterone levels. Besides the disequilibrium of salt and water homeostasis described above, hyperaldosteronism might also be causally involved in the development of the observed kidney degeneration in SPRED2-deficient mice. Because hyperaldosteronism provokes the same symptoms as non-functional salt and water reabsorption mechanisms, e.g. Na^+-K^+-$2Cl^-$ cotransporter, ROMK, V2R, and AQP2, including hydronephrosis and kidney damage (Lorenz et al., 2002; Rojek et al., 2006; Takahashi et al., 2000; Yang et al., 2006; Yun et al., 2000), the elevated aldosterone levels in the SPRED2 KOs might contribute to hydronephrosis. In general, besides the well-known effects of aldosterone on the regulation of sodium and water homeostasis, aldosterone can also produce deleterious structural changes in tissues, especially heart and kidney. Aldosterone mediates vascular injury, hypertrophy, and dysregulation of

proliferation and apoptosis leading to fibrosis and tissue remodeling, all processes that might be involved in the kidney phenotype of SPRED2 KOs (Dooley et al., 2011; Hollenberg, 2004).

The main stimulators of aldosterone release are K^+, Ang II, and ACTH. An increase of serum K^+, which can stimulate aldosterone release and thus aldosterone-mediated renal tubular K^+ secretion, did not seem to be involved in the generation of hyperaldosteronism because K^+ levels were rather decreased in SPRED2 KO animals.

Dependent on the site of origin, hyperaldosteronism occurs in two forms: while the primary form is caused directly in the adrenal gland, where aldosterone biosynthesis takes place, the secondary form is provoked by overactivity of the RAS and hence is a result of excessive circulating Renin. Because the determination of Ang II levels revealed a decrease in serum Ang II by over 50% in the KOs, we conclude that hyperaldosteronism develops independently of an augmented RAS activity and thus is rather of primary nature. Aldosterone inhibits Renin release from the juxtaglomerular apparatus since it exerts negative feedback on the RAS indirectly by volume expansion (Kaufman et al., 1980). Renin secretion and hence the production of Ang II could be additionally impaired in SPRED2 KOs because Renin is produced by juxtaglomerular cells in the kidney (Tobian, 1962). Therefore, its synthesis and secretion might be disturbed in the atrophic kidney, which provides an additional explanation for the very low Ang II levels and RAS activity in the KOs.

Primary hyperaldosteronism, also known as Conn´s syndrome, first has been described in 1955 and was caused by an aldosterone-secreting adenoma of the adrenal (Conn, 1955). Aside from increased serum aldosterone in parallel to a lower RAS activity, hypernatremia and hypokalemia are common consequences of primary hyperaldosteronism as also observed in our SPRED2 KO mice. However, the classic feature of hypertension is lacking. Blood pressure measurements by both the non-invasive tail cuff method in conscious mice and by invasive catheterization revealed that SPRED2 KO mice were normotensive until the age of 12 months (data not shown). Although aldosterone-induced volume overload leads to hypertension in most human patients, not all mouse strains develop hypertension in response to aldosterone. Especially C57BL/6 and C57BL/6 intercrosses like our SPRED2 KO mice, which are kept on a comparably mixed background, seem to be less susceptible to mineralocorticoid-induced hypertension (Hartner et al., 2003; Sontia et al., 2008). Furthermore, since normal mouse chow, which is mainly based on vegetable ingredients, contains low sodium but high potassium, it is likely that the common consequences of hyperaldosteronism, i.e. hypokalemia, hypernatremia, and hypertension are less pronounced in mice than in humans.

Besides adrenal adenoma, further causes of primary hyperaldosteronism include adrenal carcinoma, glucocorticoid-remediable aldosteronism, and adrenal hyperplasia. In comparison to WTs, the adrenal weight/body weight ratios in SPRED2 KOs were significantly elevated and, although body weights were reduced due to dwarfism, the absolute weights of adrenals even

tended to be higher in the KO mice. This points towards a hypertrophic or hyperplastic event occurring in both adrenals. Indeed, in bilateral adrenal hyperplasia, which accounts for about 30% of all cases of hyperaldosteronism, the adrenal zona glomerulosa cells become hyperplastic resulting in excessive secretion of aldosterone (Davis et al., 1967).

During aldosterone biosynthesis, the last steps from 11-deoxycorticosterone are mediated by aldosterone synthase, an enzyme exclusively expressed in the adrenal zona glomerulosa (Domalik et al., 1991; Ogishima et al., 1992). In our SPRED2 KO mice, immunohistochemical staining of aldosterone synthase in adrenal gland sections demonstrated an obviously augmented aldosterone synthase expression as compared to WT controls. A very similar phenotype is observed in female TASK1 (TWIK-related acid-sensitive K^+ channel) KO mice, which resemble our SPRED2 KO mice in the increase and expansion of aldosterone synthase expression, hyperaldosteronism, hypokalemia, and diminished RAS activity (Heitzmann et al., 2008). In the TASK1-deficient mice, aldosterone synthase was absent the zona glomerulosa, the outer zone of the adrenal cortex, and the common site of aldosterone production. Instead, it was expressed to a greater extent than usually in deeper cortical zones corresponding to the zona faciculata and the zona reticularis. Similarly, in our SPRED2 KO mouse model, although aldosterone synthase expression was observed in the zona glomerulosa, the site of expression was obviously broadened. To our opinion, this increase in aldosterone synthase was either due to hyperplasia or hypertrophy of aldosterone synthase producing zona glomerulosa cells or due to repression of the zona fasciculata. The functional corticosterone synthesis and release from the zona fasciculata was attested by augmented serum corticosterone levels. In combination with the elevated adrenal weight/body weight ratios, in our opinion a hyperplasia or hypertrophy of aldosterone producing cells in the zona glomerulosa is more likely than to a mislocalization in the zona fasciculata. This assumption was further supported because SPRED2 expression in WT adrenals and endogenous *Spred2* promoter activity in HET and KO adrenals were predominantly observed within the thin layer of the zona glomerulosa. Similar to TASK1, SPRED2 and the Ras/ERK/MAPK pathway might be involved in mechanisms required for the regular adrenocortical zonation and appropriate aldosterone synthase expression in the zona glomerulosa. In consequence of loss of SPRED2-mediated inhibition, the hyperplasia of aldosterone producing cells might be provoked by an upregulated Ras/ERK/MAPK signaling. In line with that, increased ERK phosphorylation has been shown to induce proliferation in adrenal zona glomerulosa cells in response to a multiplicity of stimuli, amongst others ACTH, Ang II, and FGF (Hoeflich and Bielohuby, 2009). In our mice, due to SPRED2 deficiency hyperproliferation of aldosterone-releasing cells might take place even independent of simulation, and overshooting ERK activity might be a possible cause of the observed bilateral adrenal hyperplasia and hyperaldosteronism in SPRED2 KOs.

Besides augmented aldosterone expression, serum ACTH levels were found to be increased by 30% in the SPRED2 KOs. Aside from the trophic effect, which ACTH exerts on the adrenal gland alone or in combination with different stimuli and by activating amongst others the Ras/ERK/MAPK pathway (Hoeflich and Bielohuby, 2009; Ramachandran et al., 1977), it also mediates steroidogenic effects. Acutely, ACTH leads to the initiation of steroidogenesis and the mobilization of cholesterol, which is indispensable for the subsequent synthesis of corticosterone in the adrenal zona fasciculata and of aldosterone in the zona glomerulosa. Chronically, ACTH stimulates the transcription of all genes encoding the enzymes required for steroidogenesis (Sewer and Waterman, 2002, 2003), especially of 11β-hydroxylase, the critical enzyme in corticosterone synthesis (Kramer et al., 1983) but not of aldosterone synthase. In fact, aldosterone synthase expression is mainly stimulated by Ang II and K^+, and especially chronic ACTH stimulation rather decreases aldosterone synthase transcription (Holland and Carr, 1993). However, in mice biosynthesis pathways of aldosterone and corticosterone are homologous up to corticosterone. Therefore, a combination of both the augmented ACTH levels and the elevated aldosterone synthase expression in adrenal zona glomerulosa cells might contribute to the hyperaldosteronism in our SPRED2-deficient mice. On the one hand, increased ACTH may lead to the mobilization of more cholesterol, which is required for the initiation of steroidogenesis and which results in a greater availability of steroidogenic aldosterone precursors, i.e. of pregnenolone, progesterone, 11-deoxycorticosterone, and corticosterone. On the other hand, the elevated number of aldosterone synthase-containing cells, which may be associated with increased ERK activity in the adrenals of SPRED2 KO mice, causes an enhanced aldosterone synthesis from the abundant precursors, i.e. 11-deoxycorticosterone, corticosterone, and 18-hydroxy-corticosterone.

6.6. Hyperactivity of the HPA Axis in SPRED2-deficient Mice – Elevated Release of Stress and Growth Hormones

ACTH, due to its ability to stimulate especially 11β-hydroxylase, has a greater impact on glucocorticoid than on mineralocorticoid regulation (Kramer et al., 1983). Therefore, the hypercorticosteronism in SPRED2 KO mice, characterized by a more than doubled serum coricosterone level, is likely provoked by the elevated serum ACTH. Hypersecretion of ACTH is due to its role as stimulator of glucocorticoid synthesis associated with diseases affecting the glucocorticoid metabolism. One of them is Addison´s disease or primary adrenal insufficiency

leading to hypocorticism due to adrenal dysgenesis, due to impaired functionality of steroidogenic enzymes, or due to autoimmune adrenal destruction. This insufficient glucocorticoid production leads to an impaired feedback regulation on ACTH release and hence to augmented serum ACTH. A second disease is Cushing's disease, which describes the signs and symptoms of hypercorticism elicited by different causes. Cushing's syndrome, the primary form of hypercorticism is caused by augmented cortisol production due to adrenal gland tumors, hyperplastic adrenal glands, or an excess of exogenously administered corticosteroids. However, the most common cause of Cushing's syndrome responsible for 70% of all cases is secondary hypercorticism. Here, augmented glucocorticoid levels are due to increased ACTH release, which is mostly caused by a benign pituitary adenoma or by excess production of hypothalamic CRH, the latter also called tertiary hypercorticism. Because elevated ACTH levels were accompanied by hypercorticosteronism, Addison´s disease seemed unlikely in our SPRED2-deficient mice, but we considered that they might display a mild form of Cushing´s disease. In a comparable mouse model, the deletion of the neuroendocrine protein 7B2, a binding protein of PC2, which is involved in the processing of ACTH, causes a lethal form of Cushing´s disease in mice (Westphal et al., 1999). Reminiscent of SPRED2 KO mice, circulating ACTH together with corticosterone was markedly elevated and associated with adrenocortical expansion and hypoglycemia (Westphal et al., 1999).

Because hypothalamic CRH is the main endogenous stimulator of ACTH and thus indirectly also of the further downstream corticosterone, we determined CRH levels in brain lysates in order to enlighten ACTH overproduction. Since we detected a substantial elevation of hypothalamic CRH release by about 30% in SPRED2 KOs, we could demonstrate an upregulation of the entire HPA axis and of the released hormones CRH, ACTH, corticosterone, and aldosterone. In accordance to our SPRED2 KO mouse model, other transgenic mouse lines that overexpress CRH also exhibited augmented ACTH and corticosterone secretion associated with adrenal hypertrophy (Groenink et al., 2002; Stenzel-Poore et al., 1992) and displayed a Cushing´s disease-like phenotype (Stenzel-Poore et al., 1992). *Vice versa*, genomic ablation of CRH in mice resulted in low corticosterone levels, while levels of POMC and serum ACTH were unaltered. However, the diurnal variation of serum ACTH and corticosterone was completely absent, a phenomenon that might be involved in the observed atrophy of the adrenal cortex in this CRH KO mouse model (Venihaki and Majzoub, 1999). Thus, an appropriate regulation of HPA axis activity is required to maintain the morphology of the involved tissues, the circadian rhythmicity of stress hormone release, and the physiological responses to stress in general.

Not only stress hormones are released from hypothalamus and pituitary in a sequential manner but also growth hormones. Similar to the hypothalamic CRH-stimulated pituitary ACTH release further resulting in adrenal corticosterone and aldosterone secretion, the hypothalamic release of growth-hormone-releasing hormone stimulates the secretion of GH from the anterior pituitary,

which further mediates the production of IGF-1 in the liver. Despite the hypochondroplasia-like dwarfism observed in the SPRED2 KOs, serum levels of both GH and IGF-1 were surprisingly found to be elevated. In our SPRED2 KO mouse model, the dwarf phenotype seemed to be caused by loss of SPRED2-mediated inhibition of FGFR3-dependent ERK activation (Bundschu et al., 2005). Accordingly, FGFR3 gain-of-function mutations are causative for different forms of dwarfism like achondroplasia, hypochondroplasia, and thanatophoric hyperplasia both in men (Bellus et al., 1995; Rousseau et al., 1994; Shiang et al., 1994; Tavormina et al., 1995) and mice (Chen et al., 1999a; Wang et al., 1999). Aside from FGFR3 signaling, a multiplicity of other mechanism regulate long bone growth, hereunder GH and IGF (Isaksson et al., 1982; Isgaard et al., 1988). Therefore, a common treatment of achondroplasia in humans is the administration of GH, which improves the disturbed bone growth because the GH-stimulated IGF-1 release prevents chondrogenic apoptosis induced by activating FGFR3 mutations (Koike et al., 2003). Taken together, on the one hand, overproduction of GH and IGF-1 might be a consequence of the generalized upregulation of the HPA axis in SPRED2 KO mice. On the other hand, it might represent an intrinsic mechanism to compensate the FGFR3-provoked defect in long bone growth. However, the increased GH and IGF-1 levels do not seem to be sufficient to overcome the hypochondroplasia-like dwarf phenotype of the SPRED2 KOs.

6.7. Excessive Grooming in SPRED2 KOs - A Result of HPA Axis Overactivity and Evidence of Endogenous Stress

In addition to metabolic disorders, upregulation of stress hormone secretion from the HPA axis has also been shown to be involved in a variety of stress-associated and affective disorders, e.g. obsessive-compulsive disorder, depression, anxiety disorder, chronic pain, eat disorders, insomnia, and neurodegenerative disorders (Arborelius et al., 1999; Bao et al., 2008; Bomholt et al., 2004; Kluge et al., 2007; Stokes and Sikes, 1991). SPRED2 KO mice older than four months developed severe skin lesions, which were a consequence of excessive and injurious self-grooming. We assume that this enhanced grooming behavior results from an obsessive-compulsive disorder (OCD).

OCD is a common psychiatric disorder and defined by the presence of persistent intrusive, obsessive thoughts and repetitive, compulsive actions often encompassed by anxiety and depressive symptoms (Miguel et al., 2005). Very strikingly, two mouse models carrying loss-of-function mutations of brain-specific proteins show a remarkable phenotypical similarity to our

SPRED2 KOs. While the first mouse model lacks SAP90/PSD95-associated protein 3 (SAPAP3), a postsynaptic scaffolding protein highly expressed at striatal excitatory synapses (Welch et al., 2007), the second one is deficient of SLIT and NTRK-like protein-5 (SLITRK5), a neuron-specific transmembrane protein (Shmelkov et al., 2010). In agreement with our SPRED2 KO mice, these mouse lines develop bloody and purulent facial skin lesions and hair loss due to an obsessive-compulsive grooming disorder, which was associated with increased anxiety-like behaviors (Shmelkov et al., 2010; Welch et al., 2007). SAPAP3 and SLITRK5 are brain-specific, structural proteins, and thus it is not astonishing that their deficiency is associated with behavioral effects. However, SPRED2 is a Ras/MAPK/ERK signaling inhibitor but is highly expressed in brain and also involved in the regulation of CRH production and HPA axis activity. Indeed, CRH overexpressing mouse models are also susceptible to stress-associated diseases and anxiety-like behavior (Stenzel-Poore et al., 1994; van Gaalen et al., 2002). Similar to CRH overexpression, intracerebroventricular administration of CRH produces a significant increase in grooming, rearing, and locomotor activity in rat, which is consistent with its role as a mediator of the stress response (Dunn and Berridge, 1990; Sutton et al., 1982). Hence, the observed obsessive-compulsive grooming of our SPRFED2 KO mice is very likely a consequence of the excessive endogenous stress caused by overproduction of hormones released from the HPA axis.

6.8. SPRED2 - A Novel Regulator of CRH Gene Transcription and Release

SPRED1 has been shown to be expressed predominantly in neural tissues, i.e. in brain and in the central nervous system (Engelhardt et al., 2004; Kato et al., 2003). There, it participates in cortical development, neural stem cell proliferation, and vesicular trafficking (Engelhardt et al., 2004; Phoenix and Temple, 2010). In addition to a generally similar expression pattern of SPRED2 in brain (Bundschu et al., 2006a; Engelhardt et al., 2004), we could demonstrate both *Spred2* promoter activity and SPRED2 expression especially in hypothalamus and pituitary gland. Both tissues are part of the HPA axis and the release of HPA stress hormones from these tissues is triggered by the limbic system. The latter contains a multiplicity of brain structures including the limbic cortex, hippocampus, amygdala, and also the hypothalamus, which initiates HPA axis activity by CRH release.

Based on SPRED2 expression in the hypothalamus, which is in parallel the most upstream trigger of the HPA axis, based on the elevated hypothamalmic CRH release in the SPRED2 KOs, and based on the described functions of SPREDs as Ras/MAPK/ERK pathway inhibitors, we aimed to unravel the mechanism how SPREDs could be involved in the regulation of CRH release and HPA axis activity. Investigation of MAPK/ERK activity in PVN region-containing brain lysates of SPRED2 KO mice revealed a significantly increased ERK phosphorylation. This clearly demonstrated an upregulated hypothalamic Ras/ERK/MAPK signaling as a consequence of the lacking suppressive effect of SPRED2.

Because the Ras/ERK/MAPK cascade is well-known to be involved in transcriptional regulation of a great variety of target genes, we considered that it might also have an impact on CRH transcription. With our studies using a CRH promoter reporter containing the RE-1/NRSE regulatory element, we could confirm that CRH transcription in general is dependent on the RE-1/NRSE, which represses transcriptional activity of the CRH promoter (Seth and Majzoub, 2001). In studies using a CRH promoter reporter lacking the RE-1/NRSE, we could show that under these conditions the CRH promoter is active and that SPREDs indeed are able to inhibit CRH promoter activity and transcription in hypothalamic mHypoE-44 cells. *In vivo*, in hypothalami of SPRED2-deficient mice, levels of CRH mRNA were accordingly higher. Amongst others, activation of CRH transcription involves the phosphorylation and nuclear translocation of CREB and its recruitment to the CRE (cAMP responsive element) on the CRH promoter (Seasholtz et al., 1988). Multiple kinases can phosphorylate CREB, such as PKC, Ca^{2+}/calmodulin-dependent protein kinase (CaMK), PKA, but also MAPKs. Indeed, in hypothalamic PVN neurons producing CRH, the Ras/ERK/MAPK signaling pathway is activated in response to various stimuli, e.g. chronic stress, catecholamines, hypoglycemia, lipopolysaccharides, and prolactin. This increase in ERK phosphorylation induces an activation and phosphorylation of downstream transcription factors in the hypothalamus (Blume et al., 2009; Khan and Watts, 2004; Singru et al., 2008) and in the limbic system (Gerrits et al., 2006). It also provokes a parallel activation of CRH transcription in these neurons (Blume et al., 2009; Khan and Watts, 2004; Singru et al., 2008). Thus, we have confirmed that the Ras/ERK/MAPK cascade is in fact a potent regulator of CRH promoter activity both *in vitro* and *in vivo* and hence identified SPREDs as novel suppressors of CRH transcription.

In order to enlighten, which of the various target transcription factors might be the mediator between Ras/ERK/MAPK pathway activation and induction of CRH transcription, we performed a second reporter assay in mHypoE-44 cells, which was able to demonstrate the effect of SPREDs on Ets-dependent transcription. The Ets transcription factor family was of special interest for us because the CRH promoter comprises at least four binding sites for Ets,1 and because Ets1 is a well-known target of Ras/ERK/MAPK signaling (Wasylyk et al., 1998). In fact, in our reporter assay, SPREDs were also able to suppress Ets1-mediated transcription. The Ets

protein family is one of the largest families of transcription factors and contains a highly conserved DNA-binding domain, the Ets domain. It is common for all family members, which are sub-classified into twelve subfamilies comprising together at least 27 members in mammals (Sharrocks, 2001). The structure of the Ets domain is a variant of the winged helix-turn-helix motif and binds specifically to 11 bp DNA sequences that comprise a central GGA motif. That especially MAPK pathways have been linked with numerous regulatory events that involve Ets domain transcription factors is underlined by the identified docking domains for MAPKs in Ets domain proteins. For ERK, these special docking sites have been identified in the Ets family transcription factors Lin1, Elk1, and Ets1 (Jacobs et al., 1998; Jacobs et al., 1999; Tan et al., 1998; Yang et al., 1998a; Yang et al., 1998b). Taken together, Ets transcription factors, due to their multiple family members and even greater number of targets, regulate various developmental processes, e.g. neurogenesis, hematopoiesis, and angiogenesis (Sharrocks, 2001). Their involvement in HPA axis activity and CRH transcription, however, has been identified in this study first.

Aside from CRH promoter activity and transcription, also CRH production and release was influenced by SPREDs. While CRH secretion was inhibited by SPREDs in mHypoE-44 cells *in vitro*, it was increased *in vivo* in SPRED2-deficient mice.

In sum, we could demonstrate that SPRED2 is not only expressed in tissues of the HPA axis but also plays a critical role in the regulation of the HPA axis. Thus, the loss of SPRED-mediated Ras/ERK/MAPK suppression in our SPRED2 KO mice elicits an upregulated hypothalamic ERK signaling. This is followed by an augmented Ets-dependent CRH transcription and release and results in an overproduction of stress hormones at all levels of the HPA axis. The dysregulation of HPA hormone secretion has very far reaching consequences for the complete body. Therefore, the identification of SPRED2 as a critical regulator of HPA axis activity is a very valuable explanation, why SPRED2 deficiency leads to the observed very complex and versatile phenotype in mice, affecting multiple organs, hormonal, water, and electrolyte homeostasis, and mood.

6.9. SPRED1 and SPRED2 Deficiency - Redundancy in Protein Function and Impact on Cancer and Rasopathies

While SPRED3 expression has been described exclusively in brain, most tissues show overlapping expression of both SPRED1 and SPRED2. SPRED1, which is found predominantly

in neural tissues, is also detectable in most other organs similar to SPRED2, which is expressed almost ubiquitously throughout the whole body (Bundschu et al., 2006a; Engelhardt et al., 2004; Kato et al., 2003). While in mice, neither the sole deficiency of SPRED1 nor that of SPRED2 affects embryonic survival, SPRED1/2 double-deficient mice suffer from embryonic lethality due to severe subcutaneous hemorrhage and edema (Taniguchi et al., 2007). Thus, overlapping expression and overlapping protein functions might explain the viability and the comparatively mild phenotype of single SPRED1 (Denayer et al., 2008; Inoue et al., 2005; Nonami et al., 2004; Phoenix and Temple, 2010) and single SPRED2 KO mice (Nobuhisa et al., 2004; Wakabayashi et al., 2012). A comprehensive phenotypical characterization is not available for the SPRED-deficient mouse models generated by the other groups, and no serious impairments of these mouse models have been published. Nevertheless, the phenotype of the SPRED2 KO mouse model generated in our lab (Bundschu et al., 2005) seems to be particularly versatile and complex, especially in mice older than three months (Ullrich et al., 2011). In comparison to the SPRED2 KOs from the Japanese group, the putative more severe phenotype of our SPRED2 KO mice might be on the one hand dependent on the genetic background. While the Japanese SPRED1 and SPRED2 KO mice were backcrossed to C57BL/6 and are kept on a defined genetic background, the SPRED2 KO mouse line generated by us is kept on a mixed C57BL/6 x 129P2/OlaHsd background. On the other hand, the expression of the EVH1-β-geo fusion protein especially in our mouse model might play a role. The function of this fusion protein, i.e. if it might exert any dominant negative effect, is still a point of discussion and it might be dependent on the tissue and the regulated process (6.1.).

Due to the embryonic lethality of conventional SPRED1/2 double-deficient mice, it has been impossible to study the function and contribution of individual SPRED family members to the integrity of special organs. In order to investigate both the specific and the common functions of the different SPREDs, the generation of conditional KO mice is indispensable. Conditional SPRED KO models would also allow to discriminate between effects caused by a single *Spred1* or *Spred2* gene deficiency in a specific organ and to exclude systematic effects, comorbidities, and affection of other organs present in our global SPRED2 KO mouse model. Therefore, we already cloned SPRED1 and SPRED2 KO targeting vectors based on the Cre-loxP-system and allowing the generation of both global and conditional KOs. By mating our floxed SPRED mouse lines with tissue-specific Cre-expressing mouse lines, we will be able to investigate specific SPRED functions in a tissue-specific background. Additionally, due to the great potential of the targeting vectors to vary the SPRED1 and SPRED2 KO strategies, and due to the ability to mate the different conditional and/or global SPRED1 and SPRED2 KO mouse models with each other, we will be able to investigate all possible genotype combinations.

The consequence, which its deficiency causes in humans, is a very important question especially regarding SPRED2 protein function. SPRED1 deficiency in humans has been linked

to neurofibromatosis type 1-like Legius syndrome characterized predominantly by café-au-lait spots on the skin, facial abnormalities, and behavioral and learning problems (Brems et al., 2007; Messiaen et al., 2009; Pasmant et al., 2009b; Spurlock et al., 2009). In fact, SPRED1 KO mice very strikingly reflect the phenotype of Legius syndrome patients because they also show learning disabilities (Denayer et al., 2008) and facial dysmorphism (Brems et al., 2007; Inoue et al., 2005). Thus, our SPRED2 KO mouse model likely demonstrates also classical features of germ-line loss-of-function mutations of SPRED2 in humans. Interestingly the reduced body weight and the facial abnormalities described for the SPRED1 KOs (Brems et al., 2007; Inoue et al., 2005) may relate to dwarfism and the shortened face seen in our SPRED2 KO mice (Bundschu et al., 2005). Consistent with the elevated ACTH levels in SPRED2 KOs, SPRED1 deficiency leads to the development of café-au-lait spots in the skin. These brown macules contain melanin deposits probably caused by elevated levels of α-MSH, a cleavage product of ACTH and a stimulator of melanin production and release by melanocytes in skin and hair (Schwindinger and Levine, 1993). Besides the lethal phenotype of SPRED1/2 double KO mice (Taniguchi et al., 2007), these are further hints towards functional redundancy for SPRED1 and SPRED2.

Because Legius syndrome belongs to the rasopathies, a group of diseases all caused by a hyperactivated Ras/ERK/MAPK signaling, SPRED2 deficiency very likely also results in a rasopathy-like disease pattern. Characteristic symptoms very strongly reminiscent of the rasopathies (Tidyman and Rauen, 2009) and also present in our SPRED2 KO mice are short stature, recognizable facial features, renal anomalies, and cardiac disorders (hypertrophy, arrhythmias; data not shown). There are further indications for developmental delay, mental retardation and learning issues, and malabsorption; however, these assumptions have to be verified by suitable experiments. Furthermore, the consequences of SPRED2 germline loss-of-function mutations are still unknown but a genetic screen for SPRED2 mutations in DNA samples from rasopathy patients has been initiated by us and is in progress.

A large number of Ras/Raf/ERK pathway components were initially identified as proto-oncogenes, e.g. overexpression or activating mutants of growth factors like FGF (Delli Bovi et al., 1987), growth factor receptors, e.g. EGFR (Velu et al., 1987), Ras (Chang et al., 1982a; Chang et al., 1982b), Raf (Rapp et al., 1983), and various transcription factors targeted by the Ras/ERK/MAPK pathway, amongst others the above mentioned c-Fos (Miller et al., 1984), c-Jun (Maki et al., 1987), NF-κB (Kieran et al., 1990), c-Myc (Roussel et al., 1979; Weiss, 1982), and Ets1 (Watson et al., 1985). In some cases, rasopathy patients show an elevated predisposition to benign tumors like neurofibromas, Lisch nodules, lipomas but also to malignancies, e.g. astromas, gliomas, leukemias (Brems et al., 2007; Messiaen et al., 2009; Pasmant et al., 2009a). However, although the deficiency of SPREDs also leads to a

consecutive upregulation of Ras/Raf/ERK signaling, it basically does not result in the development of tumors or a special form of cancer.

Conclusion and Outlook 7

With this study, we initially demonstrated that SPRED2 is indispensable for appropriate regulation of HPA axis activity and body homeostasis. For the first time, we could show that SPRED2, by downregulating MAPK signaling via inhibition of ERK phosphorylation, suppresses Ets transcription factor-dependent activation of the CRH promoter and thus reduces CRH transcription and release (Figure 35). In line with that, our SPRED2 KO mice show an upregulated ERK activity in PVN-containing hypothalamic brain regions accompanied by both increased hypothalamic CRH mRNA levels and elevated release. The inhibitory effect of SPREDs could be confirmed by *in vitro* studies using the hypothalamic cell line mHypoE-44 and showing that both SPRED1 and SPRED2 are able to suppress Ets factor-dependent transcription, CRH promoter activity, and CRH secretion. This elevated production of CRH, the most upstream regulator of the HPA axis, elicits an elevated hormone secretion from all levels of the HPA axis, including downstream pituitary ACTH and adrenal corticosterone and aldosterone. This HPA axis upregulation resulting in hypercorticism is very likely causative for the obsessive grooming behavior and the consecutive wound development in SPRED2 KO mice. HPA axis hyperactivity in combination with the augmented adrenal aldosterone synthase expression induces hyperaldosteronism leading to salt and water imbalances (Figure 35). Due to the increase of serum aldosterone, the observed hypernatremia, hyperchloremia, and hyperosmolality can not be compensated by augmented water consumption. Water deprivation showed a substantial higher loss of body fluid in SPRED2 KOs and that polydispia develops independent of an AVP release disorder. Excessive drinking might causally be involved in the development of hydronephrosis further associated with renal atrophy, lymphocytic infiltration, apoptosis, and kidney damage. The complex and manifold phenotype of our SPRED2 KO mice might be further reinforced by the putative dominant negative effect of the expressed EVH1-β-geo fusion protein.

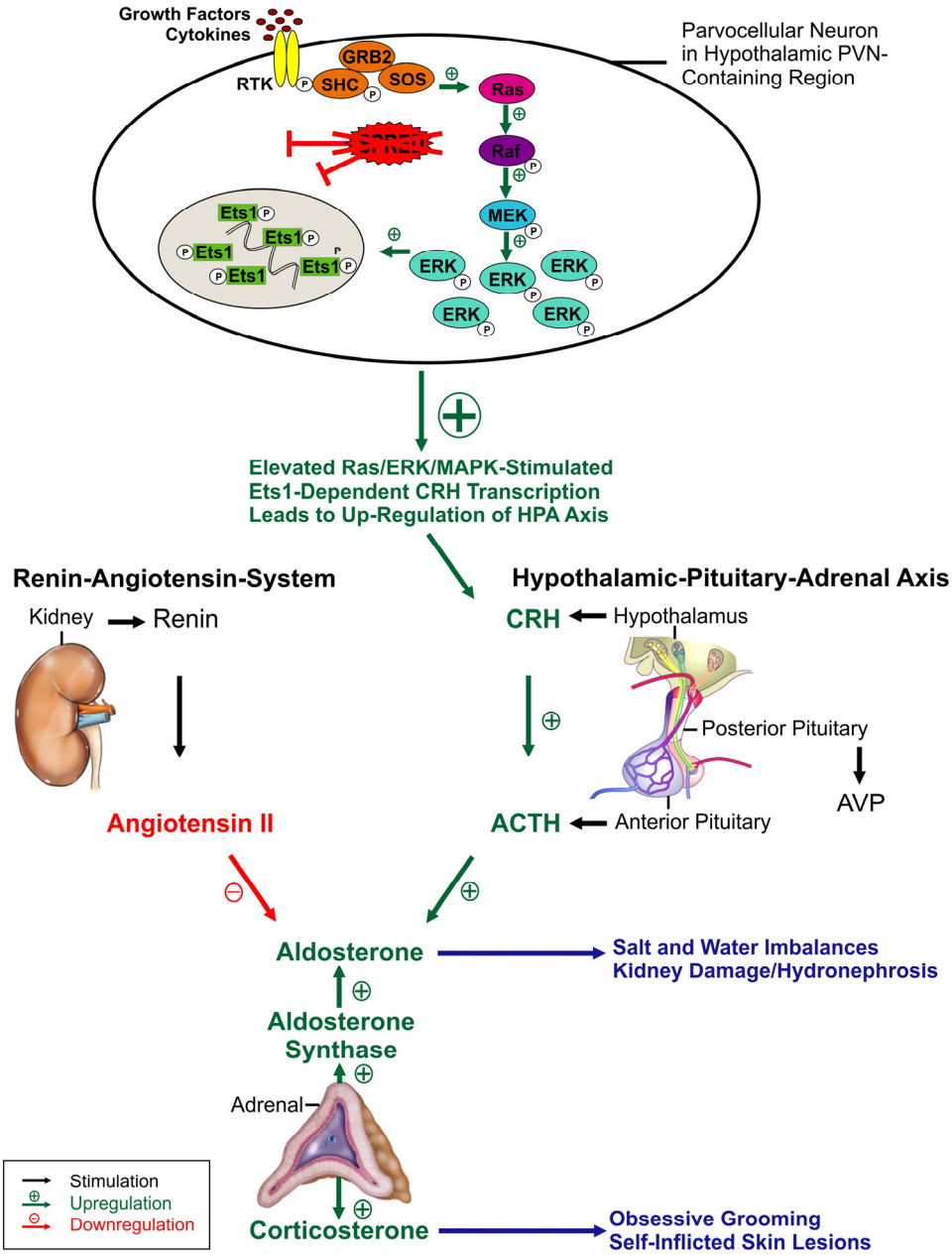

Figure 35: Putative Mechanism How SPRED2 Controls Hypothalamic-Pituitary-Adrenal Hormone Secretion

In our SPRED2 KO mouse model, due to the loss of SPRED2-mediated inhibition, Ras/ERK/MAPK signaling is upregulated in parvocellular neurons of the hypothalamic PVN. Increased ERK phosphorylation and activity leads to increased activation of Ets1 transcription factors, which in turn bind to Ets1 binding sites in the CRH promoter region and enhance CRH transcription. The resulting augmented CRH-release from the hypothalamus induces a complete upregulation of hormone secretion from the HPA axis, including elevated pituitary ACTH, adrenal corticosterone, and adrenal aldosterone release. The hyperaldosteronism develops independently of the RAS, as seen by downregulated Ang II levels, but is a consequence of HPA axis overactivation and of increased aldosterone synthase expression in adrenals of SPRED2 KO mice. This dysregulation of hormonal cascades causes both salt and water imbalances associated with kidney deterioration and altered stress-associated behavior in SPRED2 KO Mice. Thus, our study identifies SPREDs as novel regulators of hormone secretion and body homeostasis. *Figure in part reproduced from http://histoblog.viabloga.com/images/hypophyse_1_t.800.jpg, form http://www.gru.edu/mcg/phy/raineylab/images/webfigure2.jpg, and from http://www.paradisi.de/images_artikel/1/12556_0.jpg.*

Taken together, our study indicates that missing SPRED2-dependent inhibition of the Ras/ERK/MAPK pathway contributes to overshooting HPA hormone production, to the pathogenesis of hyperaldosteronism, and to obsessive-compulsive disorders.

7.1. SPRED2 – A Critical Mediator of Synaptic Transmission and Regulator of Behavior?

Based on the overactivated HPA axis and the obsessive grooming of our SPRED2 KO mice, we performed further studies to investigate how the elevated endogenous stress response impacts behavior, emotional state, and brain structure and functions. Because excessive stress hormone release from the HPA axis is associated with a great variety of behavioral and mood disorders in humans and mice (Arborelius et al., 1999; Bao et al., 2008; Bomholt et al., 2004; Kluge et al., 2007; Stokes and Sikes, 1991), we performed a set of behavioral standard tests with our SPRED2 KO mice and WT littermate controls, including elevated plus maze, open field, light dark box, and forced swim test. All these tests especially investigating anxiety and depression indicated a reduced anxiety in the SPRED2 KOs, which correlated with increasing age and the incidence of compulsive grooming. The stress hormone production of the HPA axis is subject to the control of neural afferents, which project from structures of the limbic system such as amygdala to the hypothalamus. The amygdala projects amongst others to the hypothalamic PVN from where CRH release takes place. It is instrumental in the development of anxiety and plays an important role in emotional evaluation and recognition of situations. Because incoming neural inputs to the amygdala are often of thalamic origin and because SPRED2 expression could be confirmed in both thalamus and amygdala, we performed electrophysiological measurements on acute brain slices to study synaptic transmission from thalamic nerve fibers to the amygdala. In our SPRED2 KO mice, we detected elevated excitatory postsynaptic currents (EPSCs), and the stimulation current required for triggering an action potential was reduced. Further studies revealed an increased synaptic depression and decreased frequencies and amplitudes of spontaneous vesicle fusions. In order to unravel if these changes in thalamic-amygdalal synaptic transmission are either due to pre- or postsynaptic events, we performed expression studies of both characteristic pre- and postsynaptic proteins by quantitative RT-PCR and Western Blot. Both amygdalal mRNA and protein levels of the postsynaptic metabotropic glutamate receptors mGluR2 and mGluR5 and the postsynaptic density protein 95 (PSD95) were accordingly upregulated, whilst that of presynaptic bassoon was downregulated. These data suggest counter-regulating mechanisms

between presynaptic and postsynaptic activities reflected by the dysregulated protein expressions. Another indication for a functional role of SPREDs in synaptic transmission is the confirmed colocalization of SPREDs with vesicles (Engelhardt et al., 2004; Phoenix and Temple, 2010) and their interaction with tubulin because microtubules amongst others mediate vesicle transport. Recently, the interaction with both α- and β-tubulines has been detected by us in a GST-EVH1-SPRED2 pulldown assay and confirmed by a tubulin-dimer pulldown assay. Electron microscopy studies demonstrated the general structural integrity of amygdalal synapses; however, detailed investigations are needed to determine e.g. the number and size of vesicles, dendritic counts, and the postsynaptic density. Because fluoxetine is a common drug for the treatment of mood disorders, especially obsessive-compulsive disorders and depression, we tried to rescue the excessive grooming by oral fluoxetine treatment. The antidepressant of the selective serotonin reuptake inhibitor class was administered at a dose of 20mg/kg/day within white chocolate and for the duration of four weeks. In fact, photo documentations on day zero, after two weeks, and after four weeks demonstrated a reduced severity and occurrence of wounds. In line, video documentations in the same time intervals also indicated a reduced grooming behavior after fluoxetine treatment, which further underlines the existence of a mood disorder in our SPRED2 KOs.

Taken together, this continuation study demonstrated that SPRED deficiency results in obsessive-compulsive grooming and in altered anxiety behavior, which is associated with increased synaptic transmission from thalamus to amygdala and can be rescued by fluoxetine treatment. Both efferent amygdalal nerve fibers, which trigger hypothalamic CRH release (Herman and Cullinan, 1997), and CRH, which binds to CRH1 receptors also abundant in the amygdala (Potter et al., 1994), may contribute to the behavioral disorders in the SPRED2 KOs. Increased synaptic transmission is accompanied by altered expression of pre- and postsynaptic proteins in the amygdala, very likely again mediated by loss of SPRED-dependent transcriptional inhibition of the dysregulated proteins. Thus, our study indicates a causal context between SPREDs, Ras/ERK/MAPK signaling, and obsessive-compulsive disorders for the first time and describes novel and detailed function of SPREDs in the brain.

7.2. SPRED2 – A Novel Regulator of Cardiac Hypertrophy and Electrical Conduction in the Heart?

A second study was conducted on the basis of the observation that dissections of SPRED2 KO mice older than three months did not only demonstrate kidney damage but also obviously

enlarged hearts. Calculated heart weight/body weight ratios were also elevated in the SPRED2 KOs. This was not a secondary effect of dwarfism because average absolute KO heart weights in comparison to that of WTs, which have an increased average body weight, were even slightly augmented. Thus, this was clear indication for cardiac hypertrophy. Because the manifest hyperaldosteronism and the reduced survival probability also indicate a cardiac phenotype, we investigated the cardiac performance of SPRED2 KO mice in a comprehensive and systematic manner by invasive and non-invasive standard procedures. Echocardiographic measurements performed in papillar and apical views and in systolic and diastolic dimensions confirmed the increased heart weight/body weight ratio by revealing an increased thickness of left-ventricular posterior walls in SPRED2 KO mice. Accordingly, the end-systolic and end-diastolic inner diameters of the left ventricle were decreased. These echocardiographic investigations, which allow the precise measurement of cardiac dimensions, were further confirmed and supplemented by invasive hemodynamics allowing real time measurements of left-ventricular pressure volume loops. Hemodynamics additionally and unexpectedly revealed an increased stroke volume, an elevated ejection fraction, and an augmented peak rate of pressure rise. Associated with this, calculated cardiac output and cardiac index were also increased in SPRED2 KOs. In order to be able to determine the heart rate, to investigate electrical conduction, and to detect possible arrhythmias, we performed high resolution electrocardiographs (ECGs) both under resting and stress conditions. These ECGs demonstrated an accelerated heart rate already under basal conditions, which together with the elevated stroke volume contributes to the increased cardiac output. Under stress simulation by isoproterenol administration, the heart rate between KOs and WTs did not differ. The increase of basal heart rate was characterized by a shortened TP segment in the SPRED2 KO mice, which reflects the time between ventricular repolarization and atrial depolarization. This is likely caused by premature depolarization of pacemaker cells, while the resulting positive chronotropic and inotropic effect did not seem to be beneficial for the SPRED2 KO mice. In sum, ECG recordings demonstrated that SPRED2 KOs are prone to develop various forms of spontaneous arrhythmias, e.g. different forms of AV blocks and extrasystoles. To investigate the susceptibility of KOs to develop arrhythmias also under stress conditions, we applied intracardiac overdrive pacing using an octapolar electrophysiological catheter. Pacing of atriae at decreasing pulse pause frequencies and increasing heart rates (50, 33, 25, 20 ms ≙ 1200, 1800, 2400, 3000 bpm) elicited atrial fibrillation in KOs starting at a pacing rate of 1800 bpm, whereas electrical conduction was not affected in WT controls under the same stimulus-provoked conditions. Furthermore, atrial pacing at a heart rate of 700 bpm indicated impaired sinus node function by prolonged sinus node recovery times in the SPRED2 KOs. Profound SPRED2 expression in the heart has been demonstrated on mRNA level by RT-PCR and on protein level by Western blot. X-Gal-stainings further detected *Spred2* promoter activity in both

atriae and ventricles. Upregulation of Ras/ERK/MAPK signaling in the heart is a critical marker of cardiac hypertrophy. In fact, the deletion of the ERK/MAPK inhibitor SPRED2 leads to cardiac hypertrophy and an increased cardiac ERK phosphorylation, which was determined by Western blot of heart lysates. In order to examine if cardiac dysfunction is caused directly by ablation of SPRED2 or indirectly by SPRED2 deficiency-mediated hyperaldosteronism, we rescued the hyperaldosteronism by treatment of SPRED2 KO mice and WT littermate controls with the aldosterone antagonist eplerenone. Eplerenone was administered by normal chow at a dose of 100mg/kg/day. All the above mentioned experiments to characterize cardiac performance were repeated in the same manner with the eplerenone-treated mice. Although the data analyses are still in progress, the heart weight/body weight ratio of the rescued mice is still elevated in SPRED2 KOs and does not significantly differ from the untreated groups, which indicates that the cardiac phenotype is at least to a great extent mediated by SPRED2 deficiency.

In sum, SPRED2 deficiency in mice provokes cardiac hypertrophy, which is confirmed by the increased heart weight/body weight ratio, the elevated left-ventricular wall thickness, the accordingly decreased systolic and endsystolic diameters, and the overactivated Ras/ERK-MAPK cascade. Surprisingly, cardiac ouput and index were higher in the SPRED2 KOs, which is caused by elevated stroke volume/ejection fraction and heart rate, the latter presumably caused by facilitated or premature excitation of pacemaker cells. The resulting positive chronotropic and inotropic effect is not beneficial for the SPRED2 KO mice since it is accompanied by arrhythmias both under resting and stress conditions. The causative mechanisms are still under investigation and hyperaldosteronism alone does not seem to be responsible for the cardiac phenotype of our SPRED2 KOs. Thus, this study might identify SPREDs as novel modulators of cardiac hypertrophy and electrical conduction in the heart.

7.3. SPRED2 Deficiency – A Cause of Rasopathy in Humans?

Apart from our SPRED2 KO model, which is undisputedly a very useful tool to study *Spred2 gene* function *in vivo,* we are engaged in correlating our mouse data with a human disease pattern. Human loss-of-function mutations of SPRED1 cause Legius syndrome, which is very similar to neurofibromatosis and belongs to the disease group of rasopaties. Therefore, we perform exon screening of SPRED2 mutations in DNA samples from rasopathy patients in cooperation with the Department of Human Genetics at the Universitaetsklinikum Hamburg-Eppendorf. Patients showing characteristic features of rasopathy syndromes, e.g. that of Costello syndrome, but lacking a characteristic mutation in the described disease causing gene,

i.e. in H-Ras, are of special interest for us. Based on the phenotype of our SPRED2 KO mouse model, which is already indicative for a rasopathy-like disease, and based on our recently initiated genetic screen for germline loss-of-function in humans, we are confident to identify a human correlate of SPRED2 deficiency in the near future.

References

8

Aguilera, G. (1998). Corticotropin releasing hormone, receptor regulation and the stress response. Trends in endocrinology and metabolism: TEM *9*, 329-336.

Aguilera, G., and Liu, Y. (2012). The molecular physiology of CRH neurons. Frontiers in neuroendocrinology *33*, 67-84.

Aguilera, G., Subburaju, S., Young, S., and Chen, J. (2008). The parvocellular vasopressinergic system and responsiveness of the hypothalamic pituitary adrenal axis during chronic stress. Prog Brain Res *170*, 29-39.

Alonso, G., Szafarczyk, A., Balmefrezol, M., and Assenmacher, I. (1986). Immunocytochemical evidence for stimulatory control by the ventral noradrenergic bundle of parvocellular neurons of the paraventricular nucleus secreting corticotropin releasing hormone and vasopressin in rats. Brain Res *397*, 297-307.

Amore, A., and Coppo, R. (2000). Role of apoptosis in pathogenesis and progression of renal diseases. Nephron *86*, 99-104.

Anderson, J.V., Struthers, A.D., Payne, N.N., Slater, J.D., and Bloom, S.R. (1986). Atrial natriuretic peptide inhibits the aldosterone response to angiotensin II in man. Clin Sci (Lond) *70*, 507-512.

Aoki, Y., Niihori, T., Kawame, H., Kurosawa, K., Ohashi, H., Tanaka, Y., Filocamo, M., Kato, K., Suzuki, Y., Kure, S.*, et al.* (2005). Germline mutations in HRAS proto-oncogene cause Costello syndrome. Nature genetics *37*, 1038-1040.

Arborelius, L., Owens, M.J., Plotsky, P.M., and Nemeroff, C.B. (1999). The role of corticotropin-releasing factor in depression and anxiety disorders. The Journal of endocrinology *160*, 1-12.

Arriza, J.L., Weinberger, C., Cerelli, G., Glaser, T.M., Handelin, B.L., Housman, D.E., and Evans, R.M. (1987). Cloning of human mineralocorticoid receptor complementary DNA: structural and functional kinship with the glucocorticoid receptor. Science (New York, NY *237*, 268-275.

Atlas, S.A. (2007). The renin-angiotensin aldosterone system: pathophysiological role and pharmacologic inhibition. J Manag Care Pharm *13*, 9-20.

Avrith, D., and Fitzsimons, J.T. (1978). Intracranial angiotensin II stimulates sodium appetite in the rat [proceedings]. J Physiol *282*, 40P-41P.

Ball, L.J., Jarchau, T., Oschkinat, H., and Walter, U. (2002). EVH1 domains: structure, function and interactions. FEBS Lett *513*, 45-52.

Bao, A.M., Meynen, G., and Swaab, D.F. (2008). The stress system in depression and neurodegeneration: focus on the human hypothalamus. Brain research reviews *57*, 531-553.

Bassett, M.H., Suzuki, T., Sasano, H., White, P.C., and Rainey, W.E. (2004). The orphan nuclear receptors NURR1 and NGFIB regulate adrenal aldosterone production. Mol Endocrinol *18*, 279-290.

Basso, N., and Terragno, N.A. (2001). History about the discovery of the renin-angiotensin system. Hypertension *38*, 1246-1249.

Beaumont, K., and Fanestil, D.D. (1983). Characterization of rat brain aldosterone receptors reveals high affinity for corticosterone. Endocrinology *113*, 2043-2051.

Beesley, A.H., Hornby, D., and White, S.J. (1998). Regulation of distal nephron K+ channels (ROMK) mRNA expression by aldosterone in rat kidney. J Physiol *509 (Pt 3)*, 629-634.

Bellus, G.A., McIntosh, I., Smith, E.A., Aylsworth, A.S., Kaitila, I., Horton, W.A., Greenhaw, G.A., Hecht, J.T., and Francomano, C.A. (1995). A recurrent mutation in the tyrosine kinase domain of fibroblast growth factor receptor 3 causes hypochondroplasia. Nature genetics *10*, 357-359.

Benetos, A., Gavras, I., and Gavras, H. (1987). Stimulation of vasopressin by calcium microinjections in the area of the paraventricular nucleus of the hypothalamus. Brain Res *412*, 182-184.

Bhargava, A., Fullerton, M.J., Myles, K., Purdy, T.M., Funder, J.W., Pearce, D., and Cole, T.J. (2001). The serum- and glucocorticoid-induced kinase is a physiological mediator of aldosterone action. Endocrinology *142*, 1587-1594.

Birnbaumer, M. (2000). Vasopressin receptors. Trends in endocrinology and metabolism: TEM *11*, 406-410.

Birnberg, N.C., Lissitzky, J.C., Hinman, M., and Herbert, E. (1983). Glucocorticoids regulate proopiomelanocortin gene expression in vivo at the levels of transcription and secretion. Proceedings of the National Academy of Sciences of the United States of America *80*, 6982-6986.

Blaine, E.H., and Davis, J.O. (1971). Evidence for a renal vascular mechanism in renin release: new observations with graded stimulation by aortic constriction. Circ Res *28*, Suppl 2:118-126.

Blum, A., and Friedland, G.W. (1983). Urinary tract abnormalities due to chronic psychogenic polydipsia. Am J Psychiatry *140*, 915-916.

Blum, A., Tempey, F.W., and Lynch, W.J. (1983). Somatic findings in patients with psychogenic polydipsia. J Clin Psychiatry *44*, 55-56.

Blume, A., Torner, L., Liu, Y., Subburaju, S., Aguilera, G., and Neumann, I.D. (2009). Prolactin activates mitogen-activated protein kinase signaling and corticotropin releasing hormone transcription in rat hypothalamic neurons. Endocrinology *150*, 1841-1849.

Bomholt, S.F., Harbuz, M.S., Blackburn-Munro, G., and Blackburn-Munro, R.E. (2004). Involvement and role of the hypothalamo-pituitary-adrenal (HPA) stress axis in animal models of chronic pain and inflammation. Stress *7*, 1-14.

Bos, J.L., Rehmann, H., and Wittinghofer, A. (2007). GEFs and GAPs: critical elements in the control of small G proteins. Cell *129*, 865-877.

Bottari, S.P., de Gasparo, M., Steckelings, U.M., and Levens, N.R. (1993). Angiotensin II receptor subtypes: characterization, signalling mechanisms, and possible physiological implications. Frontiers in neuroendocrinology *14*, 123-171.

Bradley, A., Evans, M., Kaufman, M.H., and Robertson, E. (1984). Formation of germ-line chimaeras from embryo-derived teratocarcinoma cell lines. Nature *309*, 255-256.

Brems, H., Chmara, M., Sahbatou, M., Denayer, E., Taniguchi, K., Kato, R., Somers, R., Messiaen, L., De Schepper, S., Fryns, J.P.*, et al.* (2007). Germline loss-of-function mutations in SPRED1 cause a neurofibromatosis 1-like phenotype. Nature genetics *39*, 1120-1126.

Brems, H., Pasmant, E., Van Minkelen, R., Wimmer, K., Upadhyaya, M., Legius, E., and Messiaen, L. (2012). Review and update of SPRED1 mutations causing Legius syndrome. Hum Mutat *33*, 1538-1546.

Brenner, B.M., Ballermann, B.J., Gunning, M.E., and Zeidel, M.L. (1990). Diverse biological actions of atrial natriuretic peptide. Physiol Rev *70*, 665-699.

Brinster, R.L., Chen, H.Y., Trumbauer, M., Senear, A.W., Warren, R., and Palmiter, R.D. (1981). Somatic expression of herpes thymidine kinase in mice following injection of a fusion gene into eggs. Cell *27*, 223-231.

Buehr, M., Meek, S., Blair, K., Yang, J., Ure, J., Silva, J., McLay, R., Hall, J., Ying, Q.L., and Smith, A. (2008). Capture of authentic embryonic stem cells from rat blastocysts. Cell *135*, 1287-1298.

Bula, C.M., Huhtakangas, J., Olivera, C., Bishop, J.E., Norman, A.W., and Henry, H.L. (2005). Presence of a truncated form of the vitamin D receptor (VDR) in a strain of VDR-knockout mice. Endocrinology *146*, 5581-5586.

Bultman, S.J., Michaud, E.J., and Woychik, R.P. (1992). Molecular characterization of the mouse agouti locus. Cell *71*, 1195-1204.

Bundschu, K. (2005). Generation and Characterization of Spred-2 Knockout Mice (Wuerzburg, Julius-Maximilians-Unuversitaet).

Bundschu, K., Gattenlohner, S., Knobeloch, K.P., Walter, U., and Schuh, K. (2006a). Tissue-specific Spred-2 promoter activity characterized by a gene trap approach. Gene Expr Patterns *6*, 247-255.

Bundschu, K., Knobeloch, K.P., Ullrich, M., Schinke, T., Amling, M., Engelhardt, C.M., Renne, T., Walter, U., and Schuh, K. (2005). Gene disruption of Spred-2 causes dwarfism. The Journal of biological chemistry *280*, 28572-28580.

Bundschu, K., Walter, U., and Schuh, K. (2006b). The VASP-Spred-Sprouty domain puzzle. The Journal of biological chemistry *281*, 36477-36481.

Bundschu, K., Walter, U., and Schuh, K. (2007). Getting a first clue about SPRED functions. Bioessays *29*, 897-907.

Calfa, G., Percy, A.K., and Pozzo-Miller, L. (2011). Experimental models of Rett syndrome based on Mecp2 dysfunction. Exp Biol Med (Maywood) *236*, 3-19.

Callebaut, I., Cossart, P., and Dehoux, P. (1998). EVH1/WH1 domains of VASP and WASP proteins belong to a large family including Ran-binding domains of the RanBP1 family. FEBS Lett *441*, 181-185.

Carpenter, C.C., Davis, J.O., and Ayers, C.R. (1961). Relation of renin, angiotensin II, and experimental renal hypertension to aldosterone secretion. The Journal of clinical investigation *40*, 2026-2042.

Casci, T., Vinos, J., and Freeman, M. (1999). Sprouty, an intracellular inhibitor of Ras signaling. Cell *96*, 655-665.

Cawthon, R.M., O'Connell, P., Buchberg, A.M., Viskochil, D., Weiss, R.B., Culver, M., Stevens, J., Jenkins, N.A., Copeland, N.G., and White, R. (1990). Identification and characterization of transcripts from the neurofibromatosis 1 region: the sequence and genomic structure of EVI2 and mapping of other transcripts. Genomics *7*, 555-565.

Chang, E.H., Furth, M.E., Scolnick, E.M., and Lowy, D.R. (1982a). Tumorigenic transformation of mammalian cells induced by a normal human gene homologous to the oncogene of Harvey murine sarcoma virus. Nature *297*, 479-483.

Chang, E.H., Gonda, M.A., Ellis, R.W., Scolnick, E.M., and Lowy, D.R. (1982b). Human genome contains four genes homologous to transforming genes of Harvey and Kirsten murine sarcoma viruses. Proceedings of the National Academy of Sciences of the United States of America *79*, 4848-4852.

Chang, F., Steelman, L.S., Lee, J.T., Shelton, J.G., Navolanic, P.M., Blalock, W.L., Franklin, R.A., and McCubrey, J.A. (2003). Signal transduction mediated by the Ras/Raf/MEK/ERK pathway from cytokine receptors to transcription factors: potential targeting for therapeutic intervention. Leukemia *17*, 1263-1293.

Chardin, P., Camonis, J.H., Gale, N.W., van Aelst, L., Schlessinger, J., Wigler, M.H., and Bar-Sagi, D. (1993). Human Sos1: a guanine nucleotide exchange factor for Ras that binds to GRB2. Science (New York, NY *260*, 1338-1343.

Chatelain, D., Montel, V., Dickes-Coopman, A., Chatelain, A., and Deloof, S. (2003). Trophic and steroidogenic effects of water deprivation on the adrenal gland of the adult female rat. Regulatory peptides *110*, 249-255.

Chen, L., Adar, R., Yang, X., Monsonego, E.O., Li, C., Hauschka, P.V., Yayon, A., and Deng, C.X. (1999a). Gly369Cys mutation in mouse FGFR3 causes achondroplasia by affecting both chondrogenesis and osteogenesis. The Journal of clinical investigation *104*, 1517-1525.

Chen, R., Lewis, K.A., Perrin, M.H., and Vale, W.W. (1993). Expression cloning of a human corticotropin-releasing-factor receptor. Proceedings of the National Academy of Sciences of the United States of America *90*, 8967-8971.

Chen, S.Y., Bhargava, A., Mastroberardino, L., Meijer, O.C., Wang, J., Buse, P., Firestone, G.L., Verrey, F., and Pearce, D. (1999b). Epithelial sodium channel regulated by aldosterone-

induced protein sgk. Proceedings of the National Academy of Sciences of the United States of America *96*, 2514-2519.

Cherradi, N., Brandenburger, Y., and Capponi, A.M. (1998). Mitochondrial regulation of mineralocorticoid biosynthesis by calcium and the StAR protein. European journal of endocrinology / European Federation of Endocrine Societies *139*, 249-256.

Clark, B.J., Ranganathan, V., and Combs, R. (2000). Post-translational regulation of steroidogenic acute regulatory protein by cAMP-dependent protein kinase A. Endocr Res *26*, 681-689.

Clem, B.F., Hudson, E.A., and Clark, B.J. (2005). Cyclic adenosine 3',5'-monophosphate (cAMP) enhances cAMP-responsive element binding (CREB) protein phosphorylation and phospho-CREB interaction with the mouse steroidogenic acute regulatory protein gene promoter. Endocrinology *146*, 1348-1356.

Condon, J.C., Pezzi, V., Drummond, B.M., Yin, S., and Rainey, W.E. (2002). Calmodulin-dependent kinase I regulates adrenal cell expression of aldosterone synthase. Endocrinology *143*, 3651-3657.

Conn, J.W. (1955). Primary aldosteronism. J Lab Clin Med *45*, 661-664.

Costantini, F., and Lacy, E. (1981). Introduction of a rabbit beta-globin gene into the mouse germ line. Nature *294*, 92-94.

Couet, J., Sargiacomo, M., and Lisanti, M.P. (1997). Interaction of a receptor tyrosine kinase, EGF-R, with caveolins. Caveolin binding negatively regulates tyrosine and serine/threonine kinase activities. The Journal of biological chemistry *272*, 30429-30438.

Coulombe, P., and Meloche, S. (2007). Atypical mitogen-activated protein kinases: structure, regulation and functions. Biochim Biophys Acta *1773*, 1376-1387.

Crews, C.M., Alessandrini, A., and Erikson, R.L. (1992). The primary structure of MEK, a protein kinase that phosphorylates the ERK gene product. Science (New York, NY *258*, 478-480.

Cullinan, W.E., Ziegler, D.R., and Herman, J.P. (2008). Functional role of local GABAergic influences on the HPA axis. Brain Struct Funct *213*, 63-72.

D'Arcangelo, G., Miao, G.G., Chen, S.C., Soares, H.D., Morgan, J.I., and Curran, T. (1995). A protein related to extracellular matrix proteins deleted in the mouse mutant reeler. Nature *374*, 719-723.

Dallman, M.F., Akana, S.F., Levin, N., Walker, C.D., Bradbury, M.J., Suemaru, S., and Scribner, K.S. (1994). Corticosteroids and the control of function in the hypothalamo-pituitary-adrenal (HPA) axis. Ann N Y Acad Sci *746*, 22-31; discussion 31-22, 64-27.

Davalos, M., Frega, N.S., Saker, B., and Leaf, A. (1978). Effect of exogenous and endogenous angiotensin II in the isolated perfused rat kidney. Am J Physiol *235*, F605-610.

Davies, H., Bignell, G.R., Cox, C., Stephens, P., Edkins, S., Clegg, S., Teague, J., Woffendin, H., Garnett, M.J., Bottomley, W.*, et al.* (2002). Mutations of the BRAF gene in human cancer. Nature *417*, 949-954.

Davis, W.W., Newsome, H.H., Jr., Wright, L.D., Jr., Hammond, W.G., Easton, J., and Bartter, F.C. (1967). Bilateral adrenal hyperplasia as a cause of primary aldosteronism with hypertension, hypokalemia and suppressed renin activity. Am J Med *42*, 642-647.

de Bold, A.J. (1985). Atrial natriuretic factor: a hormone produced by the heart. Science (New York, NY *230*, 767-770.

de Gasparo, M., Catt, K.J., Inagami, T., Wright, J.W., and Unger, T. (2000). International union of pharmacology. XXIII. The angiotensin II receptors. Pharmacol Rev *52*, 415-472.

de Maximy, A.A., Nakatake, Y., Moncada, S., Itoh, N., Thiery, J.P., and Bellusci, S. (1999). Cloning and expression pattern of a mouse homologue of drosophila sprouty in the mouse embryo. Mechanisms of development *81*, 213-216.

Delli Bovi, P., Curatola, A.M., Kern, F.G., Greco, A., Ittmann, M., and Basilico, C. (1987). An oncogene isolated by transfection of Kaposi's sarcoma DNA encodes a growth factor that is a member of the FGF family. Cell *50*, 729-737.

DeMille, M.M., Kimmel, B.E., and Rubin, G.M. (1996). A Drosophila gene regulated by rough and glass shows similarity to ena and VASP. Gene *183*, 103-108.

Denayer, E., Ahmed, T., Brems, H., Van Woerden, G., Borgesius, N.Z., Callaerts-Vegh, Z., Yoshimura, A., Hartmann, D., Elgersma, Y., D'Hooge, R.*, et al.* (2008). Spred1 is required for synaptic plasticity and hippocampus-dependent learning. J Neurosci *28*, 14443-14449.

Denayer, E., Chmara, M., Brems, H., Kievit, A.M., van Bever, Y., Van den Ouweland, A.M., Van Minkelen, R., de Goede-Bolder, A., Oostenbrink, R., Lakeman, P.*, et al.* (2011). Legius syndrome in fourteen families. Hum Mutat *32*, E1985-1998.

Dhillon, A.S., Hagan, S., Rath, O., and Kolch, W. (2007). MAP kinase signalling pathways in cancer. Oncogene *26*, 3279-3290.

di Bari, M.G., Lutsiak, M.E., Takai, S., Mostbock, S., Farsaci, B., Semnani, R.T., Wakefield, L.M., Schlom, J., and Sabzevari, H. (2009). TGF-beta modulates the functionality of tumor-infiltrating CD8+ T cells through effects on TCR signaling and Spred1 expression. Cancer Immunol Immunother *58*, 1809-1818.

Di, S., Malcher-Lopes, R., Halmos, K.C., and Tasker, J.G. (2003). Nongenomic glucocorticoid inhibition via endocannabinoid release in the hypothalamus: a fast feedback mechanism. J Neurosci *23*, 4850-4857.

Digilio, M.C., Conti, E., Sarkozy, A., Mingarelli, R., Dottorini, T., Marino, B., Pizzuti, A., and Dallapiccola, B. (2002). Grouping of multiple-lentigines/LEOPARD and Noonan syndromes on the PTPN11 gene. Am J Hum Genet *71*, 389-394.

Doetschman, T., Gregg, R.G., Maeda, N., Hooper, M.L., Melton, D.W., Thompson, S., and Smithies, O. (1987). Targetted correction of a mutant HPRT gene in mouse embryonic stem cells. Nature *330*, 576-578.

Domalik, L.J., Chaplin, D.D., Kirkman, M.S., Wu, R.C., Liu, W.W., Howard, T.A., Seldin, M.F., and Parker, K.L. (1991). Different isozymes of mouse 11 beta-hydroxylase produce mineralocorticoids and glucocorticoids. Mol Endocrinol *5*, 1853-1861.

Dooley, R., Harvey, B.J., and Thomas, W. (2011). The regulation of cell growth and survival by aldosterone. Front Biosci *16*, 440-457.

Dunn, A.J., and Berridge, C.W. (1990). Physiological and behavioral responses to corticotropin-releasing factor administration: is CRF a mediator of anxiety or stress responses? Brain Res Brain Res Rev *15*, 71-100.

Dunn, F.L., Brennan, T.J., Nelson, A.E., and Robertson, G.L. (1973). The role of blood osmolality and volume in regulating vasopressin secretion in the rat. The Journal of clinical investigation *52*, 3212-3219.

Eberle, A.N., ed. (1988). The Melanotropins (Basel, Karger).

Egan, S.E., Giddings, B.W., Brooks, M.W., Buday, L., Sizeland, A.M., and Weinberg, R.A. (1993). Association of Sos Ras exchange protein with Grb2 is implicated in tyrosine kinase signal transduction and transformation. Nature *363*, 45-51.

Eigenthaler, M., Engelhardt, S., Schinke, B., Kobsar, A., Schmitteckert, E., Gambaryan, S., Engelhardt, C.M., Krenn, V., Eliava, M., Jarchau, T.*, et al.* (2003). Disruption of cardiac Ena-VASP protein localization in intercalated disks causes dilated cardiomyopathy. Am J Physiol Heart Circ Physiol *285*, H2471-2481.

Engelhardt, C.M. (2004). Identification and Characterization of the SPRED Protein Family (Wuerzburg, Julius-Maximilians-Universitaet).

Engelhardt, C.M., Bundschu, K., Messerschmitt, M., Renne, T., Walter, U., Reinhard, M., and Schuh, K. (2004). Expression and subcellular localization of Spred proteins in mouse and human tissues. Histochem Cell Biol *122*, 527-538.

Epstein, A.N., Fitzsimons, J.T., and Simons, B.J. (1969). Drinking caused by the intracranial injection of angiotensin into the rat. J Physiol *200*, 98P-100P.

Evans, M.J., and Kaufman, M.H. (1981). Establishment in culture of pluripotential cells from mouse embryos. Nature *292*, 154-156.

Fedorov, A.A., Fedorov, E., Gertler, F., and Almo, S.C. (1999). Structure of EVH1, a novel proline-rich ligand-binding module involved in cytoskeletal dynamics and neural function. Nat Struct Biol *6*, 661-665.

Fish, J.E., Santoro, M.M., Morton, S.U., Yu, S., Yeh, R.F., Wythe, J.D., Ivey, K.N., Bruneau, B.G., Stainier, D.Y., and Srivastava, D. (2008). miR-126 regulates angiogenic signaling and vascular integrity. Dev Cell *15*, 272-284.

Freeman, M., Kimmel, B.E., and Rubin, G.M. (1992). Identifying targets of the rough homeobox gene of Drosophila: evidence that rhomboid functions in eye development. Development (Cambridge, England) *116*, 335-346.

Funder, J.W., Pearce, P.T., Smith, R., and Smith, A.I. (1988). Mineralocorticoid action: target tissue specificity is enzyme, not receptor, mediated. Science (New York, NY *242*, 583-585.

Fyhrquist, F., and Saijonmaa, O. (2008). Renin-angiotensin system revisited. Journal of internal medicine *264*, 224-236.

Galen, F.X., Devaux, C., Houot, A.M., Menard, J., Corvol, P., Corvol, M.T., Gubler, M.C., Mounier, F., and Camilleri, J.P. (1984). Renin biosynthesis by human tumoral juxtaglomerular cells. Evidences for a renin precursor. The Journal of clinical investigation *73*, 1144-1155.

Gantz, I., and Fong, T.M. (2003). The melanocortin system. American journal of physiology *284*, E468-474.

Gekle, M., and Grossmann, C. (2009). Actions of aldosterone in the cardiovascular system: the good, the bad, and the ugly? Pflugers Arch *458*, 231-246.

Gerrits, M., Westenbroek, C., Koch, T., Grootkarzijn, A., and ter Horst, G.J. (2006). Increased limbic phosphorylated extracellular-regulated kinase 1 and 2 expression after chronic stress is reduced by cyclic 17beta-estradiol administration. Neuroscience *142*, 1293-1302.

Gertler, F.B., Niebuhr, K., Reinhard, M., Wehland, J., and Soriano, P. (1996). Mena, a relative of VASP and Drosophila Enabled, is implicated in the control of microfilament dynamics. Cell *87*, 227-239.

Getting, S.J. (2006). Targeting melanocortin receptors as potential novel therapeutics. Pharmacol Ther *111*, 1-15.

Gillies, G.E., Linton, E.A., and Lowry, P.J. (1982). Corticotropin releasing activity of the new CRF is potentiated several times by vasopressin. Nature *299*, 355-357.

Giroud, C.J., Stachenko, J., and Venning, E.H. (1956). Secretion of aldosterone by the zona glomerulosa of rat adrenal glands incubated in vitro. Proc Soc Exp Biol Med *92*, 154-158.

Gobe, G.C., and Axelsen, R.A. (1987). Genesis of renal tubular atrophy in experimental hydronephrosis in the rat. Role of apoptosis. Laboratory investigation; a journal of technical methods and pathology *56*, 273-281.

Gordon, J.W., and Ruddle, F.H. (1981). Integration and stable germ line transmission of genes injected into mouse pronuclei. Science (New York, NY *214*, 1244-1246.

Gordon, J.W., Scangos, G.A., Plotkin, D.J., Barbosa, J.A., and Ruddle, F.H. (1980). Genetic transformation of mouse embryos by microinjection of purified DNA. Proceedings of the National Academy of Sciences of the United States of America *77*, 7380-7384.

Gordon, R.D., Kuchel, O., Liddle, G.W., and Island, D.P. (1967). Role of the sympathetic nervous system in regulating renin and aldosterone production in man. The Journal of clinical investigation *46*, 599-605.

Grammatopoulos, D.K., and Chrousos, G.P. (2002). Functional characteristics of CRH receptors and potential clinical applications of CRH-receptor antagonists. Trends in endocrinology and metabolism: TEM *13*, 436-444.

Gridley, T. (1991). Insertional versus targeted mutagenesis in mice. New Biol *3*, 1025-1034.

Groenink, L., Dirks, A., Verdouw, P.M., Schipholt, M., Veening, J.G., van der Gugten, J., and Olivier, B. (2002). HPA axis dysregulation in mice overexpressing corticotropin releasing hormone. Biological psychiatry *51*, 875-881.

Gunther, S. (1984). Characterization of angiotensin II receptor subtypes in rat liver. The Journal of biological chemistry *259*, 7622-7629.

Hacohen, N., Kramer, S., Sutherland, D., Hiromi, Y., and Krasnow, M.A. (1998). sprouty encodes a novel antagonist of FGF signaling that patterns apical branching of the Drosophila airways. Cell *92*, 253-263.

Hadari, Y.R., Kouhara, H., Lax, I., and Schlessinger, J. (1998). Binding of Shp2 tyrosine phosphatase to FRS2 is essential for fibroblast growth factor-induced PC12 cell differentiation. Mol Cell Biol *18*, 3966-3973.

Hancock, J.F., Magee, A.I., Childs, J.E., and Marshall, C.J. (1989). All ras proteins are polyisoprenylated but only some are palmitoylated. Cell *57*, 1167-1177.

Harbers, K., Jahner, D., and Jaenisch, R. (1981). Microinjection of cloned retroviral genomes into mouse zygotes: integration and expression in the animal. Nature *293*, 540-542.

Harmer, N.J., Sivak, J.M., Amaya, E., and Blundell, T.L. (2005). 1.15 A crystal structure of the X. tropicalis Spred1 EVH1 domain suggests a fourth distinct peptide-binding mechanism within the EVH1 family. FEBS Lett *579*, 1161-1166.

Hartner, A., Cordasic, N., Klanke, B., Veelken, R., and Hilgers, K.F. (2003). Strain differences in the development of hypertension and glomerular lesions induced by deoxycorticosterone acetate salt in mice. Nephrol Dial Transplant *18*, 1999-2004.

Hashimoto, S., Nakano, H., Singh, G., and Katyal, S. (2002). Expression of Spred and Sprouty in developing rat lung. Mechanisms of development *119 Suppl 1*, S303-309.

Hasuwa, H., Kaseda, K., Einarsdottir, T., and Okabe, M. (2002). Small interfering RNA and gene silencing in transgenic mice and rats. FEBS Lett *532*, 227-230.

Hattangady, N.G., Olala, L.O., Bollag, W.B., and Rainey, W.E. (2012). Acute and chronic regulation of aldosterone production. Mol Cell Endocrinol *350*, 151-162.

Haystead, T.A., Dent, P., Wu, J., Haystead, C.M., and Sturgill, T.W. (1992). Ordered phosphorylation of p42mapk by MAP kinase kinase. FEBS Lett *306*, 17-22.

Hayward, J.N. (1975). Neural control of the posterior pituitary. Annu Rev Physiol *37*, 191-210.

Heitzmann, D., Derand, R., Jungbauer, S., Bandulik, S., Sterner, C., Schweda, F., El Wakil, A., Lalli, E., Guy, N., Mengual, R.*, et al.* (2008). Invalidation of TASK1 potassium channels disrupts adrenal gland zonation and mineralocorticoid homeostasis. The EMBO journal *27*, 179-187.

Herman, J.P., and Cullinan, W.E. (1997). Neurocircuitry of stress: central control of the hypothalamo-pituitary-adrenocortical axis. Trends in neurosciences *20*, 78-84.

Herman, J.P., Figueiredo, H., Mueller, N.K., Ulrich-Lai, Y., Ostrander, M.M., Choi, D.C., and Cullinan, W.E. (2003). Central mechanisms of stress integration: hierarchical circuitry controlling hypothalamo-pituitary-adrenocortical responsiveness. Frontiers in neuroendocrinology *24*, 151-180.

Heyeraas, K.J., and Aukland, K. (1987). Interlobular arterial resistance: influence of renal arterial pressure and angiotensin II. Kidney international *31*, 1291-1298.

Hilger, R.A., Scheulen, M.E., and Strumberg, D. (2002). The Ras-Raf-MEK-ERK pathway in the treatment of cancer. Onkologie *25*, 511-518.

Hoeflich, A., and Bielohuby, M. (2009). Mechanisms of adrenal gland growth: signal integration by extracellular signal regulated kinases1/2. Journal of molecular endocrinology *42*, 191-203.

Hoffmeyer, A., Avots, A., Flory, E., Weber, C.K., Serfling, E., and Rapp, U.R. (1998). The GABP-responsive element of the interleukin-2 enhancer is regulated by JNK/SAPK-activating pathways in T lymphocytes. The Journal of biological chemistry *273*, 10112-10119.

Holgado-Madruga, M., Emlet, D.R., Moscatello, D.K., Godwin, A.K., and Wong, A.J. (1996). A Grb2-associated docking protein in EGF- and insulin-receptor signalling. Nature *379*, 560-564.

Holland, O.B., and Carr, B. (1993). Modulation of aldosterone synthase messenger ribonucleic acid levels by dietary sodium and potassium and by adrenocorticotropin. Endocrinology *132*, 2666-2673.

Hollenberg, N.K. (2004). Aldosterone in the development and progression of renal injury. Kidney international *66*, 1-9.

Inoue, H., Kato, R., Fukuyama, S., Nonami, A., Taniguchi, K., Matsumoto, K., Nakano, T., Tsuda, M., Matsumura, M., Kubo, M.*, et al.* (2005). Spred-1 negatively regulates allergen-induced airway eosinophilia and hyperresponsiveness. J Exp Med *201*, 73-82.

Isaksson, O.G., Jansson, J.O., and Gause, I.A. (1982). Growth hormone stimulates longitudinal bone growth directly. Science (New York, NY *216*, 1237-1239.

Isgaard, J., Moller, C., Isaksson, O.G., Nilsson, A., Mathews, L.S., and Norstedt, G. (1988). Regulation of insulin-like growth factor messenger ribonucleic acid in rat growth plate by growth hormone. Endocrinology *122*, 1515-1520.

Ishikawa, S., and Schrier, R.W. (1983). Role of calcium in osmotic and nonosmotic release of vasopressin from rat organ culture. Am J Physiol *244*, R703-708.

Jacobs, D., Beitel, G.J., Clark, S.G., Horvitz, H.R., and Kornfeld, K. (1998). Gain-of-function mutations in the Caenorhabditis elegans lin-1 ETS gene identify a C-terminal regulatory domain phosphorylated by ERK MAP kinase. Genetics *149*, 1809-1822.

Jacobs, D., Glossip, D., Xing, H., Muslin, A.J., and Kornfeld, K. (1999). Multiple docking sites on substrate proteins form a modular system that mediates recognition by ERK MAP kinase. Genes & development *13*, 163-175.

Jaenisch, R. (1976). Germ line integration and Mendelian transmission of the exogenous Moloney leukemia virus. Proceedings of the National Academy of Sciences of the United States of America *73*, 1260-1264.

Jaenisch, R. (1988). Transgenic animals. Science (New York, NY *240*, 1468-1474.

Jaenisch, R., and Mintz, B. (1974). Simian virus 40 DNA sequences in DNA of healthy adult mice derived from preimplantation blastocysts injected with viral DNA. Proceedings of the National Academy of Sciences of the United States of America *71*, 1250-1254.

Jenks, B.G. (2009). Regulation of proopiomelanocortin gene expression: an overview of the signaling cascades, transcription factors, and responsive elements involved. Ann N Y Acad Sci *1163*, 17-30.

Johne, C., Matenia, D., Li, X.Y., Timm, T., Balusamy, K., and Mandelkow, E.M. (2008). Spred1 and TESK1--two new interaction partners of the kinase MARKK/TAO1 that link the microtubule and actin cytoskeleton. Mol Biol Cell *19*, 1391-1403.

Johns, D.W., Peach, M.J., Gomez, R.A., Inagami, T., and Carey, R.M. (1990). Angiotensin II regulates renin gene expression. Am J Physiol *259*, F882-887.

Jonat, C., Rahmsdorf, H.J., Park, K.K., Cato, A.C., Gebel, S., Ponta, H., and Herrlich, P. (1990). Antitumor promotion and antiinflammation: down-modulation of AP-1 (Fos/Jun) activity by glucocorticoid hormone. Cell *62*, 1189-1204.

Jorgensen, P.L. (1972). The role of aldosterone in the regulation of (Na + + K +)-ATPase in rat kidney. J Steroid Biochem *3*, 181-191.

Kachroo, N., Valencia, T., Warren, A.Y., and Gnanapragasam, V.J. (2013). Evidence for downregulation of the negative regulator SPRED2 in clinical prostate cancer. Br J Cancer *108*, 597-601.

Kaschina, E., and Unger, T. (2003). Angiotensin AT1/AT2 receptors: regulation, signalling and function. Blood Press *12*, 70-88.

Kato, R., Nonami, A., Taketomi, T., Wakioka, T., Kuroiwa, A., Matsuda, Y., and Yoshimura, A. (2003). Molecular cloning of mammalian Spred-3 which suppresses tyrosine kinase-mediated Erk activation. Biochem Biophys Res Commun *302*, 767-772.

Kaufman, J.S., Hamburger, R.J., and Flamenbaum, W. (1980). Renal renin responses to changes in volume status and perfusion pressure. Am J Physiol *238*, F488-490.

Keegan, C.E., and Hammer, G.D. (2002). Recent insights into organogenesis of the adrenal cortex. Trends in endocrinology and metabolism: TEM *13*, 200-208.

Keller-Wood, M.E., and Dallman, M.F. (1984). Corticosteroid inhibition of ACTH secretion. Endocrine reviews *5*, 1-24.

Kemendy, A.E., Kleyman, T.R., and Eaton, D.C. (1992). Aldosterone alters the open probability of amiloride-blockable sodium channels in A6 epithelia. Am J Physiol *263*, C825-837.

Khan, A.M., and Watts, A.G. (2004). Intravenous 2-deoxy-D-glucose injection rapidly elevates levels of the phosphorylated forms of p44/42 mitogen-activated protein kinases (extracellularly regulated kinases 1/2) in rat hypothalamic parvicellular paraventricular neurons. Endocrinology *145*, 351-359.

Kieran, M., Blank, V., Logeat, F., Vandekerckhove, J., Lottspeich, F., Le Bail, O., Urban, M.B., Kourilsky, P., Baeuerle, P.A., and Israel, A. (1990). The DNA binding subunit of NF-kappa B is identical to factor KBF1 and homologous to the rel oncogene product. Cell *62*, 1007-1018.

Kim, H.J., and Bar-Sagi, D. (2004). Modulation of signalling by Sprouty: a developing story. Nat Rev Mol Cell Biol *5*, 441-450.

King, A.J., Wireman, R.S., Hamilton, M., and Marshall, M.S. (2001). Phosphorylation site specificity of the Pak-mediated regulation of Raf-1 and cooperativity with Src. FEBS Lett *497*, 6-14.

King, J.A., Corcoran, N.M., D'Abaco, G.M., Straffon, A.F., Smith, C.T., Poon, C.L., Buchert, M., I, S., Hall, N.E., Lock, P.*, et al.* (2006). Eve-3: a liver enriched suppressor of Ras/MAPK signaling. J Hepatol *44*, 758-767.

King, J.A., Straffon, A.F., D'Abaco, G.M., Poon, C.L., I, S.T., Smith, C.M., Buchert, M., Corcoran, N.M., Hall, N.E., Callus, B.A.*, et al.* (2005). Distinct requirements for the Sprouty domain for functional activity of Spred proteins. Biochem J *388*, 445-454.

Kiryluk, K., and Isom, R. (2007). Thiazolidinediones and fluid retention. Kidney international *72*, 762-768.

Kluge, M., Schussler, P., Kunzel, H.E., Dresler, M., Yassouridis, A., and Steiger, A. (2007). Increased nocturnal secretion of ACTH and cortisol in obsessive compulsive disorder. J Psychiatr Res *41*, 928-933.

Koike, M., Yamanaka, Y., Inoue, M., Tanaka, H., Nishimura, R., and Seino, Y. (2003). Insulin-like growth factor-1 rescues the mutated FGF receptor 3 (G380R) expressing ATDC5 cells from apoptosis through phosphatidylinositol 3-kinase and MAPK. J Bone Miner Res *18*, 2043-2051.

Koshimizu, T.A., Nakamura, K., Egashira, N., Hiroyama, M., Nonoguchi, H., and Tanoue, A. (2012). Vasopressin V1a and V1b receptors: from molecules to physiological systems. Physiol Rev *92*, 1813-1864.

Kouhara, H., Hadari, Y.R., Spivak-Kroizman, T., Schilling, J., Bar-Sagi, D., Lax, I., and Schlessinger, J. (1997). A lipid-anchored Grb2-binding protein that links FGF-receptor activation to the Ras/MAPK signaling pathway. Cell *89*, 693-702.

Kovacs, K.J., Foldes, A., and Sawchenko, P.E. (2000). Glucocorticoid negative feedback selectively targets vasopressin transcription in parvocellular neurosecretory neurons. J Neurosci *20*, 3843-3852.

Kramer, R.E., Simpson, E.R., and Waterman, M.R. (1983). Induction of 11 beta-hydroxylase by corticotropin in primary cultures of bovine adrenocortical cells. The Journal of biological chemistry *258*, 3000-3005.

Kramer, S., Okabe, M., Hacohen, N., Krasnow, M.A., and Hiromi, Y. (1999). Sprouty: a common antagonist of FGF and EGF signaling pathways in Drosophila. Development (Cambridge, England) *126*, 2515-2525.

Kretz, O., Reichardt, H.M., Schutz, G., and Bock, R. (1999). Corticotropin-releasing hormone expression is the major target for glucocorticoid feedback-control at the hypothalamic level. Brain Res *818*, 488-491.

Kunath, T., Gish, G., Lickert, H., Jones, N., Pawson, T., and Rossant, J. (2003). Transgenic RNA interference in ES cell-derived embryos recapitulates a genetic null phenotype. Nat Biotechnol *21*, 559-561.

Kyriakis, J.M., App, H., Zhang, X.F., Banerjee, P., Brautigan, D.L., Rapp, U.R., and Avruch, J. (1992). Raf-1 activates MAP kinase-kinase. Nature *358*, 417-421.

Lander, E.S., Linton, L.M., Birren, B., Nusbaum, C., Zody, M.C., Baldwin, J., Devon, K., Dewar, K., Doyle, M., FitzHugh, W.*, et al.* (2001). Initial sequencing and analysis of the human genome. Nature *409*, 860-921.

Laycock-van Spyk, S., Jim, H.P., Thomas, L., Spurlock, G., Fares, L., Palmer-Smith, S., Kini, U., Saggar, A., Patton, M., Mautner, V.*, et al.* (2011). Identification of five novel SPRED1 germline mutations in Legius syndrome. Clin Genet *80*, 93-96.

Leevers, S.J., Paterson, H.F., and Marshall, C.J. (1994). Requirement for Ras in Raf activation is overcome by targeting Raf to the plasma membrane. Nature *369*, 411-414.

Legeai-Mallet, L., Benoist-Lasselin, C., Delezoide, A.L., Munnich, A., and Bonaventure, J. (1998). Fibroblast growth factor receptor 3 mutations promote apoptosis but do not alter chondrocyte proliferation in thanatophoric dysplasia. The Journal of biological chemistry *273*, 13007-13014.

Legius, E., Schrander-Stumpel, C., Schollen, E., Pulles-Heintzberger, C., Gewillig, M., and Fryns, J.P. (2002). PTPN11 mutations in LEOPARD syndrome. Journal of medical genetics *39*, 571-574.

Li, D., Jackson, R.A., Yusoff, P., and Guy, G.R. (2010). Direct association of Sprouty-related protein with an EVH1 domain (SPRED) 1 or SPRED2 with DYRK1A modifies substrate/kinase interactions. The Journal of biological chemistry *285*, 35374-35385.

Li, P., Tong, C., Mehrian-Shai, R., Jia, L., Wu, N., Yan, Y., Maxson, R.E., Schulze, E.N., Song, H., Hsieh, C.L.*, et al.* (2008). Germline competent embryonic stem cells derived from rat blastocysts. Cell *135*, 1299-1310.

Liakos, P., Chambaz, E.M., Feige, J.J., and Defaye, G. (1998). Expression of ACTH receptors (MC2-R and MC5-R) in the glomerulosa and the fasciculata-reticularis zones of bovine adrenal cortex. Endocr Res *24*, 427-432.

Lim, J., Yusoff, P., Wong, E.S., Chandramouli, S., Lao, D.H., Fong, C.W., and Guy, G.R. (2002). The cysteine-rich sprouty translocation domain targets mitogen-activated protein kinase inhibitory proteins to phosphatidylinositol 4,5-bisphosphate in plasma membranes. Mol Cell Biol *22*, 7953-7966.

Liu, F., Qin, H.B., Xu, B., Zhou, H., and Zhao, D.Y. (2012). Profiling of miRNAs in pediatric asthma: upregulation of miRNA-221 and miRNA-485-3p. Mol Med Rep *6*, 1178-1182.

Liu, X.Y., Yang, Y.F., Wu, C.T., Xiao, F.J., Zhang, Q.W., Ma, X.N., Li, Q.F., Yan, J., Wang, H., and Wang, L.S. (2010). Spred2 is involved in imatinib-induced cytotoxicity in chronic myeloid leukemia cells. Biochem Biophys Res Commun *393*, 637-642.

Lock, P., I, S.T., Straffon, A.F., Schieb, H., Hovens, C.M., and Stylli, S.S. (2006). Spred-2 steady-state levels are regulated by phosphorylation and Cbl-mediated ubiquitination. Biochem Biophys Res Commun *351*, 1018-1023.

Lolait, S.J., O'Carroll, A.M., McBride, O.W., Konig, M., Morel, A., and Brownstein, M.J. (1992). Cloning and characterization of a vasopressin V2 receptor and possible link to nephrogenic diabetes insipidus. Nature *357*, 336-339.

Lorenz, J.N., Baird, N.R., Judd, L.M., Noonan, W.T., Andringa, A., Doetschman, T., Manning, P.A., Liu, L.H., Miller, M.L., and Shull, G.E. (2002). Impaired renal NaCl absorption in mice lacking the ROMK potassium channel, a model for type II Bartter's syndrome. The Journal of biological chemistry *277*, 37871-37880.

Lovenberg, T.W., Liaw, C.W., Grigoriadis, D.E., Clevenger, W., Chalmers, D.T., De Souza, E.B., and Oltersdorf, T. (1995). Cloning and characterization of a functionally distinct corticotropin-releasing factor receptor subtype from rat brain. Proceedings of the National Academy of Sciences of the United States of America *92*, 836-840.

Lowenstein, E.J., Daly, R.J., Batzer, A.G., Li, W., Margolis, B., Lammers, R., Ullrich, A., Skolnik, E.Y., Bar-Sagi, D., and Schlessinger, J. (1992). The SH2 and SH3 domain-containing protein GRB2 links receptor tyrosine kinases to ras signaling. Cell *70*, 431-442.

Ma, X.M., Levy, A., and Lightman, S.L. (1997). Rapid changes in heteronuclear RNA for corticotrophin-releasing hormone and arginine vasopressin in response to acute stress. The Journal of endocrinology *152*, 81-89.

Ma, X.N., Liu, X.Y., Yang, Y.F., Xiao, F.J., Li, Q.F., Yan, J., Zhang, Q.W., Wang, L.S., Li, X.Y., and Wang, H. (2011). Regulation of human hepatocellular carcinoma cells by Spred2 and correlative studies on its mechanism. Biochem Biophys Res Commun *410*, 803-808.

Macdonald, S.G., Crews, C.M., Wu, L., Driller, J., Clark, R., Erikson, R.L., and McCormick, F. (1993). Reconstitution of the Raf-1-MEK-ERK signal transduction pathway in vitro. Mol Cell Biol *13*, 6615-6620.

Maki, Y., Bos, T.J., Davis, C., Starbuck, M., and Vogt, P.K. (1987). Avian sarcoma virus 17 carries the jun oncogene. Proceedings of the National Academy of Sciences of the United States of America *84*, 2848-2852.

Malumbres, M., and Barbacid, M. (2003). RAS oncogenes: the first 30 years. Nat Rev Cancer *3*, 459-465.

Mangelsdorf, D.J., Thummel, C., Beato, M., Herrlich, P., Schutz, G., Umesono, K., Blumberg, B., Kastner, P., Mark, M., Chambon, P.*, et al.* (1995). The nuclear receptor superfamily: the second decade. Cell *83*, 835-839.

Manna, P.R., Eubank, D.W., Lalli, E., Sassone-Corsi, P., and Stocco, D.M. (2003). Transcriptional regulation of the mouse steroidogenic acute regulatory protein gene by the cAMP response-element binding protein and steroidogenic factor 1. Journal of molecular endocrinology *30*, 381-397.

Marais, R., Light, Y., Paterson, H.F., and Marshall, C.J. (1995). Ras recruits Raf-1 to the plasma membrane for activation by tyrosine phosphorylation. The EMBO journal *14*, 3136-3145.

Mardakheh, F.K., Yekezare, M., Machesky, L.M., and Heath, J.K. (2009). Spred2 interaction with the late endosomal protein NBR1 down-regulates fibroblast growth factor receptor signaling. J Cell Biol *187*, 265-277.

Marney, A.M., and Brown, N.J. (2007). Aldosterone and end-organ damage. Clin Sci (Lond) *113*, 267-278.

Martin, G.R. (1981). Isolation of a pluripotent cell line from early mouse embryos cultured in medium conditioned by teratocarcinoma stem cells. Proceedings of the National Academy of Sciences of the United States of America *78*, 7634-7638.

Matthews, R.P., Guthrie, C.R., Wailes, L.M., Zhao, X., Means, A.R., and McKnight, G.S. (1994). Calcium/calmodulin-dependent protein kinase types II and IV differentially regulate CREB-dependent gene expression. Mol Cell Biol *14*, 6107-6116.

McCann, S.M., Dhariwal, P.S., and Porter, J.C. (1968). Regulation of the adenohypophysis. Annu Rev Physiol *30*, 589-640.

McCann, S.M., and Porter, J.C. (1969). Hypothalamic pituitary stimulating and inhibiting hormones. Physiol Rev *49*, 240-284.

McClive, P., Pall, G., Newton, K., Lee, M., Mullins, J., and Forrester, L. (1998). Gene trap integrations expressed in the developing heart: insertion site affects splicing of the PT1-ATG vector. Dev Dyn *212*, 267-276.

McDill, B.W., Li, S.Z., Kovach, P.A., Ding, L., and Chen, F. (2006). Congenital progressive hydronephrosis (cph) is caused by an S256L mutation in aquaporin-2 that affects its phosphorylation and apical membrane accumulation. Proceedings of the National Academy of Sciences of the United States of America *103*, 6952-6957.

Meisler, M.H. (1992). Insertional mutation of 'classical' and novel genes in transgenic mice. Trends Genet *8*, 341-344.

Mene, P., and Amore, A. (1998). Apoptosis: potential role in renal diseases. Nephrol Dial Transplant *13*, 1936-1943.

Meng, S., Zhang, M., Pan, W., Li, Z., Anderson, D.H., Zhang, S., Ge, B., and Wang, C. (2012). Tyrosines 303/343/353 within the Sprouty-related domain of Spred2 are essential for its interaction with p85 and inhibitory effect on Ras/ERK activation. Int J Biochem Cell Biol *44*, 748-758.

Menzies, A.S., Aszodi, A., Williams, S.E., Pfeifer, A., Wehman, A.M., Goh, K.L., Mason, C.A., Fassler, R., and Gertler, F.B. (2004). Mena and vasodilator-stimulated phosphoprotein are required for multiple actin-dependent processes that shape the vertebrate nervous system. J Neurosci *24*, 8029-8038.

Messiaen, L., Yao, S., Brems, H., Callens, T., Sathienkijkanchai, A., Denayer, E., Spencer, E., Arn, P., Babovic-Vuksanovic, D., Bay, C.*, et al.* (2009). Clinical and mutational spectrum of neurofibromatosis type 1-like syndrome. Jama *302*, 2111-2118.

Miguel, E.C., Leckman, J.F., Rauch, S., do Rosario-Campos, M.C., Hounie, A.G., Mercadante, M.T., Chacon, P., and Pauls, D.L. (2005). Obsessive-compulsive disorder phenotypes: implications for genetic studies. Mol Psychiatry *10*, 258-275.

Miller, A.D., Curran, T., and Verma, I.M. (1984). c-fos protein can induce cellular transformation: a novel mechanism of activation of a cellular oncogene. Cell *36*, 51-60.

Miyoshi, K., Wakioka, T., Nishinakamura, H., Kamio, M., Yang, L., Inoue, M., Hasegawa, M., Yonemitsu, Y., Komiya, S., and Yoshimura, A. (2004). The Sprouty-related protein, Spred, inhibits cell motility, metastasis, and Rho-mediated actin reorganization. Oncogene *23*, 5567-5576.

Momeny, M., Khorramizadeh, M.R., Ghaffari, S.H., Yousefi, M., Yekaninejad, M.S., Esmaeili, R., Jahanshiri, Z., and Nooridaloii, M.R. (2008). Effects of silibinin on cell growth and invasive properties of a human hepatocellular carcinoma cell line, HepG-2, through inhibition of extracellular signal-regulated kinase 1/2 phosphorylation. Eur J Pharmacol *591*, 13-20.

Montagut, C., and Settleman, J. (2009). Targeting the RAF-MEK-ERK pathway in cancer therapy. Cancer Lett *283*, 125-134.

Morel, A., O'Carroll, A.M., Brownstein, M.J., and Lolait, S.J. (1992). Molecular cloning and expression of a rat V1a arginine vasopressin receptor. Nature *356*, 523-526.

Morohashi, K., Baba, T., and Tanaka, M. (2013). Steroid hormones and the development of reproductive organs. Sex Dev *7*, 61-79.

Mountjoy, K.G., Robbins, L.S., Mortrud, M.T., and Cone, R.D. (1992). The cloning of a family of genes that encode the melanocortin receptors. Science (New York, NY *257*, 1248-1251.

Muram-Zborovski, T.M., Stevenson, D.A., Viskochil, D.H., Dries, D.C., Wilson, A.R., and Rong, M. (2010). SPRED 1 mutations in a neurofibromatosis clinic. J Child Neurol *25*, 1203-1209.

Narasaka, T., Suzuki, T., Moriya, T., and Sasano, H. (2001). Temporal and spatial distribution of corticosteroidogenic enzymes immunoreactivity in developing human adrenal. Mol Cell Endocrinol *174*, 111-120.

Nasjetti, A., and Masson, G.M. (1971). Hepatic origin of renin substrate. Can J Physiol Pharmacol *49*, 931-932.

Ng, K.K., and Vane, J.R. (1967). Conversion of angiotensin I to angiotensin II. Nature *216*, 762-766.

Niebuhr, K., Ebel, F., Frank, R., Reinhard, M., Domann, E., Carl, U.D., Walter, U., Gertler, F.B., Wehland, J., and Chakraborty, T. (1997). A novel proline-rich motif present in ActA of Listeria monocytogenes and cytoskeletal proteins is the ligand for the EVH1 domain, a protein module present in the Ena/VASP family. The EMBO journal *16*, 5433-5444.

Nielsen, S., Marples, D., Frokiaer, J., Knepper, M., and Agre, P. (1996). The aquaporin family of water channels in kidney: an update on physiology and pathophysiology of aquaporin-2. Kidney international *49*, 1718-1723.

Niihori, T., Aoki, Y., Narumi, Y., Neri, G., Cave, H., Verloes, A., Okamoto, N., Hennekam, R.C., Gillessen-Kaesbach, G., Wieczorek, D.*, et al.* (2006). Germline KRAS and BRAF mutations in cardio-facio-cutaneous syndrome. Nature genetics *38*, 294-296.

Nobuhisa, I., Kato, R., Inoue, H., Takizawa, M., Okita, K., Yoshimura, A., and Taga, T. (2004). Spred-2 suppresses aorta-gonad-mesonephros hematopoiesis by inhibiting MAP kinase activation. J Exp Med *199*, 737-742.

Nonami, A., Kato, R., Taniguchi, K., Yoshiga, D., Taketomi, T., Fukuyama, S., Harada, M., Sasaki, A., and Yoshimura, A. (2004). Spred-1 negatively regulates interleukin-3-mediated ERK/mitogen-activated protein (MAP) kinase activation in hematopoietic cells. The Journal of biological chemistry *279*, 52543-52551.

Nonami, A., Taketomi, T., Kimura, A., Saeki, K., Takaki, H., Sanada, T., Taniguchi, K., Harada, M., Kato, R., and Yoshimura, A. (2005). The Sprouty-related protein, Spred-1, localizes in a lipid raft/caveola and inhibits ERK activation in collaboration with caveolin-1. Genes Cells *10*, 887-895.

Ogishima, T., Suzuki, H., Hata, J., Mitani, F., and Ishimura, Y. (1992). Zone-specific expression of aldosterone synthase cytochrome P-450 and cytochrome P-45011 beta in rat adrenal cortex: histochemical basis for the functional zonation. Endocrinology *130*, 2971-2977.

Ortiz, A. (2000). Renal cell loss through cell suicide. Kidney international *58*, 2235-2236.

Oster, H., Damerow, S., Kiessling, S., Jakubcakova, V., Abraham, D., Tian, J., Hoffmann, M.W., and Eichele, G. (2006). The circadian rhythm of glucocorticoids is regulated by a gating mechanism residing in the adrenal cortical clock. Cell Metab *4*, 163-173.

Pandit, B., Sarkozy, A., Pennacchio, L.A., Carta, C., Oishi, K., Martinelli, S., Pogna, E.A., Schackwitz, W., Ustaszewska, A., Landstrom, A.*, et al.* (2007). Gain-of-function RAF1 mutations cause Noonan and LEOPARD syndromes with hypertrophic cardiomyopathy. Nature genetics *39*, 1007-1012.

Papadimitriou, A., and Priftis, K.N. (2009). Regulation of the hypothalamic-pituitary-adrenal axis. Neuroimmunomodulation *16*, 265-271.

Papadopoulos, A.S., and Cleare, A.J. (2012). Hypothalamic-pituitary-adrenal axis dysfunction in chronic fatigue syndrome. Nat Rev Endocrinol *8*, 22-32.

Pariante, C.M. (2003). Depression, stress and the adrenal axis. J Neuroendocrinol *15*, 811-812.

Pasmant, E., Ballerini, P., Lapillonne, H., Perot, C., Vidaud, D., Leverger, G., and Landman-Parker, J. (2009a). SPRED1 disorder and predisposition to leukemia in children. Blood *114*, 1131.

Pasmant, E., Sabbagh, A., Hanna, N., Masliah-Planchon, J., Jolly, E., Goussard, P., Ballerini, P., Cartault, F., Barbarot, S., Landman-Parker, J.*, et al.* (2009b). SPRED1 germline mutations caused a neurofibromatosis type 1 overlapping phenotype. Journal of medical genetics *46*, 425-430.

Penhoat, A., Jaillard, C., and Saez, J.M. (1989). Corticotropin positively regulates its own receptors and cAMP response in cultured bovine adrenal cells. Proceedings of the National Academy of Sciences of the United States of America *86*, 4978-4981.

Pezzi, V., Clark, B.J., Ando, S., Stocco, D.M., and Rainey, W.E. (1996). Role of calmodulin-dependent protein kinase II in the acute stimulation of aldosterone production. J Steroid Biochem Mol Biol *58*, 417-424.

Phoenix, T.N., and Temple, S. (2010). Spred1, a negative regulator of Ras-MAPK-ERK, is enriched in CNS germinal zones, dampens NSC proliferation, and maintains ventricular zone structure. Genes & development *24*, 45-56.

Plotnikov, A., Zehorai, E., Procaccia, S., and Seger, R. (2011). The MAPK cascades: signaling components, nuclear roles and mechanisms of nuclear translocation. Biochim Biophys Acta *1813*, 1619-1633.

Potter, E., Sutton, S., Donaldson, C., Chen, R., Perrin, M., Lewis, K., Sawchenko, P.E., and Vale, W. (1994). Distribution of corticotropin-releasing factor receptor mRNA expression in the rat brain and pituitary. Proceedings of the National Academy of Sciences of the United States of America *91*, 8777-8781.

Pratt, W.B., Morishima, Y., Murphy, M., and Harrell, M. (2006). Chaperoning of glucocorticoid receptors. Handb Exp Pharmacol, 111-138.

Quintanar-Audelo, M., Yusoff, P., Sinniah, S., Chandramouli, S., and Guy, G.R. (2011). Sprouty-related Ena/VASP homology 1-domain-containing protein (SPRED) 1, a SHP2 substrate in the Ras/ERK pathway. The Journal of biological chemistry.

Ralph, M.R., Foster, R.G., Davis, F.C., and Menaker, M. (1990). Transplanted suprachiasmatic nucleus determines circadian period. Science (New York, NY *247*, 975-978.

Ramachandran, J., Rao, A.J., and Liles, S. (1977). Studies of the trophic action of ACTH. Ann N Y Acad Sci *297*, 336-348.

Raman, M., Chen, W., and Cobb, M.H. (2007). Differential regulation and properties of MAPKs. Oncogene *26*, 3100-3112.

Rapp, U.R., Goldsborough, M.D., Mark, G.E., Bonner, T.I., Groffen, J., Reynolds, F.H., Jr., and Stephenson, J.R. (1983). Structure and biological activity of v-raf, a unique oncogene transduced by a retrovirus. Proceedings of the National Academy of Sciences of the United States of America *80*, 4218-4222.

Ray, A., and Prefontaine, K.E. (1994). Physical association and functional antagonism between the p65 subunit of transcription factor NF-kappa B and the glucocorticoid receptor. Proceedings of the National Academy of Sciences of the United States of America *91*, 752-756.

Razzaque, M.A., Nishizawa, T., Komoike, Y., Yagi, H., Furutani, M., Amo, R., Kamisago, M., Momma, K., Katayama, H., Nakagawa, M.*, et al.* (2007). Germline gain-of-function mutations in RAF1 cause Noonan syndrome. Nature genetics *39*, 1013-1017.

Reich, A., Sapir, A., and Shilo, B. (1999). Sprouty is a general inhibitor of receptor tyrosine kinase signaling. Development (Cambridge, England) *126*, 4139-4147.

Reinhard, M., Jarchau, T., and Walter, U. (2001). Actin-based motility: stop and go with Ena/VASP proteins. Trends Biochem Sci *26*, 243-249.

Reinhard, M., Jouvenal, K., Tripier, D., and Walter, U. (1995). Identification, purification, and characterization of a zyxin-related protein that binds the focal adhesion and microfilament protein VASP (vasodilator-stimulated phosphoprotein). Proceedings of the National Academy of Sciences of the United States of America *92*, 7956-7960.

Reinhard, M., Rudiger, M., Jockusch, B.M., and Walter, U. (1996). VASP interaction with vinculin: a recurring theme of interactions with proline-rich motifs. FEBS Lett *399*, 103-107.

Renfranz, P.J., and Beckerle, M.C. (2002). Doing (F/L)PPPPs: EVH1 domains and their proline-rich partners in cell polarity and migration. Curr Opin Cell Biol *14*, 88-103.

Rivier, C., Brownstein, M., Spiess, J., Rivier, J., and Vale, W. (1982). In vivo corticotropin-releasing factor-induced secretion of adrenocorticotropin, beta-endorphin, and corticosterone. Endocrinology *110*, 272-278.

Rivier, C., and Vale, W. (1983). Modulation of stress-induced ACTH release by corticotropin-releasing factor, catecholamines and vasopressin. Nature *305*, 325-327.

Roberts, A.E., Araki, T., Swanson, K.D., Montgomery, K.T., Schiripo, T.A., Joshi, V.A., Li, L., Yassin, Y., Tamburino, A.M., Neel, B.G.*, et al.* (2007). Germline gain-of-function mutations in SOS1 cause Noonan syndrome. Nature genetics *39*, 70-74.

Rodriguez-Viciana, P., Tetsu, O., Tidyman, W.E., Estep, A.L., Conger, B.A., Cruz, M.S., McCormick, F., and Rauen, K.A. (2006). Germline mutations in genes within the MAPK pathway cause cardio-facio-cutaneous syndrome. Science (New York, NY *311*, 1287-1290.

Rojek, A., Fuchtbauer, E.M., Kwon, T.H., Frokiaer, J., and Nielsen, S. (2006). Severe urinary concentrating defect in renal collecting duct-selective AQP2 conditional-knockout mice. Proceedings of the National Academy of Sciences of the United States of America *103*, 6037-6042.

Rousseau, F., Bonaventure, J., Legeai-Mallet, L., Pelet, A., Rozet, J.M., Maroteaux, P., Le Merrer, M., and Munnich, A. (1994). Mutations in the gene encoding fibroblast growth factor receptor-3 in achondroplasia. Nature *371*, 252-254.

Roussel, M., Saule, S., Lagrou, C., Rommens, C., Beug, H., Graf, T., and Stehelin, D. (1979). Three new types of viral oncogene of cellular origin specific for haematopoietic cell transformation. Nature *281*, 452-455.

Rusak, B., and Zucker, I. (1979). Neural regulation of circadian rhythms. Physiol Rev *59*, 449-526.

Russell, L.B., Hunsicker, P.R., Cacheiro, N.L., Bangham, J.W., Russell, W.L., and Shelby, M.D. (1989). Chlorambucil effectively induces deletion mutations in mouse germ cells. Proceedings of the National Academy of Sciences of the United States of America *86*, 3704-3708.

Russell, W.L., Kelly, E.M., Hunsicker, P.R., Bangham, J.W., Maddux, S.C., and Phipps, E.L. (1979). Specific-locus test shows ethylnitrosourea to be the most potent mutagen in the mouse. Proceedings of the National Academy of Sciences of the United States of America *76*, 5818-5819.

Russell, W.L., Russell, L.B., and Kelly, E.M. (1958). Radiation dose rate and mutation frequency. Science (New York, NY *128*, 1546-1550.

Sala, C., Piech, V., Wilson, N.R., Passafaro, M., Liu, G., and Sheng, M. (2001). Regulation of dendritic spine morphology and synaptic function by Shank and Homer. Neuron *31*, 115-130.

Samarin, S., Romero, S., Kocks, C., Didry, D., Pantaloni, D., and Carlier, M.F. (2003). How VASP enhances actin-based motility. J Cell Biol *163*, 131-142.

Sasaki, A., Taketomi, T., Kato, R., Saeki, K., Nonami, A., Sasaki, M., Kuriyama, M., Saito, N., Shibuya, M., and Yoshimura, A. (2003). Mammalian Sprouty4 suppresses Ras-independent ERK activation by binding to Raf1. Nat Cell Biol *5*, 427-432.

Sasaki, A., Taketomi, T., Wakioka, T., Kato, R., and Yoshimura, A. (2001). Identification of a dominant negative mutant of Sprouty that potentiates fibroblast growth factor- but not epidermal growth factor-induced ERK activation. The Journal of biological chemistry *276*, 36804-36808.

Savill, J. (1994). Apoptosis and the kidney. J Am Soc Nephrol *5*, 12-21.

Savill, J., Mooney, A., and Hughes, J. (1996). Apoptosis and renal scarring. Kidney Int Suppl *54*, S14-17.

Sawchenko, P.E., Swanson, L.W., and Vale, W.W. (1984). Co-expression of corticotropin-releasing factor and vasopressin immunoreactivity in parvocellular neurosecretory neurons of the adrenalectomized rat. Proceedings of the National Academy of Sciences of the United States of America *81*, 1883-1887.

Schubbert, S., Zenker, M., Rowe, S.L., Boll, S., Klein, C., Bollag, G., van der Burgt, I., Musante, L., Kalscheuer, V., Wehner, L.E.*, et al.* (2006). Germline KRAS mutations cause Noonan syndrome. Nature genetics *38*, 331-336.

Schwindinger, W.F., and Levine, M.A. (1993). McCune-Albright syndrome. Trends in endocrinology and metabolism: TEM *4*, 238-242.

Seasholtz, A.F., Thompson, R.C., and Douglass, J.O. (1988). Identification of a cyclic adenosine monophosphate-responsive element in the rat corticotropin-releasing hormone gene. Mol Endocrinol *2*, 1311-1319.

Sebaai, N., Lesage, J., Alaoui, A., Dupouy, J.P., and Deloof, S. (2002). Effects of dehydration on endocrine regulation of the electrolyte and fluid balance and atrial natriuretic peptide-binding sites in perinatally malnourished adult male rats. European journal of endocrinology / European Federation of Endocrine Societies *147*, 835-848.

Seger, R., and Krebs, E.G. (1995). The MAPK signaling cascade. Faseb J *9*, 726-735.

Seth, K.A., and Majzoub, J.A. (2001). Repressor element silencing transcription factor/neuron-restrictive silencing factor (REST/NRSF) can act as an enhancer as well as a repressor of corticotropin-releasing hormone gene transcription. The Journal of biological chemistry *276*, 13917-13923.

Sewer, M.B., and Waterman, M.R. (2002). cAMP-dependent transcription of steroidogenic genes in the human adrenal cortex requires a dual-specificity phosphatase in addition to protein kinase A. Journal of molecular endocrinology *29*, 163-174.

Sewer, M.B., and Waterman, M.R. (2003). ACTH modulation of transcription factors responsible for steroid hydroxylase gene expression in the adrenal cortex. Microsc Res Tech *61*, 300-307.

Sharrocks, A.D. (2001). The ETS-domain transcription factor family. Nat Rev Mol Cell Biol *2*, 827-837.

Shiang, R., Thompson, L.M., Zhu, Y.Z., Church, D.M., Fielder, T.J., Bocian, M., Winokur, S.T., and Wasmuth, J.J. (1994). Mutations in the transmembrane domain of FGFR3 cause the most common genetic form of dwarfism, achondroplasia. Cell *78*, 335-342.

Shimizu, K., Share, L., and Claybaugh, J.R. (1973). Potentiation by angiotensin II of the vasopressin response to an increasing plasma osmolality. Endocrinology *93*, 42-50.

Shmelkov, S.V., Hormigo, A., Jing, D., Proenca, C.C., Bath, K.G., Milde, T., Shmelkov, E., Kushner, J.S., Baljevic, M., Dincheva, I.*, et al.* (2010). Slitrk5 deficiency impairs corticostriatal circuitry and leads to obsessive-compulsive-like behaviors in mice. Nat Med *16*, 598-602, 591p following 602.

Silverstein, E., Sokoloff, L., Mickelsen, O., and Jay, G.E. (1961). Primary Polydipsia and Hydronephrosis in an Inbred Strain of Mice. Am J Pathol *38*, 143-159.

Singru, P.S., Sanchez, E., Acharya, R., Fekete, C., and Lechan, R.M. (2008). Mitogen-activated protein kinase contributes to lipopolysaccharide-induced activation of corticotropin-releasing hormone synthesizing neurons in the hypothalamic paraventricular nucleus. Endocrinology *149*, 2283-2292.

Sivak, J.M., Petersen, L.F., and Amaya, E. (2005). FGF signal interpretation is directed by Sprouty and Spred proteins during mesoderm formation. Dev Cell *8*, 689-701.

Skolnik, E.Y., Lee, C.H., Batzer, A., Vicentini, L.M., Zhou, M., Daly, R., Myers, M.J., Jr., Backer, J.M., Ullrich, A., White, M.F.*, et al.* (1993). The SH2/SH3 domain-containing protein GRB2 interacts with tyrosine-phosphorylated IRS1 and Shc: implications for insulin control of ras signalling. The EMBO journal *12*, 1929-1936.

Skott, O., and Briggs, J.P. (1987). Direct demonstration of macula densa-mediated renin secretion. Science (New York, NY *237*, 1618-1620.

Smith, A.I., and Funder, J.W. (1988). Proopiomelanocortin processing in the pituitary, central nervous system, and peripheral tissues. Endocrine reviews *9*, 159-179.

Song, K.S., Li, S., Okamoto, T., Quilliam, L.A., Sargiacomo, M., and Lisanti, M.P. (1996). Co-purification and direct interaction of Ras with caveolin, an integral membrane protein of caveolae microdomains. Detergent-free purification of caveolae microdomains. The Journal of biological chemistry *271*, 9690-9697.

Sontia, B., Montezano, A.C., Paravicini, T., Tabet, F., and Touyz, R.M. (2008). Downregulation of renal TRPM7 and increased inflammation and fibrosis in aldosterone-infused mice: effects of magnesium. Hypertension *51*, 915-921.

Spencer, E., Davis, J., Mikhail, F., Fu, C., Vijzelaar, R., Zackai, E.H., Feret, H., Meyn, M.S., Shugar, A., Bellus, G.*, et al.* (2011). Identification of SPRED1 deletions using RT-PCR, multiplex ligation-dependent probe amplification and quantitative PCR. Am J Med Genet A.

Spurlock, G., Bennett, E., Chuzhanova, N., Thomas, N., Jim, H.P., Side, L., Davies, S., Haan, E., Kerr, B., Huson, S.M.*, et al.* (2009). SPRED1 mutations (Legius syndrome): another clinically useful genotype for dissecting the neurofibromatosis type 1 phenotype. Journal of medical genetics *46*, 431-437.

Stenzel-Poore, M.P., Cameron, V.A., Vaughan, J., Sawchenko, P.E., and Vale, W. (1992). Development of Cushing's syndrome in corticotropin-releasing factor transgenic mice. Endocrinology *130*, 3378-3386.

Stenzel-Poore, M.P., Heinrichs, S.C., Rivest, S., Koob, G.F., and Vale, W.W. (1994). Overproduction of corticotropin-releasing factor in transgenic mice: a genetic model of anxiogenic behavior. J Neurosci *14*, 2579-2584.

Stevenson, D., Viskochil, D., Mao, R., and Muram-Zborovski, T. (1993). Legius Syndrome.

Stocco, D.M. (2001). StAR protein and the regulation of steroid hormone biosynthesis. Annu Rev Physiol *63*, 193-213.

Stokes, P.E., and Sikes, C.R. (1991). Hypothalamic-pituitary-adrenal axis in psychiatric disorders. Annu Rev Med *42*, 519-531.

Stokoe, D., Macdonald, S.G., Cadwallader, K., Symons, M., and Hancock, J.F. (1994). Activation of Raf as a result of recruitment to the plasma membrane. Science (New York, NY *264*, 1463-1467.

Stowe, I.B., Mercado, E.L., Stowe, T.R., Bell, E.L., Oses-Prieto, J.A., Hernandez, H., Burlingame, A.L., and McCormick, F. (2012). A shared molecular mechanism underlies the human rasopathies Legius syndrome and Neurofibromatosis-1. Genes & development *26*, 1421-1426.

Suarez, Y., and Sessa, W.C. (2009). MicroRNAs as novel regulators of angiogenesis. Circ Res *104*, 442-454.

Suda, T., Tomori, N., Yajima, F., Ushiyama, T., Sumitomo, T., Nakagami, Y., Demura, H., and Shizume, K. (1987). A short negative feedback mechanism regulating corticotropin-releasing hormone release. The Journal of clinical endocrinology and metabolism *64*, 909-913.

Sugimoto, T., Saito, M., Mochizuki, S., Watanabe, Y., Hashimoto, S., and Kawashima, H. (1994). Molecular cloning and functional expression of a cDNA encoding the human V1b vasopressin receptor. The Journal of biological chemistry *269*, 27088-27092.

Sumner, K., Crockett, D.K., Muram, T., Mallempati, K., Best, H., and Mao, R. (2011). The SPRED1 Variants Repository for Legius Syndrome. G3 (Bethesda) *1*, 451-456.

Sutton, R.E., Koob, G.F., Le Moal, M., Rivier, J., and Vale, W. (1982). Corticotropin releasing factor produces behavioural activation in rats. Nature *297*, 331-333.

Sylvestersen, K.B., Herrera, P.L., Serup, P., and Rescan, C. (2011). Fgf9 signalling stimulates Spred and Sprouty expression in embryonic mouse pancreas mesenchyme. Gene Expr Patterns *11*, 105-111.

Takahashi, N., Chernavvsky, D.R., Gomez, R.A., Igarashi, P., Gitelman, H.J., and Smithies, O. (2000). Uncompensated polyuria in a mouse model of Bartter's syndrome. Proceedings of the National Academy of Sciences of the United States of America *97*, 5434-5439.

Tan, P.B., Lackner, M.R., and Kim, S.K. (1998). MAP kinase signaling specificity mediated by the LIN-1 Ets/LIN-31 WH transcription factor complex during C. elegans vulval induction. Cell *93*, 569-580.

Taniguchi, K., Kohno, R., Ayada, T., Kato, R., Ichiyama, K., Morisada, T., Oike, Y., Yonemitsu, Y., Maehara, Y., and Yoshimura, A. (2007). Spreds are essential for embryonic lymphangiogenesis by regulating vascular endothelial growth factor receptor 3 signaling. Mol Cell Biol *27*, 4541-4550.

Taniguchi, Y., Yoshida, M., Ishikawa, K., Suzuki, M., and Kurosumi, K. (1988). The distribution of vasopressin- or oxytocin-neurons projecting to the posterior pituitary as revealed by a combination of retrograde transport of horseradish peroxidase and immunohistochemistry. Arch Histol Cytol *51*, 83-89.

Tartaglia, M., Mehler, E.L., Goldberg, R., Zampino, G., Brunner, H.G., Kremer, H., van der Burgt, I., Crosby, A.H., Ion, A., Jeffery, S.*, et al.* (2001). Mutations in PTPN11, encoding the protein tyrosine phosphatase SHP-2, cause Noonan syndrome. Nature genetics *29*, 465-468.

Tartaglia, M., Pennacchio, L.A., Zhao, C., Yadav, K.K., Fodale, V., Sarkozy, A., Pandit, B., Oishi, K., Martinelli, S., Schackwitz, W.*, et al.* (2007). Gain-of-function SOS1 mutations cause a distinctive form of Noonan syndrome. Nature genetics *39*, 75-79.

Tasker, J.G., Di, S., and Malcher-Lopes, R. (2006). Minireview: rapid glucocorticoid signaling via membrane-associated receptors. Endocrinology *147*, 5549-5556.

Tavormina, P.L., Shiang, R., Thompson, L.M., Zhu, Y.Z., Wilkin, D.J., Lachman, R.S., Wilcox, W.R., Rimoin, D.L., Cohn, D.H., and Wasmuth, J.J. (1995). Thanatophoric dysplasia (types I and II) caused by distinct mutations in fibroblast growth factor receptor 3. Nature genetics *9*, 321-328.

Temeles, G.L., Gibbs, J.B., D'Alonzo, J.S., Sigal, I.S., and Scolnick, E.M. (1985). Yeast and mammalian ras proteins have conserved biochemical properties. Nature *313*, 700-703.

Tewksbury, D.A., Dart, R.A., and Travis, J. (1981). The amino terminal amino acid sequence of human angiotensinogen. Biochem Biophys Res Commun *99*, 1311-1315.

Thomas, K.R., and Capecchi, M.R. (1987). Site-directed mutagenesis by gene targeting in mouse embryo-derived stem cells. Cell *51*, 503-512.

Tidyman, W.E., and Rauen, K.A. (2009). The RASopathies: developmental syndromes of Ras/MAPK pathway dysregulation. Curr Opin Genet Dev *19*, 230-236.

Timpl, P., Spanagel, R., Sillaber, I., Kresse, A., Reul, J.M., Stalla, G.K., Blanquet, V., Steckler, T., Holsboer, F., and Wurst, W. (1998). Impaired stress response and reduced anxiety in mice lacking a functional corticotropin-releasing hormone receptor 1. Nature genetics *19*, 162-166.

Tobian, L. (1962). Relationship of juxtaglomerular apparatus to renin and angiotensin. Circulation *25*, 189-192.

Torpy, D.J., Stratakis, C.A., and Chrousos, G.P. (1999). Hyper- and hypoaldosteronism. Vitam Horm *57*, 177-216.

Treisman, J.E., and Rubin, G.M. (1996). Targets of glass regulation in the Drosophila eye disc. Mechanisms of development *56*, 17-24.

Tremblay, A., Parker, K.L., and Lehoux, J.G. (1992). Dietary potassium supplementation and sodium restriction stimulate aldosterone synthase but not 11 beta-hydroxylase P-450 messenger ribonucleic acid accumulation in rat adrenals and require angiotensin II production. Endocrinology *130*, 3152-3158.

Truong, L.D., Petrusevska, G., Yang, G., Gurpinar, T., Shappell, S., Lechago, J., Rouse, D., and Suki, W.N. (1996). Cell apoptosis and proliferation in experimental chronic obstructive uropathy. Kidney international *50*, 200-207.

Tuduce, I.L., Schuh, K., and Bundschu, K. (2010). Spred2 expression during mouse development. Dev Dyn *239*, 3072-3085.

Ullrich, A., and Schlessinger, J. (1990). Signal transduction by receptors with tyrosine kinase activity. Cell *61*, 203-212.

Ullrich, M., Bundschu, K., Benz, P.M., Abesser, M., Freudinger, R., Fischer, T., Ullrich, J., Renne, T., Walter, U., and Schuh, K. (2011). Identification of SPRED2 (Sprouty-related Protein with EVH1 Domain 2) as a Negative Regulator of the Hypothalamic-Pituitary-Adrenal Axis. The Journal of biological chemistry *286*, 9477-9488.

Ullrich, M., and Schuh, K. (2009). Gene trap: knockout on the fast lane. Methods in molecular biology (Clifton, NJ *561*, 145-159.

Ulrich-Lai, Y.M., Figueiredo, H.F., Ostrander, M.M., Choi, D.C., Engeland, W.C., and Herman, J.P. (2006). Chronic stress induces adrenal hyperplasia and hypertrophy in a subregion-specific manner. American journal of physiology *291*, E965-973.

Vale, W., Spiess, J., Rivier, C., and Rivier, J. (1981). Characterization of a 41-residue ovine hypothalamic peptide that stimulates secretion of corticotropin and beta-endorphin. Science (New York, NY *213*, 1394-1397.

van der Geer, P., Hunter, T., and Lindberg, R.A. (1994). Receptor protein-tyrosine kinases and their signal transduction pathways. Annu Rev Cell Biol *10*, 251-337.

van Gaalen, M.M., Stenzel-Poore, M.P., Holsboer, F., and Steckler, T. (2002). Effects of transgenic overproduction of CRH on anxiety-like behaviour. The European journal of neuroscience *15*, 2007-2015.

Vander, A.J. (1965). Effect of catecholamines and the renal nerves on renin secretion in anesthetized dogs. Am J Physiol *209*, 659-662.

Vander, A.J., and Geelhoed, G.W. (1965). Inhibition of renin secretion by angiotensin. II. Proc Soc Exp Biol Med *120*, 399-403.

Velu, T.J., Beguinot, L., Vass, W.C., Willingham, M.C., Merlino, G.T., Pastan, I., and Lowy, D.R. (1987). Epidermal-growth-factor-dependent transformation by a human EGF receptor proto-oncogene. Science (New York, NY *238*, 1408-1410.

Venihaki, M., and Majzoub, J.A. (1999). Animal models of CRH deficiency. Frontiers in neuroendocrinology *20*, 122-145.

Venter, J.C., Adams, M.D., Myers, E.W., Li, P.W., Mural, R.J., Sutton, G.G., Smith, H.O., Yandell, M., Evans, C.A., Holt, R.A.*, et al.* (2001). The sequence of the human genome. Science (New York, NY *291*, 1304-1351.

Villar, V., Kocic, J., and Santibanez, J.F. (2010). Spred2 inhibits TGF-beta1-induced urokinase type plasminogen activator expression, cell motility and epithelial mesenchymal transition. Int J Cancer *127*, 77-85.

Viskochil, D., Buchberg, A.M., Xu, G., Cawthon, R.M., Stevens, J., Wolff, R.K., Culver, M., Carey, J.C., Copeland, N.G., Jenkins, N.A.*, et al.* (1990). Deletions and a translocation interrupt a cloned gene at the neurofibromatosis type 1 locus. Cell *62*, 187-192.

Visser, S., and Yang, X. (2010). Identification of LATS transcriptional targets in HeLa cells using whole human genome oligonucleotide microarray. Gene *449*, 22-29.

Wagner, E.F., Stewart, T.A., and Mintz, B. (1981a). The human beta-globin gene and a functional viral thymidine kinase gene in developing mice. Proceedings of the National Academy of Sciences of the United States of America *78*, 5016-5020.

Wagner, T.E., Hoppe, P.C., Jollick, J.D., Scholl, D.R., Hodinka, R.L., and Gault, J.B. (1981b). Microinjection of a rabbit beta-globin gene into zygotes and its subsequent expression in adult mice and their offspring. Proceedings of the National Academy of Sciences of the United States of America *78*, 6376-6380.

Wakabayashi, H., Ito, T., Fushimi, S., Nakashima, Y., Itakura, J., Qiuying, L., Win, M.M., Cuiming, S., Chen, C., Sato, M.*, et al.* (2012). Spred-2 deficiency exacerbates acetaminophen-induced hepatotoxicity in mice. Clin Immunol *144*, 272-282.

Wakioka, T., Sasaki, A., Kato, R., Shouda, T., Matsumoto, A., Miyoshi, K., Tsuneoka, M., Komiya, S., Baron, R., and Yoshimura, A. (2001). Spred is a Sprouty-related suppressor of Ras signalling. Nature *412*, 647-651.

Wallace, M.R., Marchuk, D.A., Andersen, L.B., Letcher, R., Odeh, H.M., Saulino, A.M., Fountain, J.W., Brereton, A., Nicholson, J., Mitchell, A.L.*, et al.* (1990). Type 1 neurofibromatosis gene: identification of a large transcript disrupted in three NF1 patients. Science (New York, NY *249*, 181-186.

Wang, S., Aurora, A.B., Johnson, B.A., Qi, X., McAnally, J., Hill, J.A., Richardson, J.A., Bassel-Duby, R., and Olson, E.N. (2008). The endothelial-specific microRNA miR-126 governs vascular integrity and angiogenesis. Dev Cell *15*, 261-271.

Wang, Y., Spatz, M.K., Kannan, K., Hayk, H., Avivi, A., Gorivodsky, M., Pines, M., Yayon, A., Lonai, P., and Givol, D. (1999). A mouse model for achondroplasia produced by targeting fibroblast growth factor receptor 3. Proceedings of the National Academy of Sciences of the United States of America *96*, 4455-4460.

Wasylyk, B., Hagman, J., and Gutierrez-Hartmann, A. (1998). Ets transcription factors: nuclear effectors of the Ras-MAP-kinase signaling pathway. Trends Biochem Sci *23*, 213-216.

Waterston, R.H., Lindblad-Toh, K., Birney, E., Rogers, J., Abril, J.F., Agarwal, P., Agarwala, R., Ainscough, R., Alexandersson, M., An, P.*, et al.* (2002). Initial sequencing and comparative analysis of the mouse genome. Nature *420*, 520-562.

Watson, D.K., McWilliams-Smith, M.J., Nunn, M.F., Duesberg, P.H., O'Brien, S.J., and Papas, T.S. (1985). The ets sequence from the transforming gene of avian erythroblastosis virus, E26, has unique domains on human chromosomes 11 and 21: both loci are transcriptionally active. Proceedings of the National Academy of Sciences of the United States of America *82*, 7294-7298.

Weir, M.R., and Dzau, V.J. (1999). The renin-angiotensin-aldosterone system: a specific target for hypertension management. Am J Hypertens *12*, 205S-213S.

Weiss, R. (1982). The myc oncogene in man and birds. Nature *299*, 9-10.

Welch, J.M., Lu, J., Rodriguiz, R.M., Trotta, N.C., Peca, J., Ding, J.D., Feliciano, C., Chen, M., Adams, J.P., Luo, J.*, et al.* (2007). Cortico-striatal synaptic defects and OCD-like behaviours in Sapap3-mutant mice. Nature *448*, 894-900.

Wellbrock, C., Karasarides, M., and Marais, R. (2004). The RAF proteins take centre stage. Nat Rev Mol Cell Biol *5*, 875-885.

Westphal, C.H., Muller, L., Zhou, A., Zhu, X., Bonner-Weir, S., Schambelan, M., Steiner, D.F., Lindberg, I., and Leder, P. (1999). The neuroendocrine protein 7B2 is required for peptide hormone processing in vivo and provides a novel mechanism for pituitary Cushing's disease. Cell *96*, 689-700.

Wikberg, J.E., Muceniece, R., Mandrika, I., Prusis, P., Lindblom, J., Post, C., and Skottner, A. (2000). New aspects on the melanocortins and their receptors. Pharmacol Res *42*, 393-420.

Williams, G.H. (1979). The adrenal manifestations of systemic diseases. Clin Endocrinol Metab *8*, 527-545.

Williams, G.H. (2005). Aldosterone biosynthesis, regulation, and classical mechanism of action. Heart failure reviews *10*, 7-13.

Willumsen, B.M., Christensen, A., Hubbert, N.L., Papageorge, A.G., and Lowy, D.R. (1984). The p21 ras C-terminus is required for transformation and membrane association. Nature *310*, 583-586.

Wotus, C., Levay-Young, B.K., Rogers, L.M., Gomez-Sanchez, C.E., and Engeland, W.C. (1998). Development of adrenal zonation in fetal rats defined by expression of aldosterone synthase and 11beta-hydroxylase. Endocrinology *139*, 4397-4403.

Xiao, B., Tu, J.C., and Worley, P.F. (2000). Homer: a link between neural activity and glutamate receptor function. Curr Opin Neurobiol *10*, 370-374.

Yang, B., Zhao, D., Qian, L., and Verkman, A.S. (2006). Mouse model of inducible nephrogenic diabetes insipidus produced by floxed aquaporin-2 gene deletion. Am J Physiol Renal Physiol *291*, F465-472.

Yang, S.H., Whitmarsh, A.J., Davis, R.J., and Sharrocks, A.D. (1998a). Differential targeting of MAP kinases to the ETS-domain transcription factor Elk-1. The EMBO journal *17*, 1740-1749.

Yang, S.H., Yates, P.R., Whitmarsh, A.J., Davis, R.J., and Sharrocks, A.D. (1998b). The Elk-1 ETS-domain transcription factor contains a mitogen-activated protein kinase targeting motif. Mol Cell Biol *18*, 710-720.

Yao, Z., and Seger, R. (2009). The ERK signaling cascade--views from different subcellular compartments. Biofactors *35*, 407-416.

Yoon, S., and Seger, R. (2006). The extracellular signal-regulated kinase: multiple substrates regulate diverse cellular functions. Growth Factors *24*, 21-44.

Yoshida, T., Hisamoto, T., Akiba, J., Koga, H., Nakamura, K., Tokunaga, Y., Hanada, S., Kumemura, H., Maeyama, M., Harada, M.*, et al.* (2006). Spreds, inhibitors of the Ras/ERK signal transduction, are dysregulated in human hepatocellular carcinoma and linked to the malignant phenotype of tumors. Oncogene *25*, 6056-6066.

Yun, J., Schoneberg, T., Liu, J., Schulz, A., Ecelbarger, C.A., Promeneur, D., Nielsen, S., Sheng, H., Grinberg, A., Deng, C.*, et al.* (2000). Generation and phenotype of mice harboring a nonsense mutation in the V2 vasopressin receptor gene. The Journal of clinical investigation *106*, 1361-1371.

Zhang, X.F., Settleman, J., Kyriakis, J.M., Takeuchi-Suzuki, E., Elledge, S.J., Marshall, M.S., Bruder, J.T., Rapp, U.R., and Avruch, J. (1993). Normal and oncogenic p21ras proteins bind to the amino-terminal regulatory domain of c-Raf-1. Nature *364*, 308-313.

Zhang, Y., Proenca, R., Maffei, M., Barone, M., Leopold, L., and Friedman, J.M. (1994). Positional cloning of the mouse obese gene and its human homologue. Nature *372*, 425-432.

Zhou, Y., Takahashi, G., Shinagawa, T., Okuhara, T., Yonamine, K., Aida, Y., and Tadokoro, M. (2002). Increased transforming growth factor-beta1 and tubulointerstitial fibrosis in rats with congenital hydronephrosis. Int J Urol *9*, 491-500.

Zhuang, L., Villiger, P., and Trueb, B. (2011). Interaction of the receptor FGFRL1 with the negative regulator Spred1. Cell Signal.

Zimmerman, E.A., Stillman, M.A., Recht, L.D., Antunes, J.L., Carmel, P.W., and Goldsmith, P.C. (1977). Vasopressin and corticotropin-releasing factor: an axonal pathway to portal capillaries in the zona externa of the median eminence containing vasopressin and its interaction with adrenal corticoids. Ann N Y Acad Sci *297*, 405-419.

Zimmermann, J., Jarchau, T., Walter, U., Oschkinat, H., and Ball, L.J. (2004). 1H, 13C and 15N resonance assignment of the human Spred2 EVH1 domain. J Biomol NMR *29*, 435-436.

Appendix 9

9. 1. Genotyping

Murine *Spred2* Gene with and without the pGT0 Gene Trap Vector behind Exon 4 and Appropriate Primers Used for Amplification of Specific WT and KO Fragments

Sequence Origin: ENSEMBL Database Chromosome 11: 19,924,442 - 20,022,577, Genomic DNA

WT DNA Fragment (803 bp):

164 bp – 966 bp (Pr.1 – Pr.2)

Legend:

Spred2 - Intron 4

Primer SPR2-Geno-WT/KO-Forward, Pr. 1

Primer SPR2-Geno-WT-Reverse, Pr. 2:

GAGACAGGGTTTTTCTGTGCGGCCTTGGCTGTCCTGGAACTCAATCAGAAGGACCATGCTAGCC
TTGAACTCACTGAGATCTGCTGGGACTAAATGCATGCACCAGCAGCACCCAGCTAACAAATAGT
TTTCTCTCAGTCATCAGGCTGCCTTCTCGGCCCCAGCTTGACCGGCACCCCGGTGAGCACAGGC
TCACCTCAGTAGTGTTGATCTCTTGTTAGTCAGTTGACTCTTGAGCCCTGATGATTAGCATACA
CACATTTTTAGCCAAAGTATTACAATAACATCCCTTACTCCAAGTCTAGAGAGTGTCTTTGGTA
CCCTCTGAAACCCAGAGGACCAGGCCTCCATTGTCCATGTTTCTCTCAGAATTCTTAGCTTCCA
AGATCTCTCGAGAATGACCCATTAAGTTTTCAGTCCTCACCAGGAAAAAGCCAATCCCTGAGAG

TAAAGGACAGCCAGGGCTGCAGAGACAAACCCTGCTGTCTCAGAAGGGAGTGGGGACGGGCTTT
TAGTTCTACTTGTCATAGTGTCTGGAAGCCAAGGTCAGGAATGGATCAACTATGCCCAGTCACA
GGAGAGTGGCTGGTAGGAGCCAAGTATCTATCTTCCACCATGGCCCAGTACTGTTTTTACATTT
AGAAAACCAGCTTGTCTTTCCAAGGCCTTGCTGCTGGGCCTCTCCAACCATTGAGGTAACTACT
TCATTCACATTGAGACATTCTGTTCATTCTCATGTCTAAGACAACTCAAGACTGGAAAGCCAGG
AGTGATGGTTCATATTCTATAATCCCAGCACTTGAAATGTAAAGTCTAAAAACCAAGCCAGTGT
GTGGGGGTGTGGTGGGGGCAGAGACAGAGAGATGAGATATGGCTCAAAGGTTAAAAGCACCTAC
TACTACTACTAGCACCCAGCTAAGATGGCTCACAACCACCCACCTATAAGCTCCAAGGGATCCA
GTGCCCTCTGCTGCCTCCATGGGCACCTACACTCAAATGCACATTATTAAAAATGAAATAAACT
AGGCCCATGGAGGCCAGAAAAGAGCATCAGCTCCCCCCAGACCTGGAGTTATAGGCAGTCGAAG
CTGTCTGTAGGTGGTGAGAATCTGGGCATTCAAGTCTGCTCACCCCGGGGCCCCTTCCCGCCCA
TACCTTTAAT

KO DNA Fragment (452 bp):

164 bp – 615 bp (Pr.1 – Pr.3)

Legend:

Spred2 - Intron 4

XXX: Unknown Sequence

pGTO pfs Gene Trap Vector

β-geo CDS

Primer SPR2-Geno-WT/KO-Forward, Pr. 1

Primer SPR2-Geno-KO-Reverse, Pr. 3:

Primer SPR2-Geno-WT-Reverse, Pr. 2:

GAGACAGGGTTTTTCTGTGCGGCCTTGGCTGTCCTGGAACTCAATCAGAAGGACCATGCTAGCC
TTGAACTCACTGAGATCTGCTGGGACTAAATGCATGCACCAGCAGCACCCAGCTAACAAATAGT
TTTCTCTCAGTCATCAGGCTGCCTTCTCGGCCCCAGCTTGACCGGCACCCCGGTGAGCACAGGC
TCACCTCAGTAGTGTTGATCTCTTGTTAGTCAGTTGACTCTTGAGCCCTGATGATTAGCATACA
CACATTTTTAGCCAAAGTATTACAATAACATCCCTTACTCCAAGTCTAGAGAGTGTCTTTGGTA
CCCTCTGAAACCCAGAGGACCAGGCCTCCATTGTCCATGTTTCTCTCAGAATTCTTAGCTTCCA
AGATCTCTCGAGAATGACCCATTAAGTTTTCAGTCCTCACCAGGAAAAAGCCAATCCCTGAGAG

TAAAGGACAGCCAGGGCTGCAGAGACAAACCCTGCTGTCTCAGTGTTATCACTCATGGTTATGG
CAGCACTGCATAATTCTCTTACTGTCATGCCATCTGTAAGATGCTTTTCTGTGACTGGTGAGTA
Ctctttcccagggagggaaggaggagagtttgagatccgctccggaagtcggggttcaggtttg
agcaggccaggcctctcccgtggtctcgccctcttgtcctagaagcctcactggccaggtgtaa
gccaggtcgtgggtgccgagccctgctccctcatcctcagcatggatgtgaagaggactgtatg
gcgtgcgggtgtgtgtgaccgtgggtacacttaaaacaccgggttttggatctgcactgtcccg
gatgtcctctggtgctcaaagacccttttgggtttgccctttggtaagagcgccgggatctact
tgtctggaggccagggagtcctcagccgaggcttgccgcccctgactgcactgcactgagtagt
ggatgggagagtctggtaccgcactgccggtttcctccaccatccccgcagcgcagggcagtgc
attccgtcctggctgcgaaggggatggtcgggccttctccagcctcttccgcttctagcgaag
gggccttgatggaagggcccgcatgtctccaaagttgattcatgcttcttgcacagagaaagac
cagaaagaaggtctcaagttttagccggtagcccggatggccttttcctgcacggcaccatatg
aaccttgtgaccctgactttgagacccctctaacccaaggcccctaccactttacccttccct
ttgaaggctttcccacaccaccctccacacttnccccaaacactgccaactatgtaggaggaag
gggttgggactaacagaagaacccgttgtggggaagctgttgggagggtcactttatgttcttg
cccaaggtcagttgggtggcctgcttctgatgaggtggtcccaaggtctggggtagaaggtgag
agggacaggccaccaaggtcagccccccccccctatcccataggagccaggtccctctcctgga
caggaagactgaaggggagatgccagagactcagtgaagcctggggtaccctattggagtcctt
caaggaaacaaacttggcctcaccaggcctcagccttggctcctcctgggaactctactgccct
tgggatcccttgtagttgtgggttacataggaaggggacggattccccttgactggctagccta
ctcttttcttcagtcttctccatctcctctcaccgttctctcgacccttccctaggatagact
tggaaaaagataaggggagaaaaacaaatgcaaacgaggccagaaagattttggctgggcattc
cttccgctagcttttattgggatcccctagtttgtgataggccttttagctacatctgccaatc
catctcattttcacacacacacaccactttccttctggtcagtgggcacatgtccagcctca
agtttatatcaccacccccaatgcccaacacttgtatggccttggcgggtcatccccccccccca
cccccagtatctgcaacctcaagctagcttgggtgcgttggttgtggataagtagctagactcc
agcaaccagtaacctctgccctttctcctccatgacaaccagGTCCCAGGTCCCGAAAACCAAA
GAAGAAGAACGCAGATCCAGAAGTTCCTATTCCGAAGTTCCTATTCTCTAGAAAGTATAGGAAC
TTCTCAGATCTGGACTCTAGAGGATCCCGTCGTTTTACAACGTCGTGACTGGGAAAACCCTGGC
GTTACCCAACTTAATCGCCTTGCAGCACATCCCCCTTTCGCCAGCTGGCGTAATAGCGAAGAGG
CCCGCACCGATCGCCCTTCCCAACAGTTGCGCAGCCTGAATGGCGAATGGCGCTTTGCCTGGTT
TCCGGCACCAGAAGCGGTGCCGGAAAGCTGGCTGGAGTGCGATCTTCCTGAGGCCGATACTGTC
GTCGTCCCCTCAAACTGGCAGATGCACGGTTACGATGCGCCCATCTACACCAACGTAACCTATC
CCATTACGGTCAATCCGCCGTTTGTTCCCACGGAGAATCCGACGGGTTGTTACTCGCTCACATT

TAATGTTGATGAAAGCTGGCTACAGGAAGGCCAGACGCGAATTATTTTTGATGGCGTTAACTCG
GCGTTTCATCTGTGGTGCAACGGGCGCTGGGTCGGTTACGGCCAGGACAGTCGTTTGCCGTCTG
AATTTGACCTGAGCGCATTTTTACGCGCCGGAGAAAACCGCCTCGCGGTGATGGTGCTGCGTTG
GAGTGACGGCAGTTATCTGGAAGATCAGGATATGTGGCGGATGAGCGGCATTTTCCGTGACGTC
TCGTTGCTGCATAAACCGACTACACAAATCAGCGATTTCCATGTTGCCACTCGCTTTAATGATG
ATTTCAGCCGCGCTGTACTGGAGGCTGAAGTTCAGATGTGCGGCGAGTTGCGTGACTACCTACG
GGTAACAGTTTCTTTATGGCAGGGTGAAACGCAGGTCGCCAGCGGCACCGCGCCTTTCGGCGGT
GAAATTATCGATGAGCGTGGTGGTTATGCCGATCGCGTCACACTACGTCTGAACGTCGAAAACC
CGAAACTGTGGAGCGCCGAAATCCCGAATCTCTATCGTGCGGTGGTTGAACTGCACACCGCCGA
CGGCACGCTGATTGAAGCAGAAGCCTGCGATGTCGGTTTCCGCGAGGTGCGGATTGAAAATGGT
CTGCTGCTGCTGAACGGCAAGCCGTTGCTGATTCGAGGCGTTAACCGTCACGAGCATCATCCTC
TGCATGGTCAGGTCATGGATGAGCAGACGATGGTGCAGGATATCCTGCTGATGAAGCAGAACAA
CTTTAACGCCGTGCGCTGTTCGCATTATCCGAACCATCCGCTGTGGTACACGCTGTGCGACCGC
TACGGCCTGTATGTGGTGGATGAAGCCAATATTGAAACCCACGGCATGGTGCCAATGAATCGTC
TGACCGATGATCCGCGCTGGCTACCGGCGATGAGCGAACGCGTAACGCGAATGGTGCAGCGCGA
TCGTAATCACCCGAGTGTGATCATCTGGTCGCTGGGGAATGAATCAGGCCACGGCGCTAATCAC
GACGCGCTGTATCGCTGGATCAAATCTGTCGATCCTTCCCGCCCGGTGCAGTATGAAGGCGGCG
GAGCCGACACCACGGCCACCGATATTATTTGCCCGATGTACGCGCGCGTGGATGAAGACCAGCC
CTTCCCGGCTGTGCCGAAATGGTCCATCAAAAAATGGCTTTCGCTACCTGGAGAGACGCGCCCG
CTGATCCTTTGCGAATACGCCCACGCGATGGGTAACAGTCTTGGCGGTTTCGCTAAATACTGGC
AGGCGTTTCGTCAGTATCCCCGTTTACAGGGCGGCTTCGTCTGGGACTGGGTGGATCAGTCGCT
GATTAAATATGATGAAAACGGCAACCCGTGGTCGGCTTACGGCGGTGATTTTGGCGATACGCCG
AACGATCGCCAGTTCTGTATGAACGGTCTGGTCTTTGCCGACCGCACGCCGCATCCAGCGCTGA
CGGAAGCAAAACACCAGCAGCAGTTTTTCCAGTTCCGTTTATCCGGGCAAACCATCGAAGTGAC
CAGCGAATACCTGTTCCGTCATAGCGATAACGAGCTCCTGCACTGGATGGTGGCGCTGGATGGT
AAGCCGCTGGCAAGCGGTGAAGTGCCTCTGGATGTCGCTCCACAAGGTAAACAGTTGATTGAAC
TGCCTGAACTACCGCAGCCGGAGAGCGCCGGGCAACTCTGGCTCACAGTACGCGTAGTGCAACC
GAACGCGACCGCATGGTCAGAAGCCGGGCACATCAGCGCCTGGCAGCAGTGGCGTCTGGCGGAA
AACCTCAGTGTGACGCTCCCCGCCGCGTCCCACGCCATCCCGCATCTGACCACCAGCGAAATGG
ATTTTTGCATCGAGCTGGGTAATAAGCGTTGGCAATTTAACCGCCAGTCAGGCTTTCTTTCACA
GATGTGGATTGGCGATAAAAAACAACTGCTGACGCCGCTGCGCGATCAGTTCACCCGTGCACCG
CTGGATAACGACATTGGCGTAAGTGAAGCGACCCGCATTGACCCTAACGCCTGGGTCGAACGCT
GGAAGGCGGCGGGCCATTACCAGGCCGAAGCAGCGTTGTTGCAGTGCACGGCAGATACACTTGC
TGATGCGGTGCTGATTACGACCGCTCACGCGTGGCAGCATCAGGGGAAAACCTTATTTATCAGC

CGGAAAACCTACCGGATTGATGGTAGTGGTCAAATGGCGATTACCGTTGATGTTGAAGTGGCGA
GCGATACACCGCATCCGGCGCGGATTGGCCTGAACTGCCAGCTGGCGCAGGTAGCAGAGCGGGT
AAACTGGCTCGGATTAGGGCCGCAAGAAAACTATCCCGACCGCCTTACTGCCGCCTGTTTTGAC
CGCTGGGATCTGCCATTGTCAGACATGTATACCCCGTACGTCTTCCCGAGCGAAAACGGTCTGC
GCTGCGGGACGCGCGAATTGAATTATGGCCCACACCAGTGGCGCGGCGACTTCCAGTTCAACAT
CAGCCGCTACAGTCAACAGCAACTGATGGAAACCAGCCATCGCCATCTGCTGCACGCGGAAGAA
GGCACATGGCTGAATATCGACGGTTTCCATATGGGGATTGGTGGCGACGACTCCTGGAGCCCGT
CAGTATCGGCGGAATTCCAGCTGAGCGCCGGTCGCTACCATTACCAGTTGGTCTGGTGTCAGGG
GATCCCCCGGGCTGCAGCCAATATGGGATCGGCCATTGAACAAGATGGATTGCACGCAGGTTCT
CCGGCCGCTTGGGTGGAGAGGCTATTCGGCTATGACTGGGCACAACAGACAATCGGCTGCTCTG
ATGCCGCCGTGTTCCGGCTGTCAGCGCAGGGGCGCCCGGTTCTTTTTGTCAAGACCGACCTGTC
CGGTGCCCTGAATGAACTGCAGGACGAGGCAGCGCGGCTATCGTGGCTGGCCACGACGGGCGTT
CCTTGCGCAGCTGTGCTCGACGTTGTCACTGAAGCGGGAAGGGACTGGCTGCTATTGGGCGAAG
TGCCGGGGCAGGATCTCCTGTCATCTCACCTTGCTCCTGCCGAGAAAGTATCCATCATGGCTGA
TGCAATGCGGCGGCTGCATACGCTTGATCCGGCTACCTGCCCATTCGACCACCAAGCGAAACAT
CGCATCGAGCGAGCACGTACTCGGATGGAAGCCGGTCTTGTCGATCAGGATGATCTGGACGAAG
AGCATCAGGGGCTCGCGCCAGCCGAACTGTTCGCCAGGCTCAAGGCGCGCATGCCCGACGGCGA
GGATCTCGTCGTGACCCATGGCGATGCCTGCTTGCCGAATATCATGGTGGAAAATGGCCGCTTT
TCTGGATTCATCGACTGTGGCCGGCTGGGTGTGGCGGACCGCTATCAGGACATAGCGTTGGCTA
CCCGTGATATTGCTGAAGAGCTTGGCGGCGAATGGGCTGACCGCTTCCTCGTGCTTTACGGTAT
CGCCGCTCCCGATTCGCAGCGCATCGCCTTCTATCGCCTTCTTGACGAGTTCTTCTGAgcggga
ctctggggttcgaaatgaccgaccaagcgacgcccaacctgccatcacgagatttcgattccac
cgccgccttctatgaaaggttgggcttcggaatcgttttccgggacgccggctggatgatcctc
cagcgcggggatctcatgctggagttcttcgcccacccccggatctaagctctagccggccgc
ctcgagaagttcctattccgaagttcctattctctagaaagtataggaacttctaaggacgagc
tgtgattgaattccgcccccccccccccccctctccctcccccccccctaacgttactggccg
aagccgcttggaataaggccggtgtgcgtttgtctatatgttattttccaccatattgccgtct
tttggcaatgtgagggcccggaaacctggccctgtcttcttgacgagcattcctaggggtcttt
cccctctcgccaaaggaatgcaaggtctgttgaatgtcgtgaaggaagcagttcctctggaagc
ttcttgaagacaaacaacgtctgtagcgacccttgcaggcagcggaacccccacctggcgac
aggtgcctctgcggccaaaagccacgtgtataagatacacctgcaaaggcggcacaaccccagt
gccacgttgtgagttggatagttgtggaaagagtcaaatggctctcctcaagcgtattcaacaa
ggggctgaaggatgcccagaaggtaccccattgtatgggatctgatctggggcctcggtgcaca
tgctttacgtgtgtttagtcgaggttaaaaaacgtctaggccccccgaaccacggggacgtggt

tttcctttgaaaaacacgatgataatatggccacaaccatgctgctgctgctgctgctgctggg
cctgaggctacagctctccctgggcatcatcccagttgaggaggagaacccggacttctggaac
cgcgaggcagccgaggccctgggtgccgccaagaagctgcagcctgcacagacagccgccaaga
acctcatcatcttcctgggcgatgggatgggggtgtctacggtgacagctgccaggatcctaaa
agggcagaagaaggacaaactggggcctgagataccctggccatggaccgcttcccatatgtg
gctctgtccaagacatacaatgtagacaaacatgtgccagacagtggagccacagccacggcct
acctgtgcggggtcaagggcaacttccagaccattggcttgagtgcagccgcccgctttaacca
gtgcaacacgacacgcggcaacgaggtcatctccgtgatgaatcgggccaagaaagcagggaag
tcagtgggagtggtaaccaccacacgagtgcagcacgcctcgccagccggcacctacgcccaca
cggtgaaccgcaactggtactcggacgccgacgtgcctgcctcggcccgccaggaggggtgcca
ggacatcgctacgcagctcatctccaacatggacattgatgtgatcctaggtggaggccgaaag
tacatgtttcgcatgggaaccccagaccctgagtacccagatgactacagccaaggtgggacca
ggctggacgggaagaatctggtgcaggaatggctcggcgaacgccagggtgcccggtacgtgtg
gaaccgcactgagctcatgcaggcttccctggacccgtctgtgacccatctcatgggtctcttt
gagcctggagacatgaaatacgagatccaccgagactccacactggacccctccctgatggaga
tgacagaggctgccctgcgcctgctgagcagacacccccgcggcttcttcctcttcgtggaggg
tggtcgcatcgaccatggtcatcatgaaagcagggcttaccgggcactgactgagacgatcatg
ttcgacgacgccattgagagggcgggccagctcaccagcgaggaggacacgctgagcctcgtca
ctgccgaccactcccacgtcttctccttcggaggctacccccctgcgagggagctccttcatcgg
gctggccgctggcaaggcccgggacaggaaggcctacacggtcctcctatacggaaacggtcca
ggctatgtgctcaaggacggcgcccggccggatgttaccgagagcgagagcgggagccccgagt
atcggcagcagtcagcagtgcccctggacgaagagacccacgcaggcgaggacgtggcggtgtt
cgcgcgcggcccgcaggcgcacctggttcacggcgtgcaggagcagaccttcatagcgcacgtc
atggccttcgccgcctgcctggagccctacaccgcctgcgacctggcgcccccccgccggcacca
ccgacgccgcgcacccggggcggtccgtggtccccgcgttgcttcctctgctggccgggaccct
gctgctgctggagacggccactgctccctgagtgtcccgtccctggggctcctgcttccccatc
ccggagttctcctgctccccacctcctgtcgtcctgcctggcctccagcccgagtcgtcatccc
cggagtccctatacagaggtcctgccatggaaccttcccctccccgtgcgctctggggactgag
cccatgacaccaaacctgccccttggctgctctcggactccctaccccaaccccagggactgca
ggttgtgccctgtggctgcctgcaccccaggaaaggaggggctcaggccatccagccaccacc
tacagcccagtgggtcgctctagagcgacctcgaggggctaganntgatcataatcagccatac
cacatttgtagaggttttacttgctttaaaaaacctcccacacctccccctgaacctgaaacat
aaaatgaatgcaattgttgttgttaacttgtttattgcagcttataatggttacaaataaagca
atagcatcacaaatttcacaaataaagcatttttttcactgcattctagttgtggtttgtccaa

actcatcaatgtatcttatcatgtctggatccccgggcgagctcgaattcgtaatcatggtcat
agctgtttcctgtgtgaaattgttatccgctcacaattccacacaacatacgagccggaagcat
aaagtgtaaagcctggggtgcctaatgagtgagctaactcacattaattgcgttgcgctcactg
cccgctttccagtcgggaaacctgtcgtgccagctgcattaatgaatcggccaacgcgcgggga
gaggcggtttgcgtattgggcgctcttccgcttcctcgctcactgactcgctgcgctcggtcgt
tcggctgcggcgagcggtatcagctcactcaaaggcggtaatacggttatccacagaatcaggg
gataacgcaggaaagaacatgtgagcaaaaggccagcaaaaggccaggaaccgtaaaaaggccg
cgttgctggcgtttttccataggctccgccccctgacgagcatcacaaaaatcgacgctcaag
tcagaggtggcgaaacccgacaggactataaagataccaggcgtttccccctggaagctccctc
gtgcgctctcctgttccgaccctgccgcttaccggatacctgtccgcctttctcccttcgggaa
gcgtggcgctttctcatagctcacgctgtaggtatctcagttcggtgtaggtcgttcgctccaa
gctgggctgtgtgcacgaacccccgttcagcccgaccgctgcgccttatccggtaactatcgt
cttgagtccaacccggtaagacacgacttatcgccactggcagcagccactggtaacaggatta
gcagagcgaggtatgtaggcggtgctacagagttcttgaagtggtggcctaactacggctacac
tagaaggacagtatttggtatctgcgctctgctgaagccagttaccttcggaaaaagagttggt
agctcttgatccggcaaacaaaccaccgctggtagcggtggtttttttgtttgcaagcagcaga
ttacgcgcagaaaaaaaggatctcaagaagatcctttgatcttttctacggggtctgacgctca
gtggaacgaaaactcacgttaagggattttggtcatgagattatcaaaaaggatcttcacctag
atccttttaaattaaaaatgaagttttaaatcaatctaaagtatatatgagtaaacttggtctg
acagttaccaatgcttaatcagtgaggcacctatctcagcgatctgtctatttcgttcatccat
agttgcctgactccccgtcgtgtagataactacgatacgggagggcttaccatctggccccagt
gctgcaatgataccgcgagacccacgctcaccggctccagatttatcagcaataaaccagccag
ccggaagggccgagcgcagaagtggtcctgcaactttatccgcctccatccagtctattaattg
ttgccgggaagctagagtaagtagttcgccagttaatagtttgcgcaacgttgttgccattgct
acaggcatcgtggtgtcacgctcgtcgtttggtatggcttcattcagctccggttcccaacgat
caaggcgagttacatgatcccccatgttgtgcaaaaaagcggttagctccttcggtcctccgat
cgttgtcagaagtaagttggccgcagtgttatcactcatggttatggcagcactgcataattct
cttactgtcatgccatccgtaagatgcttttctgtgactggtgagtactcaaccaagtcattct
gagaatagtgtatgcggcgaccgagttgctcttgcccggcgtcaatacgggataataccgcgcc
acatagcagaactttaaaagtgctcatcattggaaaacgttcttcggggcgaaaactctcaagg
atcttaccgctgttgagatccagttcgatgtaacccactcgtgcacccaactgatcttcagcat
cttttactttcaccagcgtttctgggtgagcaaaaacaggaaggcaaaatgccgcaaaaaaggg
aataagggcgacacggaaatgttgaatactcatactcttccttttttcaatattattgaagcatt
tatcagggttattgtctcatgagcggatacatatttgaatgtatttagaaaaataaacaaatag

gggttccgcgcacatttccccgaaaagtgccacctgacgtctaagaaaccattattatcatgac
attaacctataaaaataggcgtatcacgaggccctttcgtctcgcgcgtttcggtgatgacggt
gaaaacctctgacacatgcagctcccggagacggtcacagcttgtctgtaagcggatgccggga
gcagacaagcccgtcagggcgcgtcagcgggtgttggcgggtgtcggggctggcttaactatgc
ggcatcagagcagattgtactgagagtgcaccatatgcggtgtgaaataccgcacagatgcgta
aggagaaaataccgcatcaggcgccattcgccattcaggctgcgcaactgttgggaagggcgat
cggtgcgggcctcttcgctattacgccagctggcgaaaggggatgtgctgcaaggcgattaag
ttgggtaacgccagggttttcccagtcacgacgttgtaaaacgacggccagtgccaagctgcgt
cgacAAGGGAGTGGGGACGGGCTTTTAGTTCTACTTGTCATAGTGTCTGGAAGCCAAGGTCAGG
AATGGATCAACTATGCCCAGTCACAGGAGAGTGGCTGGTAGGAGCCAAGTATCTATCTTCCACC
ATGGCCCAGTACTGTTTTTACATTTAGAAAACCAGCTTGTCTTTCCAAGGCCTTGCTGCTGGGC
CTCTCCAACCATTGAGGTAACTACTTCATTCACATTGAGACATTCTGTTCATTCTCATGTCTAA
GACAACTCAAGACTGGAAAGCCAGGAGTGATGGTTCATATTCTATAATCCCAGCACTTGAAATG
TAAAGTCTAAAAACCAAGCCAGTGTGTGGGGGTGTGGTGGGGGCAGAGACAGAGAGATGAGATA
TGGCTCAAAGGTTAAAAGCACCTACTACTACTACTAGCACCCAGCTAAGATGGCTCACAACCAC
CCACCTATAAGCTCCAAGGGATCCAGTGCCCTCTGCTGCCTCCATGGGCACCTACACTCAAATG
CACATTATTAAAAATGAAATAAACTAGGCCCATGGAGGCCAGAAAAGAGCATCAGCTCCCCCCA
GACCTGGAGTTATAGGCAGTCGAAGCTGTCTGTAGGTGGTGAGAATCTGGGCATTCAAGTCTGC
TCACCCCGGGGCCCCTTCCCGCCCATACCTTTAAT

9.2. EVH1-β-geo Fusion Protein

Murine *Spred2* Gene Containing the pGT0 Gene Trap Vector behind Exon 4 and Appropriate Primers Used for Amplification of the EVH1-β-geo Fusion Protein and the β-geo Reporter Protein

Sequence Origin: ENSEMBL Database Chromosome 11: 19,924,442 - 20,022,577, Corresponding mRNA

Cloned EVH1-β-geo Fusion Protein (4,422 bp):

1 bp – 4,422 bp (Pr.4 – Pr.6)

Cloned β-geo Reporter Protein (3,984 bp):

439 bp - 4,422 bp (Pr.5 – Pr.6)

Legend:

Spred2 - Exon 1

Spred2 - Exon 2

Spred2 - Exon 3

Spred2 - Exon 4

β-geo CDS

Primer S2/EVH1-β-geo -Forward, Pr. 4

Primer β-geo-Forward, Pr. 5:

Primer Reverse (for both), Pr. 6:

ATGACCGAAGAAACACACCCGGACGATGACAGCTATATTGTGCGTGTCAAGGCTGTGGTTATGA
CCAGAGATGACTCCAGCGGGGGATGGTTCCCACAGGAAGGAGGCGGGATCAGTCGCGTCGGCGT
GTGTAAGGTCATGCACCCTGAAGGCAACGGACGAAGCGGCTTTCTCATCCATGGCGAGCGACAG
AAAGACAAACTGGTGGTATTGGAATGCTATGTCAGAAAGGACTTGGTCTACACCAAAGCCAATC
CGACGTTTCATCATTGGAAGGTTGATAACAGGAAGTTTGGACTTACTTTCCAAAGTCCTGCAGA
TGCACGAGCCTTTGACAGGGGCGTGAGAAAAGCCATTGAAGACCTTATAGAAGGTTCAACGACC
TCCTCTTCCACTCTCCATAACGAAGCTGAGCTCGGAGACGATGACGTTTTCACGGTCCCAGGTC
CCGAAAACCAAAGAAGAAGAACGCAGATCCAGAAGTTCCTATTCCGAAGTTCCTATTCTCTAGA

AAGTATAGGAACTTCTCAGATCTGGACTCTAGAGGATCCCGTCGTTTTACAACGTCGTGACTGG
GAAAACCCTGGCGTTACCCAACTTAATCGCCTTGCAGCACATCCCCCTTTCGCCAGCTGGCGTA
ATAGCGAAGAGGCCCGCACCGATCGCCCTTCCCAACAGTTGCGCAGCCTGAATGGCGAATGGCG
CTTTGCCTGGTTTCCGGCACCAGAAGCGGTGCCGGAAAGCTGGCTGGAGTGCGATCTTCCTGAG
GCCGATACTGTCGTCGTCCCCTCAAACTGGCAGATGCACGGTTACGATGCGCCCATCTACACCA
ACGTAACCTATCCCATTACGGTCAATCCGCCGTTTGTTCCCACGGAGAATCCGACGGGTTGTTA
CTCGCTCACATTTAATGTTGATGAAAGCTGGCTACAGGAAGGCCAGACGCGAATTATTTTTGAT
GGCGTTAACTCGGCGTTTCATCTGTGGTGCAACGGGCGCTGGGTCGGTTACGGCCAGGACAGTC
GTTTGCCGTCTGAATTTGACCTGAGCGCATTTTTACGCGCCGGAGAAAACCGCCTCGCGGTGAT
GGTGCTGCGTTGGAGTGACGGCAGTTATCTGGAAGATCAGGATATGTGGCGGATGAGCGGCATT
TTCCGTGACGTCTCGTTGCTGCATAAACCGACTACACAAATCAGCGATTTCCATGTTGCCACTC
GCTTTAATGATGATTTCAGCCGCGCTGTACTGGAGGCTGAAGTTCAGATGTGCGGCGAGTTGCG
TGACTACCTACGGGTAACAGTTTCTTTATGGCAGGGTGAAACGCAGGTCGCCAGCGGCACCGCG
CCTTTCGGCGGTGAAATTATCGATGAGCGTGGTGGTTATGCCGATCGCGTCACACTACGTCTGA
ACGTCGAAAACCCGAAACTGTGGAGCGCCGAAATCCCGAATCTCTATCGTGCGGTGGTTGAACT
GCACACCGCCGACGGCACGCTGATTGAAGCAGAAGCCTGCGATGTCGGTTTCCGCGAGGTGCGG
ATTGAAAATGGTCTGCTGCTGCTGAACGGCAAGCCGTTGCTGATTCGAGGCGTTAACCGTCACG
AGCATCATCCTCTGCATGGTCAGGTCATGGATGAGCAGACGATGGTGCAGGATATCCTGCTGAT
GAAGCAGAACAACTTTAACGCCGTGCGCTGTTCGCATTATCCGAACCATCCGCTGTGGTACACG
CTGTGCGACCGCTACGGCCTGTATGTGGTGGATGAAGCCAATATTGAAACCCACGGCATGGTGC
CAATGAATCGTCTGACCGATGATCCGCGCTGGCTACCGGCGATGAGCGAACGCGTAACGCGAAT
GGTGCAGCGCGATCGTAATCACCCGAGTGTGATCATCTGGTCGCTGGGGAATGAATCAGGCCAC
GGCGCTAATCACGACGCGCTGTATCGCTGGATCAAATCTGTCGATCCTTCCCGCCCGGTGCAGT
ATGAAGGCGGCGGAGCCGACACCACGGCCACCGATATTATTTGCCCGATGTACGCGCGCGTGGA
TGAAGACCAGCCCTTCCCGGCTGTGCCGAAATGGTCCATCAAAAAATGGCTTTCGCTACCTGGA
GAGACGCGCCCGCTGATCCTTTGCGAATACGCCCACGCGATGGGTAACAGTCTTGGCGGTTTCG
CTAAATACTGGCAGGCGTTTCGTCAGTATCCCCGTTTACAGGGCGGCTTCGTCTGGGACTGGGT
GGATCAGTCGCTGATTAAATATGATGAAAACGGCAACCCGTGGTCGGCTTACGGCGGTGATTTT
GGCGATACGCCGAACGATCGCCAGTTCTGTATGAACGGTCTGGTCTTTGCCGACCGCACGCCGC
ATCCAGCGCTGACGGAAGCAAAACACCAGCAGCAGTTTTTCCAGTTCCGTTTATCCGGGCAAAC
CATCGAAGTGACCAGCGAATACCTGTTCCGTCATAGCGATAACGAGCTCCTGCACTGGATGGTG
GCGCTGGATGGTAAGCCGCTGGCAAGCGGTGAAGTGCCTCTGGATGTCGCTCCACAAGGTAAAC
AGTTGATTGAACTGCCTGAACTACCGCAGCCGGAGAGCGCCGGGCAACTCTGGCTCACAGTACG
CGTAGTGCAACCGAACGCGACCGCATGGTCAGAAGCCGGGCACATCAGCGCCTGGCAGCAGTGG

CGTCTGGCGGAAAACCTCAGTGTGACGCTCCCCGCCGCGTCCCACGCCATCCCGCATCTGACCA
CCAGCGAAATGGATTTTTGCATCGAGCTGGGTAATAAGCGTTGGCAATTTAACCGCCAGTCAGG
CTTTCTTTCACAGATGTGGATTGGCGATAAAAAACAACTGCTGACGCCGCTGCGCGATCAGTTC
ACCCGTGCACCGCTGGATAACGACATTGGCGTAAGTGAAGCGACCCGCATTGACCCTAACGCCT
GGGTCGAACGCTGGAAGGCGGCGGGCCATTACCAGGCCGAAGCAGCGTTGTTGCAGTGCACGGC
AGATACACTTGCTGATGCGGTGCTGATTACGACCGCTCACGCGTGGCAGCATCAGGGGAAAACC
TTATTTATCAGCCGGAAAACCTACCGGATTGATGGTAGTGGTCAAATGGCGATTACCGTTGATG
TTGAAGTGGCGAGCGATACACCGCATCCGGCGCGGATTGGCCTGAACTGCCAGCTGGCGCAGGT
AGCAGAGCGGGTAAACTGGCTCGGATTAGGGCCGCAAGAAAACTATCCCGACCGCCTTACTGCC
GCCTGTTTTGACCGCTGGGATCTGCCATTGTCAGACATGTATACCCCGTACGTCTTCCCGAGCG
AAAACGGTCTGCGCTGCGGGACGCGCGAATTGAATTATGGCCCACACCAGTGGCGCGGCGACTT
CCAGTTCAACATCAGCCGCTACAGTCAACAGCAACTGATGGAAACCAGCCATCGCCATCTGCTG
CACGCGGAAGAAGGCACATGGCTGAATATCGACGGTTTCCATATGGGGATTGGTGGCGACGACT
CCTGGAGCCCGTCAGTATCGGCGGAATTCCAGCTGAGCGCCGGTCGCTACCATTACCAGTTGGT
CTGGTGTCAGGGGATCCCCCGGGCTGCAGCCAATATGGGATCGGCCATTGAACAAGATGGATTG
CACGCAGGTTCTCCGGCCGCTTGGGTGGAGAGGCTATTCGGCTATGACTGGGCACAACAGACAA
TCGGCTGCTCTGATGCCGCCGTGTTCCGGCTGTCAGCGCAGGGGCGCCCGGTTCTTTTTGTCAA
GACCGACCTGTCCGGTGCCCTGAATGAACTGCAGGACGAGGCAGCGCGGCTATCGTGGCTGGCC
ACGACGGGCGTTCCTTGCGCAGCTGTGCTCGACGTTGTCACTGAAGCGGGAAGGGACTGGCTGC
TATTGGGCGAAGTGCCGGGGCAGGATCTCCTGTCATCTCACCTTGCTCCTGCCGAGAAAGTATC
CATCATGGCTGATGCAATGCGGCGGCTGCATACGCTTGATCCGGCTACCTGCCCATTCGACCAC
CAAGCGAAACATCGCATCGAGCGAGCACGTACTCGGATGGAAGCCGGTCTTGTCGATCAGGATG
ATCTGGACGAAGAGCATCAGGGGCTCGCGCCAGCCGAACTGTTCGCCAGGCTCAAGGCGCGCAT
GCCCGACGGCGAGGATCTCGTCGTGACCCATGGCGATGCCTGCTTGCCGAATATCATGGTGGAA
AATGGCCGCTTTTCTGGATTCATCGACTGTGGCCGGCTGGGTGTGGCGGACCGCTATCAGGACA
TAGCGTTGGCTACCCGTGATATTGCTGAAGAGCTTGGCGGCGAATGGGCTGACCGCTTCCTCGT
GCTTTACGGTATCGCCGCTCCCGATTCGCAGCGCATCGCCTTCTATCGCCTTCTTGACGAGTTC
TTCTGA

9.3. CRH Promoter Reporter Assay

Murine CRH Promoter Region and Appropriate Primers Used for Amplification of the CRH Promoter Region Including the RE-1/NRSE Regulatory Element

Generation of CRH Promoter Region Lacking the RE-1/NRSE Regulatory Element by Eco91I Restriction Endonuclease Digest

Sequence Origin: ENSEMBL Database Chromosome 3:19,593,401 – 19,595,396, Genomic DNA

Illustrated and Analyzed CRH Promoter Region:

6,996 bp (until end of Exon 2)

Cloned CRH Promoter Region Including RE-1/NRSE (5,834 bp):

42 bp – 5,875 bp (Pr.7 – Pr.8)

Cloned CRH Promoter Region Lacking RE-1/NRSE (5,669 bp):

42 bp – 5,710 bp (Pr.7 – Eco91I Site)

Legend:

CRH-Exon 1/2

Primer CRH-RE-1/NRSE-Forward, Pr. 7

Primer CRH-RE-1/NRSE-Reverse, Pr. 8

REGULATORY ELEMENT (RE-1/NRSE)

G/GTCACC : Eco91I Site

ACTTCTAATTCCCAGGATCTTAGAAGGAACTGATTTGAGAAATGGCCTTTCCAAGGGTAATTCA
GTAAAATTAGGTCAAAGGCAAATGCTTGTGCCATATTTTAAGCGGTTGGGAGTAATAGCTGTGG
ATTTGCTCTAAGGATTGTATTATGTTAATTGGGTTCCAAAATTTGCATGAGAATCCGCAGCATG
TAAGACTCTGAGGGTCCCTGCACACAGTTGGTTTGGATTGGTAAATAAAGTTGCTGGAGGCCAA
TGGCTGGGCAGGGAGGGACACAGAGGCAAGACTTTAGGATTCCCTGGCAAGGGAACAGAGAGAG
GATGGAGGAGAAAGATTTGCCCTGGAGGGAAAGGAGAAAGACCAGGCCTGAGAAGTGTAGGACA

GAAAGACTGTTAACATGTAAGAGTCAGGTATCCTGGCCCAGAAGGGTTGCAAGCCTAGGGTATG
GGGTGGCTAGGATGGAATATAGGTTTTAGTAAGTAATAATTCAGGAATATCATAGGGGAGAGTG
TGCTAACTTCATGGAAGTTCGGAGGTGTCCAGCCATTGAGCTCTTTAAGGCATATTAAAACAAA
AGTCTGTGTGTGTGTCTTTTATTCAGGAACCCAGAACACTGGGGTAGGTAGAGAGGACAAGGCC
AGGCAATTTGAGCAAGAGTAACTGGCCTACCACAACAGGAAATAATAGAATACAGTTGTGCTAT
TTAGTTATTTTATGATGATATAGTTCTAGATGAATTTTCTGTCCTGCGTTATTCAATGAACTAT
GGAGTATCCACTGCACTTGCTTAGCTTTTGGAGTGACCACTGCATTAATTCAACAGGCAAGAAA
TACGAGCTGTACTCAACAGGCTAAGCAATGTCTACTACATTTATTCAAAAGTCTGGGGAGTAGC
CACTGCACATATTCAACAGTCTTGGGAATATCCACTGCATTTATTCAACAGGATTTAGAGTGTC
CACTGCACTCATTAAACAGAAGAGTGACCACTACATTCTTTCAATAGGCTAGCAAGTATCCACT
GAATGGACTCAACAGACAAGGGAGTAGCTTCTGGATTTATTTAACAGGCCAAGGAATGAATATC
CATTGTGTTTTGAGAAGGAACTTATACAGAAAACCCATGCCCTGTCACACAGTGTCCAGTCTAT
GCTGTGCCAGTGACTAGTGAAATGTGAGATTTATGCTGAAAGACATCCATGATTTTAGCAGAAC
ATAAGCATACAGGTCCTAAACTTAATCTCAGAAAGAGTCCCACAACAAAACACTTGTTAATGAA
ATAATTAATGTGCATTGCCAATAACACACACAGCATGCAACATATTTTGATATATATATAATAG
AACATGATAGAACATCTAAGTGGAACCAACTAACCTGTATGTCACCTTACATACCATTTCCTAT
GGTAAGAATATTTAAAATCACTCCCTCCCTCTTTTTTTCTTTACATTTAAGTTTTAAAATGTAG
GTTTTATTTTAAAGTAGAGATCACAGTTAAGACCACAGTATTAGTCCAATTAAGAAAAATATAT
GATCTCATCACAAACCTTTGGGGACAGGTAACAAAGTGGTAAATGTGATTAGCTTTGGCATTCA
GAAGAATTTTGTACAGTGTTGTTTGGCCAAGTCTTACAATTTATGCCAGGCTGACTTCCAGCTT
GCAGTTCTGCTGTCCACTGAAGGTGCTGCGATTAGAGATGTGTGCCTCCACAGCTGGCTTACAT
GCTCCATTGTGTTTTTCAGAATCTTCCATGTTCTCTATAGAGAGGATGTATGGCTTTGACACCA
GAAGAGATTGCTAGCAGTTACAATATTGTTCCCAGGAAAGCAGTAAGGTATTTATGTTTTTGAA
ATCCTTTCTTTATCATCTTATGATGATGGCTCTCAAATCTACCTAAAGTGCAGTGACCACAATG
ATTAAGCAACCTGACTGTGAGTAAACATGACAGATTAATGTCAACTCAGCAAACTTGGAGAGTG
TATGATGGCCTGGATTTTGCCAATAGGAGTATATAAAAGTGCAAAGAGATGCAGGCTCTGAGGA
GGTACCTGCTCTCTGTCTCTTTGTGTCTTGTTCTTAAAATCTGTCTCTGTCTCTGTCTCTCTCT
GTCTCTCTGTCTCTCTGTCTCTGTCTCTGTCTCTCTCTCTCTCTCTCTCTCTGTGTATGT
GTGTGCCTATGTGTCTATGTGCCTGTGTGTGTGTGTGTGTGTGTGTGTGTGTGTGTGTGT
GTGTGTGTGAGGTACTATGGCTTGAACCCAGGGCAAGTTCTTTGTCACTGAGGCCCATACCCTA
CCCTCTTGTTTCTCTTTTATTTAATTAATCTGTGTTCCATATTATTTAACTCACTCCTATGTTA
TATTGCTTTTGATAAAGTATTTTGAACAGGAATTAATCACTACTTGGTGCCCATATTTCTTGAA
CAGTGTTTCTAGGATATAAAAGCATTTGTGTTGGTCCTTTTATGATTCCTTTCAGTAAGTGAAG
TGCTATCTCTTGGTGTGAGTCTTGTAATAGAGATTATTAGTGTCTTGTGTAGATCATATCTACA

TTGTTATGTCTGTAATCACACATCAATGACATAATTTCAAGAATCCTCCCTACTCCCTATATTC
TATAAAAAGATAAAATTAATTCTTTTATTTTTGTGTGAATTTTTATTTTGCATTTTCATTTTTA
GGTGCATCAGTGCACTGAAAAACCTCACATCACAAGATTCAGCTAACATGAAAATAGCAGTGTG
CACATACAGACATTTAAAGCCAAGGGGCACTGCACAAAGAATTTCTGTGTTCTTGTGCCTTGGG
AATAAAAGGAAACCCCACGAAAAGGCCTCCAAGAGCTGATATGTGTGTTGCTCCACCTCGTCCA
CTCGTCTCTGCTCATTCGTGTGCCTGTGCTGGGAAAGAAAGCACAAAGGATGCCGTGATGCTGT
GTAAATAGTGAGGCCAGCAGTAAAGAACTGGGTTCTTGTTCTGACTTTATCACTCGCTGAGTAA
CTTCAGATTCCCTCTGGTTCTCATTTAAGCCAAGCGAGCATTTCTAACACGAGTTCTCTGAGAT
TTGCTTCAGTAAATTATGGTACTTCACAATTTATATTCCAGGTAAGCCCCGTGGCAAAGGCTCA
ACAGCAATAGTGGAGCCCGAGTAAAAACACGTCTCCTGATGGTCCGATGGGAGGGATCTTGAGG
GCCAGGAGGTTAGCAAGAGCCCATGTGTGCCACTTCTTCCCCCAGGGACCCTCCCTGACTTCTC
CTGGAAAGCCCATAGGCATGTCTCTCTCTTACTTCCTCTTCAGGACTCATTGGCCTCCTTTCCC
TCTCCAGACTGGCACTTAAGCTGAACTTTATGAATGGGCAAAGAATTGGTCAGGAATGAAAGTT
AAAACAAAACAGAGACCAACAAACAAAAATCCCAAACACTGAGGTGAATTTTAACCTCTAAAAT
GCCCACTGTAACAATAGTGAAGGTTCTGCAGGCCTCCTGGTCAATGTAAACCCACTTTTCCTCT
AAAGCACAATTTGATCATTATTTATTAATGAATCACACTTCTCCTGTGGACAGAATCCTTCCTG
TGTTCTCTTCTATCAGAAATGCATCCCATTCATTCACCTATGAGCTGACTTTTCTGCAACCTCC
AGTGTGAAAACACCTTCCTCTTGTTTCAAGAAGAGTTATCAATTAGTACAGGCCCCAAACAGGG
GTGGAAATCTGCATTGCATTACTTGTGACAGAGAAAATGGCAGACATAACCAGAAACAGGGAAC
AGGAAATTTTGGATAAACAGTAGTGGTGGTTATGAAGCAGCTGAAGCGAATCCCAGACACTAGA
GTTTGTAACAGCATCTTGAATTGCAGGATTAAAGGTAACTACTTCCCACTTAGACATAATCTCC
ATTCAACTCAAAATTTGAGAGTAGATTTATAGACATGGCATTGTGTTCTATAATAGTGCCAGAA
AGCAATAACTAAAGACACTTGTGGTGCACATTTGAATGTGGAGAAAAGAACAGAACACATAATA
AATAACTTGAGTGGTTTGCTCTGCATACCATCATGGTTTCACAGTACACGGAGGTGAAATGAAT
GATTCTCATTTACAGACTCAATAACTGATTTTTTTTCAGGCTATCAAACAGCTTAAGTTTTTTC
AACACAAGAGAACAATGCCTCTCTCATTGGGTTTGCGGTGTAGACTCCGAACAGAGTGTTTAAT
ATACACAGCTCACCCTGCTCTTCTTGGGGGAACAGTCCTGATTAACTTTAGATTCTAAGAGAAC
CATAGGAGGCCTGAGATTCACTTGAAACTGAGGCTTTTAAGAGACTTTGTTTATGGCCTTCCTC
GTTAGAATAGCTCTTTTCTTGTGAAGGAAAACACTAAGCTGGTTTCAAAAAAACGTACTGGCCT
TGTCTTCAGCTCCATAATTCCTATGTATGCTCTTGGGAGGGCTAAGTGGATAAAAACTCAGACC
TGGTTGTCTCTGTCCCCTAGTTCTTCATTCTCCTCCAGGCAGAAAGATGGCAGGCCATAGTAAC
GACAGATTTCAGATACTGAGATGTTTCCTGAGAGGACAACCTGACAGAAGAGTTAGGTGGGGGT
GCTGAGGCACCAGGAAATGTCCAGATCCACCCCTTTAATGGTAACTACCTTCTTGGAAGCTCTG
CACTCCCCACCTCTTCTTCTTTCCCCTCCCACTCTCTGTCTCTTTTCTGGTCCGTATCTGGCCT

ATCATAGTAAGAGGTCAGTCTGTTTTCCACACTTGGATAGTCTCATTCAAAAATTTTTGTCAAT
GGACAAGTCATAAGAAACCCTTCCATTTTCGGGCTCGTTGACGTCACCAAGGAGGCGATAAATA
TCTGTTGATATAATTGGATGTGAGATTCAGTGTTGAAATAGCAGAACTCTGTCCCTCGCTCCTT
GGCAGGGCCCTATTATTTATGCAGGAGCAGAGGCAGCACGCAATCGAGCTGTCAAGAGAGCGTC
AGCTTATTAGGCAAATGCTGCGTGCTTTCTGAAGAGGGTCGACATTATAAAATCTCACTCCAGG
CTCTGGTGTGGAGAAACTCAGAGCCCAAGTACGTTGAGAGACTGAAGAGAAAGGGAAAAGGCAA
AAGAAAAAAAGAAGAGAAAGGAGAAGAGGAAGAAAACCTGCAGGAGGCATCCTGAGAGAAGTCC
CTCTGCAGAGGCAGCAGTGCGGGCTCACCTACCAAGGGAGGAGAAGGTAGGCAGCGCCTAGACG
GGCGCCACCAACTTTGTGCTGCCTGAGCTGCTGTGGTGAGCCCCGGAGCCAGCTGCCCATGTGC
TGGAATGCCTGTGCCTATGCATGTATGTGTGTCGCTAACTGTGCCTTAAAATTCCGATGACAGT
GGCGATTTGAAAAAGCGAAGTTAGACGGCGGCTGCTCATCTTTATCCACTCAATCCAATCTGCC
ACTCACTGCTCATAGTCTGTGCAAAGAATGGCTCCCCTATTGCATCCCATGTCCCCAAGCAAAC
GGAGTAAGGGCAGGAATGGAGACAGAGAAGGTTGTTCTCAATTTGGCAGAAAAGGATGTCCGAA
AGGGGGCGATTAGGGTGTGCGACAGCTTAAACCTGTGGCACTTGTCCGGGCTCAGGGAAGTCGG
TTTAGGGAAGACGTTTGGGAGGTCCTTAGGAAGAGGAGCCAGGGGTTGTCCCTTCTAGGTCTCC
AAAGAAGGGTCACCGCGGGCTCGCACCAGTTGAGCTTTGCAGGTACCTAGCTTCAGCACCGCGG
ACAGCGTCACCGAAGCCTAGAGCCTGTCTTGTCTGTGGGTGTCCGATAGGAAGCCCCGCTGCAC
CTTCCAGCTGAGCTAAACTCTGACCAATCTTACCTTTCTCCCCCACCTTCTCTCTCCCCCGACC
TCAACCTCGGTGCTTCAGAGAGCGCCCCTAACATGCGGCTGCGGCTGCTGGTGTCCGCGGGCAT
GCTGCTGGTGGCTCTGTCGTCCTGCCTGCCTTGCAGGGCCCTGCTCAGCAGGGGATCCGTCCCC
CGAGCGCCGCGGGCCCCGCAGCCCTTGAATTTCTTGCAGCCGGAGCAGCCCCAGCAACCTCAGC
CGGTTCTGATCCGCATGGGTGAAGAATACTTCCTCCGCCTGGGGAATCTCAACAGAAGTCCCGC
TGCTCGGCTGTCCCCCAACTCCACGCCCCTCACCGCGGGTCGCGGCAGCCGCCCCTCGCACGAC
CAGGCTGCGGCTAACTTTTTCCGCGTGTTGCTGCAGCAGCTGCAGATGCCTCAGCGCTCGCTCG
ACAGCCGCGCGGAGCCGGCCGAACGCGGCGCCGAGGATGCCCTCGGTGGCCACCAGGGGGCGCT
GGAGAGGGAGAGGCGGTCGGAGGAGCCGCCCATCTCTCTGGATCTCACCTTCCACCTTCTGCGG
GAAGTCTTGGAAATGGCCCGGGCAGAGCAGTTAGCTCAGCAAGCTCACAGCAACAGGAAACTGA
TGGAGATTATCGGGAAATGAAATGTTGCGCTTGGCCAAAACGATTCTGCATTTAGCACACAAGT
AAAAATAAAAATTTAAAACACAGTATTCTGTACCATATCGCAGCTCCGATATCATTTGTTTATT
TTTATATAGCTTGAAGCATAGAAGATGTACAGGGAGAGAGCCTATATACCCCTTAATTAGCATG
CACAAAGTGTATTTCTGTGTCGTAACAAAACAGCGTTATTTGTATTGCCCATGCTTAATTTCTA
TGTGCAAATAAGCGTCTTTATAGCGATATCTTAAAGAAAATGTGGCCCCAAGGAGGAAACCTTT
GAAAAAGCAGATGGGAGTCATCCAGTTGTTTTTATTTGGAGCTGCAGTGGAAGAGAATTCATTC
TTGAGGGGTGGCTAGGACGAAATGTGTAAGCTCTTTGAATCAACTTTTTCTTGTAAATGTTTCA

GTAATAAAACATCTTTCTGATTCTTGGTCAATTTGGTTGTGTAAGAGAACGTTAAATATATTTT
TAATAAAATCTGCAAAGGTT

9.4. Vector Cards

Plasmids with pcDNA3.1/*myc*-His(-) A Vector Backbone

(Invitrogen, Cat. No. V855-20)

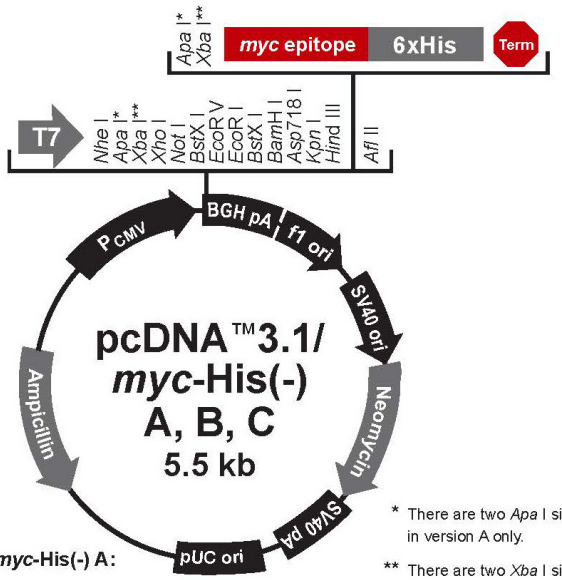

* There are two *Apa* I sites in version A only.

** There are two *Xba* I sites in version B only.

Comments for pcDNA™3.1/*myc*-His(-) A: 5522 nucleotides

CMV promoter: bases 209-863
T7 promoter/priming site: bases 863-882
Multiple cloning site: bases 895-1006
myc epitope: bases 1007-1036
Polyhistidine tag: bases 1052-1069
BGH reverse priming site: bases 1113-1130
BGH polyadenylation signal: bases 1116-1343
f1 origin: bases 1389-1817
SV40 promoter and origin: bases 1844-2152
Neomycin resistance gene: bases 2227-3021
SV40 polyadenylation signal: bases 3195-3325
pUC origin: bases 3708-4381
Ampicillin resistance gene: bases 4526-5386 (complementary strand)

pcDNA3.1-SPRED1 and pcDNA3.1-SPRED2

Full-length cDNAs of murine *Spred1* and *Spred2* including their endogenous stop codons were cloned into the NotI and HindIII sites of the pcDNA3.1/*myc*-His(-) A vector. With these constructs, SPRED1 and SPRED2 are expressed without *myc*-His tags (Bundschu, 2005).

Plasmids with pcDNA3.1/*myc*-His(-) B Vector Backbone

(Invitrogen, Cat. No. V855-20)

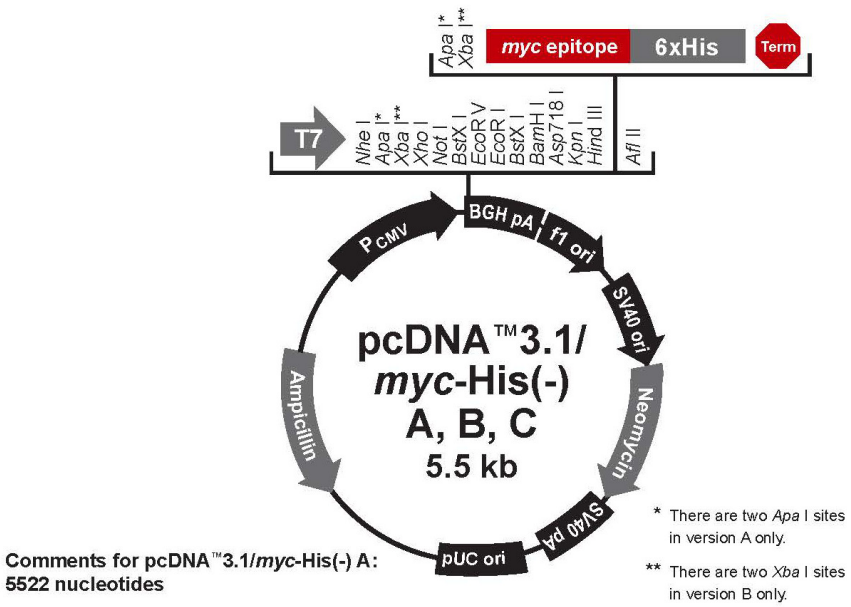

Comments for pcDNA™3.1/*myc*-His(-) A: 5522 nucleotides

CMV promoter: bases 209-863
T7 promoter/priming site: bases 863-882
Multiple cloning site: bases 895-1006
myc epitope: bases 1007-1036
Polyhistidine tag: bases 1052-1069
BGH reverse priming site: bases 1113-1130
BGH polyadenylation signal: bases 1116-1343
f1 origin: bases 1389-1817
SV40 promoter and origin: bases 1844-2152
Neomycin resistance gene: bases 2227-3021
SV40 polyadenylation signal: bases 3195-3325
pUC origin: bases 3708-4381
Ampicillin resistance gene: bases 4526-5386 (complementary strand)

pcDNA3.1-EVH1-β-geo and pcDNA3.1-β-geo

Full-length cDNAs of *EVH1-β-geo* and *β-geo* including their endogenous stop codons were cloned into the NotI and HindIII sites of the pcDNA3.1/*myc*-His(-) B vector. With these constructs, EVH1-β-geo and β-geo are expressed without *myc*-His tags (4.3.1./5.3.2/Appendix 9.2.)

Plasmids with pGL3 Basic Vector Backbone

(Promega, Cat. No. E1751)

3.A. pGL3-Basic Vector

The pGL3-Basic Vector lacks eukaryotic promoter and enhancer sequences, allowing maximum flexibility in cloning putative regulatory sequences. Expression of luciferase activity in cells transfected with this plasmid depends on insertion and proper orientation of a functional promoter upstream from *luc+*. Potential enhancer elements can also be inserted upstream of the promoter or in the BamHI or SalI sites downstream of the *luc+* gene.

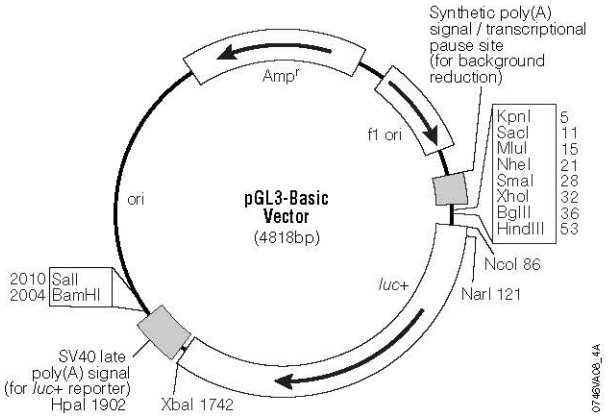

Figure 1. pGL3-Basic Vector circle map. Additional description: *luc+*, cDNA encoding the modified firefly luciferase; Amp^r, gene conferring ampicillin resistance in *E. coli*; f1 ori, origin of replication derived from filamentous phage; ori, origin of replication in *E. coli*. Arrows within *luc+* and the Amp^r gene indicate the direction of transcription; the arrow in the f1 ori indicates the direction of ssDNA strand synthesis.

pGL3-Basic Vector Sequence Reference Points:

Promoter	(none)
Enhancer	(none)
Multiple cloning region	1–58
Luciferase gene (*luc+*)	88–1740
GLprimer2 binding site	89–111
SV40 late poly(A) signal	1772–1993
RVprimer4 binding site	2080–2061
ColE1-derived plasmid replication origin	2318
β-lactamase gene (Amp^r)	3080–3940
f1 origin	4072–4527
upstream poly(A) signal	4658–4811
RVprimer3 binding site	4760–4779

pGL3-CRH$_{Prom-RE}$ and pGL3-CRH$_{Prom}$

A 5.7 kb region of the murine CRH promoter region containing exon 1 was cloned into the XhoI site of the pGL3 Basic Vector. pGL3-CRH$_{Prom-RE}$ includes the RE-1/NRSE regulatory element in the intron between CRH exons 1 and 2, pGL3-CRH$_{Prom}$ lacks it (4.3.2./5.14.2/Appendix 9.3.). The activity of the cloned promoter sequence can be monitored because it drives the expression of the downstream firefly luciferase reporter gene.

Plasmids with pGL2 Basic Vector Backbone

(Promega, Cat. No. E1641)

3.A. pGL2 Basic Vector

The pGL2-Basic Vector lacks eukaryotic promoter and enhancer sequences, allowing maximum flexibility in cloning putative regulatory sequences. Expression of luciferase activity in cells transfected with this plasmid depends on insertion and proper orientation of a functional promoter upstream from *luc*. Potential enhancer elements can also be inserted upstream of the promoter or in the BamHI or SalI sites downstream of the luciferase gene.

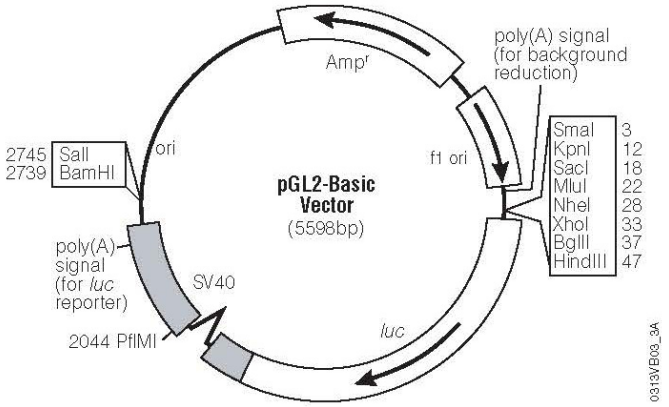

Figure 1. pGL2-Basic Vector map.

pGL2-Basic Vector Sequence Reference Points:

SV40 Promoter	(none)
SV40 Enhancer	(none)
Multiple cloning region	1–53
GLprimer2 binding site	77–99
Luciferase gene (*luc*)	76–1728
SV40 late poly(A) signal	2518–2739
RVprimer4 binding site	2796–2815
β-lactamase (Amp^r) gene	3815–4675
ColE1-derived plasmid replication origin	3053
f1 origin	4807–5262
GLprimer1 binding site	5565–5587

pGL2-4xEts1

4 Ets1 binding sites were cloned into the SmaI site of the pGL2 Basic Vector by blunt end ligation. Ets1 factor-dependent transcription can be monitored by firefly luciferase reporter gene expression (Appendix 9.5.).

pRL-TK

(Promega, Cat. No. E2241)

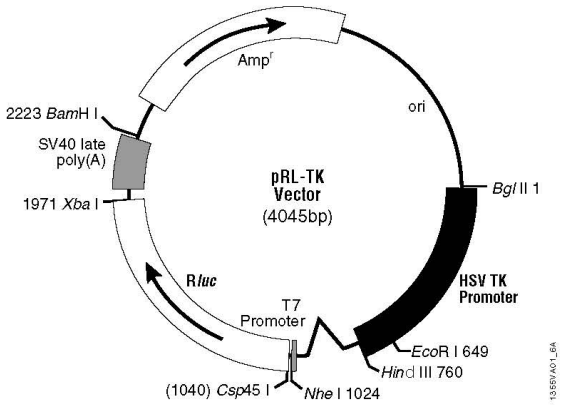

Figure 1. The pRL-TK Vector circle map and sequence reference points.

Sequence reference points:	
HSV-TK promoter	7–759
Chimeric intron	826–962
T7 RNA polymerase promoter (–17 to +2)	1006–1024
T7 RNA polymerase transcription initiation site	1023
R*luc* reporter gene	1034–1969
SV40 late polyadenylation signal	2011–2212
β-lactamase (Amp^r) coding region	2359–3219

pRL-TK contains a *Renilla* luciferase reporter gene, whose expression is driven by the constitutive active HSV-TK promoter. It was used as an internal control reporter plasmid in combination with the CRH promoter and 4xEts1 firefly luciferase reporter vectors.

9.5. 4xEts1 Reporter Assay

Sequence of and Transcription Factor Binding Site Prediction in the 4xEts1 Reporter

Sequence Origin: Eurofins MWG Operon Sequence Analysis of the 4xEts1 Promoter Reporter (pGL2-4xETS1)

Sequence of 4xETS1-Insert:

CCCCTAGAGCTCGACTGTGCTCAGTTAGTCACTTCCTCGACTGTGCTCAGTTAGTCACTTCCTC
GACTGTGCTCAGTTAGTCACTTCCTCGACTGTGCTCAGTTAGTCACTTCCTCGAGGATCCAAGC
TAGCTTGTGACCTCACCCTGCAGAGCCACACCCTGGTGTTGGCCAATCTACACACGGGGTAGGG
ATTACATAGTTCAGGACTTGGGCATAAAAGGCAGAGCAGGGCAGCTGCTGCTTACACTTGCTTA
GATCTAAGTAAGCTGGCATCCGTACCGTA

The Insert Contains 4 Ets1 Binding Sites:

1. 28 bp – 37 bp
2. 54 bp – 63 bp
3. 80 bp – 89 bp
4. 106 bp – 115 bp

Legend:

c-Ets-1 Binding Site

AliBaba2.1 predicts the following sites in your sequence:

```
================================================================================
seq(    0..   59)     cccctagagctcgactgtgctcagttagtcacttcctcgactgtgctcagttagtcactt
Segments:
1.1.1.1     21   30                        ====JunD==
1.1.1.5     23   32                          ====GCN4==
9.9.29      24   33                           ====AP-1==
9.9.32      24   33                           ====AP-1==
2.3.1.0     27   36                              ====Sp1===
3.5.2.0     28   37                               ==c-Ets-1=
1.1.1.1     47   56                                                  ====JunD==
```

```
1.1.1.5     49   58                                                  ====GCN4==
9.9.29      50   59                                                   ====AP-1==
9.9.32      50   59                                                   ====AP-1==
2.3.1.0     53   62                                                      ====Sp1
3.5.2.0     54   63                                                       ==c-Et
================================================================================
seq(   60..  119)     cctcgactgtgctcagttagtcacttcctcgactgtgctcagttagtcacttcctcgagg
Segments:
2.3.1.0     53   62     ===
3.5.2.0     54   63     s-1=
1.1.1.1     73   82                  ====JunD==
1.1.1.5     75   84                    ====GCN4==
9.9.29      76   85                     ====AP-1==
9.9.32      76   85                     ====AP-1==
2.3.1.0     79   88                        ====Sp1===
3.5.2.0     80   89                         ==c-Ets-1=
1.1.1.1     99   108                                        ====JunD==
1.1.1.5     101  110                                          ====GCN4==
9.9.29      102  111                                           ====AP-1==
9.9.32      102  111                                           ====AP-1==
2.3.1.0     105  114                                              ====Sp1===
3.5.2.0     106  115                                               ==c-Ets-1=
================================================================================
seq(  120..  179)     atccaagctagcttgtgacctcaccctgcagagccacaccctggtgttggccaatctaca
Segments:
2.1.2.1     131  140              =RAR-alph=
9.9.45      131  140              ===ARP-1==
2.1.2.2     133  142                ==RXR-beta
2.1.2.3     133  142                =REV-ErbA=
2.1.1.4     133  144                ======ER====
1.1.1.6     134  143                 ==CRE-BP1=
2.3.3.0     134  143                 =CPE_bind=
1.1.1.1     135  144                  ===c-Jun==
1.1.3.0     135  144                  =C/EBPalp=
9.9.51      135  144                  ====ATF===
9.9.77      136  145                   =CACCC-bi=
2.3.1.0     137  147                    =====Sp1===
2.3.1.0     152  162                                 =====Sp1===
1.1.3.0     165  174                                              =C/EBPalp=
9.9.539     167  176                                                ====NF-1==
1.3.1.2     178  187
================================================================================
seq(  180..  239)     cacggggtagggattacatagttcaggacttgggcataaaaggcagagcagggcagctgc
Segments:
1.3.1.2     178  187    ==USF===
```

```
2.3.1.0     181   193     ======Sp1====
1.1.3.0     192   201                =C/EBPalp=
4.3.2.0     207   216                                  ====SRF===
2.3.2.2     211   220                                      =====Kr===
1.2.1.0     233   242                                                          =====E1
1.2.2.0     233   242                                                          ====Myo
3.5.1.2     233   242                                                          ===Adf-
================================================================================
seq(  240..  285)     tgcttacacttgcttagatctaagtaagctggcatccgtaccgta
Segments:
1.2.1.0     233   242   ===
1.2.2.0     233   242   D==
3.5.1.2     233   242   1==

47 segments in this sequence identified as potential binding sites
```

9.6. Transcription Factor Binding Site Prediction in the Murine CRH Promoter

Focus on Predicted Ets1 Binding Sites

Sequence Origin: ENSEMBL Database Chromosome 3:19,593,401 - 19,595,396, Genomic DNA

Illustrated and Analyzed CRH Promoter Region:

5,906 bp (until end of *CRH*-Intron 1)

Cloned CRH Promoter Region Including RE-1/NRSE (5,834 bp):

42 bp – 5,875 bp (Pr.7 – Pr.8)

Contains 4 Ets1 Binding Sites:

1. 673 bp – 682 bp
2. 3576 bp – 3585 bp
3. 3772 bp – 3783 bp
4. 4617 bp – 4626 bp

Cloned CRH Promoter Region Lacking RE-1/NRSE (5,669 bp):

42 bp – 5,710 bp (Pr.7 – Eco91I Site)

Contains 4 Ets1 Binding Sites:

1. 673 bp – 682 bp
2. 3576 bp – 3585 bp
3. 3772 bp – 3783 bp
4. 4617 bp – 4626 bp

Legend:

c-Ets-1 Binding Site

CRH-Exon 1/2

Primer CRH-RE-1/NRSE-Forward, Pr. 7

Primer CRH-RE-1/NRSE-Reverse, Pr. 8

REGULATORY ELEMENT (RE-1/NRSE)

G/GTCACC : Eco91I Site

AliBaba2.1 predicts the following sites in your sequence:

```
================================================================================
     seq(    0..   59)     acttctaattcccaggatcttagaaggaactgatttgagaaatggcctttccaagggtaa
Segments:
3.5.2.0     23   32                              ====PU.1==
1.1.3.0     32   41                                    =C/EBPalp=
3.1.2.2     34   43                                      ===Oct-1==
9.9.590     42   51                                            =NF-kappaB
================================================================================
     seq(   60..  119)     ttcagtaaaattaggtcaaaggcaaatgcttgtgccatattttaagcggttgggagtaat
Segments:
4.3.2.0     68   77            ====SRF===
2.1.1.4     70   79              =====ER===
2.1.2.1     72   81              =RAR-alph=
2.1.2.3     72   81              =REV-ErbA=
2.1.2.10    72   81              ====COUP==
4.3.1.1     97   106                                   ===MEB-1==
4.3.1.2     97   106                                   ====GLO===
================================================================================
     seq(  120..  179)     agctgtggatttgctctaaggattgtattatgttaattgggttccaaaatttgcatgaga
Segments:
1.1.3.0     125  134       =C/EBPalp=
9.9.539     160  169                                       ====NF-1==
1.1.3.0     168  177                                              =C/EBPalp=
3.1.2.2     168  177                                              ===Oct-1==
================================================================================
     seq(  180..  239)     atccgcagcatgtaagactctgagggtccctgcacacagttggtttggattggtaaataa
Segments:
1.1.3.0     227  236                                                  =C/EBPalp=
3.1.1.12    229  238                                                    ===HNF-1==
3.1.2.2     229  238                                                    ===Oct-1==
4.5.1.0     231  240                                                      ====TBP==
1.1.3.0     234  243                                                         =C/EBP
================================================================================
     seq(  240..  299)     agttgctggaggccaatggctgggcagggagggacacagaggcaagactttaggattccc
Segments:
4.5.1.0     231  240   =
1.1.3.0     234  243   alp=
2.3.1.0     243  252      ====Sp1===
9.9.539     248  257           ====NF-1==
9.9.150     250  259             ====CP1===
2.3.1.0     257  268                   =====Sp1====
2.3.1.0     263  274                         =====Sp1====
2.1.1.1     271  280                               =====GR===
1.1.3.0     279  288                                     =C/EBPgam=
9.9.539     295  304                                                 ====N
9.9.535     298  307                                                    ==
```

```
2.3.1.0     299  308                                                                    =
================================================================================
     seq(  300..  359)     tggcaagggaacagagagaggatggaggagaaagatttgccctggagggaaaggagaaag
Segments:
9.9.539     295  304   F-1==
9.9.535     298  307   ==NF-1==
2.3.1.0     299  308   ===Sp1===
2.3.1.0     320  329                        ====Sp1===
================================================================================
     seq(  360..  419)     accaggcctgagaagtgtaggacagaaagactgttaacatgtaagagtcaggtatcctgg
Segments:
2.1.1.2     385  394                             =====PR===
1.1.1.5     400  409                                       ====GCN4==
9.9.32      401  410                                        ====AP-1==
================================================================================
     seq(  420..  479)     cccagaagggttgcaagcctagggtatggggtggctaggatggaatataggttttagtaa
Segments:
9.9.726     449  458                                 =represso=
3.1.1.2     479  488                                                                =
================================================================================
     seq(  480..  539)     gtaataattcaggaatatcataggggagagtgtgctaacttcatggaagttcggaggtgt
Segments:
3.1.1.2     479  488   ==Zen-1==
2.3.1.0     500  509                        ====Sp1===
1.1.3.0     504  513                            =C/EBPbeta
================================================================================
     seq(  540..  599)     ccagccattgagctctttaaggcatattaaaacaaaagtctgtgtgtgtgtcttttattc
Segments:
3.3.2.0     566  575                             ===HNF-3==
3.5.1.2     577  589                                   =====RAP1====
3.3.2.0     591  600                                                ===HNF-3=
3.1.2.1     593  602                                                  ===Pit-
9.9.29      594  603                                                   ====AP
================================================================================
     seq(  600..  659)     aggaacccagaacactggggtaggtagagaggacaaggccaggcaatttgagcaagagta
Segments:
3.3.2.0     591  600   =
3.1.2.1     593  602   1a=
9.9.29      594  603   -1==
9.9.150     629  638                                 ====CP1===
1.1.3.0     640  654                                       ===C/EBPalpha==
9.9.32      654  663                                                    ====AP
================================================================================
     seq(  660..  719)     actggcctaccacaacaggaaataatagaatacagttgtgctatttagttattttatgat
Segments:
9.9.32      654  663   -1==
3.5.2.0     673  682              =c-Ets-1 =
9.9.590     673  682              =NF-kappaB
1.1.3.0     676  685                 ===C/EBP==
2.2.1.1     676  685                 ===GATA-1=
1.1.3.0     693  702                              =C/EBPbeta
3.1.2.2     701  710                                    ===Oct-1==
1.1.3.0     701  714                                    ===C/EBPalpha=
3.1.1.2     705  714                                        ====Antp==
================================================================================
     seq(  720..  779)     gatatagttctagatgaattttctgtcctgcgttattcaatgaactatggagtatccact
Segments:
1.1.3.0     748  757                               =C/EBPbeta
================================================================================
     seq(  780..  839)     gcacttgcttagcttttggagtgaccactgcattaattcaacaggcaagaaatacgagct
Segments:
2.1.2.3     801  810                          =REV-ErbA=
================================================================================
     seq(  840..  899)     gtactcaacaggctaagcaatgtctactacatttattcaaaagtctggggagtagccact
Segments:
1.1.3.0     840  849   =C/EBPalp=
3.1.1.2     867  876                               ====Dfd===
3.1.2.2     873  882                                    ===Oct-1==
```

```
2.3.1.0     882  894                                                ======Sp1====
1.1.3.0     896  905                                                      =C/E
4.3.2.0     899  908                                                        =
================================================================================
     seq(  900..  959)     gcacatattcaacagtcttgggaatatccactgcatttattcaacaggatttagagtgtc
Segments:
1.1.3.0     896  905   BPalp=
4.3.2.0     899  908   ===SRF===
4.1.1.0     918  927                  ===c-Rel==
9.9.590     919  928                   =NF-kappaB
9.9.592     919  928                   =NF-kappa=
9.9.594     919  928                   ====RelA==
3.1.1.2     931  940                          ====Dfd===
3.1.2.1     933  942                            ===Pit-1a=
================================================================================
     seq(  960.. 1019)     cactgcactcattaaacagaagagtgaccactacattctttcaataggctagcaagtatc
Segments:
3.1.1.12    967  976        ===HNF-1==
3.6.1.0     990  999                          ====TEC1==
================================================================================
     seq( 1020.. 1079)     cactgaatggactcaacagacaagggagtagcttctggatttatttaacaggccaaggaa
Segments:
4.3.2.0    1023 1032     ====SRF===
9.9.539    1035 1044               ====NF-1==
2.3.1.0    1043 1052                     ====Sp1===
9.9.539    1070 1079                                          ====NF-1==
3.6.1.0    1074 1083                                              ====TE
================================================================================
     seq( 1080.. 1139)     tgaatatccattgtgttttgagaaggaacttatacagaaaacccatgccctgtcacacag
Segments:
3.6.1.0    1074 1083  C1==
3.1.2.2    1082 1091    ===Oct-1==
3.5.2.0    1102 1111                ====PU.1==
3.5.1.2    1119 1128                          ====RAP1==
2.3.1.0    1122 1131                             ====Sp1===
2.1.2.3    1123 1132                              =T3R-alpha
2.3.1.0    1128 1137                                   ====Sp1===
================================================================================
     seq( 1140.. 1199)     tgtccagtctatgctgtgccagtgactagtgaaatgtgagatttatgctgaaagacatcc
Segments:
9.9.29     1157 1166               ====AP-1==
1.1.3.0    1169 1178                         =C/EBPbeta
================================================================================
     seq( 1200.. 1259)     atgattttagcagaacataagcatacaggtcctaaacttaatctcagaaagagtcccaca
Segments:
1.1.3.0    1202 1211   =C/EBPalp=
2.1.1.1    1210 1219         =====GR===
3.1.2.2    1216 1225              ===Oct-1==
1.1.3.0    1217 1226               =C/EBPbeta
1.1.3.0    1236 1245                          =C/EBPbeta
1.1.1.5    1245 1254                                ====GCN4==
1.1.3.0    1256 1265                                      =C/E
2.3.2.2    1258 1267                                        ==
================================================================================
     seq( 1260.. 1319)     acaaaacacttgttaatgaaataattaatgtgcattgccaataacacacacagcatgcaa
Segments:
1.1.3.0    1256 1265  BPalp=
2.3.2.2    1258 1267  =LyF-1==
3.1.2.2    1273 1282         ===Oct-1==
1.1.3.0    1275 1287           ==C/EBPalpha=
3.1.1.2    1279 1288               ===Zen-1==
3.1.2.2    1286 1295                     ===Oct-1==
2.2.1.1    1287 1296                      ===GATA-1=
9.9.539    1291 1303                          =====NF-1====
1.1.3.0    1294 1303                             =C/EBPalp=
3.1.1.12   1294 1303                             ===HNF-1==
9.9.535    1294 1303                             ====NF-1==
9.9.537    1294 1303                             ====NF-1==
```

```
2.3.2.3     1302 1311                                                  =WT1_I_-K=
4.6.1.0     1302 1311                                                  ===Sox-2==
9.9.1840    1302 1311                                                  ===WT1_I==
9.9.1841    1302 1311                                                  ==WT1-del2
9.9.1842    1302 1311                                                  =WT1_I-de=
3.1.2.2     1311 1320                                                        ===Oct-1=
1.1.3.0     1313 1322                                                          =C/EBPa
================================================================================
     seq( 1320.. 1379)     catattttgatatatatataatagaacatgatagaacatctaagtggaaccaactaacct
Segments:
3.1.2.2     1311 1320  =
1.1.3.0     1313 1322  lp=
1.1.3.0     1321 1330   =C/EBPalp=
4.5.1.0     1329 1341          ======TBP====
3.1.2.1     1331 1340            ===Pit-1a=
2.1.1.1     1339 1348                  =====GR===
================================================================================
     seq( 1380.. 1439)     gtatgtcaccttacataccatttcctatggtaagaatatttaaaatcactccctccctct
Segments:
2.3.1.0     1396 1405                ====Sp1===
1.1.3.0     1398 1407                  =C/EBPalp=
9.9.590     1399 1408                   =NF-kappaB
3.1.2.2     1414 1423                            ===Oct-1==
1.1.3.0     1418 1427                               =C/EBPalp=
2.1.1.4     1420 1429                                 =====ER===
2.3.1.0     1426 1436                                       =====Sp1===
4.5.1.0     1434 1443                                             ====TB
9.9.820     1434 1443                                             ===TFI
2.3.3.0     1435 1444                                              =CPE_
1.1.1.5     1438 1447                                                 ==
2.3.2.2     1439 1449                                                  =
================================================================================
     seq( 1440.. 1499)     ttttttctttacatttaagttttaaaatgtaggtttatttaaagtagagatcacagtt
Segments:
4.5.1.0     1434 1443  P===
9.9.820     1434 1443  ID==
2.3.3.0     1435 1444  bind=
1.1.1.5     1438 1447  ==GCN4==
2.3.2.2     1439 1449  ====Hb====
2.2.1.1     1443 1452     ===GATA-1=
3.1.2.2     1444 1457      =====Oct-1====
3.1.1.2     1447 1456         ===Zen-1==
3.1.1.2     1472 1481                        ====Antp==
3.1.2.2     1475 1484                           ===Oct-1==
4.3.1.1     1475 1484                           ===MEB-1==
2.1.1.4     1489 1498                                    =====ER===
================================================================================
     seq( 1500.. 1559)     aagaccacagtattagtccaattaagaaaaatatatgatctcatcacaaacctttgggga
Segments:
1.1.3.0     1513 1522              =C/EBPalp=
3.1.1.0     1518 1527                   =MATalpha1
3.1.2.2     1518 1527                   ===Oct-1==
4.3.1.3     1518 1527                   ====MCM1==
1.1.3.0     1519 1528                    =C/EBPalp=
2.3.1.0     1555 1564                                                ====S
2.2.1.1     1557 1566                                                  ===
================================================================================
     seq( 1560.. 1619)     caggtaacaaagtggtaaatgtgattagctttggcattcagaagaattttgtacagtgtt
Segments:
2.3.1.0     1555 1564  p1===
2.2.1.1     1557 1566  GATA-1=
2.1.1.1     1564 1573      =====GR===
2.2.1.1     1568 1577          ===GATA-1=
1.1.3.0     1605 1614                                        =C/EBPalp=
2.1.1.1     1607 1616                                          =====GR===
4.3.2.0     1617 1626                                                ===
9.9.537     1619 1628                                                 =
================================================================================
```

```
     seq( 1620.. 1679)     gtttggccaagtcttacaatttatgccaggctgacttccagcttgcagttctgctgtcca
Segments:
4.3.2.0     1617 1626  =SRF===
9.9.537     1619 1628  ===NF-1==
9.9.539     1622 1631    ====NF-1==
3.1.2.2     1633 1642               ===Oct-1==
9.9.539     1639 1648                     ====NF-1==
9.9.29      1651 1660                           ====AP-1==
================================================================================
     seq( 1680.. 1739)     ctgaaggtgctgcgattagagatgtgtgcctccacagctggcttacatgctccattgtgt
Segments:
1.3.1.4     1710 1719                           ====AP-4==
================================================================================
     seq( 1740.. 1799)     ttttcagaatcttccatgttctctatagagaggatgtatggctttgacaccagaagagat
Segments:
3.4.1.0     1746 1755         ====HSF===
3.1.1.2     1777 1786                                 ====Antp==
1.1.3.0     1794 1803                                                =C/EBP
================================================================================
     seq( 1800.. 1859)     tgctagcagttacaatattgttcccaggaaagcagtaaggtatttatgtttttgaaatcc
Segments:
1.1.3.0     1794 1803  alp=
2.3.1.0     1823 1832                     ====Sp1===
9.9.539     1825 1834                       ====NF-1==
1.1.3.0     1840 1849                                 =C/EBPalp=
1.1.3.0     1849 1858                                          =C/EBPgam=
================================================================================
     seq( 1860.. 1919)     tttctttatcatcttatgatgatggctctcaaatctacctaaagtgcagtgaccacaatg
Segments:
2.2.1.1     1861 1870   ===GATA-1=
3.5.2.0     1862 1871    ===Erg-1==
1.6.1.0     1883 1892                     =AP-2alph=
3.1.2.2     1913 1922                                                ===Oct-
1.1.3.0     1919 1928                                                    =
================================================================================
     seq( 1920.. 1979)     attaagcaacctgactgtgagtaaacatgacagattaatgtcaactcagcaaacttggag
Segments:
3.1.2.2     1913 1922  1==
1.1.3.0     1919 1928  C/EBPalp=
1.1.3.0     1937 1946               =C/EBPalp=
3.1.1.12    1937 1946               ===HNF-1==
3.3.2.0     1937 1946               ===HNF-3==
9.9.29      1942 1951                    ====AP-1==
================================================================================
     seq( 1980.. 2039)     agtgtatgatggcctggattttgccaataggagtatataaaagtgcaaagagatgcaggc
Segments:
1.1.3.0     1996 2008               ==C/EBPalpha=
9.9.537     1999 2008                  ====NF-1==
9.9.539     2000 2009                   ====NF-1==
3.1.2.2     2012 2021                         ===Oct-1==
4.5.1.0     2012 2022                         =====TBP===
4.5.1.0     2013 2023                          =====TBP===
1.1.3.0     2037 2046                                              =C/
================================================================================
     seq( 2040.. 2099)     tctgaggaggtacctgctctctgtctctttgtgtcttgttcttaaaatctgtctctgtct
Segments:
1.1.3.0     2037 2046  EBPalp=
2.3.1.0     2043 2052     ====Sp1===
1.1.1.5     2073 2082                         ====GCN4==
2.1.1.1     2073 2082                         =====GR===
2.1.1.2     2076 2085                            =====PR===
================================================================================
     seq( 2100.. 2159)     ctgtctctctctgtctctctgtctctctgtctctgtctctgtctctctctctctctct
Segments:
================================================================================
     seq( 2160.. 2219)     ctctctctgtgtatgtgtgtgcctatgtgtctatgtgcctgtgtgtgtgtgtgtgtgt
Segments:
3.5.1.2     2167 2178           =====RAP1===
```

```
3.5.1.2     2200 2209                                          ====RAP1==
3.5.1.2     2212 2221                                                    ====RAP1
================================================================================
     seq( 2220.. 2279)     gtgtgtgtgtgtgtgtgtgtgtgtgtgaggtactatggcttgaacccagggcaagttc
Segments:
3.5.1.2     2212 2221  ==
3.5.1.2     2226 2235        ====RAP1==
3.5.1.2     2239 2248                  ====RAP1==
9.9.539     2256 2265                             ====NF-1==
================================================================================
     seq( 2280.. 2339)     tttgtcactgaggcccataccctaccctcttgtttctcttttatttaattaatctgtgtt
Segments:
2.3.1.0     2299 2308                  ====Sp1===
3.5.3.0     2311 2320                        ===ICSBP==
9.9.428     2311 2320                        ===ISGF-3=
1.1.1.5     2316 2325                             ====GCN4==
3.3.2.0     2317 2326                              ===HNF-3==
4.5.1.0     2317 2326                              ====TBP===
3.1.1.12    2319 2328                                ===HNF-1==
2.3.2.2     2321 2330                                  =====Hb===
3.1.2.2     2321 2330                                  ===Oct-1==
3.1.2.2     2338 2347                                                       ==
================================================================================
     seq( 2340.. 2399)     ccatattatttaactcactcctatgttatattgcttttgataaagtattttgaacaggaa
Segments:
3.1.2.2     2338 2347  =Oct-1==
1.1.3.0     2342 2351    =C/EBPbeta
3.1.1.2     2345 2354       ====Ftz===
3.1.1.8     2345 2354       ====Eve===
3.1.1.2     2368 2377                        ====Antp==
1.1.3.0     2394 2403                                                  =C/EBP
================================================================================
     seq( 2400.. 2459)     ttaatcactacttggtgcccatatttcttgaacagtgtttctaggatataaaagcatttg
Segments:
1.1.3.0     2394 2403  alp=
3.1.1.12    2400 2409  ===HNF-1C=
1.2.8.0     2401 2410   ====Id3===
4.1.3.0     2401 2410   ==NF-ATc3=
1.1.3.0     2415 2424               =C/EBPbeta
4.3.2.0     2415 2424               ====SRF===
9.9.539     2415 2424               ====NF-1==
4.5.1.0     2443 2452                                  ====TBP===
================================================================================
     seq( 2460.. 2519)     tgttggtccttttatgattcctttcagtaagtgaagtgctatctcttggtgtgagtcttg
Segments:
4.3.2.0     2466 2475        ====SRF===
4.5.1.0     2469 2478           ====TBP===
3.1.2.1     2470 2479            ===Pit-1a=
2.2.1.1     2494 2503                        ===GATA-1=
1.1.3.0     2513 2523                                                  =C/EBPa
1.1.3.0     2514 2523                                                   =C/EBP
================================================================================
     seq( 2520.. 2579)     taatagagattattagtgtcttgtgtagatcatatctacattgttatgtctgtaatcaca
Segments:
1.1.3.0     2513 2523  lpha
1.1.3.0     2514 2523  alp=
2.2.1.1     2524 2533      ===GATA-1=
3.1.1.12    2543 2552                ===HNF-1==
3.1.2.2     2551 2560                      ===Oct-1==
================================================================================
     seq( 2580.. 2639)     catcaatgacataatttcaagaatcctccctactccctatattctataaaaagataaaat
Segments:
2.3.3.0     2582 2591    =CPE_bind=
1.1.2.0     2584 2593      ====CREB==
1.1.1.6     2585 2594       ==CRE-BP1=
4.5.1.0     2621 2630                                  ====TBP===
4.3.1.1     2622 2631                                   ===RSRFC4=
2.2.1.1     2627 2636                                        ===GATA-1=
```

```
1.1.3.0     2635 2644                                                                    =C/EB
================================================================================
     seq( 2640.. 2699)     taattcttttatttttgtgtgaatttttatttgcattttcatttttaggtgcatcagtg
Segments:
1.1.3.0     2635 2644  Pbeta
1.1.1.5     2644 2653      ====GCN4==
3.1.2.2     2644 2653      ===Oct-1==
3.3.2.0     2645 2654       ===HNF-3==
9.9.51      2658 2667                 ====ATF===
1.1.3.0     2663 2672                      =C/EBPalp=
3.1.2.2     2667 2678                          ====Oct-1A==
2.2.1.1     2668 2677                           ===GATA-1=
9.9.539     2668 2677                           ====NF-1==
3.5.3.0     2677 2686                                   ===ICSBP==
================================================================================
     seq( 2700.. 2759)     cactgaaaaacctcacatcacaagattcagctaacatgaaaatagcagtgtgcacataca
Segments:
3.1.2.2     2733 2742                                   ===Oct-1==
2.3.1.0     2745 2754                                         ====Sp1===
================================================================================
     seq( 2760.. 2819)     gacatttaaagccaaggggcactgcacaaagaatttctgtgttcttgtgccttgggaata
Segments:
9.9.539     2766 2777        =====NF-1===
2.3.1.0     2770 2779            ====Sp1===
================================================================================
     seq( 2820.. 2879)     aaaggaaaccccacgaaaaggcctccaagagctgatatgtgtgttgctccacctcgtcca
Segments:
2.3.1.0     2824 2833      ====Sp1===
2.3.1.0     2840 2849                ====Sp1===
2.3.1.0     2865 2874                                   ====Sp1===
================================================================================
     seq( 2880.. 2939)     ctcgtctctgctcattcgtgtgcctgtgctgggaaagaaagcacaaaggatgccgtgatg
Segments:
1.1.3.0     2939 2948                                                                =
================================================================================
     seq( 2940.. 2999)     ctgtgtaaatagtgaggccagcagtaaagaactgggttcttgttctgactttatcactcg
Segments:
1.1.3.0     2939 2948  C/EBPalp=
2.3.1.0     2952 2961             ====Sp1===
2.3.1.0     2967 2976                  ====Sp1===
2.1.1.1     2977 2986                       =====GR===
2.2.1.1     2990 2999                            ===GATA-1=
1.1.1.2     2998 3007                                  ==
9.9.32      2998 3007                                  ==
1.1.1.1     2998 3008                                  ==
================================================================================
     seq( 3000.. 3059)     ctgagtaacttcagattccctctggttctcatttaagccaagcgagcatttctaacacga
Segments:
1.1.1.2     2998 3007  =c-Fos==
9.9.32      2998 3007  ==AP-1==
1.1.1.1     2998 3008  ==c-Jun==
9.9.29      3000 3009  ====AP-1==
1.1.1.5     3001 3010   ====AP-1==
9.9.590     3013 3022         =NF-kappaB
1.3.1.2     3024 3033              ====USF===
4.6.1.0     3046 3055                        ===SOX-9==
================================================================================
     seq( 3060.. 3119)     gttctctgagatttgcttcagtaaattatggtacttcacaatttatattccaggtaagcc
Segments:
3.1.2.2     3068 3079          ====Oct-1===
1.1.3.0     3072 3081              =C/EBPalp=
1.1.3.0     3093 3102                   =C/EBPalp=
2.3.1.0     3109 3118                             ====Sp1===
1.1.5.2     3117 3126                                   ===
================================================================================
     seq( 3120.. 3179)     ccgtggcaaaggctcaacagcaatagtggagcccgagtaaaaacacgtctcctgatggtc
Segments:
1.1.5.2     3117 3126  TAF-1==
```

```
2.1.1.1     3171 3180                                                                  =====GR==
================================================================================
     seq( 3180.. 3239)     cgatgggagggatcttgagggccaggaggttagcaagagcccatgtgtgccacttcttcc
Segments:
2.1.1.1     3171 3180  =
2.3.1.0     3182 3193    =====Sp1====
9.9.539     3197 3206                ====NF-1==
2.3.1.0     3197 3207                =====Sp1===
1.1.3.0     3210 3219                      =C/EBPalp=
1.3.1.2     3218 3227                           ====USF===
9.9.539     3222 3231                               ====NF-1==
2.3.1.0     3228 3237                                   ====Sp1===
2.3.1.0     3238 3247                                        ==
================================================================================
     seq( 3240.. 3299)     cccagggaccctccctgacttctcctggaaagcccataggcatgtctctctcttacttcc
Segments:
2.3.1.0     3238 3247  ==Sp1===
2.3.1.0     3245 3258       ======Sp1=====
1.1.3.0     3255 3264             =C/EBPalp=
2.3.1.0     3256 3265              ====Sp1===
4.1.1.0     3265 3274                    =NF-kappa=
9.9.590     3265 3274                    =NF-kappaB
3.5.2.0     3294 3303                                                    ====PU
2.3.1.0     3295 3304                                                     ====S
================================================================================
     seq( 3300.. 3359)     tcttcaggactcattggcctcctttccctctccagactggcacttaagctgaactttatg
Segments:
3.5.2.0     3294 3303  .1==
2.3.1.0     3295 3304  p1===
9.9.539     3311 3320        ====NF-1==
2.3.1.0     3320 3333                ======Sp1=====
2.3.1.0     3331 3340                      ====Sp1===
9.9.539     3336 3345                           ====NF-1==
2.1.2.1     3347 3356                                =RAR-alph=
2.1.2.3     3347 3356                                =REV-ErbA=
2.1.2.11    3347 3356                                =HNF-4alp=
3.1.2.1     3356 3365                                     ===P
2.3.1.0     3359 3368                                      =
================================================================================
     seq( 3360.. 3419)     aatgggcaaagaattggtcaggaatgaaagttaaaacaaaacagagaccaacaaacaaaa
Segments:
3.1.2.1     3356 3365  it-1a=
2.3.1.0     3359 3368  ===Sp1===
2.1.1.1     3363 3372     =====GR===
9.9.1202    3372 3381           ====CP1===
3.6.1.0     3379 3388                ====TEC1==
3.3.2.0     3392 3401                     ===HNF-3==
1.1.3.0     3393 3402                      =C/EBPalp=
1.1.3.0     3409 3418                                =C/EBPalp=
9.9.590     3418 3427                                      =N
================================================================================
     seq( 3420.. 3479)     atcccaaacactgaggtgaattttaacctctaaaatgcccactgtaacaatagtgaaggt
Segments:
9.9.590     3418 3427  F-kappaB
3.5.1.2     3422 3431    ====RAP1==
4.3.1.1     3438 3447                ===MEB-1==
4.3.1.2     3438 3447                ====GLO===
================================================================================
     seq( 3480.. 3539)     tctgcaggcctcctggtcaatgtaaacccactttcctctaaagcacaatttgatcatta
Segments:
2.3.1.0     3484 3493       ====Sp1===
2.1.1.4     3493 3502            =====ER===
3.1.2.2     3496 3505               ===Oct-1==
4.1.1.0     3510 3519                     =NF-kappa=
3.1.1.12    3532 3541                                ===HNF-1
1.1.3.0     3534 3547                                  ===C/E
```

```
     seq( 3540.. 3599)     tttattaatgaatcacacttctcctgtggacagaatccttcctgtgttctcttctatcag
Segments:
3.1.1.12    3532 3541  ==
1.1.3.0     3534 3547  BPalpha=
1.1.1.1     3545 3554       ===c-Jun==
1.1.1.5     3546 3555        ====GCN4==
3.5.2.0     3576 3585                                    =c-Ets-1 =
2.1.1.1     3580 3589                                        =====GR===
2.1.1.2     3582 3591                                          =====PR===
2.2.1.1     3590 3601                                                ====GATA-1
================================================================================
     seq( 3600.. 3659)     aaatgcatcccattcattcacctatgagctgacttttctgcaacctccagtgtgaaaaca
Segments:
2.2.1.1     3590 3601  ==
9.9.539     3603 3612     ====NF-1==
3.1.2.1     3611 3620           ===Pit-1a=
1.3.1.2     3623 3632                 ====USF===
3.5.2.0     3635 3644                      ===Erg-1==
================================================================================
     seq( 3660.. 3719)     ccttcctcttgtttcaagaagagttatcaattagtacaggccccaaacaggggtggaaat
Segments:
2.3.1.0     3660 3669  ====Sp1===
3.5.2.0     3660 3669  ====PU.1==
9.9.322     3661 3670   ====GCR1==
2.1.1.2     3675 3684         =====PR===
2.3.1.0     3694 3703                ====Sp1===
2.3.1.0     3707 3716                     ====Sp1===
3.1.2.2     3716 3730                          ====
================================================================================
seq( 3720.. 3779)     ctgcattgcattacttgtgacagagaaaatggcagacataaccagaaacagggaacagga
Segments:
3.1.2.2     3716 3730  ==Oct-1====
9.9.539     3720 3729  ====NF-1==
2.1.1.4     3732 3741       =====ER===
3.1.1.2     3741 3750            ====Ftz===
3.5.2.0     3772 3783                          ==c-Ets-
1.1.3.0     3773 3782                           =C/EBPa
9.9.590     3773 3782                           =NF-kap
================================================================================
seq( 3780.. 3839)     aattttggataaacagtagtggtggttatgaagcagctgaagcgaatcccagacactaga
Segments:
3.5.2.0     3772 3783  1 68
1.1.3.0     3773 3782  lp=
9.9.590     3773 3782  paB
9.9.539     3781 3790   ====NF-1==
1.1.3.0     3836 3845                                          =C/E
================================================================================
seq( 3840.. 3899)     gtttgtaacagcatcttgaattgcaggattaaaggtaactacttcccacttagacataat
Segments:
1.1.3.0     3836 3845  BPalp=
3.1.1.2     3854 3863         ====Ftz===
================================================================================
seq( 3900.. 3959)     ctccattcaactcaaaatttgagagtagatttatagacatggcattgtgttctataatag
Segments:
1.1.5.3     3935 3944                                ====GBF1==
2.1.1.1     3943 3952                                     =====GR===
9.9.539     3955 3964                                          ====N
================================================================================
seq( 3960.. 4019)     tgccagaaagcaataactaaagacacttgtggtgcacatttgaatgtggagaaaagaaca
Segments:
9.9.539     3955 3964  F-1==
3.1.1.12    3971 3980       ===HNF-1==
3.1.2.2     3997 4006                      ===Oct-1==
4.3.2.0     4002 4011                           ====SRF===
1.1.3.0     4004 4013                             =C/EBPalp=
2.1.1.1     4013 4022                                   =====GR
================================================================================
seq( 4020.. 4079)     gaacacataataaataacttgagtggtttgctctgcataccatcatggtttcacagtaca
```

```
Segments:
2.1.1.1     4013 4022  ===
3.1.1.12    4028 4037          ===HNF-1C=
9.9.15      4028 4037          ====AFP1==
1.1.3.0     4029 4038           =C/EBPalp=
1.1.3.0     4043 4052                      =C/EBPalp=
3.1.2.2     4048 4057                           ===Oct-1==
2.3.1.0     4078 4087                                                ==
================================================================================
seq( 4080.. 4139)     cggaggtgaaatgaatgattctcatttacagactcaataactgatttttttttcaggctat
Segments:
2.3.1.0     4078 4087  ==Sp1===
3.1.1.12    4113 4122                                ===HNF-1==
1.1.3.0     4114 4123                                 =C/EBPdel=
1.1.3.0     4123 4132                                          =C/EBPalp=
2.3.2.2     4123 4132                                          =====Hb===
================================================================================
seq( 4140.. 4199)     caaacagcttaagttttttcaacacaagagaacaatgcctctctcattgggtttgcggtg
Segments:
9.9.173     4180 4189                                               ====CTF===
9.9.233     4180 4189                                               ====EFI===
================================================================================
seq( 4200.. 4259)     tagactccgaacagagtgtttaatatacacagctcaccctgctcttcttgggggaacagt
Segments:
2.1.1.1     4208 4217          =====GR===
4.5.1.0     4220 4229                ====TBP===
2.3.1.0     4229 4238                     ====Sp1===
2.3.1.0     4236 4245                          ====Sp1===
================================================================================
seq( 4260.. 4319)     cctgattaactttagattctaagagaaccataggaggcctgagattcacttgaaactgag
Segments:
2.3.1.0     4292 4301                               ====Sp1===
3.5.3.0     4311 4320                                                ===ICSBP=
================================================================================
seq( 4320.. 4379)     gcttttaagagactttgtttatggccttcctcgttagaatagctcttttcttgtgaagga
Segments:
3.5.3.0     4311 4320  =
2.1.1.1     4362 4371                                          =====GR===
2.2.1.1     4364 4373                                            ===GATA-1=
================================================================================
seq( 4380.. 4439)     aaacactaagctggtttcaaaaaaacgtactggccttgtcttcagctccataattcctat
Segments:
1.1.3.0     4395 4404           =C/EBPalp=
2.3.2.2     4397 4406             ===LyF-1==
2.2.1.1     4411 4420                      ===GATA-1=
1.1.3.0     4437 4446                                                =C/
================================================================================
seq( 4440.. 4499)     gtatgctcttgggagggctaagtggataaaaactcagacctggttgtctctgtcccctag
Segments:
1.1.3.0     4437 4446  EBPalp=
2.3.1.0     4447 4456        ====Sp1===
================================================================================
seq( 4500.. 4559)     ttcttcattctcctccaggcagaaagatggcaggccatagtaacgacagatttcagatac
Segments:
3.6.1.0     4501 4510   ====TEC1==
2.3.1.0     4505 4514       ====Sp1===
2.3.1.0     4523 4532                 ====YY1===
================================================================================
seq( 4560.. 4619)     tgagatgtttcctgagaggacaacctgacagaagagttaggtgggggtgctgaggcacca
Segments:
1.1.3.0     4565 4574       ===C/EBP==
2.3.1.0     4599 4608                                    ====Sp1===
3.5.1.2     4599 4608                                    ====RAP1==
9.9.77      4599 4608                                    =CACCC-bi=
1.1.3.0     4605 4616                                          ==C/EBPgamma
9.9.29      4607 4616                                            ====AP-1==
9.9.31      4607 4616                                            ====AP-1==
1.1.3.0     4616 4625                                                  =C/E
```

```
3.5.2.0     4617 4626                                                                  =c-
1.2.2.0     4618 4627                                                                  ==
================================================================================
seq( 4620.. 4679)     ggaaatgtccagatccacccctttaatggtaactaccttcttggaagctctgcactcccc
Segments:
1.1.3.0     4616 4625  BPalp=
3.5.2.0     4617 4626  Ets-1 =
1.2.2.0     4618 4627  ==MyoD==
4.3.2.0     4624 4633      ====SRF===
2.3.1.0     4631 4643            ======Sp1====
4.3.2.0     4639 4648                  ====SRF===
3.1.1.2     4640 4649                   ===Zen-1==
2.3.1.0     4665 4674                                        ====Sp1===
2.3.1.0     4672 4686                                              =======S
3.5.2.0     4678 4687                                                    ==
================================================================================
seq( 4680.. 4739)     acctcttcttctttcccctcccactctctgtctcttttctggtccgtatctggcctatca
Segments:
2.3.1.0     4672 4686  p1=====
3.5.2.0     4678 4687  =Elk-1==
2.3.1.0     4693 4703            =====Sp1===
2.3.1.0     4729 4738                                                ====Sp1===
2.2.1.1     4733 4742                                                    ===GATA
================================================================================
seq( 4740.. 4799)     tagtaagaggtcagtctgttttccacacttggatagtctcattcaaaaatttttgtcaat
Segments:
2.2.1.1     4733 4742  -1=
2.1.2.1     4743 4752     =RAR-alph=
2.1.2.2     4743 4752     =RXR-beta2
2.1.1.4     4747 4756         =====ER===
4.3.2.0     4762 4771                ====SRF===
9.9.537     4766 4775                    ====NF-1==
1.1.3.0     4781 4790                                =C/EBPalp=
2.3.2.2     4786 4795                                     =====Hb===
3.1.1.2     4787 4796                                      ===HOXA4==
1.1.3.0     4792 4801                                           =C/EBPal
================================================================================
seq( 4800.. 4859)     ggacaagtcataagaaacccttccattttcgggctcgttgacgtcaccaaggaggcgata
Segments:
1.1.3.0     4792 4801  p=
3.5.1.2     4816 4825           ====REB1==
1.1.3.0     4820 4829               =C/EBPalp=
3.5.1.2     4835 4844                        ===Adf-1==
9.9.51      4835 4844                        ====ATF===
2.1.2.3     4836 4845                         =REV-ErbA=
1.1.2.0     4836 4846                         ====CREB===
1.1.1.6     4837 4846                          ==CRE-BP1=
1.1.1.1     4838 4847                           ===c-Jun==
2.3.3.0     4838 4847                           =CPE bind=
2.3.1.0     4847 4856                                  ====Sp1===
1.1.3.0     4857 4866                                        =C/
2.2.1.1     4859 4868                                         =
3.1.2.2     4859 4868                                         =
================================================================================
seq( 4860.. 4919)     aatatctgttgatataattggatgtgagattcagtgttgaaatagcagaactctgtccct
Segments:
1.1.3.0     4857 4866  EBPalp=
2.2.1.1     4859 4868  ==GATA-1=
3.1.2.2     4859 4868  ==Oct-1==
================================================================================
seq( 4920.. 4979)     cgctccttggcagggccctattatttatgcaggagcagaggcagcacgcaatcgagctgt
Segments:
9.9.173     4921 4930   ====CTF===
9.9.539     4925 4934       ====NF-1==
2.3.1.0     4927 4937         =====Sp1===
4.5.1.0     4941 4950                ====TBP===
1.1.3.0     4944 4953                   =C/EBPalp=
================================================================================
```

```
seq( 4980.. 5039)     caagagagcgtcagcttattaggcaaatgctgcgtgctttctgaagagggtcgacattat
Segments:
1.1.3.0     4996 5005                  =C/EBPalp=
2.3.1.0     5021 5031                                  =====Sp1===
1.1.3.0     5035 5049                                              ===C/
================================================================================
seq( 5040.. 5099)     aaaatctcactccaggctctggtgtggagaaactcagagcccaagtacgttgagagactg
Segments:
1.1.3.0     5035 5049  EBPalpha==
1.1.3.0     5061 5070                       =C/EBPalp=
4.1.1.0     5066 5075                            =====Dl===
================================================================================
seq( 5100.. 5159)     aagagaaagggaaaaggcaaaagaaaaaaagaagagaaaggagaaggaggaagaaaacctg
Segments:
3.5.3.0     5104 5113      ===IRF-1==
9.9.428     5104 5113      ===ISGF-3=
9.9.701     5107 5116         =PTF1-beta
1.1.3.0     5109 5118           =C/EBPalp=
2.3.2.2     5119 5128                 =====Hb===
3.1.2.2     5123 5132                    ===Oct-1==
2.2.1.1     5129 5138                         ===GATA-1=
3.5.3.0     5129 5138                         ===ICSBP==
2.3.1.0     5140 5151                               =====Sp1====
3.5.2.0     5143 5152                                  ===Elf-1==
2.3.1.0     5156 5165                                           ====
================================================================================
seq( 5160.. 5219)     caggaggcatcctgagagaagtccctctgcagaggcagcagtgcgggctcacctaccaag
Segments:
2.3.1.0     5156 5165  Sp1===
2.3.1.0     5162 5171    ====Sp1===
4.1.1.0     5175 5184               =NF-kappa=
9.9.590     5175 5184               =NF-kappaB
2.3.1.0     5180 5189                    ====Sp1===
2.3.1.0     5217 5227                                        ===
================================================================================
seq( 5220.. 5279)     ggaggagaaggtaggcagcgcctagacgggcgccaccaactttgtgctgcctgagctgct
Segments:
2.3.1.0     5217 5227  ==Sp1===
2.3.1.0     5233 5242            ====Sp1===
2.3.1.0     5244 5257                 ======Sp1=====
1.2.1.0     5265 5274                                =====E4===
2.1.1.4     5269 5278                                    =====ER===
================================================================================
seq( 5280.. 5339)     gtggtgagccccggagccagctgcccatgtgctggaatgcctgtgcctatgcatgtatgt
Segments:
2.3.1.0     5288 5298         =====Sp1===
1.3.1.2     5293 5302              ====USF===
1.2.1.0     5295 5304                =====E1===
1.2.2.0     5295 5304                ===Myf-3==
2.3.1.0     5295 5304                ====Sp1===
1.3.1.2     5301 5310                     ====USF===
3.5.1.2     5333 5342                                          ====RAP
================================================================================
seq( 5340.. 5399)     gtgtcgctaactgtgccttaaaattccgatgacagtggcgatttgaaaaagcgaagttag
Segments:
3.5.1.2     5333 5342  1==
1.1.3.0     5379 5388                                  =C/EBPalp=
================================================================================
seq( 5400.. 5459)     acggcggctgctcatctttatccactcaatccaatctgccactcactgctcatagtctgt
Segments:
3.5.1.2     5401 5410   ===Adf-1==
2.2.1.1     5407 5416        ===GATA-1=
2.1.1.1     5433 5442                            =====GR===
2.3.1.0     5438 5447                                 ====Sp1===
2.2.1.1     5455 5464                                          ===GA
================================================================================
seq( 5460.. 5519)     gcaaagaatggctcccctattgcatcccatgtccccaagcaaacggagtaagggcaggaa
Segments:
```

```
2.2.1.1     5455 5464  TA-1=
1.6.1.0     5467 5476        ====AP-2==
1.3.1.2     5485 5494                  ====USF===
3.6.1.0     5515 5524                                       ====T
================================================================================
seq( 5520.. 5579)     tggagacagagaaggttgttctcaatttggcagaaaaggatgtccgaaaggggcgatta
Segments:
3.6.1.0     5515 5524  EC1==
1.1.3.0     5538 5547             =C/EBPalp=
9.9.535     5542 5551                 ====NF-1==
9.9.539     5543 5552                  ====NF-1==
2.1.1.1     5545 5554                    =====GR===
3.5.2.0     5553 5562                           ====PEA3==
2.3.1.0     5566 5575                                    ====Sp1===
3.5.1.2     5577 5586                                          ===
================================================================================
seq( 5580.. 5639)     gggtgtgcgacagcttaaacctgtggcacttgtccgggctcagggaagtcggtttaggga
Segments:
3.5.1.2     5577 5586  =RAP1==
1.1.3.0     5584 5593      =C/EBPbeta
9.9.539     5603 5612                 ====NF-1==
2.3.1.0     5614 5623                       ====Sp1===
1.1.1.6     5636 5645                                  ==CR
1.1.2.0     5636 5645                                  ====
================================================================================
seq( 5640.. 5699)     agacgtttgggaggtccttaggaagaggagccaggggttgtcccttctaggtctccaaag
Segments:
1.1.1.6     5636 5645  E-BP1=
1.1.2.0     5636 5645  CREB==
2.3.1.0     5648 5657          ====Sp1===
2.3.1.0     5661 5673                ======Sp1====
2.3.1.0     5672 5681                      ====Sp1===
2.3.1.0     5679 5688                            ====Sp1===
4.3.2.0     5694 5703                                     ====SR
================================================================================
seq( 5700.. 5759)     aaggtcaccgcgggctcgcaccagttgagctttgcaggtacctagcttcagcaccgcgg
Segments:
4.3.2.0     5694 5703  F===
9.9.32      5705 5714       ====AP-1==
2.3.1.0     5709 5718           ====Sp1===
================================================================================
seq( 5760.. 5819)     acagcgtcaccgaagcctagagcctgtcttgtctgtgggtgtccgataggaagccccgct
Segments:
2.3.3.0     5762 5771    =CPE bind=
4.4.1.0     5767 5776         =====E2===
3.5.1.2     5790 5799                   ====RAP1==
2.3.1.0     5791 5800                    ====Sp1===
2.2.1.1     5802 5811                         ===GATA-1=
2.3.1.0     5809 5822                               ======Sp1==
================================================================================
seq( 5820.. 5879)     gcaccttccagctgagctaaactctgaccaatcctacctttctcccccaccttctctctc
Segments:
2.3.1.0     5809 5822  ===
2.1.1.4     5840 5849            =====ER===
2.3.1.0     5861 5873                       ======Sp1====
2.3.1.0     5874 5886                                ======
2.3.3.0     5876 5885                                  =CPE
================================================================================
seq( 5880.. 5906)     ccccgacctcaacctcggtgcttcag
Segments:
2.3.1.0     5874 5886  Sp1====
2.3.3.0     5876 5885   bind=
2.3.1.0     5880 5889  ====Sp1===
2.3.1.0     5886 5895       ====Sp1===
3.1.2.2     5898 5906
```

9.7. Northern Blot

Murine CRH Promoter Region and Appropriate Primers Used for Amplification of the CRH Probe

Sequence Origin: ENSEMBL Database Chromosome 3:19,593,401 - 19,595,396, Genomic DNA

Illustrated CRH Promoter Region:

5,000 bp (Start of *CRH*-Exon 1) - 6,996 bp (End of *CRH*-Exon 2)

Cloned CRH Probe (357 bp):

6,036 bp – 6,392 bp (Pr.9 – Pr.10)

Amplification from corresponding mRNA by RT-PCR

Legend:

CRH-Exon 1/2

Primer CRH-Ex2-Forward, Pr. 9

Primer CRH-Ex2-Reverse, Pr. 10

Probe (357 bp)

AGGCAAATGCTGCGTGCTTTCTGAAGAGGGTCGACATTATAAAATCTCACTCCAGGCTCTGGTG
TGGAGAAACTCAGAGCCCAAGTACGTTGAGAGACTGAAGAGAAAGGGAAAAGGCAAAAGAAAAA
AAGAAGAGAAAGGAGAAGAGGAAGAAAACCTGCAGGAGGCATCCTGAGAGAAGTCCCTCTGCAG
AGGCAGCAGTGCGGGCTCACCTACCAAGGGAGGAGAAGGTAGGCAGCGCCTAGACGGGCGCCAC
CAACTTTGTGCTGCCTGAGCTGCTGTGGTGAGCCCCGGAGCCAGCTGCCCATGTGCTGGAATGC
CTGTGCCTATGCATGTATGTGTGTCGCTAACTGTGCCTTAAAATTCCGATGACAGTGGCGATTT
GAAAAAGCGAAGTTAGACGGCGGCTGCTCATCTTTATCCACTCAATCCAATCTGCCACTCACTG
CTCATAGTCTGTGCAAAGAATGGCTCCCCTATTGCATCCCATGTCCCCAAGCAAACGGAGTAAG
GGCAGGAATGGAGACAGAGAAGGTTGTTCTCAATTTGGCAGAAAAGGATGTCCGAAAGGGGGCG
ATTAGGGTGTGCGACAGCTTAAACCTGTGGCACTTGTCCGGGCTCAGGGAAGTCGGTTTAGGGA
AGACGTTTGGGAGGTCCTTAGGAAGAGGAGCCAGGGGTTGTCCCTTCTAGGTCTCCAAAGAAGG
GTCACCGCGGGCTCGCACCAGTTGAGCTTTGCAGGTACCTAGCTTCAGCACCGCGGACAGCGTC
ACCGAAGCCTAGAGCCTGTCTTGTCTGTGGGTGTCCGATAGGAAGCCCCGCTGCACCTTCCAGC
TGAGCTAAACTCTGACCAATCTTACCTTTCTCCCCCACCTTCTCTCTCCCCCGACCTCAACCTC
GGTGCTTCAGAGAGCGCCCCTAACATGCGGCTGCGGCTGCTGGTGTCCGCGGGCATGCTGCTGG
TGGCTCTGTCGTCCTGCCTGCCTTGCAGGGCCCTGCTCAGCAGGGGATCCGTCCCCCGAGCGCC
GCGGGCCCCGC**AGCCCTTGAATTTCTTGCAG**CCGGAGCAGCCCCAGCAACCTCAGCCGGTTCTG
ATCCGCATGGGTGAAGAATACTTCCTCCGCCTGGGGAATCTCAACAGAAGTCCCGCTGCTCGGC
TGTCCCCCAACTCCACGCCCCTCACCGCGGGTCGCGGCAGCCGCCCCTCGCACGACCAGGCTGC

GGCTAACTTTTTCCGCGTGTTGCTGCAGCAGCTGCAGATGCCTCAGCGCTCGCTCGACAGCCGC
GCGGAGCCGGCCGAACGCGGCGCCGAGGATGCCCTCGGTGGCCACCAGGGGGCGCTGGAGAGGG
AGAGGCGGTCGGAGGAGCCGCCCATCTCTCTGGATCTCACCTTCCACC

9.8. Abbreviations

ACE	Angiotensin converting enzyme
ACTH	Adrenocorticotropic hormone
ADP	Adenosine diphosphate
AGM	Aorta-gonad-mesonephros
Ang	Angiotensin
ANP	Atrial natriuretic peptide
AP-1	Activator Protein 1
APS	Ammonium persulfate
AQP	Aquaporin
AS	Aldosterone synthase
AT	Angiotensin receptor
ATF1	cAMP-dependent transcription factor
ATP	Adenosine triphosphate
AVP	Arginine vasopressin
B	Basal
BRCA1	Breast Cancer 1
BSA	Bovine serum albumine
BW	Body weight
Ca^{2+}	Calcium
CaMK	Ca^{2+}/calmodulin-dependent protein kinase
cAMP	Cyclic adenosine monophosphate
Cat. No.	Catalog number
Cbl	Casitas B-lineage lymphoma
CD	Cluster of differentiation
CK	Creatine Kinase
Cl^-	Chloride
CLIP	Corticotropin-like intermediate peptide
CNS	Central nervous system
Cre	Causes recombination
CRE	cAMP-responsive element
CREB	cAMP-responsive element binding protein

CRH	Corticotropin-releasing hormone
CRH_{Prom}	CRH promoter reporter including RE-1/NRSE regulatory element
$CRH_{Prom-RE}$	CRH promoter reporter lacking RE-1/NRSE regulatory element
CRH-R	Corticotropin-releasing hormone receptor
DAPI	4',6-Diamidino-2-phenylindole
DEPC	Diethylpyrocarbonate
DHEA	Dehydroepiandrosterone
DMEM	Dulbecco's modified Eagle's medium
DNA	Deoxyribonucleic acid
dUTP	Deoxyuridine triphosphate
ECG	Electrocardiography
ECL	Enhanced chemoluminescence
EDTA	Ethylenediaminetetraacetic acid
EGF	Epidermal growth factor
EGFR	Epidermal growth factor receptor
EGTA	Ethylene glycol tetraacetic acid
EIA	Enzyme immuoassay
ELISA	Enzyme-linked immunosorbent assay
En2 intron 1	*Engrailed2* intron 1
Ena	Enabled
ENaC	Epithelial sodium channel
ENU	N-Ethyl-N-nitrosourea
EPSC	Excitatory postsynaptic current
EPSP	Excitatory postsynaptic potential
ERK	Extracellular signal-regulated kinase
ES cell	Embryonic stem cell
EST	Expressed sequence tag
Ets	E-twenty six
Eve	EVH1 enhanced
EVH1	Ena/VASP homology 1 domain
Ex	Exon
FBS	Fetal bovine serum
FGF	Fibroblast growth factor
FGFR	Fibroblast growth factor receptor

FGFRL	Fibroblast growth factor receptor-like
FLP	Flippase
FRS2	Fibroblast growth factor receptor substrate 2
FRT	Flippase recognition target
FSH	Follicle-stimulating hormone
GABA	γ-Aminobutyric acid
GAB1	GRB2-associated binding protein 1
GDP	Guanosine diphosphate
GF	Growth factor
GFR	Glomerular filtration rate
GGT	γ-Glutamyltransferase
GH	Growth hormone
GHRH	Growth hormone-releasing hormone
GnRH	Gonadotropin-releasing hormone
GOT/AST	Glutamate oxaloacetate transaminase/Aspartate aminotransferase
GPT/ALT	Glutamate pyruvate transaminase/Alanine aminotransferase
GR	Glucocorticoid receptor
GRB2	Growth factor receptor-bound protein 2
GRE	Glucocorticoid response element
GTP	Guanosine triphosphate
h	Hour
H&E	Hematoxylin & Eosin
HCC	Hepatocellular carcinoma
HEK	Human embryonic kidney
HEPES	4-(2-Hydroxyethyl)-1-piperazineethanesulfonic acid
HET	Heterozygous
HGF	Hepatocyte growth factor
HPA	Hypothalamic-pituitary-adrenal
HSD11B2/11β-HSD type II	11β-Hydroxysteroid-dehydrogenase type 2
HSD3B/ 3β-HSD	3β-Hydroxysteroid-dehydrogenase
IGF-1	Insulin-like growth factor 1
IgG	Immunoglobulin G
IGTC	International gene trap consortium
IMPC	International mouse phenotyping consortium

IL	Interleukin
IRS-1/2	Insulin receptor substrate 1/2
JNK	c-Jun N-terminal kinase
K^+	Potassium
KBD	c-Kit binding domain
kDa	Kilodalton
KO	Knockout
lacZ	β-Galactosidase gene
LATS	Large tumor suppressor
LH	Luteinizing hormone
LoxP	Locus of X-over P1
LPH	Lipotropin
Luc	Luciferase
M	Marker
MAPK	Mitogen-activated protein kinase
MAPKK/MEK	Mitogen-activated protein kinase kinase
MAPKKK	Mitogen-activated protein kinase kinase kinase
MARKK	Microtubule affinity-regulating kinase-activating kinase
MCR	Melanocortin receptor
mGluR	Metabotropic glutamate receptor
mHypoE-44	Embryonic mouse hypothalamic cell line N44
min	Minute
MMP	Matrix metalloproteinases
MNK	MAPK interacting kinases
MOPS	3-(N-Morpholino)propanesulfonic acid
MSH	Melanocyte-stimulating hormone
MSK	Mitogen- and stress-activated kinase
n	Number
Na^+	Sodium
NBR1	Neighbor of BRCA1
neoR	Neomycin resistance gene
NF1	Neurofibromin 1
NF-KB	Nuclear factor `kappa-light-chain-enhancer´ of activated B cells
NGF	Nerve growth factor

NGF1B	Nerve growth factor 1 B
NGFR	Nerve growth factor receptor
NPC	Neural progenitor cell
NURR1	Nuclear receptor related 1
OCD	Obsessive-compulsive disorder
p	Probability
P450aldo/CYP11B2	Aldosterone synthase
P450c11/CYP11B1	11β-Hydroxylase
P450c17/CYP17A1	17α-Hydroxylase
P450c21/CYP21A2	21α-Hydroxylase
P450scc/CYP11A1	Cholesterol side-chain cleavage monooxygenase
pA	Simian virus 40 polyadenylation site
PBS	Phosphate buffered saline
PCR	Polymerase chain reaction
PDGF	Platelet-derived growth factor receptor
PDGFR	Platelet-derived growth factor
PDV	Tumorigenic murine keratinocyte cell line
PFA	Paraformaldehyde
PKA	Protein kinase A
PKC	Protein kinase C
PO_4^{3-}	Phosphate
POMC	Proopiomelanocortin
Pr.	Primer
PRL	Prolactin
PSD 95	Postsynaptic density protein 95
PTB	Phosphotyrosine-binding
pUC	pUC vector backbone
PVN	Paraventricular nucleus
Rab	Ras-related protein
Raf	Rapidly accelerated fibrosarcoma
Ras	Rat sarcoma
RAS	Renin-Angiotensin system
RasGAP	Ras GTPase-activating protein
RasGEF	Ras guanine nucleotide exchange factor
RBM	Raf-binding motif

RE-1/NRSE	Repressor element-1/neuron-restrictive silencing element
RhoA	Ras homolog gene family, member A
RNA	Ribonucleic acid
RNAi	RNA interference
ROCK	Rho-associated protein kinase
ROMK	Renal outer medullary potassium channel
RSK	Ribosomal S6 kinase
RTK	Receptor tyrosine kinase
RT-PCR	Reverse transcription polymerase chain reaction
s	Second
SA	Splice acceptor
SAPAP3	SAP90/PSD95-associated protein 3
SCF	Stem cell factor
SCN	Suprachiasmatic nucleus
SD	Standard deviation
SDS	Sodium dodecyl sulphate
SDS-PAGE	Sodium dodecyl sulphate-polyacrylamide gel electrophoresis
SGK1	Serum and glucocorticoid-inducible kinase 1
SH2	Src homology 2
SH3	Src homology 3
SHC	Src homology and collagen protein
SHP2/PTPN11	Src homology 2 domain containing protein-tyrosine phosphatase 2 / Tyrosine-protein phosphatase non-receptor type 11
siRNA	Small interfering RNA
SLITRK5	SLIT and NTRK-like protein-5
SON	Supraoptic nucleus
SOS	Son of sevenless
SPR2	SPRED2
SPRED	Sprouty-related protein with EVH1 domain
Src	Sarcoma
SSC	Saline-sodium citrate
StAR	Steroidogenic acute regulatory protein
STAT	Signal transducers and activators of transcription
TASK	TWIK-related acid-sensitive K+ channel

TEMED	Tetramethylethylendiamin
TESK	Testis-specific protein kinase 1
TGF-β1	Transforming growth factor β 1
TNF α	Tumor necrosis factor α
TRH	Thyrotropin-releasing hormone
TSH	Thyroid-stimulating hormone
TUNEL	Terminal deoxynucleotidyl transferase dUTP nick end labeling
U	Unit
uPA	Urokinase type plasminogen activator
UV	Ultraviolett
V1a/1b/2R	Vasopressin receptor 1a, 1b, 2
VASP	Vasodilator-stimulated phosphoprotein
VEGF	Vascular endothelial growth factor
VEGFR	Vascular endothelial growth factor receptor
WASP	Wiskott-Aldrich syndrome protein
WD	Water deprivation
WT	Wild-type
X-Gal	5-Bromo-4-chloro-3-indolyl-beta-D-galactopyranoside
β-gal	β-galactosidase
β-geo	Fusion gene composed of β-galactosidase gene (lacZ) and neomycin resistance gene (neoR)